Quantitative magnetic resonance imaging in optic neuritis

Simon James Hickman

A thesis submitted to the University of London for the degree of Doctor of Philosophy

2004

NMR Research Unit
Department of Neuroinflammation
Institute of Neurology
University College London
Queen Square
London
WC1N 3BG
United Kingdom

ProQuest LLC
789 East Eisenhower Parkway
P.O. Box 1346
Ann Arbor, MI 48106-1346

Abstract

The major event in relapsing remitting multiple sclerosis (MS) is the acute relapse. The majority of patients with MS present with such an event. Most early relapses are followed by complete or near complete recovery, however partial recovery or significant disability can result from an individual relapse. Study of relapses *in vivo* is therefore desirable. Magnetic resonance imaging (MRI) is very sensitive at detecting MS lesions. Unfortunately, in the brain and spinal cord, it has been difficult to reliably identify the lesion that is responsible for the symptoms of an individual relapse and most new brain lesions which are apparent on MRI are clinically silent.

Optic neuritis provides an attractive model to study the effects of relapses in MS. Optic neuritis is a frequent manifestation of MS and has been regarded as a *forme fruste* of the disease. The natural history of acute optic neuritis mirrors that of an acute MS relapse elsewhere in the central nervous system (CNS) and the response to corticosteroid therapy is the same. Visual function can be measured accurately in a rater-independent fashion and it is possible to measure the latency and amplitude of the visual evoked potential (VEP) which gives information about the integrity of the visual conducting pathways.

Developments in imaging technology and application now means that, potentially more pathologically specific imaging sequences can be applied to the study of the optic nerves. This thesis will investigate the application of these new imaging techniques, along with clinical and VEP measures, to the study of optic neuritis in order to gain new insights into the effect of individual lesions on structure and function in the CNS in the short- and long-term.

Declaration

Patient recruitment and examinations for the studies in Chapter 3.1 and 3.2 were performed by Dr. Peter Brex in London and Dr. Charlotte Brierley in Cambridge. The images were reported by Dr. Ivan Moseley. Statistical advice was provided by Dr. Martin King.

Patient recruitment and examinations for the study in Chapter 3.3 were performed by Dr. R. Kapoor, Dr. G.T. Plant, Dr. S.J. Jones, Dr. A. Brusa, Dr. A. Gass, Dr. C.P. Hawkins, Dr. R. Page, Prof. N.W. Wood, Prof. D.A.S. Compston, Dr. I.F. Moseley, Prof. W.I. McDonald, Mr. D.G. MacManus, and Mrs. M. Galton. Statistical analysis was performed by Dr. Daniel Altmann.

In Chapter 4 visual evoked potentials were recorded and analysed by Dr. Stephen Jones. The conventional MRIs were reported by Dr. Katherine Miszkiel. Statistical analysis was performed by Dr. Daniel Altmann.

Acknowledgements

I would first like to thank all the willing participants, both patients and controls, who volunteered to spend endless hours in the imager and have numerous clinical tests. Without them all this would not have been possible.

Dr. Peter Brex and our collaborators in Cambridge: Dr. Charlotte Brierley, Prof. Neil Scolding and Prof. Alastair Compston provided patients for the studies in Chapter 3, which enabled me to get started and develop the segmentation methodology for optic nerve atrophy measurement.

Patient recruitment for the studies in Chapter 4 was carried out in the Neuro-Ophthalmology clinic at Moorfield's Eye Hospital. I am indebted to Michelle Peppiatt for organising the optic neuritis clinic and to Dr. Gordon Plant for kindling my interest in the field of Neuro-Ophthalmology.

I would like to thank the radiographers David MacManus, Andrew Lowe, Ros Gordon and Chris Benton for putting up with me and for imaging all the subjects. Reporting of the images was performed by Dr. Ivan Moseley and Dr. Katherine Miszkiel. Dr. Steve Jones did all the hard work performing and analysing the visual evoked potential experiments. His was also the voice of reason making sure that I did not get too carried away with outlandish conclusions.

The support of the fellows' room kept me going; firstly Drs. Jackie Foong, Manny Bagary and Stefania Bruno and latterly Drs. Declan Chard, Ahmed Toosy, Gordon Ingle, Gerard Davies, Waqar Rashid, Olga Ciccarelli, Tony Traboulsee, Catherine Dalton and Jaume Sastre-Garriga.

This work would not have been possible without the technical support of the Physicists, particularly Drs. Geoff Parker and Claudia Wheeler-Kingshott, and Prof. Gareth Barker who also acted as my secondary supervisor, providing sage advice. Statistical advice and support was also vital and I am indebted to Drs. Martin King and Daniel Altmann for getting me to think more clearly about the data.

Profs. Alan Thompson and David Miller conceived the idea for this project and secured the funding to enable it to proceed. Prof. Miller also acted as my principal supervisor. He displayed a good mix of gentle support when it was needed and a firm hand to make sure that I kept the writing-up going to publish the data and produce this work. I would like to thank him especially for his help.

The NMR Research Unit is supported by the Multiple Sclerosis Society of Great Britain and Northern Ireland. Their financial support keeps the Unit going. I was supported by a project grant from The Wellcome Trust. I am indebted to these two organisations for enabling me to complete this PhD.

Lastly I would like to thank my wife Rosemary and children Stephanie and Alistair for putting up with me for the last few years and for always being there.

Publications associated with this thesis

Hickman SJ, Brex PA, Brierley CMH, Silver NC, Barker GJ, Scolding NJ, Compston DAS, Moseley IF, Plant GT, Miller DH. Detection of optic nerve atrophy following a single episode of unilateral optic neuritis by MRI using a fat saturated short echo fast FLAIR sequence. *Neuroradiology* 2001;**43**:123-128.

Hickman SJ, Brierley CMH, Brex PA, MacManus DG, Scolding NJ, Compston DAS, Miller DH. Continuing optic nerve atrophy following optic neuritis: A serial MRI study. *Mult Scler* 2002;**8**:339-342.

Hickman SJ, Dalton CM, Miller DH, Plant GT. Management of acute optic neuritis. *Lancet* 2002;**360**:1953-1962.

Hickman SJ, Kapoor R, Jones SJ, Altmann DR, Plant GT, Miller DH. Corticosteroids do not prevent optic nerve atrophy following optic neuritis. *J Neurol Neurosurg Psychiatry* 2003;**74**:1139-1141.

Hickman SJ, Toosy AT, Jones SJ, Altmann DR, Miszkiel KA, MacManus DG, Barker GJ, Plant GT, Thompson AJ, Miller DH. Serial magnetization transfer imaging in acute optic neuritis. *Brain* 2004;**127**:692-700.

Hickman SJ, Toosy AT, Miszkiel KA, Jones SJ, Altmann DR, MacManus DG, Plant GT, Thompson AJ, Miller DH. Visual recovery following acute optic neuritis: A clinical, electrophysiological and magnetic resonance imaging study. *J Neurol* 2004, in press.

Table of Contents

Abbreviations

2D	Two-dimensional
3D	Three-dimensional
ACE	Angiotensin converting enzyme
ACTH	Adrenocorticotrophic hormone
ANA	Antinuclear antibodies
ADC	Apparent diffusion coefficient
ARR	Adjusted rate ratio
AZOOR	Acute zonal occult outer retinopathy
BOLD	Blood oxygen level dependent
CDMS	Clinically definite multiple sclerosis
CF	Central field
CI	Confidence interval
CIS	Clinically isolated syndrome suggestive of multiple sclerosis
CNS	Central nervous system
CPD	Cycles per degree
CPMS	Clinically probable multiple sclerosis
CRION	Chronic relapsing inflammatory optic neuropathy
CSF	Cerebrospinal fluid
CV	Coefficient of variation
CT	Computerised tomography
CXR	Chest radiograph
DMDs	Disease modifying drugs
DWI	Diffusion-weighted imaging
EAE	Experimental allergic encephalomyelitis
EDSS	Expanded disability status scale
EPI	Echo planar imaging
ESR	Erythrocyte sedimentation rate

ETL	Echo-train length
FA	Fractional anisotropy
fMRI	Functional magnetic resonance imaging
FM 100	Farnsworth Munsell 100 hue test
FOV	Field of view
FSE	Fast spin echo
FLAIR	Fluid-attenuated inversion recovery
GCA	Giant cell arteritis
GE	Gradient echo
GM	Grey matter
ICC	Intraclass correlation coefficient
IM	Intramuscular
iNOS	Inducible NO synthase
IV	Intravenous
IVIG	Intravenous immunoglobulin
IVMP	Intravenous methylprednisolone
LGN	Lateral geniculate nucleus
MDM	Magnetic dipole moment
MP	Methylprednisolone
MRI	Magnetic resonance imaging
MS	Multiple sclerosis
MSFC	Multiple sclerosis functional composite
MT	Magnetisation transfer
MTR	Magnetisation transfer ratio
M_0	Signal intensity in absence of the magnetisation transfer pre-pulse
M_S	Signal intensity in the presence of the magnetisation transfer pre-pulse
NEX	Number of excitations
NO	Nitric oxide

NPL	No perception of light
NS	Not significant
OCT	Ocular coherence tomography
ON	Optic neuritis
ONTT	Optic neuritis treatment trial
PD	Proton density
PERG	Pattern electroretinogram
PION	Posterior ischaemic optic neuropathy
PSA-NCAM	Polysialylated form of neural cell adhesion molecule
pu	Percent units
QDS	Four times per day
RAPD	Relative afferent pupillary defect
REM	Rapid eye movement
RF	Radiofrequency
RNFL	Retinal nerve fibre layer
ROI	Region of interest
RRMS	Relapsing remitting multiple sclerosis
SD	Standard deviation
SFV	Semliki Forest virus
SLP	Scanning laser polarimetry
SNR	signal-to-noise ratio
sTE fFLAIR	Short echo fast fluid-attenuated inversion recovery
SPIR-FLAIR	Selective partial inversion recovery – fluid-attenuated inversion recovery with fast spin-echo acquisition
SPMS	Secondary progressive multiple sclerosis
STIR	Short *tau* inversion recovery
T	Tesla
TE	Echo time

TEef	Effective echo time
TI	Inversion time
TR	Repetition time
VA	Visual acuity
VEP	Visual evoked potential
VER	Visual evoked response
WF	Whole field
WM	White matter
ZOOM-EPI	Zonal oblique multi-slice echo planar imaging

Figures

Tables

Chapter 1 Optic Neuritis

1.1 Anatomy and physiology of the optic nerve

1.1.1 Gross anatomy

The optic nerve is an offshoot of the brain and is covered by a sheath, made up of the full three layers of meninges in continuity with the leptomeninges of the brain, which transmits the cerebrospinal fluid (CSF) (Tamraz, 1994). Its blood supply comes from the ophthalmic artery, a branch of the internal carotid artery (Sadun, 1998). The optic nerve in adult humans is about 40-50mm long and is subdivided into four parts with varying lengths and cross-sectional areas (Table 1.1 and Table 1.2). The two optic nerves fuse in the cranial cavity to form the optic chiasm where the nerve fibres from the nasal half of each retina decussate (Sadun, 1998).

1.1.2 Optic nerve head

The optic nerve head is approximately 1mm long (anterior-posterior) by 1.5mm horizontally and 1.8mm vertically. The anterior surface is the optic disc that is visible on fundus examination (Tamraz, 1994; Sadun, 1998).

1.1.3 Intraorbital optic nerve

The intraorbital optic nerve is 20-30mm long (Blinkov & Glezier, 1968; Tamraz, 1994; Sadun, 1998), and has a sinuous course from the back of the globe to the optic foramen. The intraorbital optic nerve is approximately 6mm longer than the distance it has to traverse to allow for movements of the eye (Williams *et al.*, 1989). The nerve is 3mm in diameter at the globe, increasing to 4.5mm at the orbital apex (Sadun, 1998), with an average diameter in the globe of 3.5mm (Tamraz, 1994) and is circular in shape (Sylvester & Ari, 1961; Barker, 2000), The nerve is surrounded by the nerve sheath, containing the CSF, and then orbital fat containing the ciliary vessels and nerves (Williams *et al.*, 1989). The dura fuses anteriorly with the sclera and posteriorly with the periosteum of the optic canal (Tamraz, 1994). At the orbital apex the optic nerve is

surrounded by the annulus of Zinn, the origin of the four rectus muscles of the orbit (Sadun, 1998).

Portion of optic nerve	Approximate anterior-posterior length
i) Optic nerve head	1mm
ii) Intraorbital optic nerve	20-30mm
iii) Intracanalicular optic nerve	4-10mm
iv) Intracranial optic nerve	3-16mm
Total optic nerve length	40-50mm
Optic chiasm	4-13mm

Table 1.1: Approximate anterior-posterior length of adult human optic nerve according to position within the nerve (Blinkov & Glezier, 1968; Williams *et al.*, 1989; Tamraz, 1994; Sadun, 1998; Slamovits, 1998).

Portion of optic nerve		Optic nerve mean cross-sectional area
Intraorbital		6.75-6.95mm^2
Intracanalicular	(i) Anterior	6.16mm^2
	(ii) Middle	6.66mm^2
	(iii) Posterior	7.71mm^2
Intracranial		9.93-12.09mm^2

Table 1.2: Optic nerve mean areas according to position within the optic nerve from human adult autopsy studies (Donaldson & Bolton, 1891; Sylvester & Ari, 1961; Dolman *et al.*, 1980; Jonas *et al.*, 1990; Rimmer *et al.*, 1993; Chou *et al.*, 1995).

1.1.4 Intracanalicular optic nerve

The optic nerve enters the optic canal through the orbital foramen. The canal is formed by the union of the two roots of the lesser wings of the sphenoid bone. The canal is 4-10mm long (Blinkov & Glezier, 1968; Tamraz, 1994; Sadun, 1998), is approximately 21mm^2 in cross-sectional area anteriorly, narrowing to 16mm^2 at its mid-point, and increasing again to 18mm^2 posteriorly (Chou *et al.*, 1995). Each canal runs posteriorly

and medially. The sphenoid sinus and the posterior ethmoidal air cells lie medial to the optic canal. Infero-laterally the optic strut, which joins the lesser wing of the sphenoid bone to its main body, separates the canal from the superior orbital fissure (Sadun, 1998). The optic strut joins with the anterior clinoid posteriorly (Goldberg *et al.*, 1992). Superiorly is a plate of bone, over which lies the frontal lobe of the brain, although occasionally the frontal sinus extends this far back. Unlike the intraorbital optic nerve the intracanalicular portion is fixed and cannot move freely as the eye moves. The dura is adherent to the bones of the canal on one side and the optic nerve on the other (Sadun, 1998). The limited space within the canal and its bony walls makes the optic nerve vulnerable to damage from blunt trauma (Chou *et al.*, 1995) and from compression due to swelling of the optic nerve, possibly explaining the previous observation of a poorer prognosis when the intracanalicular optic nerve is involved in optic neuritis (Miller *et al.*, 1988).

1.1.5 Intracranial optic nerve

The optic nerves exit the canal into the cranial cavity. The intracranial optic nerves are 3-16mm in length and 4.5-5mm in diameter (Blinkov & Glezier, 1968; Tamraz, 1994; Sadun, 1998), but are elliptical in shape (Sylvester & Ari, 1961; Barker, 2000), and take a posterior, superior and medial course to join at the optic chiasm. The frontal lobes of the brain lie superiorly. The olfactory tracts here are separated from the optic nerve by the anterior cerebral and anterior communicating arteries. Laterally, lie the internal carotid artery and its branches. The ophthalmic artery is given off here and enters the canal infero-laterally to the optic nerve. Infero-medially lies the sphenoid sinus (Sadun, 1998).

1.1.6 Optic chiasm

Within the optic chiasm nerve fibres from the nasal retina (serving the temporal visual field) cross to the contralateral optic tract, whereas temporal fibres (serving nasal vision) continue within the ipsilateral optic tract. The chiasm has a transverse diameter of 10-20mm, an anterior-posterior width of 4-13mm and is 3-5mm thick (Blinkov & Glezier, 1968; Tamraz, 1994; Sadun, 1998). The chiasm overlies the tuberculum sellae of the sphenoid bone and the pituitary gland, hence its vulnerability to damage from

supra-sellar extension of pituitary tumours. In 79% of cases the chiasm is postfixed, overlying the posterior two-thirds of the sella. In 12% of cases it is over the middle sella, in 4% it is over and behind the dorsum sellae and in 5% it is in the chiasmatic sulcus. This explains the variation in position of the chiasm on imaging (Tamraz, 1994) and the differences in length seen in the intracranial optic nerves (Sadun, 1998). Inferolateral to the chiasm lies the cavernous sinuses and laterally are the supraclinoid portions of the internal carotid arteries. Posteriorly is the third ventricle, anteriorly the anterior communicating arteries, and superiorly lies the lamina terminalis (Sadun, 1998).

1.1.7 Optic nerve histology and physiology

The axons of the optic nerve start at the retinal ganglion cells and synapse in the lateral geniculate nucleus (LGN), either ipsilateral or contralateral depending on their path through the optic chiasm. Some fibres terminate in the optic tectum in the brainstem and may play a role in pupillary responses. There are in addition efferent fibres which are thought to terminate in the retina. These may be involved in a feedback system to modulate the visual response (Sadun, 1998).

As in the central nervous system (CNS) the nerve fibres are myelinated by oligodendrocytes rather than Schwann cells which myelinate peripheral nerves. Astrocytes are also present. All of the axons subserving vision are myelinated after they pass through the lamina cribrosa in the optic nerve head. In one study the optic nerves were reported to contain 1,010,000±84,000 myelinated fibres each, and in addition a large number of unmyelinated fibres which may be the efferent fibres mentioned above (Blinkov & Glezier, 1968). The presence of unmyelinated fibres is disputed (Anderson & Hoyt, 1969). Two further studies recorded mean fibre counts of 1,244,005±20,033 (Balazsi *et al.*, 1984) and 1,159,000±196,000 (Jonas *et al.*, 1990) respectively. The cross-sectional area of the intra-orbital optic nerve is 6.75-6.95mm^2 (Table 2) (Dolman *et al.*, 1980; Jonas *et al.*, 1990; Rimmer *et al.*, 1993). The density of myelinated fibres is therefore approximately 150,000 per mm^2.

The mean diameter of axons is 0.96±0.09μm. 95% of axons are between 0.3 and 2μm across (Repka & Quigley, 1989). Mean axonal area is 0.644±0.361μm^2. The axons are

about one tenth of the size of spinal ventral root axons with myelin sheaths approximately one half as thick (Kunii *et al.*, 1999). There are two classes of retinal ganglion cells in humans. About 80-90% of them are small-to-medium sized, are concentrated in the macula and project to the parvocellular layers of the dorsal LGN. These P-cells have colour-opponent physiology and are thought to subserve high-contrast, high-spatial frequency resolution. In contrast, the remainder are large cells which project to the magnocellular layers of the LGN (the M-cells) and are primarily involved with non-colour information of high temporal and low spatial frequency (Sadun, 1998).

The inner layer of the meninges, the pia mater wraps around the optic nerve. From its inner surface fibrous septa, containing collagen, enter the nerve subdividing it into longitudinal polygonal sections occupied by fascicles of axons, approximately 1000 fascicles in all (Williams *et al.*, 1989). Separation is incomplete and communication between different fascicles without a connective tissue barrier can occur at different points along the nerve length (Anderson & Hoyt, 1969). With the exception of the central retinal vessels within a central connective tissue core most blood vessels in the optic nerve are very small. These arterioles, venules and capillaries all run in the connective tissue septa. The arterial input to the nerve derives chiefly from the surrounding plial plexus (Sadun, 1998). The presence of these septa distinguishes the optic nerve from other CNS white matter tracts.

1.2 Optic neuritis

Optic neuritis is a common condition, having an incidence of 1-5 per 100,000/year (Rodriguez *et al.*, 1995; Jin *et al.*, 1998; MacDonald *et al.*, 2000). The incidence is highest in Caucasians (Optic Neuritis Study Group, 1991), in countries from higher latitudes (Jin *et al.*, 1998) and in spring (Jin *et al.*, 1999). The age group principally affected is 20-49 years, females being more commonly affected (Jin *et al.*, 1998). It usually presents as subacute unilateral loss of vision, although bilateral visual loss can occur, either simultaneous or sequential. Most cases of optic neuritis are due to idiopathic inflammatory demyelination, which may occur in isolation, or as a manifestation of multiple sclerosis (MS) (Optic Neuritis Study Group, 1997a). The causes of optic neuritis/MS are currently unknown. A genetic predisposition exits as suggested by the epidemiology of the condition, although the genetic component is not Mendelian and linkages have been proposed at chromosomes 1p, 6p, 10p, 17q and 19q (Compston & Coles, 2002). Environmental factors, in particular exposure to viruses, are probably also important although, as yet, no reliable candidate has been identified.

1.2.1 Presentation of optic neuritis

The typical presenting features of optic neuritis are listed in Table 1.3 (Perkin & Rose, 1979; Optic Neuritis Study Group, 1991; Beck, 1998). Optic neuritis usually presents as a painful subacute unilateral loss of vision, which progresses over a period of a few days to two weeks. In about 10% of cases no pain is reported. Phosphenes (photopsias) may be seen by the patient on eye movement (Davis *et al.*, 1976). Clearly, subclinical cases are very common as some patients present with Uhthoff's phenomenon (visual deterioration on getting warm, or during exercise) (Selhorst & Saul, 1995) and delayed visual evoked potentials (VEP) are not uncommon in early MS, even without a previous history of optic neuritis (Feinsod & Hoyt, 1975).

The maximal visual loss varies from minor blurring to no perception of light (NPL) in the diseased eye. Abnormal colour vision, reduced contrast sensitivity, visual field loss and a relative afferent pupillary defect (RAPD) are usually present in the affected eye (Levatin, 1959; Perkin & Rose, 1979; Optic Neuritis Study Group, 1991). Whilst any type of visual field defect may be seen, and the type of defect may vary over time, the

most characteristic finding is a central or para-central scotoma (Keltner *et al.*, 1993). The presence of an RAPD is a useful objective sign of a unilateral optic neuropathy, although it is not specific for optic neuritis. The lack of an RAPD may reflect mild clinical involvement in the affected eye, previous optic neuritis in the contralateral eye or subclinical optic neuropathy in the contralateral eye (Cox *et al.*, 1981).

Typical features of optic neuritis
20-49 age group
Female>male
Caucasian
Peri-ocular pain and pain on eye movement
Pain may precede onset of visual symptoms
Progressive visual loss over a few days
Phosphenes (photopsias) provoked by eye movement
Previous history of multiple sclerosis or previous neurological symptoms
Spontaneous improvement in vision
Uhthoff's phenomenon (usually not noticed until the recovery phase)
Fading of vision (usually not noticed until the recovery phase)
Pulfrich's effect (usually not noticed until the recovery phase)

Typical signs of optic neuritis
Decreased visual acuity
Decreased colour vision
Decreased contrast sensitivity
Any type of visual field defect
Relative afferent pupillary defect
Normal or swollen optic disc
Normal macula and peripheral retina
Uveitis or retinal phlebitis may be detected

Table 1.3: Typical symptoms and signs of optic neuritis.

Slit lamp examination occasionally reveals cells in the anterior chamber or vitreous but is usually normal (Lightman *et al.*, 1987). However, intermediate uveitis, pars planitis, panuveitis and granulomatous uveitis have all been associated with optic neuritis and MS. The uveitis may be present for some years before the onset of optic neuritis or MS (Malinowski *et al.*, 1993; Biousse *et al.*, 1999). The optic disc appears swollen in 36-58% of cases at presentation (Perkin & Rose, 1979; Optic Neuritis Study Group 1991). Small flame-shaped haemorrhages or marked optic disc swelling with cotton wool spots on the retina are seen occasionally. In cases where there is no disc swelling the condition is often labelled retrobulbar neuritis. Retinal examination is usually unremarkable. However, in a series of 50 consecutive patients with optic neuritis, peripheral retinal peri-phlebitis (peri-venous sheathing) was seen in six patients and fluoroscein leakage was seen in 10 (Lightman *et al.*, 1987). The presence of these abnormalities was linked with an increased risk for subsequent development of MS. Retinal peri-phlebitis can also be seen in MS in the absence of optic neuritis and on occasion it can be so severe as to cause retinal ischaemia and peripheral retinal neovascularisation (Vine, 1992). It is uncertain whether eyes affected by optic neuritis will show a higher incidence of retinal peri-phlebitis than eyes of MS patients which have not been affected by optic neuritis.

1.2.2 Fellow eye involvement

One of the most surprising aspects of unilateral optic neuritis is that asymptomatic deficits may be detected in the contralateral eye. In the North American Optic Neuritis Treatment Trial (ONTT) abnormalities were seen on visual acuity testing (logMAR >0.0) in 12.2%, contrast sensitivity testing (Pelli-Robson <1.67 log units) in 13.4%, colour vision testing (Farnsworth Munsell 100 Hue Test [FM 100] square root of error score >10.5) in 19.9% and visual field testing (Humphrey mean deviation <-3.0) in 46.3% of patients without a previous history of optic neuritis in that eye (Beck *et al.*, 1993b). The presence of fellow eye abnormalities was not associated with previous MS or lesions on brain MRI suggesting that dissemination of the disease was not responsible. The Japanese Multicentre Treatment Trial discovered abnormal visual fields in 53%, abnormal colour vision ($\geq$1 error using Ishihara pseudoisochromatic plates) in 7.7%, reduced contrast sensitivity at one or more spatial frequencies in 14.6% and critical flicker fusion frequency less than 35Hz in 16.1% of contralateral eyes

(Wakakura *et al.*, 1999b). Previous asymptomatic optic neuritis may account for some of these effects although the majority of fellow eyes with abnormalities in the ONTT recovered to normal after six months' follow-up suggesting that acute inflammation in the fellow optic nerve was responsible (Beck *et al.*, 1993b). Another possibility is that the effects are due to chiasmal or retro-chiasmal involvement in the symptomatic side. The ONTT demonstrated chiasmal or retro-chiasmal visual field defects in 13.2% of patients at least once during the first year of follow-up (Keltner *et al.*, 1994).

1.2.3 Recovery

In optic neuritis the pain rarely lasts more than a few days and vision deteriorates over a period of a few days to two weeks before spontaneously improving (Beck, 1998). In the placebo group of the ONTT 79% had begun to show signs of improvement ($\geq$ one line on chart) within three weeks of onset, and 93% by five weeks (Beck, 1998). The initial period of recovery is rapid. In one study (Perkin & Rose, 1979), at three weeks after onset ~40% had a visual acuity of counting fingers or worse, ~30% were 6/18 to 6/60 and ~30% were 6/12 or better. At four weeks ~17% were counting fingers or worse, ~33% were 6/18 to 6/60 and ~50% were 6/12 or better. Amongst patients who were followed for at least six months 85.7% reached a final visual acuity of between 6/6 and 6/12, 9.6% were between 6/18 and 6/60, and 4.7% between counting fingers and NPL. The mean period of recovery to 6/6 amongst those who reached this level was 8.1 weeks, which was not affected by the severity of visual impairment at presentation. In a different series (Bradley & Whitty, 1967), vision had improved to normal (defined as Snellen acuity of 6/9 or better) in half of the patients after one month, and in three-quarters by six months. The recovery here was slower in those with poor vision at onset (6/60 or worse).

For most patients in the ONTT, recovery of visual acuity was nearly complete by five weeks after onset of symptoms. Further improvement however, was noted even up to one year after onset. The mean visual acuity at one year after entry into the study was 20/15, with less than 10% having a visual acuity worse than 20/40 (Beck, 1998). The amount of visual improvement after optic neuritis does not seem to be related to age, gender, ethnicity, concurrent presence of multiple sclerosis, or abnormalities on brain magnetic resonance imaging (Beck *et al.*, 1994). Severity of the initial visual loss in the

ONTT was related to final visual outcome, although still most patients recovered well. Of 187 patients with visual acuity worse than 20/200 on admission to the ONTT, only 6% had this level of acuity or worse at 6 months. Of 28 patients with light perception only or worse, 64% recovered to 20/40 or better (Beck & Cleary, 1993b). In another patient group, of 12 patients who presented with NPL in the diseased eye, five recovered to 20/20 or better, three to 20/40 or better and four had peripheral recovery but dense central scotomata and visual acuities of less than 3/60 (Slamovits *et al.*, 1991).

Other visual parameters tend to improve in parallel with the improvement in visual acuity, but subjective residual deficits are common (Beck, 1998). In one study of 58 patients one year after untreated optic neuritis 59% reported that their vision had not returned to normal, although only 5 (8.0%) patients had a visual acuity in the diseased eye worse than 6/9 (Frederiksen *et al.*, 1997). The vision after optic neuritis may show marked variation during the day and from one day to the next (Wall *et al.*, 1998) and may deteriorate in specific situations, for example Uhthoff's phenomenon (Selhorst & Saul, 1995) and fatigue or fading of vision (Enoch *et al.*, 1979). Pulfrich's phenomenon (misperception of the trajectory of moving objects) is also occasionally seen (Slagsvold, 1978).

The optic disc usually becomes pale, either diffusely or more often in the temporal region, despite improvements in vision (Beck, 1998). Abnormalities in the retinal nerve fibre layer (RNFL) have also been seen following optic neuritis and reflect axonal loss (Steel & Waldock, 1998). The RAPD may disappear on recovery although, particularly in cases where there is poor recovery, it may be persistent.

1.2.4 Differential diagnosis

The differential diagnosis of optic neuritis with appropriate investigations is considered in Table 1.4. Misdiagnosis of optic neuritis has been reported in clinical trials. Out of 457 patients enrolled in the ONTT, three were subsequently diagnosed as having anterior ischaemic optic neuropathy, two had compressive lesions (one ophthalmic artery aneurysm and one pituitary tumour) and two had connective tissue diseases in addition to optic neuritis (Optic Neuritis Study Group, 1991; Beck *et al.*, 1992).

Diagnosis	Usual clinical features	Tests to consider
Corticosteroid responsive optic neuropathies Sarcoidosis Systemic lupus erythematosus Autoimmune optic neuritis Chronic relapsing inflammatory optic neuropathy Optic peri-neuritis Behçet's disease Neuromyelitis optica (Devic's disease)	Progressive severe visual loss May be very painful Often bilateral (simultaneous or sequential) Isolated or as part of a multi-system disorder More common in Africans or Afro-Caribbeans (sarcoidosis) Corticosteroid dependent	Contrast-enhanced MRI orbits and brain Lumbar puncture ANA serum ACE CXR ^{67}Gallium scan Biopsy of accessible tissue (sarcoid)
Other inflammatory optic neuropathies Post-infectious Post-vaccination Acute disseminated encephalomyelitis Neuroretinitis	Bilateral and simultaneous Often in childhood Usually excellent prognosis Swollen disc and macular star Spontaneous recovery	Contrast-enhanced MRI orbits and brain Lumbar puncture Bartonella, borrelia and syphilis serology
Compressive optic neuropathies Primary tumours, eg meningiomas, gliomas and pituitary tumours Metastases Tuberculomas Thyroid ophthalmopathy Arterial aneurysms Sinus mucocoeles	Painless (rarely painful, eg aneurysms and mucocoeles) Progressive visual loss Optic atrophy at presentation Past history of, or evidence for primary tumour (metastases)	Contrast-enhanced CT or MRI orbits and brain Biopsy if appropriate
Infectious optic neuropathies Syphilis Tuberculosis Lyme disease Viral optic neuritis	Progressive visual loss with exposure to infectious agent Severe optic disc oedema Cellular reaction in vitreous	Appropriate serology Lumbar puncture CXR Tuberculin test
Ischaemic optic neuropathies Anterior ischaemic optic neuropathy Posterior ischaemic optic neuropathy (PION) Giant cell arteritis (GCA) Diabetic papillopathy	Usually older age group Sudden onset Painless (except GCA) Swollen optic disc (except PION) Altitudinal field defect	ESR
Toxic and nutritional optic neuropathies Vitamin B_{12} deficiency Tobacco-alcohol amblyopia Methanol intoxication Ethambutol toxicity Cuban and Tanzanian epidemic optic neuropathies	Bilateral and symmetrical Painless Poor prognosis	Serum vitamin B_{12}
Inherited optic neuropathies Leber's hereditary optic neuropathy	Family history Sequential (or simultaneous) bilateral painless visual loss	Genetic testing for Leber's mutation
Ocular causes Posterior scleritis Maculopathies and retinopathies including and central serous retinopathy Big blind spot syndrome and acute zonal occult outer retinopathy (AZOOR)	Severe pain Less visual symptoms Painless Metamorphopsia Preserved colour vision Visual field loss + photopsias Normal fundus	B mode ultrasound of orbits Electroretinogram Fluoroscein angiogram Electroretinogram

ACE = angiotensin converting enzyme	ANA = antinuclear antibodies
CT = computerised tomography	CXR = chest radiograph
ESR = erythrocyte sedimentation rate	MRI = magnetic resonance imaging
Metamorphopsia = distorted vision	Photopsia = spontaneous showers of light in vision

Table 1.4: Differential diagnosis of optic neuritis (Rosenberg *et al.*, 1984; Kansu *et al.*, 1989; Miller *et al.*, 1995; Dunya *et al.*, 1996; Miller & Newman, 1998; McCluskey *et al.*, 1999; Zajicek *et al.*, 1999; Acheson, 2000; Gass, 2000; Eggenberger, 2001; Purvin *et al.*, 2001; Zacks & D'Amico, 2001; Kidd *et al.*, 2002).

In a later study, out of 102 patients enrolled 17 were later excluded due to misdiagnosis (Wakakura *et al.*, 1999b). The final diagnoses in these 17 were: rhinogenic optic neuropathy (sinus mucocoeles) (n=9); brain tumour (n=3); ischaemic optic neuropathy (n=2); Leber's hereditary optic neuropathy (n=1); nutritional optic neuropathy (n=1); age-related macular degeneration (n=1).

Presentation with severe pain that restricts ocular movements or wakes the patient from sleep should alert to the possibility of posterior scleritis (McCluskey *et al.*, 1999) or an infective or granulomatous optic neuropathy, such as sarcoidosis or chronic relapsing inflammatory optic neuropathy (CRION) (Zajicek *et al.*, 1999; Kidd *et al.*, 2002). Visual loss in infective and granulomatous optic neuropathy is usually more severe than in typical optic neuritis and does not spontaneously improve. In cases of optic neuropathy due to sarcoidosis there are usually systemic features of the disease that can be detected although it may be restricted, at least initially, to the optic nerve (Zajicek *et al.*, 1999).

Children or adults may present with a typical history for optic neuritis but, on fundus examination, optic disc swelling and a macular star is seen leading to the diagnosis of neuroretinitis. This condition is usually idiopathic but may be associated with cat scratch disease, Lyme disease, syphilis, toxocariasis, toxoplasmosis or histoplasmosis (Eggenberger, 2001). Prognosis for recovery is good and there is no risk of developing MS following it (Beck, 1998). Sarcoid optic neuropathy, if it affects the anterior optic

nerve can cause disc swelling and a macular star (Ray & Gragoudas, 2001), but the clinical course is more in keeping with that for sarcoidosis than typical neuroretinitis.

1.2.5 Investigations

Generally, optic neuritis can be diagnosed on clinical grounds (Table 1.3). If any warning signs or atypical features for optic neuritis occur leading to suspicion of an alternative diagnosis (Table 1.5) then prompt investigations are required (Lee *et al.*, 2000; Eggenberger, 2001).

Optic atrophy on presentation without previous optic neuritis or multiple sclerosis
Severe optic disc oedema with vitreous reaction
Optic disc haemorrhage
Bilateral loss of vision
Previous history of neoplasia
African or Afro-Caribbean patients with vision <6/12 and no early recovery
Loss of vision to no perception of light with no early recovery
Painless loss of vision to <6/60 with no early recovery
Severe or persistent pain for >2 weeks since onset
Visual loss progressing for >2weeks since onset of visual symptoms
Lack of any recovery >3 weeks after onset of visual symptoms
Worsening of vision after withdrawal of corticosteroids

Table 1.5: Warning signs in the presentation of optic neuritis that should prompt further investigation to rule out alternative diagnoses.

The best management of some conditions, such as optic nerve compression by a sinus mucocoele or a tuberculous or granulomatous optic neuropathy, requires appropriate treatment within days of presentation as a significantly worse visual outcome may result if treatment is delayed. Thus, an expectant approach must not be adopted where clinical features are atypical.

Combined ophthalmological and neurological services is recommended to improve diagnostic accuracy and early review is important to ensure that visual recovery, either

subjectively or objectively, has started to occur. A case of optic neuropathy in which no spontaneous recovery at all has occurred is very unlikely to be optic neuritis.

Investigations should be guided by the clinical presentation (Table 1.4). It is important to have ready access to imaging facilities. Contrast-enhanced high resolution CT with fine cuts through the orbits will show up most compressive lesions (Acheson, 2000). Short *tau* inversion recovery (STIR) or fat-saturated fast spin echo (FSE) MRI is preferable in that it does not involve ionising radiation and can also demonstrate any intrinsic optic nerve lesions as in optic neuritis (Figure 1.1) (Gass & Moseley, 2000). Experimental study of optic neuritis with MRI will be considered in the subsequent chapters.

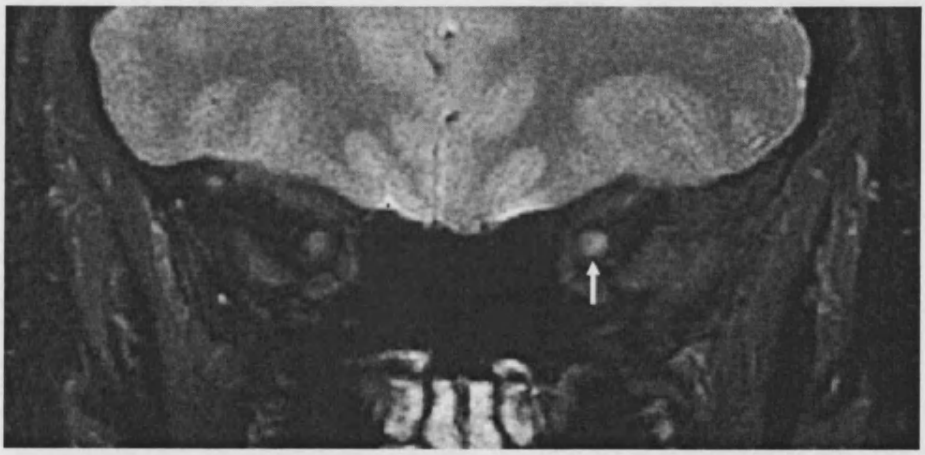

Figure 1.1: Fat-saturated proton density FSE MRI in left-sided acute optic neuritis (diseased optic nerve arrowed).

The VEP may not be helpful in differentiating between different causes of optic neuropathies in the acute phase (Acheson, 2000), although the combination of VEP with pattern electroretinogram (PERG) may be useful in differentiating macular from optic nerve disorders. In retinal disorders both the P50 (early) and N95 (late) components of the PERG are abnormal, whereas in optic nerve disorders only the N95 component is abnormal (Acheson, 2000; Holder, 2001). In acute optic neuritis however, the P50 may be reduced as well in the acute phase, which normalises during recovery (Holder, 2001). In clinical practice, the presence of a delayed but well preserved P100 wave of the VEP is most useful in confirming a diagnosis of optic neuritis if the presentation is delayed,

or in supporting a diagnosis of MS by demonstrating dissemination in space in appropriately selected patients (Halliday *et al.*, 1972; Halliday *et al.*, 1973b). The insights that VEP studies have given about the pathophysiology of optic neuritis will be considered later.

If a corticosteroid responsive optic neuropathy is suspected then both conventional and gadolinium-enhanced MRI of the orbits and brain should be performed. In sarcoidosis, CRION and optic peri-neuritis optic nerve sheath enhancement is typical (Carmody *et al.*, 1994; Purvin *et al.*, 2001; Kidd *et al.*, 2002). In addition, in sarcoidosis basal meningeal enhancement and enhancing cerebral lesions may be seen (Carmody *et al.*, 1994). White matter lesions on both T_2-weighted and gadolinium-enhanced MRI may be non-specific, occurring in both MS and other inflammatory conditions, although the former is much more common. The significance of white matter on T_2-weighted scans requires a careful consideration of the site and shape of the lesions and the age of the patient, recognising that age-related changes due to small vessel disease should not be misinterpreted as evidence for demyelination (Miller *et al.*, 1998).

Serological and other evidence for sarcoidosis, vasculitis and syphilis should be sought and tuberculosis considered in appropriate patients. In cases of suspected infectious or corticosteroid responsive optic neuropathy a lumbar puncture should also be performed. The CSF examination can look for infections, hypercellularity, a raised protein level and local or systemic production of oligoclonal bands of immunoglobulins to try to help differentiate between demyelinating optic neuritis and other causes of inflammatory optic neuritis. In optic neuritis there may be no oligoclonal bands, or local intrathecal synthesis of immunoglobulins (unmatched bands compared with serum). In CRION, sarcoidosis, vasculitis or acute disseminated encephalomyelitis there may be no oligoclonal bands or systemic production of immunoglobulins (matched oligoclonal bands in both CSF and serum) (Zajicek *et al.*, 1999; Kidd *et al.*, 2002).

1.2.6 Treatment of optic neuritis

A number of therapeutic trials have attempted to improve the prognosis with respect to visual outcome in typical optic neuritis. Early, observational studies suggested that corticosteroids might be effective, although this view was controversial (Perkin & Rose,

1979). Subsequent placebo-controlled trials of corticosteroids have been carried out and these are summarised in Table 1.6.

A meta-analysis of these trials showed that corticosteroids reduced the number of patients without clinical improvement at 30 days (odds ratio 0.60, range 0.42-0.85) but did not cause long-term improvement in visual outcome (odds ratio 0.96, range 0.71-1.31) (Brusaferri & Candelise, 2000). When the presenting visual acuity was 20/40 or better, then corticosteroids conferred no benefit in the ONTT (Beck *et al.*, 1992).

There has been a suggestion that the failure to see a long-term beneficial effect in the treatment trials may be because the corticosteroids were given too late to provide neuroprotection (Compston & Coles, 2002). Treatment trials in the hyperacute phase are required to address this issue.

Corticosteroids can cause significant side-effects. Common minor side-effects reported include insomnia, mild mood changes, stomach upsets, facial flushing, acne, oedema and weight gain (Beck *et al.*, 1992; Sellebjerg *et al.*, 1999). More serious side-effects seen in the IVMP arm (n=151) of the ONTT include one patient developing psychotic depression and another developing pancreatitis (Beck *et al.*, 1992). There have also been reports of avascular necrosis (osteonecrosis) of the femoral head (McKee *et al.*, 2001) and deaths in children due to chicken pox following short-term corticosteroid therapy (Committee on Safety of Medicines, 1994; Reynolds *et al.*, 1996).

Study	Entry criteria	Treatment groups	Visual outcome	Comments
Rawson *et al.*, 1966. Rawson & Liversedge, 1969.	Treatment to commence within 10 days of onset of symptoms.	1) IM ACTH 40 units/day for 30 days (n=25). 2) IM placebo for 30 days (n=25).	Faster recovery of VA in treatment group ($p<0.01$ at 30 days) but no effect at 1 year.	All treated patients pain-free by 2 days. Placebo group pain-free by 2 weeks.
Bowden *et al.*, 1974.	Any patient regardless of delay to the initiation of treatment.	1) IM ACTH 40 units/day for 30 days (n=27). 2) IM placebo for 30 days (n=27).	No significant treatment effect for any visual parameter at any time up to 2 years.	Mean delay to treatment of 16.7 days (ACTH group) and 18.5 days (controls).
Gould *et al.*, 1977.	Treatment to commence within 10 days. VA <6/9, abnormal colour vision, RAPD and central scotoma.	1) Retrobulbar triamcinolone 40mg (n=31). 2) No injection (n=30).	Faster rate of recovery of VA in the treatment group ($p=0.1$ at 1 week). No difference seen at 2 and 6 months.	Single blind.
Trauzettal-Klosinski *et al.*, 1993.	Randomisation within 21 days and before recovery. RAPD and ≥2 of: abnormal VA; central scotoma; abnormal VEP and/or flicker test.	1) Oral MP tapering dose over 24 days starting at 100mg/day (n=16). 2) Oral thiamine 100mg/day for 24 days (n=34).	Trend for all the parameters tested to recover faster in the treated group but with no treatment benefit at 12 months.	Not all patients blinded to treatment.
Optic Neuritis Treatment Trial Beck *et al.*, 1992, 1993a, Beck & Cleary 1993a, Beck 1995, Optic Neuritis Study Group, 1997a.	Treatment to commence within 8 days of onset of symptoms. RAPD and abnormal visual field in affected eye.	1) Oral prednisone 1mg/kg/day for 14 days (n=156). 2) IVMP 250mg QDS for 3 days then 1mg/kg/day prednisone for 11 days (n=151). 3 days of dose tapering in both treatment groups. 3) Oral placebo for 14 days (n=150).	Median VA 6/7.5 by day 4 in IVMP group compared with day 15 in the other two groups. Minimal treatment benefit at 30 days and no effect seen after 1 and 5 years. No treatment benefit from IVMP if VA ≥6/12. No benefit shown for prednisone.	No IV placebo group. Increased risk of recurrence of ON after prednisone at 5 years ($p=0.003$ vs IVMP, $p=0.004$ vs placebo). Decreased 2-year (ARR 0.34, 95% CI 0.16 to 0.74) but not 3-year rate of CDMS after IVMP.
Kapoor *et al.*, 1998.	Randomisation within 30 days. VA ≤6/9. Optic nerve lesions classified as long (≥15mm) or short on STIR MRI.	1) IVMP 1g/day for 3 days with no tapering dose (n=33). 2) IV saline for 3 days (n=33).	Trend for increased rate of recovery of VA after IVMP in all patients and in those with long lesions. No effect seen at 6 months.	No correlation between initial VA and initial lesion length. Treatment did not affect 6 month lesion length on MRI.
Sellebjerg *et al.*, 1999.	Treatment to commence within 28 days of onset of symptoms. VA ≤0.7.	1) Oral MP 500mg/day for 5 days with a tapering dose for 10 days (n=30). 2) Oral placebo for 15 days (n=30).	Improved spatial vision at 3 weeks in treatment group ($p=0.03$). No benefit after 8 weeks and 1 year.	MP did not affect the conversion to CDMS at 1 year ($p=0.8$).
Wakakura *et al.*, 1999a.	Treatment to commence within 14 days of onset of symptoms. RAPD in the affected eye.	1) IVMP 1g/day for 3 days then oral taper for 7-10 days (n=33). 2) Mecobalamin 500μg/day IV for 3 days then orally for 7 days (n=33).	Faster visual recovery for all parameters tested after IVMP but no treatment effect seen after 12 weeks and 1 year.	Mecobalamin treatment used for comparison as placebo treatment considered unethical in Japan.

ACTH = adrenocorticotrophic hormone (corticotrophin)
ARR = adjusted rate ratio
CDMS = clinically definite multiple sclerosis
CI = confidence intervals
IM = intramuscular
IV = intravenous
IVMP = intravenous methylprednisolone
MP = methylprednisolone
ON = optic neuritis
QDS = 4 times per day
VA = visual acuity

Table 1.6: Randomised controlled trials of corticosteroids in acute unilateral optic neuritis.

(i) Recommendations for management

The recommendations of the Quality Standards Subcommittee of the American Academy of Neurology were that "oral prednisone in doses of 1mg/kg/day has no demonstrated efficacy in the recovery of visual function in acute monosymptomatic optic neuritis, and therefore is of no proven value in treating this disorder. Higher dose oral or parenteral methylprednisolone or adrenocorticotrophic hormone may hasten the speed and degree of recovery of visual function in persons with in acute monosymptomatic optic neuritis. There is, however, no evidence of long-term benefit for visual function. The decision to use these medications to speed recovery but not to improve ultimate visual outcome should therefore be based on other non-evidence-based factors such as quality of life, risk to the patient, visual function in the fellow eye, or other factors that the clinician deems appropriate" (Kaufman *et al.*, 2000).

When treatment is instigated 1g/day IVMP for three days has become the preferred option (Trobe *et al.*, 1999). For convenience, this tends to be given as a single daily dose which enables outpatient treatment. In the United States of America an oral taper of prednisolone following this remains popular, although it is less commonly used in the United Kingdom and Europe (Barnes, 2000). The rationale for the use of an oral taper is concern regarding suppression of the hypothalamic-pituitary-adrenal axis, although with the short treatment regimens used fast recovery of the axis is seen and the oral taper should not normally be needed (Wenning *et al.*, 1994). Another concern is that after cessation of the IVMP worsening of symptoms may occur with recrudescence of inflammation as has been suggested from serial gadolinium-enhanced MRI studies of

the brain in MS (Miller *et al.*, 1992), however there were no reports of recovery followed by deterioration of vision in the one study that did not use an oral taper (Kapoor *et al.*, 1998). Appropriate precautions should be taken before starting treatment and all patients should be warned of the possible side-effects (British National Formulary, 2003).

If a corticosteroid responsive optic neuropathy is suspected then treatment should be with IVMP 1g/day for three day followed by 1mg/kg/day oral prednisolone. This is then slowly reduced by 10mg per month. If a relapse occurs on reducing the dose then high-dose treatment should be re-instigated and a corticosteroid-sparing agent such as azathioprine started before reducing the dose again. Protocols for osteoporosis prophylaxis need to be followed. Although these cases are rare they need to be recognised as management is entirely different from typical demyelinating optic neuritis in that early and continued treatment with corticosteroids is necessary to ensure a good visual outcome (Kidd *et al.*, 2002). In optic neuritis associated with vasculitis (eg in systemic lupus eythematosus) the visual outcome may be improved if cyclophosphamide is given at an early stage but there are no published data on this.

At present there are no treatments that can reverse established poor visual outcome following typical optic neuritis. An early report suggested that intravenous immunoglobulin (IVIG) may be helpful in promoting remyelination and improving vision (van Engelen *et al.*, 1992). A larger subsequent trial randomised 55 MS patients with persistent visual acuity loss after optic neuritis to receive either 0.4g/kg IVIG daily for five days followed by three single infusions monthly for three months, or placebo (Noseworthy *et al.*, 2001). The trial was terminated early due to negative results. Visual acuity was unchanged after six months' follow-up (p=0.766), although there was a trend for improvement after 12 months (p=0.132). The improvement was however modest, amounting to a mean difference of two letters on the logMAR acuity chart with no improvement in VEP latency. The lack of significant improvement in these patients may imply that IVIG does not induce remyelination or that irreversible disability may be largely a result of axonal degeneration. Potential future therapies could include neuro-protective agents (Guy, 2000), strategies to induce remyelination (Compston & Coles, 2002), and optic nerve transplantation (Adachi-Usami, 2001), although all are at this time experimental.

(ii) Management of bilateral optic neuritis

In cases of bilateral (simultaneous or early sequential with poor initial recovery) optic neuritis then patients should be investigated for the possibility of a corticosteroid responsive optic neuropathy. Treatment should be with parenteral followed by oral corticosteroids to hasten functional visual recovery. Patients should be followed closely as the oral prednisolone is tapered off to ensure that worsening vision does not occur.

(iii) Management of childhood optic neuritis

Childhood cases are more commonly bilateral and simultaneous (Kriss *et al.*, 1988), usually following viral infections (Morales *et al.*, 2000). Visual recovery after optic neuritis in childhood is usually good. In one cohort 78% had a visual acuity of 6/6 or better after a mean follow-up of 8.8 years (Kriss *et al.*, 1988). Another series reported better prognosis for unilateral optic neuritis than bilateral cases, although many of the bilateral cases suffered recurrent attacks of visual loss (Morales *et al.*, 2000). Prompt response to corticosteroid therapy has been reported although there have been no treatment trials of corticosteroids in childhood optic neuritis (Brady *et al.*, 1999).

1.2.7 Late outcome and the risk of recurrence of optic neuritis

The cumulative probability of having recurrent optic neuritis after five-year follow-up in the ONTT was 19% for the affected eye, 17% for the unaffected eye and 30% for either eye (Optic Neuritis Study Group, 1997b). The risk of recurrence was twice as high in patients who had developed MS and was also higher in those who were initially treated with oral prednisolone. The cumulative probability of recurrence at five years was 41% in the prednisolone group, 25% in the IVMP group (p=0.003) and 25% in the placebo group (p=0.004). The increased risk was apparent throughout the period of follow-up in the study although there is not a convincing explanation for the underlying mechanism behind this association.

Ten-year follow-up figures have recently been reported for the ONTT (Optic Neuritis Study Group, 2004). The retention of patients in the study was very good with 319 out of the original 454 participants being seen. The median visual acuity in the originally

affected eye at 10 years was logMAR -0.06 (Snellen 20/16) with only 33% having a visual acuity of worse than 0.0 (Snellen 20/20). Median Pelli-Robson contrast sensitivity score was 1.65 (33% <1.65) and median 30-2 Humphrey perimetry mean deviation was -1.25 (27% <-3.00dB). Recurrence of optic neuritis occurred in 35% (48% in those who had developed MS and 24% in those who had not). Only six patients (2%) had visual acuity of less than 20/40 in each eye, usually due to recurrence of the disease. The long-term visual prognosis following optic neuritis is therefore very good.

1.2.8 The association between optic neuritis and multiple sclerosis

The association between optic neuritis and MS has been apparent for many years (Perkin & Rose, 1979). MS is a clinical diagnosis based on the dissemination of CNS lesions in time and space i.e., the occurrence of a second clinical episode at a different site in the CNS. CDMS can be diagnosed when the episodes are confirmed by a Neurologist without the need for supporting investigations (Poser *et al.*, 1983). The risk of developing MS increases with longer follow-up. In one series the 10 year risk of CDMS was 39%, the 20 year risk was 49%, the 30 year risk was 54% and the 40 year risk was 60% (Rodriguez *et al.*, 1995). The risk is increased in females (Rizzo III & Lessell, 1988), (Sandberg-Wollheim *et al.*, 1990), in those with retinal vascular abnormalities (Lightman *et al.*, 1987), in those who are HLA-DR2 positive (Sandberg-Wollheim *et al.*, 1990; Hauser *et al.*, 2000), in those who have oligoclonal bands on CSF examination (Cole *et al.*, 1998; Sandberg-Wollheim *et al.*, 1990), and in those with serum antimyelin antibodies (Berger *et al.*, 2003). The risk of MS developing following childhood and bilateral simultaneous optic neuritis is much lower (Parkin *et al.*, 1984; Kriss *et al.*, 1988).

The strongest predictor for the development of MS, that appears to exceed the factors just mentioned, is the presence of asymptomatic white matter lesions on brain MRI. The five-year risk of CDMS in the ONTT was 16% in 202 patients with no brain lesions, but was 51% in the 89 patients with three or more lesions on entry to the study (Optic Neuritis Study Group, 1997a). The 10-year risk of CDMS in the ONTT was 38%; 22% in 191 patients with no initial brain lesions, rising to 57% in 28 patients with nine or more baseline lesions (Optic Neuritis Study Group, 2003). In a different cohort

CDMS developed in 37 out of 71 patients (52%) with one or more lesion after 10 years while no patient with a normal MRI developed CDMS (Ghezzi *et al.*, 1999). The risk of early MS developing increases if asymptomatic spinal cord lesions are present at baseline in addition to brain lesions, reflecting increased dissemination in space in these patients. In a study of patients with clinically isolated syndromes suggestive of demyelination (CIS) (i.e. optic neuritis, spinal cord and brain stem syndrome patients) 10/21 (48%) patients with abnormal brain and spinal cord imaging developed MS at one year compared to 3/17 (18%) with brain lesions alone (Brex *et al.*, 1999). The risk of MS within one year also increased if new brain lesions were detected on repeat brain imaging after three months. MS occurred in 12/21 (57%) of patients with new lesions on T_2-weighted imaging and 7/11 (64%) of patients with new gadolinium-enhancing lesions, but only 1/20 (5%) of patients who had abnormal baseline imaging and no new lesions at three months.

Recently, The International Panel on MS Diagnosis published diagnostic criteria for MS ("McDonald criteria") which suggested that MRI evidence of dissemination of CNS lesions in time and space was sufficient for the diagnosis of MS even before clinical dissemination had occurred (Figure 1.2) (Table 1.7) (McDonald *et al.*, 2001).

These criteria clarify the role of MRI in clinical practice but have not been without controversy, principally regarding the reliance on imaging data when these findings on MRI can be non-specific (Poser & Brinar, 2001). However, when they have been applied to a cohort of CIS patients, the use of the criteria with repeat imaging after three months has shown a 93% specificity and an 83% positive predictive value for the development of CDMS at three years (Dalton *et al.*, 2002).

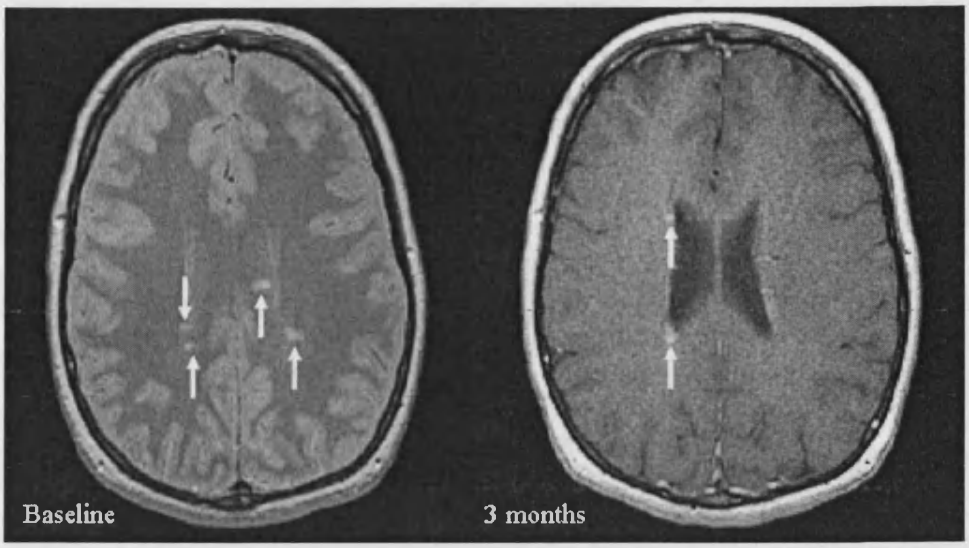

Figure 1.2: Left - baseline proton density weighted FSE MRI (left) of a 37 year-old woman with left optic neuritis demonstrating asymptomatic brain lesions (arrowed). Right – gadolinium-enhanced T_1-weighted spin echo image taken three months later demonstrating two new enhancing lesions (arrowed) sufficient to give a diagnosis of MS using the McDonald criteria.

Even if multiple sclerosis does develop following optic neuritis the prognosis for disability is usually good, it being more often associated with a benign course of the disease (odds ratio 1.73, 95% CI 1.27-2.35) (Ramsaransing *et al.*, 2001). After five years only 17 of the 105 patients who had developed CDMS (4% of the entire cohort) in the ONTT had an expanded disability status scale (EDSS) score of three or more, and only five had an EDSS of six or more, although this did include one patient who died from MS (Optic Neuritis Study Group, 1997a). As well as predicting an increased risk for the development of MS, brain MRI lesion load can also help to predict the probability of developing disability following a CIS. In a cohort of patients followed for 14 years following a CIS, EDSS correlated with both baseline lesion volume (r=0.48) and change in lesion volume in the first five years (r=0.61), suggesting that early inflammatory activity in MS is related to the later development of disability (Brex *et al.*, 2002).

MRI dissemination in space consisting of 3 out of 4 of the following:

1. One gadolinium-enhancing lesion or nine T_2 hyperintense lesions if no enhancing lesion.
2. At least one infratentorial lesion.
3. At least one juxtacortical lesion.
4. At least three periventricular lesions.

One spinal cord lesion may be substituted for one brain lesion.

or

Two or more MRI-detected lesions consistent with MS plus positive CSF (oligoclonal bands different from any such bands in the serum and/or the presence of an elevated IgG index)

and

MRI dissemination in time

First scan 3 or more months after the clinical event.

1. A gadolinium-enhancing lesion (not at the site implicated in the first clinical event) is sufficient evidence to demonstrate dissemination in time.
2. If there are no gadolinium-enhancing lesions a second scan is required more than 3 months later. A new T_2 or gadolinium-enhancing lesion is sufficient evidence for dissemination in time.

First scan less than 3 months after the clinical event.

1. A second scan done 3 or more months after the optic neuritis showing a gadolinium-enhancing lesion is sufficient evidence for dissemination in time.
2. If no enhancing lesion is seen on the second scan, a further scan performed not less than 3 months after the previous scan that shows a new T_2 or enhancing lesion will suffice.

or

A second clinical attack

Table 1.7: Diagnostic criteria to allow multiple sclerosis to be diagnosed following a monosymptomatic clinical event such as optic neuritis (McDonald *et al.*, 2001).

1.2.9 Treatments to delay the onset of multiple sclerosis after optic neuritis

Are there any treatments that alter the risk for the development of MS following clinically isolated optic neuritis? *Post hoc* analysis from the ONTT suggested that there was a decreased risk for the development of CDMS in the IVMP group (10 patients, 7.5%) compared to the other two groups (19 patients, 14.7% in the prednisolone group and 21 patients, 16.7% in the placebo group) after a follow-up period of two years in

patients with clinically isolated optic neuritis on entry to the study (n=389) (Beck *et al.*, 1993a). The adjusted rate ratio for the development of CDMS in IVMP group was 0.34 (95% CI 0.16 to 0.74) compared with the placebo group. Most of the treatment effect was seen in patients with an abnormal brain MRI on entry to the trial. The findings however, were based on a retrospective analysis with an open-label treatment (there was no intravenous placebo arm) with only small numbers developing MS. Also, data were not available for 50 of the patients, which may have had a confounding effect. The beneficial effect was lost by three years with a cumulative incidence of CDMS of 17.3% in the IVMP group, 24.7% in the prednisolone group and 21.3% in the placebo group (Beck, 1995). The significance of these findings remains uncertain. If benefit from IVMP exists to delay the onset of CDMS it is short-lived and does not affect either the eventual risk of CDMS or the development of disability (Optic Neuritis Study Group, 1997a).

Two recent trials have addressed whether β-interferon can slow down the progression from CIS to CDMS. The CHAMPS study recruited 383 patients following their first demyelinating event (192 with optic neuritis) who, in addition, had two or more clinically silent brain lesions on MRI (Jacobs *et al.*, 2000). Half the patients received once weekly 30μg intramuscular interferon β-1a and half placebo injections. The trial was stopped early after an interim analysis since the cumulative probability of the development of CDMS during the three-year follow-up period was significantly lower in the interferon group than in the placebo group (rate ratio 0.56; 95% CI 0.38-0.81; p=0.002). There was also a relative reduction in new lesion activity on MRI in the interferon group (p<0.001). The ETOMS study took a similar group of patients (n=309, 98 with optic neuritis) but four asymptomatic white matter lesions (or three if one was enhancing after administration of gadolinium) were required for entry (Comi *et al.*, 2001). Half the patients received once weekly subcutaneous 22μg interferon β-1a and half placebo injections. After two years the odds ratio for conversion to CDMS was 0.61 (95% CI 0.37-0.99; p=0.045) in the treatment group compared to the placebo group, again with less new lesion formation in the treatment group (p<0.001). The treatments were well tolerated with no excess major adverse events due to the interferons. Significant minor adverse events included influenza-like symptoms (both trials), depression (CHAMPS) and injection site reactions (ETOMS).

These results are not surprising because in essence the interferons are reducing the relapse rate, which is a well-known effect from the previous studies in relapsing remitting MS (RRMS). These patients were at high risk for the development of MS in view of the abnormal baseline brain imaging. Pooling the results with results from studies in RRMS, the interferons reduce the relapse rate by a third. The annual relapse rate in these patients is approximately 0.5/year. Interferon treatment therefore has to be given for six years to prevent one relapse in this group of patients (Ebers, 2001). There are also no long-term data that can say whether, by reducing inflammatory activity, the interferons prevent the development of disability due to MS.

(i) Recommendations for management

Brain MRI at presentation can give an indication for the prognosis for the development of MS, and if a high lesion load is present then this gives further information concerning the probability of later disability, although the association is not strong. A significant number of patients with CIS and brain lesions have a benign long-term course (Brex *et al.*, 2002).

In the UK, the Association of British Neurologists' guidelines currently recommend disease modifying drugs (DMDs) only in established MS, therefore brain imaging at presentation with optic neuritis will not alter initial treatment decisions. In the absence of evidence that earlier treatment of patients with CIS has a greater long-term effect on prognosis for disability, current UK practice is to treat only ambulant patients with clinically active, established RRMS, or secondary progressive MS (SPMS) with superimposed disabling relapses. In countries where DMDs are available for use after a CIS if asymptomatic brain lesions are present, baseline brain imaging may be useful to guide the treatment decision.

Repeat imaging of CIS patients may, however, establish an earlier diagnosis using the McDonald criteria. In some patients this will be worthwhile in order to enable a more informed discussion of diagnosis and prognosis. Further studies are needed to determine whether the subgroup of CIS patients who develop MS using the McDonald criteria will benefit usefully from long-term treatment with DMDs.

It is important that the diagnosis of optic neuritis is secure before treatment with a DMD is commenced as there has been a report of three patients with anterior ischaemic optic neuropathy and incidental white matter lesions of presumed vascular origin who were commenced on interferon β-1a on the erroneous assumption that the cause of visual loss was optic neuritis (Horton, 2002).

1.2.10 Optic neuritis pathology

There are a limited number of studies on the pathology of optic neuritis, due to the absence of autopsy material from the acute inflammatory phase of the illness. This reflects the fact that optic neuritis generally affects a young patient group and the lack of data from biopsy of lesions, unlike the situation with MS lesions in the brain. Human autopsy material has been available from patients with established multiple sclerosis, but the studies that have used this need to be interpreted with caution. The results probably represent both episodes of acute optic neuritis as well as possible insidious damage either as part of MS, or as a long-term consequence of acute episodes.

Samuel Gartner in 1953 published the first systematic study of the optic nerve in MS (Gartner, 1953). He examined under the light microscope the optic nerves of 10 MS patients who had had visual symptoms in life. Six of them had had definite or probable optic neuritis. He described atrophy of nerve fibres, particularly in the papillomacular bundle but also extending to other areas, as well as increases in glial cells, fibroblasts and lymphocytes. Atrophy of nerve fibres and ganglion cell bodies was also seen in the retina and the optic disk showed extensive gliosis with new connective tissue formation.

The introduction of electron microscopy allowed more thorough investigation. de Preux and Mair (1974) carried out a combined light and electron microscopy study of the optic nerves of patients affected by Schilder's disease, Devic's disease and disseminated sclerosis (MS). The patient with disseminated sclerosis had died due to the condition and had documented visual impairment during life. The optic nerves in Devic's disease had extensive destruction of myelin and axons with astrocytosis, absent oligodendrocytes and infiltration of the nerve bundles and fibrous septa by macrophages. The destruction of axons and myelin was mild in Schilder's disease with oligodendrocyte preservation but some astrocytosis. Myelin breakdown in the optic

nerves of the patient with disseminated sclerosis was patchy with parts showing complete demyelination and other areas only patchy demyelination. Where there was complete demyelination oligodendrocytes were absent but macrophages were present and there was an intense astrocyte proliferation around naked axons. Axonal destruction was present but not as severe as in the patient with Devic's disease. The connective tissue septa contained blood vessels with endothelial hypertrophy and hyperplasia (also seen in the other two conditions). In the partially demyelinated regions there were some degenerating demyelinated fibres with an excess of fibroblasts and frequent macrophages. Oligodendrocytes were present almost as frequently as in normal optic nerves. The myelin of degenerating fibres showed concentric splitting or a lattice pattern.

In another study, the length of plaques seen on *post mortem* examination from the optic nerves of 14 patients who died of MS varied from 3mm to 3cm with a mean of 10.5mm and plaques contained increased fibrillary astrocytic processes (McDonald, 1977; McDonald, 1986). Plaques in MS show a classical peri-venular distribution and peri-vascular cuffing has been observed in the peripheral retina, at a site where there are no myelinated nerve fibres, suggesting that primary autoimmune demyelination is not the only process occurring in MS (Fog, 1965).

Ulrich and Groebke-Lorenz (1983), in another autopsy study of MS patients, discussed some of the clinico-pathological implications of optic nerve demyelination in MS. There was a significant correlation between visual acuity taken from retrospective records before death and the rank preserved myelin (r_S –0.668, p<0.001). They also confirmed the earlier finding of areas of partial and complete demyelination and the presence of astrocytosis. They were unable to quantify the extent of axonal loss due to technical problems with the stains used. The interesting observation was that it was still possible to have a reasonable level of visual acuity despite a long segment of demyelination covering the whole cross-section of the nerve for more than one centimetre. This suggested that useful conduction of nerve impulses was possible along demyelinated nerves (this phenomenon will be discussed further in the pathophysiology of optic neuritis).

A later study further demonstrated the variable size of plaques in the optic nerves of MS patients, from 5-90% of the cross-sectional area (Mogenson, 1990). The plaques were typically coniform, with bases at the periphery. Three out of ten nerves examined also had areas with periphlebitis.

A further way of investigating the functional significance of damage to the optic nerves in MS is to investigate the differential loss of fibres in the magnocellular and parvocellular pathways. Evangelou *et al.* (2001) studied the optic nerves and LGNs from eight patients with MS and eight non-neurological controls. They found that the optic nerve cross-sectional area from the intracranial portion of the optic nerve was non-significantly reduced in the patients with MS to a median 6.44mm^2 compared to 9.25mm^2 in controls (p=0.08). Axonal density was also reduced from a median 170,118mm^{-2} in controls to 108,912mm^{-2} (p=0.05) giving a total estimated axonal number of 1,407,711 in controls and 808,003 in the patients with MS (p=0.05). In the LGN there was not a decrease in size of the nucleolated magnocellular neurons whereas there was for the parvocellular neurons: median 226μm2 compared with 230μm in controls (p=0.001), suggesting that transynaptic atrophy had occurred. The skewness of parvocellular cell distribution correlated with axonal density in the optic tract. These observations suggest that the parvocellular nerves are damaged preferentially in MS. These observations confirm the clinical finding that parvocellular cells (providing colour vision and high spatial frequency resolution) are damaged preferentially in optic neuritis compared with magnocellular cells (responsible for low spatial frequency resolution) (Wall, 1990).

All the above studies rely on autopsy material from patients with long established MS. Histopathological examination of patients with acute optic neuritis has usually not been possible due to the obvious hazards from biopsy of the optic nerve. There is one report in the literature of a 50 year old woman who presented with progressive monocular visual loss (Rush *et al.*, 1982). There was a history of retrobulbar pain and blurred vision in that eye several months previously. Visual acuity was counting fingers at 5 feet, with defective colour vision, a relative afferent pupillary defect and a pale optic disk. A computed tomography scan showed diffuse enlargement of the affected optic nerve with no enhancement. There was a positive anti-nuclear antibody titre at a dilution of 1:100 (speckled pattern) and a monoclonal immunoglobulin G band in her

serum. CSF examination showed 27mg/100ml protein, 54mg/100ml glucose, ten lymphocytes and one monocyte. Due to increasing pain and decreasing visual acuity to hand movement perception a frontotemporal craniotomy was performed. The intracranial optic nerve and anterior chiasm looked yellow, indurated and swollen. Biopsy of the intracranial optic nerve showed a perivascular lymphocytic infiltration, multifocal demyelination, and reactive astrocytosis. Electron microscopy examination revealed dense bundles of reactive astrocytes, encompassing lymphocytes with plasmacytic features (probably B lymphocytes). Axonal integrity was not commented on. No visual recovery occurred after two years follow-up despite post-operative corticosteroids. It is not definite that this case represents optic neuritis given the progressive history with no visual recovery and abnormal blood test results but it represents the only human biopsy study of possible optic neuritis.

A way around this lack of data from human cases is to use animal models. Caution needs to be taken when trying to extrapolate the results to humans in that experimental allergic optic neuritis may not be a completely accurate model for human optic neuritis.

Rao *et al.* (1977) developed a model for acute allergic optic neuritis, which they discovered in adult guinea pigs that developed experimental allergic encephalomyelitis (EAE) following sensitisation with intracutaneous injections of isogenic spinal cord emulsion in complete Freund's adjuvant. Two patterns of disease were observed. One group with absent pupillary light responses and normal fundi were classified as having "retrobulbar optic neuritis". Lesions were localised to the orbital and intracranial portions of the optic nerves with foci of mononuclear cell infiltration in the pial septa, adjacent axonal bundles and occasionally in a perivascular distribution. Demyelination was present with disrupted myelin sheaths, phagocytosis of myelin fragments and moderate axonal swelling. The other group had absent pupillary light responses with a swollen disc and oedema of the surrounding retina. These were described as suffering from "neuroretinitis". Inflammation and demyelination was observed here just posterior to the lamina scleralis. Axonal swelling was seen at the lamina retinalis, which extended into the juxtapapillary retinal nerve fibres. Foci of mononuclear cell infiltration were present in the choroid and meninges.

The pattern of acute EAE is usually that of an illness leading to the death of the animal within four to six weeks although recovery is possible. Sensitisation of juvenile guinea pigs in later experiments produced a more chronic illness with death after several months and variation of the clinical findings, including pupillary changes, suggesting a relapsing remitting course (Rao, 1979). Multiple foci of mononuclear cell infiltration and demyelination in the optic nerve were again present but gliosis was now frequently seen. Non-myelinated axons appeared normal except at sites of active inflammation where axonal swelling was observed. Raine *et al.* (1980) later questioned the validity of the chronic model for human optic neuritis as part of MS. Although active optic nerve lesions were seen up to four months after inoculation they did not observe new spontaneous lesions spread over a number of years without re-inoculation, in contrast to the situation they observed in the spinal cord. At the periphery of chronic demyelinated lesions in the optic nerve, remyelination was seen with thinly myelinated fibres and an increase in densely staining cells, presumed to be oligodendrocytes. Axonal loss was not commented upon, although optic nerve atrophy was not seen.

Guy *et al.* (1992) carried out orbital gadolinium enhanced T_1-weighted fat suppressed MRI and T_2-weighted fat suppressed MRI on adult guinea pigs with EAE. The ultrastructure of the optic nerves was then investigated with transmission electron microscopy in order to correlate the imaging and histopathological findings. Gadolinium enhancement of the optic nerve near the globe was seen early, within three days of sensitisation, before clinical signs of EAE appeared, consistent with previous observations that blood-brain barrier breakdown is the first event in an MS relapse (Kermode *et al.*, 1990). After 10 to 14 days a longer segment of the optic nerve was enhancing and this persisted at 30 days. Gadolinium enhancement preceded high signal becoming apparent on T2-weighted images. The nerves showed perineural and perivascular demyelination, axonal degeneration and decreased axonal density with expansion of the extravascular space. Inflammatory cells infiltrated the perivascular space. Expansion of the extracellular space and the inflammatory infiltrate was associated with the intensity of the gadolinium enhancement and the T_2-weighted signal aberration tied in with observed demyelination.

Hayreh *et al.* (1981) were able to record VEPs from rhesus monkeys with EAE using a flash stimulus and correlate these with histological findings. In early EAE no gross

VEP change was detectable despite a cellular infiltration of the optic nerve, mild focal demyelination and optic disk oedema. Later on in the disease evolution a flat VEP was observed in association with optic atrophy on fundus examination and extensive demyelination and axonal loss on histological examination. Pattern-reversal VEPs would have been more sensitive but it was not possible to use them in this experimental model.

Further work on the integrity of the blood-brain barrier in the optic nerve was performed by Hu *et al.* (1998) in a rat EAE model. Microglia became activated, MHC class II^+ cells increased and horseradish peroxidase leakage was visible from day seven to eight post injection. On day eight, Monastral blue leakage was present in the myelinated parts of the optic nerve with infiltration of $ED1^+$ macrophages and $\alpha\beta TCR^+$ lymphocytes. Significant clinical symptoms became apparent at day 10. Oedema was detectable on transverse sections of the optic nerve between days 10 to 14. The intensity of the leakage, cellular infiltrate and MHC class II expression was maximal at day 12 and predominantly in the myelinated region of the optic nerve. At day 10 $CD4^+$ lymphocytes predominated over $CD8^+$ cells, however this situation was reversed at day 28. In control rats MHC class II+ cells were found in the meninges surrounding the optic nerve and the lamina cribrosa. The presence of these cells may contribute to the development of optic neuritis. The first features of acute EAE were therefore activation of microglia, increasing MHC class II expression and breakdown of the blood-brain barrier in line with earlier observations. Calcium activated neural proteinase (calpain) expression was found to be increased in the activated microglia and macrophages from the optic nerves of rats with EAE in a later study (Shields *et al.*, 1998). Calpain may play a role in degradation of myelin basic protein and other myelin proteins during phagocytosis.

In a mouse model of demyelination induced by Semliki Forest virus (SFV), Ikeda and Tansey (1986) observed early (1-2 weeks post-inoculation) demyelination with peri-vascular lymphocyte cuffing, a moderate lymphocytic infiltration of the meninges, microglial proliferation and some astrocytic hypertrophy. At this time fast axonal transport, measured by [^{3}H]proline uptake in the brain after ocular injection, was increased. The height of demyelination occurred 18-21 days post-inoculation. Most demyelinated fibres were found at the periphery of the optic nerve, closest to the larger

blood vessels. There was a significant loss of small (<7μm) myelinated fibres with a corresponding increase in unmyelinated fibres compared with control optic nerves, suggesting that the smaller fibres were more susceptible to demyelination. Slow axonal transport peaked at this time and there was also a suggestion that axonal sprouting had occurred as a possible response to the injury.

Axonal cytoskeleton changes have also been observed early on in the course of acute EAE in rats induced by optic nerve microinjection of polyclonal rabbit ant-galactocerebroside antibody with guinea pig complement (Zhu *et al.*, 1999). On day one post injection moderate neurofilament and microtubule disassembly was seen in the local demyelinated area with again an increase in microglia but before any cellular infiltration was seen. From day three onwards there was an increasing inflammatory cell infiltrate of predominantly macrophages, coinciding with more axonal cytoskeleton changes. There was then more extensive demyelination, axonal swelling and loss, and subsequent gliosis. Some of the axonal swellings may have represented the occurrence of axonal transection. Axonal loss was seen in demyelinated areas with few or no inflammatory cells, suggesting that inflammation-independent mechanisms were at work. However, axonal cytoskeleton changes and axonal loss were most apparent in areas with high levels of cell infiltration in agreement with recent biopsy studies of brain MS lesions in humans (Ferguson *et al.*, 1997; Trapp *et al.*, 1998). Acute demyelination may therefore induce local axonal cytoskeleton changes, which are then further enhanced by inflammation. The cytoskeleton changes may be amongst the earliest events in the course of acute axonal loss that occurs in acute EAE/optic neuritis. From day seven axons frequently showed thin myelin sheaths, possibly representing attempts at remyelination, although partial demyelination could also have been responsible. Wallerian degeneration of axons was only occasionally observed.

Active remyelination has been observed after anti-galactocerebroside antibody mediated demyelination and oligodendrocyte destruction in the cat optic nerve (Carroll *et al.*, 1990). This was thought to be due to a new population of small glial cells, possibly derived from dedifferentiated astrocytes or progenitor cells, which differentiate to become oligodendrocytes. Bipotential glial progenitor cells have been previously identified in the rat optic nerve (ffrench-Constant & Raff, 1986). Almost complete

remyelination occurs in this model unlike in human optic neuritis suggesting that repair mechanisms in human optic neuritis may be impaired.

The above animal models demonstrate that there may be very early axonal changes with an increase in microglia and breakdown of the blood-optic nerve barrier followed by cellular infiltration. Demyelination of axons occurs focally initially but then spreads over time. Early axonal swelling may indicate acute axonal transection. The amount of axonal loss is related to the degree of inflammation, although inflammation-independent mechanisms of demyelination and axonal loss may also occur. Early remyelination by oligodendrocytes possibly derived from progenitor cells may then start. The predilection of MS to affect the optic nerves is uncertain but a possible mechanism is an inherent weakness of the blood-brain barrier in the optic nerve (Tso *et al.*, 1975). The animal studies may provide good models for early acute inflammatory changes in optic neuritis but they provide little information about the causes and effects of recurrences (relapses) of optic neuritis, which may be more akin to the human situation. More studies are also required to follow the course of EAE optic neuritis into the chronic phase to investigate the complex interplay between degeneration and repair that may be occurring following optic neuritis. In human optic neuritis remyelination is thought to occur, as witnessed by the progressive shortening of VEP latency (Jones, 1993; Frederiksen & Petrera, 1999), although its frequency and extent is unknown. It is difficult to measure visual function in animals and therefore correlate clinical findings with radiological and histological results in order to understand the functional significance of any changes observed. The pathophysiology of the acute deficits, subsequent recovery and persistent disability in optic neuritis will be discussed in the next section.

1.2.11 The pathophysiology of optic neuritis

A coherent account of the pathophysiology of optic neuritis has to include the mechanisms behind both relapse and recovery including the causes of incomplete recovery from an individual attack. Insight into these mechanisms has come from study of optic neuritis and MS *in vivo* and laboratory studies.

From studies of the pathology of optic neuritis and MS it is clear that demyelination of axons is a significant and consistent feature within all types of MS lesions (Lucchinetti *et al.*, 2000). Demyelination occurs due to breakdown of the ability of regulatory systems to prevent auto-reactive T cells from causing autoimmune damage (Compston & Coles, 2002). In optic neuritis and MS, T cells auto-reactive to myelin, access the central nervous system by expressing adhesion molecules to allow their passage through the blood-brain barrier. Once there, they recognise myelin and cause microglia to express major histocompatibility complex class II to present myelin to T cells. A pro-inflammatory loop is therefore set-up and an inflammatory demyelinating plaque results.

From experiments with demyelination induced by direct micro-injection of diphtheria toxin into the posterior columns of cat spinal cords, McDonald and Sears (1970) first demonstrated that demyelination can cause conduction block in axons, suggesting the cause for clinical relapse. Contributory evidence came from the development of electrophysiological studies *in vivo*.

Stimulation of the eye produces a cortical response. When appropriate averaging techniques are used, this visual evoked response (VER) or VEP can be measured (Halliday *et al.*, 1972). Two principal methods can be used as a stimulus: a flash of light, typically of peak intensity $1.25 \times 10^6 cd/m^2$ and a time constant of $20\mu s$; or pattern-reversal of a checkerboard pattern with individual black-and-white squares subtending 50 minutes and having a luminance of 8.6 and $110 \times 10^6 cd/m^2$ respectively. In studies of optic neuritis, flash responses are not able to differentiate accurately between diseased and healthy nerves (Halliday *et al.*, 1972). Pattern reversal VEPs in optic neuritis usually show a characteristic delay and often a reduction in the amplitude of the response. Halliday *et al.* (1972) observed delayed responses from 120ms to 155ms using pattern-evoked visual responses from eyes affected by optic neuritis compared to controls, probably due to slowing of conduction within the affected optic nerve (Table 1.8).

Study	Subjects	Results	Comments
Halliday *et al.*, 1972.	17 controls 17 acute optic neuritis (≤ 29 weeks after onset) 2 chronic optic neuritis (21 months and 5 years)	*Diseased eyes where a response could be measured* Mean lat. 155.1 ± 20.0ms Mean ampl. 3.68 ± 1.63μV *Healthy unaffected eyes* Mean lat. 121.1 ± 5.9ms Mean ampl. 8.22 ± 4.43μV *Controls* Mean lat. 120.1 ± 4.0ms Mean ampl. 7.74 ± 3.26μV	5 patients ≤ 2 weeks of onset, with visual acuity ≤ 6/60, showed no response 4 of these were re-measured subsequently and low amplitude, delayed responses were recorded 8 patients seen median 19.5 weeks after onset (range 7 weeks to 5 years) Median latency 151.5ms (range 132-206) Median visual acuity 6/6 (range 6/5 to 6/9)
Halliday *et al.*, 1973a.	53 patients recovering from optic neuritis	Correlation between VEP amplitude and visual acuity ($p<0.001$)	No correlation between VEP latency and visual acuity
Halliday *et al.*, 1973b.	51 patients with MS 24 of which having a past history of optic neuritis	All patients with previous optic neuritis had delayed VEPs 25/27 MS patients without previous optic neuritis had delayed VEPs	96% of MS patients had a delayed VEP 93% of MS patients without previous optic neuritis still had a delayed VEP
Feinsod and Hoyt, 1975.	25 patients with MS 15 of which had no visual symptoms or signs	Flash-evoked latency and amplitude abnormal in all subjects Three patterns: i) Prolonged peak latency ii) Breakdown of first negative component into 2-4 sub-components iii) Very low amplitude response	Responses due to varying degrees of conduction delay in demyelinated axons and depletion of axons in the optic pathways
Harding and Wright, 1986.	22 patients ≤ 3 days from onset of acute optic neuritis	*At 3 days* Mean P100 amplitude <1μV Mean latency unmeasurable *At 1 week* Mean P100 amplitude ~3μV Mean latency unmeasurable *At 3 weeks* Mean P100 amplitude ~5μV Mean latency ~160ms *At 4 weeks* Mean P100 amplitude ~4μV Mean latency ~130ms	Amplitude of P100 VEP but not flash VER correlated with visual acuity Over next 12 months VEP latencies decreased and 3/22 returned to normal
Kriss *et al.*, 1988.	20 childhood optic neuritis patients (4 unilateral and 16 bilateral) out of a cohort examined a mean 8.8 years after attack	45% had delayed VEP including one absent response	All unilateral cases remained abnormal. 55% of cases overall had a normal response

CF = central field, WF = whole field, SD = standard deviation

Study	Subjects	Results	Comments
Youl *et al.*, 1991.	11 patients (2 with bilateral optic neuritis) recorded a mean 6.4 (range 2-13) days after onset of acute optic neuritis 9 (1 bilateral) of whom re-examined a mean 27.8 (range 20-32) days later	*Acutely (13 eyes)* Absent VEP in 3 eyes Delayed + low ampl. in 6 Delayed only in 3 Low amplitude only in 1 *Follow-up (10 eyes)* Delayed VEPs only in 6 Delayed + low ampl. in 2 Normal in 2	VER amplitude significantly larger at follow-up (p=0.02) and associated with resolution of optic nerve gadolinium 'leakage' on STIR MRI
Jones, 1993.	376 patients examined at differing time points following acute unilateral optic neuritis	*1-4 weeks (n=64)* 89.1% abnormal, 21.8% absent *5-8 weeks (n=78)* 93.6% abnormal, 6.4% absent *9-13 weeks (n=64)* 93.7% abnormal, 1.6% absent *14-26 weeks (n=55)* 92.7% abnormal, 0% absent *27-104 weeks (n=59)* 79.7% abnormal, 0% absent *105-990 weeks (n=56)* 71.4% abnormal, 0% absent	Most apparent improvement in VEP latency between 6 months and 2 years after optic neuritis Latencies in patients with MS were prolonged at 4 weeks, but significantly shorter between 8-104 weeks, compared with isolated optic neuritis
Brusa *et al.*, 1999.	12 patients who were part of the Kapoor *et al.* 1998 IVMP trial, re-examined after 3 years	*Clinically affected eye* Shortening of mean latency between 6 months and 3 years Whole field: 131 to 123ms Central field: 136 to 125ms	*Clinically unaffected eye* Prolongation of mean latency over same time period Whole field: 110 to 113ms
Fredericksen and Petrera, 1999.	90 patients with acute optic neuritis, with follow-up after 2, 4, 12 and 52 weeks	*Baseline* 69 (77%) - abnormal VEP *Follow-up* 13 (19%) normalised 11 of the initially normal VERs became abnormal	Baseline abnormalities seen in 35% of clinically unaffected eyes (not including MS)
Brusa *et al.*, 2001.	31 patients, examined 3, 6, 9, 12, 18 and 24 months after acute optic neuritis	*At 3 months* All responses abnormal WF ampl. = 5.79 SD 3.6μV WF lat. = 129.8 SD 13.5ms CF ampl. = 4.42 SD 3.4μV CF lat. = 129.8 SD 10.1ms *At one year* WF ampl. = 6.99 SD 3.5μV WF lat. = 122.7 SD 13.4ms CF ampl. = 4.63 SD 2.9μV CF lat. = 122.4 SD 12.1ms *At two years* WF ampl. = 6.91 SD 3.5μV WF lat. = 119.7 SD 12.8ms CF ampl. = 4.51SD 2.4μV CF lat. = 118.4 SD 11.0ms	Most significant shortening between 3 and 6 months (p<0.001 for WF and CF) Between 1 and 2 years less marked shortening (p<0.05 for WF)

Table 1.8: Studies of pattern-reversal (unless indicated) VER in optic neuritis and MS.

Delayed visual evoked, somatosensory evoked and brainstem evoked responses have also been seen in the absence of clinically definite relapses in these systems and these investigations have been used to provide confirmatory evidence of other silent areas of demyelination and so assist in making the diagnosis of MS by confirming dissemination in space (McDonald, 1998).

The presence of demyelination enables some of the phenomena that some optic neuritis patients experience to be explained.

(i) Phosphenes

Spontaneous oscillatory bursts of action potentials have been observed in experimentally demyelinated optic nerves induced in mice by SFV which may be the electrophysiological representation of phosphenes seen by some optic neuritis patients (Tansey & Ikeda, 1986). This spontaneous firing, often induced by movement is thought to be analogous to Lhermitte's phenomenon in the spinal cord (Davis *et al.*, 1976).

(ii) Uhthoff's phenomenon

VEP experiments have been performed on patients who experience Uhthoff's phenomenon, before, during and after exercise (Persson & Sachs, 1981) and during heating in a hydrotherapy bath (Saul *et al.*, 1995). These experiments showed that both exercise and heat principally caused decline in VEP amplitudes, particularly in patients who showed symptomatic visual loss. The mechanism behind Uhthoff's phenomenon is thought to be the induction of conduction block in demyelinated nerve fibres by the increased temperature (Rasminsky, 1973). Demyelination is thought to reduce the ability of the nerve fibre to conduct repetitive impulses by increasing the refractory period (Schauf & Davis, 1974). Hence the safety factor for conduction is reduced.

(iii) Pulfrich's phenomenon

Pulfrich's phenomenon may be explained by a delay in the visual impulse from one eye being delayed in reaching the brain compared with the other. To measure the effect

Rushton (1975) arranged a pair of oscilloscopes with one screen being presented to each eye, so that each subject saw a fused image. A spot oscillated to and fro on the screen. The subject was asked to vary the phase angle, and hence the time lead or lag, in order to produce a fused image. The inter-ocular latency could then be calculated. In a series of patients with MS inter-ocular delays of up to 30ms were recorded. VEPs were more sensitive at detecting delayed conduction because the Pulfrich test could only detect inter-ocular delay and many of the MS patients had abnormal conduction in both eyes. This phenomenon has also been measured in patients who had recovered from optic neuritis (Slagsvold, 1978). All patients tested were however, asymptomatic for Pulfrich's phenomenon and in clinical practice it is much rarer than Uhthoff's phenomenon.

(iv) Fading of vision

Fading of vision in bright environments is thought to be due to fatigue or a saturation effect in the conduction of demyelinated optic nerves which occurs over minutes (Campos *et al.*, 1980). This effect may be due to a progressive failure to conduct nerve impulses at high firing rates (McDonald & Sears, 1970).

Remyelination can occur in optic neuritis and multiple sclerosis lesions however the new internodes are thought to be shorter and thinner than normal (Prineas & Connell, 1979). Restoration of central conduction via these new internodes however, was demonstrated, suggesting a mechanism for recovery from clinical relapses (Smith *et al.*, 1979; Smith *et al.*, 1981). Further evidence for the existence of remyelination after acute demyelinating events comes from VEP studies. Normalisation of the VEP latency has been shown to occur after optic neuritis in 0% to 38% of cases (Frederiksen & Petrera, 1999), and continues for up to two years after the acute event (Brusa *et al.*, 2001). A study of childhood optic neuritis found that normalisation occurred in 55% of cases, suggesting that remyelination may be more extensive in children (Kriss *et al.*, 1988).

However, remyelination as the mechanism for remission from relapses cannot explain completely the mechanism of recovery from a relapse. Prineas *et al.* (1993) concluded from observation of lesions from post mortem material from cases of early MS that the

interval from the beginning of a new lesion to commencing remyelination is approximately one month. From their experimental observations on cat spinal cords Smith *et al.* (1981) concluded that remyelination commences during the second week following micro-injection of lysophosphatidyl choline, with recovery of conduction stretching over three months. This is therefore too long to explain the rapid recovery in function that can sometimes be seen with relapses, particularly in optic neuritis (Youl *et al.*, 1991). Furthermore, the remyelination may only occur at the edge of lesions and is often incomplete (Prineas & Connell, 1979). There is also evidence to suggest that function is possible despite complete or almost complete demyelination of axons within lesions. Wisniewski *et al.* (1976) described: (i) two patients with functional vision who, on *post mortem* examination, had very long segments of optic nerves showing complete demyelination, and (ii) four animals in remission from EAE despite having spinal cords displaying large stretches of demyelination. Recovery of good visual acuity is also possible despite persistent increased latency of the visual evoked response (Halliday *et al.*, 1973a). In a mouse model of demyelination induced by Theiler's murine encephalomyelitis virus, normal function was possible even though there was nearly complete demyelination of the spinal cord (Rivera-Quinones *et al.*, 1998). These findings support the assertion by Charcot (1877) that "patches of sclerosis have been found, after death, occupying the whole thickness of the nerve-trunk, in the optic nerves, in cases where, during life, an enfeeblement of sight simply had been noted. This apparent disproportion between the symptom and the lesion constitutes one of the most powerful arguments which can be invoked to show that the functional continuity of the nerve-tubes is not absolutely interrupted, although these, in their course through the sclerosed patches, have been despoiled of their medullary sheaths and reduced to axis-cylinders." Conduction of nerve impulses must therefore show some recovery very quickly and be possible even in the presence of demyelination or only partial remyelination.

Youl *et al.* (1991) observed that both clinical improvement and increased P100 amplitude of the VEP occurred rapidly after acute optic neuritis. This was associated with the cessation of gadolinium "leakage" visible on STIR MRI after administration of dimeglumine gadopentate. The leakage was thought to be due to acute inflammation causing a breakdown in the blood-optic nerve barrier. Acute inflammation alone could

therefore have been responsible for conduction block and its resolution an important step in remission, prior to any significant remyelination.

Nitric oxide (NO) and the inducible form of NO synthase (iNOS) have been found in elevated concentrations in the central nervous system in MS and experimental allergic encephalomyelitis. Increased iNOS expression can be seen in activated macrophages and astrocytes. NO is thought to be an important inflammatory mediator. In experiments, Redford *et al.* (1997) observed that NO donors cause reversible conduction block in axons from both the peripheral and central nervous systems. Demyelinated and early remyelinated axons were particularly were particularly susceptible. This therefore gave experimental evidence for how inflammation can cause conduction block. It is now thought that other compounds may also be involved in producing conduction block. Brinkmeier *et al.* (2000) discovered an endogenous pentapeptide in the cerebrospinal fluid of patients with MS and Guillain-Barré syndrome, which was able to act as a sodium channel blocker and could therefore also be involved in the pathophysiology of optic neuritis and MS.

Restoration of conduction in a demyelinated axon is also thought to be due to increased expression of sodium channels along the demyelinated segment allowing continuous (albeit slowed) conduction instead of the fast saltatory conduction that occurs in normally myelinated axons (Smith & McDonald, 1999). Saxitoxin is a neurotoxin that binds and blocks sodium channels. Increased saxitoxin binding has been demonstrated in human multiple sclerosis lesions by Moll *et al.* (1991) although the resolution was not sufficient to permit differentiation of the binding into glial or axonal tissue components. More recently, Felts *et al.* (1998) showed an increase in sodium channel immunoreactivity on experimentally demyelinated axons, with an even distribution on some, but discrete foci on others. The relevance of these foci is unclear but as they occur at a time when conduction is possible their presence may be important (Smith & McDonald, 1999). Restoration of conduction in demyelinated axons has been demonstrated experimentally using intra-axonal recording. Conduction was possible over segments of demyelination exceeding several internodes although with a reduced conduction velocity and increased refractory period (Felts *et al.*, 1997). These mechanisms could therefore explain the basis of recovery of function despite evidence

of persistent demyelination and the presence of asymptomatic lesions causing delay of the visual evoked response (Halliday *et al.*, 1973a; 1973b).

The recovery from a relapse is therefore probably a combination of resolution of inflammation, increased expression of sodium channels in a demyelinated segment and the formation of new internodes by remyelination (Smith & McDonald, 1999). Inflammation may be important in the repair process. A number of inflammatory cytokines may be involved in inducing remyelination (Sharief, 1998). Interleukin-1β is a potent inducer of remyelination. It also induces astrocytes to produce other cytokines, including interleukin-6 which is involved in oligodendrocyte differentiation, migration and survival, and ciliary neurotrophic factor, which may protect oligodendrocyte precursors from cell death caused by tumour necrosis factor-α and neurotoxins. Inflammation and repair may therefore be in complex balance and governed by the availability of oligodendrocytes and their precursors and the temporal and spatial effects of inflammatory cells and their associated cytokines.

Remyelination may fail for a number of reasons. Oligodendrocyte precursors may be depleted by the inflammatory process (Franklin, 2002). In chronic plaques gliosis may act as a physical barrier to remyelination (Compston & Coles, 2002). Astrocytes have been demonstrated to express Jagged 1 in active lesions. Jagged 1 can inhibit oligodendrocyte differentiation and process production via the Notch pathway (John *et al.*, 2002). Also, axons in demyelinated plaques re-express PSA-NCAM (polysialylated form of neural cell adhesion molecule) which may inhibit remyelination (Charles *et al.*, 2002).

The failure of complete recovery from a relapse may be in part due to axonal degeneration. Axonal loss has been demonstrated to occur in acute MS lesions with the degree of axonal damage related to the amount of inflammation present (Ferguson *et al.*, 1997; Trapp *et al.*, 1998). NO may be important here. Smith *et al.* (2001) exposed axons to pathophysiological concentrations of NO for two hours and demonstrated that persistent conduction block occurred associated with axonal degeneration morphologically. The axons were vulnerable at lower concentrations of NO if they were also made to conduct impulses at 50 or 100Hz (physiological frequencies). NO may inhibit mitochondrial function and hence axons will be more susceptible to damage

if put under some metabolic stress (Smith & McDonald, 1999). It was possible to protect the axons from degenerating by preventing sodium entry into the axons or inhibiting sodium/calcium exchange using appropriate channel blocking drugs (Kapoor *et al.*, 2003). Direct autoimmune T cell axonal damage (Medana *et al.*, 2001) and glutamate excitotoxicity may also be important in the pathogenesis of acute axonal degeneration (Pitt *et al.*, 2000).

Halliday *et al.* (1973a) observed a clear relationship between the mean amplitude of the VEP and visual acuity ($p<0.001$), but not between the mean latency and visual acuity following optic neuritis. This suggested that axonal loss could have functional significance following a single episode of acute inflammation and this could explain some of the mechanisms behind the failure to recover completely from a relapse. Normal visual acuity is however possible despite abnormal VEP results following optic neuritis (Halliday *et al.*, 1973a; Frederiksen & Petrera, 1999). There may therefore, be redundancy in the number of axons required hence large numbers may need to be lost to be clinically significant. Frisen and Quigley (1984) obtained nerve fibre counts from the temporal quadrants of optic nerves with optic atrophy. The temporal quadrant was measured as it was felt that this portion of the nerve was most likely to subserve foveal vision. This was compared to the visual acuity to give an indication of the functional fraction of neural channels. This produced a parabolic relationship and the suggestion that normal (Snellen 6/6) vision can remain despite the loss of 40% of the neural substrate. Visual acuity of 6/15 seemed possible with 10% remaining of the neural substrate and 6/60 with only 1%. The recovery and/or retention of function despite continued axonal dysfunction or loss within the optic nerve may also be as a consequence of plasticity and functional remodelling within the visual system and higher centres, perhaps by utilising the redundant capacity (Sabel *et al.*, 1997; Werring *et al.*, 2000). In a series of experiments, reviewed in (Sabel *et al.*, 1997), it has been demonstrated that recovery of visual function in rats to near-normal levels was possible within two weeks despite only 10% of nerve fibres remaining following graded optic nerve crush. The remaining nerve fibres were measured by looking at the number of retinal ganglion cells that had taken up horseradish peroxidase after injection in the contralateral superior colliculus. The other neural connections of the optic nerve, including the lateral geniculate nucleus were therefore not included in assessing nerve viability and therefore it is not certain whether other pathways had nerve fibres that

were less vulnerable to injury and contributed to the visual recovery. Measurement of vision was by a behavioural task involving orienting towards a visual stimulus or ability to perform visual tests in a Y-maze. The tests were therefore examining behavioural adaptation rather than visual recovery *per se*. Nevertheless, whatever the mechanism recovery of function was possible despite significant axonal loss. Werring *et al.* (2000) observed extraoccipital activation on functional magnetic resonance imaging (fMRI) using periodic monocular 8Hz photic stimulation in seven patients with optic neuritis who had recovered back to normal visual acuity (Snellen 6/6 or better). Whilst this study demonstrates that altered cortical responses occur following optic neuritis, their functional significance in contributing to recovery of vision is unknown.

There is evidence that a more chronic process of ongoing axonal loss also occurs in MS and this may explain the development of irrecoverable disability and secondary progression in MS (Smith & McDonald, 1999). Abnormalities in the retinal nerve fibre layer in patients with MS have been seen in the absence of previous optic neuritis and visual complaints suggesting that insidious axonal loss can occur in the optic nerves (Frisen & Hoyt, 1974). Early visual evoked response abnormalities in the absence of optic neuritis have also been recorded in MS patients including both increased latency and reduction of amplitude (Feinsod & Hoyt, 1975). Other studies have shown that progressive atrophy of the brain and spinal cord occurs in MS, measured using MRI techniques. Correlations with disability have been shown in most of these studies (particularly cross-sectional studies) again providing evidence for axonal loss in MS and its functional significance (Losseff & Miller, 1998).

The amount of axonal degeneration in MS appears in part related to the amount of preceding inflammation. After administration of Campath-1H, a humanised anti-leucocyte (CD-52) monoclonal antibody Coles *et al.* (1999) observed almost complete suppression of new gadolinium enhancing lesions in patients with MS for at least 18 months. Disability progression and increasing brain atrophy still occurred in about half the patients and was correlated to the magnetic resonance imaging inflammatory load present before treatment ($p<0.001$). These progressive changes may be as a result of Wallerian degeneration of axons (Waller, 1850) becoming apparent radiologically over time (Simon *et al.*, 2000). That increased cerebral atrophy indicated axonal degeneration could be deduced from its strong correlation with decreased *N*-acetyl

aspartate concentration detected using magnetic resonance spectroscopy (Coles *et al.*, 1999).

Axonal loss in chronic plaques also occurs. The axonal loss is greater in areas of demyelination than remyelination (Kornek *et al.*, 2000). Oligodendrocytes are thought to secrete trophic factors to help maintain axonal integrity (Scolding & Franklin, 1998; Wilkins *et al.*, 2003). Remyelinated axons may not, however, be totally immune from degeneration. Raine and Cross (1989) observed axonal loss in both demyelinated and remyelinated plaques. The mechanism of damage may be related to the observation that remyelinated axons may be vulnerable to damage from physiological impulse transmission (Samtani & Smith, 1999) Axonal damage due to low-grade ongoing inflammation in chronic plaques has also been proposed as a mechanism of chronic damage (Smith & Lassmann, 2002).

Chapter 2 Magnetic Resonance Imaging in Optic Neuritis

MRI allows *in vivo* examination and there is therefore the potential of gaining valuable insights into the pathophysiology of optic neuritis. This potential will be discussed along with results of previous MRI studies in optic neuritis. The theory of MRI will be considered followed by the technical difficulties to be overcome in order to image the optic nerves.

2.1 Theory of magnetic resonance imaging

The basis of MRI (Hendrick, 1994; Horowitz, 1994; Hashemi & Bradley jr, 1997), is the utilisation of the properties of the nuclei of atoms. Nuclei contain protons which are positively charged particles. Each proton behaves as though it was spinning and so generates an electro-magnetic field (Figure 2.1).

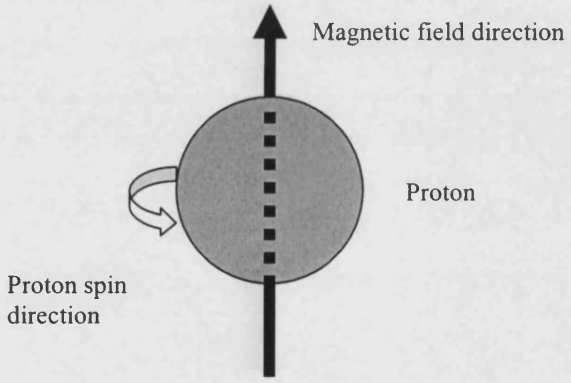

Figure 2.1: The spin of a proton will generate a magnetic field.

Depending on the number of nucleons (protons and neutrons), the nucleus may show an overall "spin", which may be an integer or a half-integer. Hence the nucleus may have a net magnetic field or magnetic dipole moment (MDM). The principal element of interest for biological MRI is hydrogen because a hydrogen atom's nucleus contains a single proton and hence an MDM, it is found in abundance in biological tissues (approximately 10^{19} hydrogen nuclei per mm^3 of tissue, principally in water and fat) and can provide a means of differentiating normal from diseased tissue as the water content often changes due to disease.

If a nucleus with an MDM is placed in an external magnetic field (the B_0 field) then the spins of its protons will line up with the magnetic field. The spin direction is not usually exactly perpendicular to the "vertical" axis (defined by the main magnetic field). The spin and hence the MDM precesses in a motion identical to a spinning top. The top spins around its axis, while the axis of the spinning top precesses (more slowly) around the vertical axis.

For MRI the magnetic field strengths used are tens of thousands of times stronger than the Earth's magnetic field (1.5 Tesla [T] ≈30,000 x Earth's magnetic field strength). If radiofrequency (RF) energy appropriate to that nucleus (at the Larmor or precession frequency, which is proportional to the magnetic field) is applied (generating the B_1 magnetic field) some protons will change the direction of their spins, or precession, to line up with the new magnetic field. The change in angle of the spins of the protons is called the "flip angle". It is proportionate to the strength and duration of the RF pulse. Commonly used flip angles are 90° and 180°. Partial flip angles (of use in gradient echo [GE] imaging, see later) of less than 90° can be achieved by lowering the strength or duration of the RF pulse. When the RF pulse is switched off the spins will return to align with the B_0 field. The magnetisation precessing in the x-y plane can induce a detectable current in a surrounding coil. This signal oscillates at the precessional frequency which can be described as a sine curve and its amplitude decays away to give the "free induction decay" or "T_2* curve".

If the signals from different protons are out of alignment such that one has a negative vector whereas another has a positive vector, although they may be precessing at the same frequency, they will not be in phase. The individual signals will therefore tend to cancel each other out. Immediately after the RF pulse, the vectors are in phase and hence the signals are additive. The decay in the T_2* curve is due to dephasing of the individual proton MDM vectors. The dephasing is caused by inhomogeneities in the external magnetic field which will change the precession frequency and by spin-spin interactions between neighbouring protons.

2.1.1 T_1 and T_2 relaxation

Relaxation is the term used to describe the realignment of proton spins back to their equilibrium state after the RF pulse is turned off.

The T_1 relaxation time is the time constant for the rate of growth of magnetization back along the longitudinal (z) axis (T_1 is the time for the signal to recover to 1-(1/e), approximately 63% of original value). The T_2 relaxation time, which is more rapid, is the time constant for the rate of decay of the spins (hence magnetization) in the x-y (transverse) directions (T_2 is the time for the signal to decay to 1/e, approximately 37% of original value). T_1 and T_2 relaxations are two independent processes occurring at two different rates and both vary according to the environment the protons lie within, ie the nature of the tissue being examined.

The T_2 decay depends on the spin-spin interactions. T_2 is therefore fixed and depends upon the properties of the tissue whereas T_2* depends on the homogeneity of the external magnetic field.

2.1.2 The spin echo pulse sequence

The spin echo pulse sequence consists of a 90° RF pulse followed by one or more 180° pulses (Figure 2.2). The 180° pulse is a rephasing or refocusing pulse which eliminates dephasing between protons caused by external magnetic field (B_0) inhomogeneities. A new T_2* decay occurs after each refocusing pulse, each with a lower amplitude due to dephasing from spin-spin interactions that cannot be corrected for and it is this decay that produces the T_2 decay curve. The time from the 90° pulse to the 180° pulse must equal the time from the180° pulse to the measurement of the signal. This allows time for the proton spins to get back in phase before the signal is measured.

In order to produce an image the RF pulse with relaxation and signal measurement need to be repeated many times. The TR is the "repetition time" or the time interval between RF pulses. The TE is the "echo time" or the time between the RF pulse and signal measurement. Both T_1 and T_2 are sensitive to the macromolecular environment of the protons and are inherent properties of the tissue being examined. T_1 and T_2 vary

depending on the tissue type and between normal and diseased tissue and by varying TR and TE the required image contrast can be produced to display the tissue and detect disease effects.

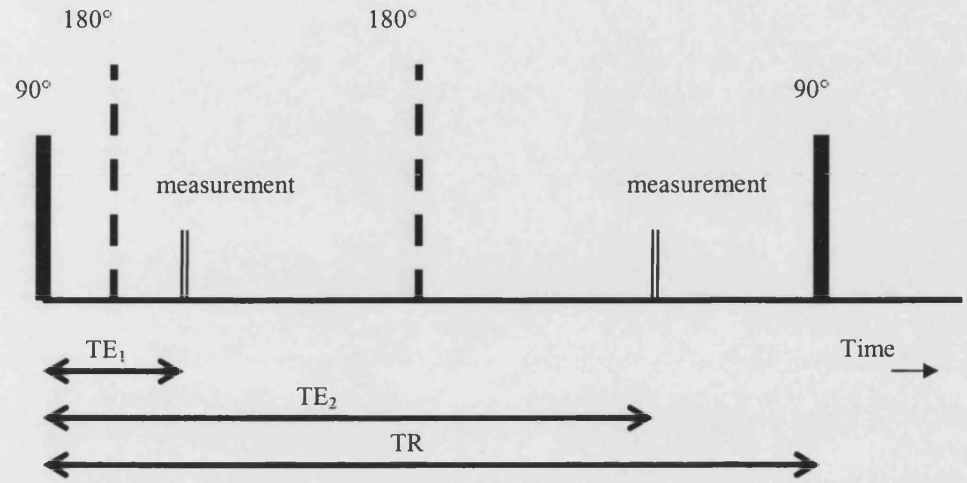

Figure 2.2: The spin-echo pulse sequence.

In order to produce a more "T_1–weighted" image in which the intensity contrast is due mainly to the T_1 relaxation properties of the tissue a short TR and a short TE are required to allow for differences in the longer T_1 times of tissues whilst minimising the effects of T_2. In order to produce a more "T_2–weighted" image longer TR and TE are required to minimise the effect of T_1 differences between tissues (to allow the longitudinal relaxation to be virtually complete in all tissues) whilst allowing more time for transverse decay. If a long TR and very short TE sequence is chosen then this will negate the effects of both T_1 and T_2 relaxation. The main factor left that can affect the signal produced by a tissue is the proton density, hence the images produced in this way are called "proton density" (PD) weighted images. The above effects are all relative as there is a spectrum from T_1- to T_2- and PD-weighted images.

If two 180° pulses are used with a long TR (usually around 2000-3000ms), two signal outputs can be measured: one with a short TE (usually around 20ms) and one with a long TE (usually around 80ms). Thus, two sets of images can be produced, one that is mildly T_1-weighted (called "PD") and one that is more T_2-weighted.

T_1 relaxation curves show the strength of the magnetisation in the z direction (Mz vector) as a function of time (Figure 2.3) given by the equation:

$$Mz = Mo\ [1\text{-}e(^{-t}/T_1)]$$

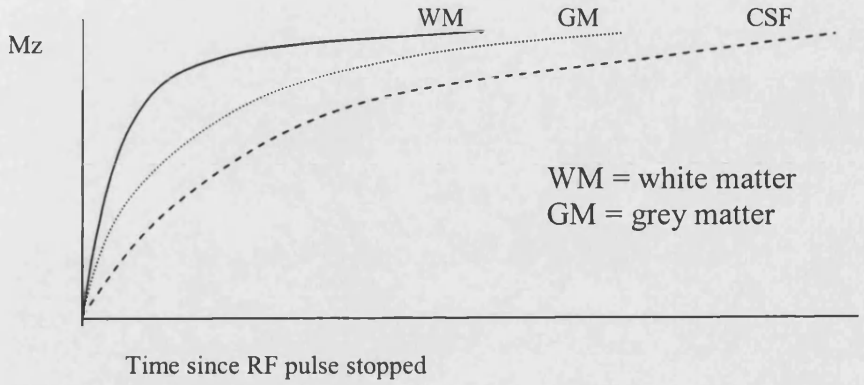

Figure 2.3: T_1 relaxation curves.

Examining the graph shows that CSF has a longer T_1 time than white matter. If a signal is measured with a short TR and TE then white matter will give high signal intensity, grey matter will give an intermediate signal and CSF will give low signal intensity. The maximum magnitude of the magnetisation is also directly proportional to the proton density.

The T_2 decay curve is a graph of the signal intensity versus TE for a given tissue. If the T_2 decay curve is considered (Figure 2.4) and a signal is measured with a long TE then CSF will give high signal intensity, grey matter will give intermediate signal intensity and white matter low signal intensity.

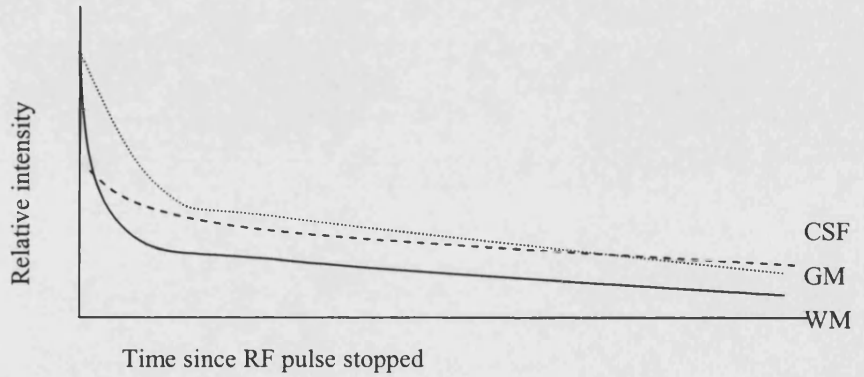

Figure 2.4: T_2 decay curves.

Acute MS lesions in cerebral white matter contain high amounts of oedema and have varying amounts of demyelination. The lesions have long T_1 relaxation curves and T_2 decay curves (although not as long as CSF). Acute lesions therefore give low signal intensity on T_1-weighted images and high signal intensity on T_2-weighted images. There may not be high contrast at a long TE between CSF and the lesion. On long TR/ relatively short TE (PD-weighted, although not true PD) images the lesions usually, because of the properties of their T_2 decay curves, give higher signal intensity than CSF. As the acute lesion resolves and the oedema subsides the T_1 relaxation speeds up.

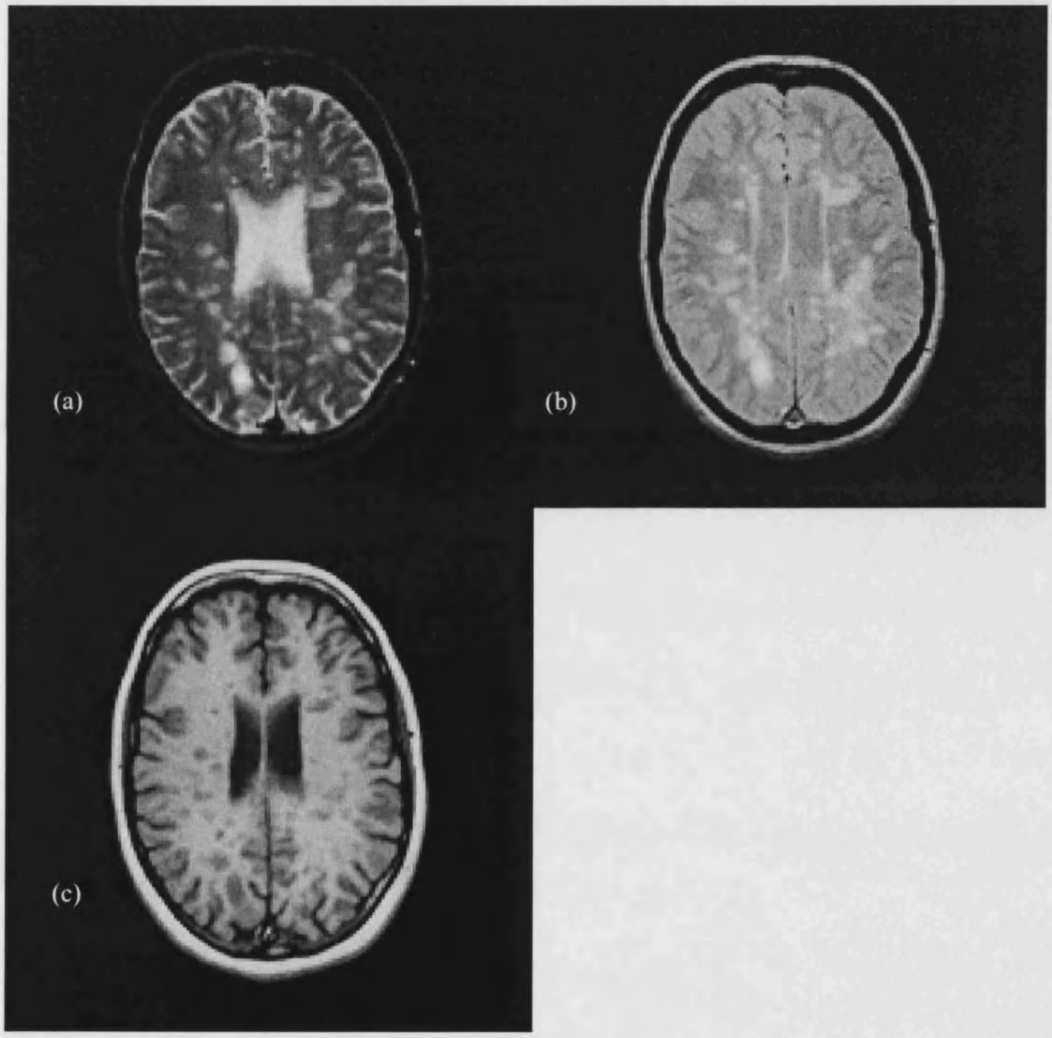

Figure 2.5: a) T_2-weighted b) PD-weighted c) T_1-weighted conventional spin echo images from a patient with SPMS demonstrating hyperintense lesions on T_2/PD-weighted images and hypointense lesions (black holes) on T_1-weighted images.

The lesions still give high signal intensity on T_2- and PD-weighted images due to demyelination and gliosis and isointensity on T_1-weighted images. However, a chronic lesion with axonal loss will have increased extracellular water and will again give low signal intensity on T_1-weighted images whilst continuing to give high signal intensity on T_2- and PD-weighted images (Figure 2.5). T_2- and PD-weighted images are very sensitive to detecting MS lesions however there is low pathological specificity for the nature of the lesions so detected (Grossman *et al.*, 2000).

2.1.3 Generating the image in space

In MRI the B_0 field is usually generated by coils of superconducting wire. Gradient coils can change the B_0 field. A transmitter coil transmits the RF pulse and receiver coils detect the RF pulses generated by the relaxing protons. The transmitter and receiver coils may be combined together (eg head coils). The gradient coil generates an intentional inhomogeneity in the B_0 field which allows spatial information to be deciphered. Three orthogonal gradient coils are used to allow three-dimensional spatial encoding in the x, y and z directions and hence the image can be constructed. The gradients are referred to as the:

1) slice-select gradient
2) phase-encoding gradient
3) frequency-encoding gradient.

The vector of application of these three gradients can be varied to vary the plane of imaging to suit the tissue being investigated (axial, sagittal, coronal or oblique). Oblique planes can be obtained by combining gradients.

2.1.4 The slice-select gradient

The slice-select gradient is produced by varying the magnitude of the B_0 field in a particular direction. The Larmor frequency of the protons therefore varies with the slice-select gradient. By using different RF pulse frequencies then different protons along the slice-select gradient can be flipped, hence an image plane can be selected. Usually a range of frequencies (the "bandwidth" of the pulse) are used. The thickness of the image slice can be varied by changing the bandwidth of the RF pulse or by changing the amplitude of the slice-select gradient. Mostly the latter is varied as there is

a limitation as to how much the bandwidth can be decreased. If contiguous slices are imaged then the edges of the consecutive slices may overlap causing interference or cross-talk. This can be overcome by having gaps between slices or by using an acquisition that images consecutive slices at different times and then interleaves them when the image is constructed. The slice-select gradient is only turned on during the application of the RF pulses.

2.1.5 The frequency-encoding gradient

Each image slice is composed of a grid of pixels. Each pixel will have its own signal intensity. In MRI the signal recorded is the sum of all the pixels. The signal intensity of each individual pixel needs to be reconstructed to generate the image. To distinguish points along the frequency-encoding gradient (or read-out gradient) a magnetic field is applied in this direction and therefore the Larmor frequency of the protons varies. The frequency-encoding gradient is applied only when the signal is measured. The signal strength at each frequency can be measured. To extract this information a Fourier transform is needed. The Fourier transform is a continuous frequency distribution curve that plots amplitude of the signal against frequency.

2.1.6 The phase-encoding gradient

Phase-encoding occurs by applying a gradient in the phase-encoding direction for a short period after the RF pulse, usually between the 90° pulse and the 180° pulse or between the 180° pulse and signal measurement. Protons at different positions in this gradient will therefore precess at a different frequency. When the gradient is switched off all protons will again precess at the same frequency but they will no longer be in phase. Differences in spatial position are therefore "phase-encoded". The number of repetitions of the pulse sequence equals the number of rows of pixels in the image. For each repetition, the phase-encoding gradient is applied with increasing amplitude and therefore the effect of phase-encoding is greater.

Most imagers use 256 or 512 frequency gradations in the frequency-encoding direction and a multiple of 64 phase-encoding rows (128, 192, 256). When the signal is recorded the frequency-encoding gradient is applied hence the protons in each pixel will have a

distinct frequency and a distinct phase, which are unique and encode the x and y coordinates for that pixel.

2.1.7 Image processing

The signal produced from each phase-encoding step is in the form of a set of sine waves comprising a composite of the signal from each pixel. The imager records the amplitude of the signal at equally-spaced intervals in time called sampling points. This is stored as a matrix of data. Each row of numbers represents a set of sampled points for each phase-encoding step and each column represents a point in time. This matrix of data can be thought of in terms of "k-space" and contains the same number of points as the final image. Each point in the image though arises from all points in k-space. The centre of k-space contains the phase-encoding steps with the weakest gradients and therefore with the highest signal. This area provides contrast. The periphery of k-space contains the phase-encoding steps with the largest gradients and hence the least signal. This area gives information about boundaries and gives sharpness to the final image.

By a mathematical transformation (Fourier transformation) the sine waves are converted into a matrix of data consisting of individual pixels. Each pixel has x and y coordinates and an intensity value (representing the amplitude of the signal at that point). The image can therefore be reconstructed.

2.2 Optic nerve imaging

MRI of the optic nerve is challenging for many reasons (Barker, 2000). These principally are:

1) Its small size and tortuosity
2) Its mobility
3) The surrounding CSF
4) Orbital fat
5) The bones of the orbital canal and air-fluid interfaces from the adjacent sphenoid and ethmoid sinuses

The optic nerves are approximately 40-50mm long and 3-5mm in diameter (Williams *et al.*, 1989; Tamraz, 1994; Sadun, 1998). Resolution of the small structures or lesions contained within the nerves is dependent upon the voxel size. If the voxel size is too large then resolution will be impaired due to partial volume effects (ie mixing of signal from neighbouring structures). The voxel size can be reduced by increasing the matrix size, however if the voxel size is too small then there may not be enough signal resolved to produce an image because the signal-to-noise ratio (SNR) is reduced. Resolution and SNR can be increased by increasing the acquisition time or by increasing the magnetic field strength. Increasing the magnetic field strength however will increase the longitudinal relaxation time of the tissue being imaged, also potentially leading to increased acquisition time. There is also the possibility of more susceptibility artefacts (see later) from surrounding tissues at higher field strengths leading to worsening of the SNR (Horsfield, 2000). Signal averaging can also improve the SNR and thereby improve the resolution, again at the expense of increased acquisition time (Barker, 2000). Increasing acquisition time will lead to more movement artefact, particularly in the mobile optic nerve. Fast imaging techniques are therefore required to give high SNR with an acceptable acquisition time (Gass *et al.*, 1995).

The optic nerves are surrounded by a CSF-filled nerve sheath and, in the orbit, by lipid (Williams *et al.*, 1989; Sadun, 1998). Due to its high PD lipid typically gives high signal intensity on both T_1- and PD/T_2-weighted imaging (Figure 2.6). CSF gives high signal intensity on PD- and T_2-weighted imaging. This may cause problems due to obscuring the edge of the optic nerves and hence CSF suppression may be desirable. In

certain circumstances however the bright CSF may assist in identification of the nerve (Barker, 2000).

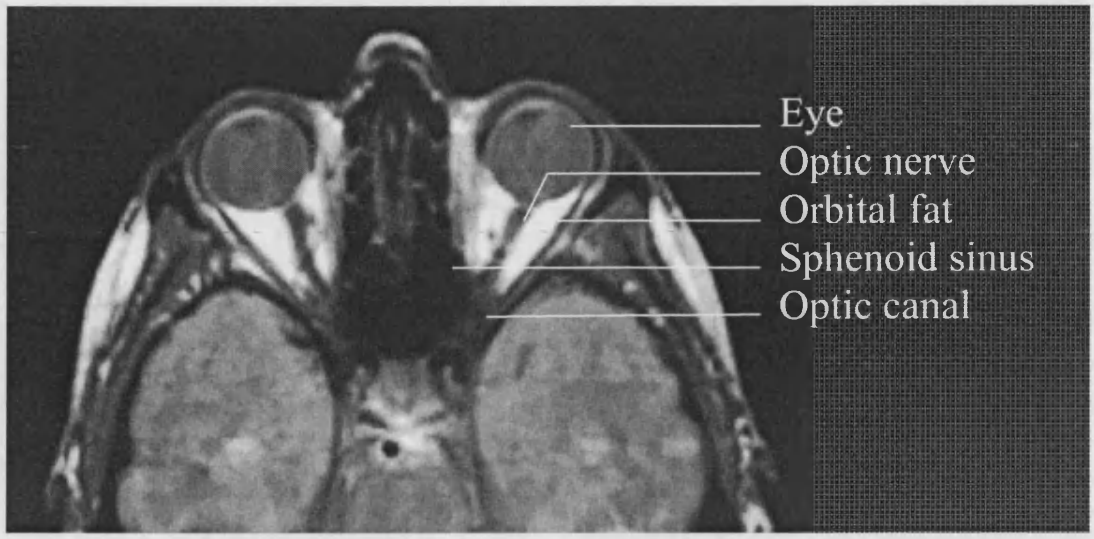

Figure 2.6: Axial PD-weighted FSE image demonstrating optic nerve anatomy.

2.2.1 Artefact

There is also a considerable potential for artefact in optic nerve imaging, more so than in the brain. The most important sources of artefact with possible solutions are discussed below:

(i) Chemical shift artefacts

As has been discussed, the optic nerves are surrounded by lipid in the orbits. Orbital fat produces a signal that is much more intense than the water signal leading to excessive partial volume effects. In addition chemical shift artefacts can occur at lipid-water boundaries. Due to their differing chemical environments protons in lipid have a lower precession frequency than protons in water. The lipid protons are therefore misregistered relative to the water protons in the frequency encoding direction (Soila *et al.*, 1984). This can lead to decreased signal where the lipid is displaced away from water and high signal where lipid and water overlap. This chemical shift artefact is more prominent at higher field strengths (Barker, 2000). High signal and chemical shift artefacts from orbital fat can be suppressed using STIR imaging (Johnson *et al.*, 1987)

or a frequency-selective fat saturation excitation pulse prior to imaging time (Gass *et al.*, 1995).

(ii) Motion artefacts

Motion in a structure causes image blurring in the direction of movement and "ghost" artefacts in the phase-encoding direction due to the signal being reconstructed over and over. The major motion problem in optic nerve imaging is random motion due to eye movements. On ocular movement the intra-orbital portion of the optic nerve shifts against the direction of gaze with an increasing extent from the relatively fixed posterior part at the orbital apex anteriorly (Liu *et al.*, 1992). Motion artefacts can be reduced by using fast imaging techniques with multiple signal acquisitions and signal averaging or by using GE rather than spin echo techniques because a 180° refocusing pulse is not required in GE imaging (mobile protons may have moved before the 180° pulse has been applied (Taber *et al.*, 1998; Barker, 2000). Subjects undergoing optic nerve imaging can also be encouraged to relax, close their eyes and avoid deliberate eye movements. Taping down the eyelids has been suggested (Iwasawa *et al.*, 1997), although this seems a little extreme.

(iii) Susceptibility artefacts

Susceptibility artefacts occur at interfaces between different tissues, due to the different magnetic properties of the tissues. It is more apparent at higher field strengths and can cause rapid dephasing of spins with signal loss and mismapping artefacts (Hashemi & Bradley jr, 1997). It is a particular problem in the canalicular portion of the optic nerves due to the bony cavity of the optic canal and air from the adjacent sphenoid and ethmoid sinuses. Metals, particularly iron, can cause a lot of image distortion and subjects should be carefully screened for metal in clothing before imaging commences. Susceptibility artefacts can be reduced by using spin echo rather than GE or echo planar imaging (EPI) because the spin echo sequence includes a refocusing pulse (Barker, 2000).

Imaging of the optic nerves is therefore a trade-off between imaging time, resolution, SNR and the amount of artefact induced.

2.3 Magnetic resonance imaging in optic neuritis

MRI provides a valuable opportunity for *in vivo* study of the pathological evolution of optic neuritis and, by inference, other central nervous system inflammatory /demyelinating lesions with clinical and electrophysiological correlation. There follows a summary of the studies and pulse sequences used in optic neuritis.

2.3.1 Short *tau* inversion recovery imaging

The first imaging technique used to investigate optic neuritis was the STIR sequence. This utilises a 180° RF pulse prior to the excitation pulse to invert the net magnetisation. A short inversion time (TI) is then used so that the lipid signal is approximately zero (due to its short T_1 relaxation time) whilst other tissues continue to give a negative signal (Johnson *et al.*, 1987; Brown & Semelka, 1999). Thus when the 90° excitation pulse is applied these tissues will be flipped whereas the fat signal will remain zero. This suppresses the fat signal relative to, in particular, water. The images are displayed with reversed polarity to make most tissues appear bright and lipid dark.

In a study of 37 patients following an episode of optic neuritis using STIR imaging (TR 1500ms, TE 40ms, TI 150ms, matrix 256x256, field of view [FOV] 15cmx15cm, number of excitations [NEX] 2, 5mm contiguous slices, Picker 0.5T imager) lesions were detected in 84% of symptomatic nerves and 20% of asymptomatic nerves (Miller *et al.*, 1988). Slow (>4 weeks for vision to improve to 6/9) or poor (<6/9 at 6 months) visual recovery was associated with longer lesions (mean number of abnormal 5mm coronal slices 3.50 versus 1.84, $p<0.01$) although there was no correlation between lesion length and latency or amplitude of the P100 response of the VEP. Eleven out of 15 patients (73%) with lesions involving the optic canal also had a poor recovery which was thought to be due to compression of the swollen optic nerve within the tight confines of the bony canal. These findings were confirmed by Dunker and Wiegand (1996). They examined 22 patients acutely and again after a mean of 4.7 years (range 2.5-8 years) with STIR MRI of the optic nerves (TR 1800ms, TE 35ms, TI 140ms, Siemens 0.5T imager at baseline; TR 2100ms, TE 20ms, TI 150ms, Siemens 1.0T imager at follow-up). Lesions less than 17.5mm long either acutely or chronically were correlated with complete visual recovery (visual acuity >20/25, no visual field, colour

vision or contrast sensitivity defect). Intracanalicular lesions correlated with incomplete visual recovery (visual acuity >20/25 but other deficits present).

Kakisu *et al.* (1991) demonstrated that although the lesion length on STIR (TR 1500ms, TE 40ms, TI 100ms, Picker 0.5T imager) was not correlated with pattern-reversal VEP findings in the acute phase, there was a significant correlation in the chronic phase (r=0.68, p<0.005). There was however, no correlation between lesion length and visual acuity.

High signal in optic nerves following optic neuritis remains chronically despite improvements in vision and VEP findings (Youl *et al.*, 1996) and may be seen in MS in the absence of acute attacks of optic neuritis (Davies *et al.*, 1998).

Subsequently a study was performed to see whether STIR MRI of the optic nerves could help to predict whether corticosteroids could be targeted more effectively in optic neuritis (Kapoor *et al.*, 1998). Sixty-six patients with acute unilateral optic neuritis had their optic nerves imaged with the STIR sequence (TR 2500ms, TE 40ms, TI 175ms, matrix 256x128, FOV 16cmx16cm, NEX 2, 5mm contiguous slices, General Electric 1.5T imager). They were then randomized to receive either 1g/day IVMP for three days or placebo. Patients were stratified into those with short or long ($\geq$ 3 involved coronal slices) lesions. The presence of canalicular involvement was also noted. Patients with longer lesions tended to present earlier (mean 8.4 versus 12.1 days, p<0.05) however there was no correlation between initial visual acuity and initial lesion length. Treatment with IVMP was not associated with improved visual outcome at six-months in those patients with long or canalicular lesions and treatment did not affect six month lesion length on repeat imaging. An association between initial canalicular involvement and poor recovery was not seen, however after six months canalicular involvement was seen in all 16 patients with a poor visual recovery compared with only 31 out of 45 patients with a good recovery (p<0.01).

The STIR sequence has some drawbacks. A long TR is required to enable all the T_1 relaxation to occur in the different tissues prior to the next inversion pulse, leading to an increased acquisition time. Tissues with T_1 similar to fat will have their signal suppressed and the contrast between other tissues may be reduced. There may also be a

signal void at fat-water interfaces. Care must be taken when interpreting images after administration of gadolinium as this is a T_1 contrast agent. The STIR sequence will result in decreased signal from tissues that have taken up the contrast agent rather than enhanced T_1 signal that is normally expected and easier to depict (see later) (Brown & Semelka, 1999).

2.3.2 Chemical shift imaging

This technique involves a spin echo acquisition followed by a sequence with the read-out timing adjusted to vary the relative amounts of water and fat signal in each voxel. The images are combined so that images containing only water or fat can be produced (Brown & Semelka, 1999). Optimisation of the field homogeneity is crucial for consistent image appearance. This method however doubles the imaging time and requires post-processing. A derivation of this technique using chopper fat suppression has been reported (Lee *et al.*, 1991). Here normal signal averaging is employed with the first acquisition having the 90° and 180° pulses in phase and the second reversing the phase of the 90° and having the 180° pulse offset by a delay. With pre-saturation of fat and subtraction of the second data set from the first during signal averaging, a fat-suppressed single image dataset is produced with no increase in imaging time. Using this sequence (TR 2000-2500ms, TE 30-35 or 70-80ms, 128 phase steps, FOV 20cmx20cm, 3mm slices with 1-1.5mm intersection gap, Signa 1.5T imager) the sensitivity for detecting optic neuritis lesions was 89% with 100% specificity and 86% accuracy.

2.3.3 Frequency selective fat saturation

By applying a narrow bandwidth RF pulse centred at the precession frequency of fat in the absence of a gradient the resulting transverse magnetisation can be dephased by spoiler gradients. Any imaging sequence can then be used including T_1- or T_2-weighted images and after the administration of contrast signal enhancement results leading to easier to interpret images. The suppression of fat signal is not as high as with STIR imaging due to T_1 relaxation occurring between the fat saturation pulse and the imaging pulse. The degree of suppression will also be affected by magnetic field

inhomogeneities as the precession frequency varies with magnetic field strength (Brown & Semelka, 1999).

2.3.4 Fat saturated fast spin echo imaging

The major disadvantage of spin echo imaging is the poor resolution possible within an acceptable acquisition time (Barker, 2000). Imaging time can be decreased using multiple echoes to reduce the number of excitation pulses required. The rapid acquisition with relaxation enhancement sequence, now more commonly known as FSE, uses multiple echo trains from a single TR, each using slightly different amount of phase encoding gradient to build up the image in k-space, rather than each line in k-space coming from different TRs as in spin echo imaging (Hennig *et al.*, 1986; Brown & Semelka, 1999). The amplitude variations between the echoes are due to both the phase-encoding amplitude and the TE. The effective TE (TEef) is recorded as this is the TE of a multi-echo sequence at the centre of k-space where image contrast principally occurs. The echo train length (ETL) is the number of echoes delivered for each TR. For optic nerve imaging with fat saturation the FSE sequence allows for increased resolution and image quality with an acceptable acquisition time. In a study comparing STIR (TR 2000ms, TE 50ms, TI 175ms, NEX 1, matrix 256x256, FOV 20cmx20cm, in-plane resolution 0.8x0.8mm, 5mm slices with 0.5mm inter-slice gap, 2 acquisitions, General Electric 1.5T imager with 13min acquisition time) with fat-saturated FSE (TR 3250ms, TEef 68ms, ETL 16, NEX 4 , 512x512 matrix, 24cm rectangular FOV, in-plane resolution 0.5x0.5mm, 3mm interleaved contiguous slices, General Electric 1.5T imager with 11min acquisition time) lesions were detected in 18 out of 21 symptomatic optic nerves with acute optic neuritis using STIR compared with 20/21 using FSE (Gass *et al.*, 1996). Mean lesion length was 15.4mm on STIR images and 17.3mm on FSE images. Using fat-saturated FSE dual echo imaging is possible giving both PD- and T_2-weighted images from the same acquisition if appropriate TEefs are chosen (Barker, 2000). It is not yet known how results of imaging using FSE in optic neuritis relate to visual impairment in the acute phase and prognosis for recovery of vision.

2.3.5 Combined fat and water suppression imaging

On FSE and, particularly the lower resolution STIR, CSF gives high signal which may obscure the signal from the optic nerves (Gass *et al.*, 1996). It is possible to suppress the signal from CSF using fluid-attenuated inversion recovery (FLAIR) techniques. The FLAIR sequence uses an inversion pulse with a long TI for CSF suppression which increases the acquisition time. For optic nerve imaging fat saturation and fast acquisitions are required hence a combined selective partial inversion recovery pre-pulse with a FLAIR sequence and FSE acquisition (SPIR-FLAIR) has been developed to try to achieve these aims (Jackson *et al.*, 1998). SPIR-FLAIR (TR 8000ms, TE 120ms, TI 2200ms, ETL 21, matrix 256x256, FOV 16cmx16cm, 3mm slices with 1mm intersection gap, 2 acquisitions, Philips 1.5T imager with 4min acquisition time) was compared with both SPIR (TR 3085ms, TE 120ms, ETL 12, matrix 512x512, FOV 18cmx18cm, 3mm slices with 1mm intersection gap, 2 acquisitions, Philips 1.5T imager with 4min 25s acquisition time) and STIR (TR 1560ms, TE 50ms, TI 165ms, ETL 4, matrix 256x256, FOV 18cmx18cm, 3mm slices with 1mm intersection gap, 2 acquisitions, Philips 1.5T imager with 2min 41s acquisition time) imaging in the assessment of optic neuritis. Both SPIR-FLAIR and SPIR detected lesions in all 21 symptomatic optic nerves imaged whereas STIR imaging detected only 20/21. Lesion lengths were also longest on the SPIR-FLAIR images (17.2mm on SPIR-FLAIR, 15.8mm on SPIR and 13.8mm on STIR, $p<0.01$) even though the in-plane resolution was less than with SPIR imaging.

2.3.6 New pulse sequences and methods of analysis

Although the above conventional MRI techniques are sensitive in detecting the lesions of optic neuritis there is a lack of pathological specificity to allow prediction of the chronological age of these lesions. This is because oedema, demyelination and gliosis all demonstrate high signal on T_2-weighted images (Miller *et al.*, 1998). As has been discussed imaging of the optic nerves is particularly limited by issues of poor resolution. Increasing the SNR requires very large increases in acquisition time. Using conventional imaging techniques at present is therefore limited by the technology available (Horsfield, 2000). The only pointers to age the lesion have been a subjective impression of optic nerve swelling in the acute phase and atrophy in the chronic phase

(Miller *et al.*, 1988; Gass *et al.*, 1996; Jackson *et al.*, 1998; Kapoor *et al.*, 1998). Other techniques have been developed which are able to study the optic nerves in order to understand better the pathophysiology of optic neuritis. These have principally been applied in brain imaging in MS but, with recent technological advances, optic nerve imaging using these techniques has also been possible.

2.3.7 Gadolinium "enhancement"

Dimeglumine gadopentate is the most common contrast agent used in MRI as gadolinium is a paramagnetic substance. In areas of acute inflammation where there is blood vessel wall leakage gadolinium will accumulate and show up as high signal on T_1-weighted imaging due to shortening of T_1. Optic nerve imaging imposes some constraints due to the need for fat suppression. If STIR imaging is used then the signal from gadolinium is also suppressed hence a drop in signal is indicative of acute inflammation and gadolinium "leakage" rather than gadolinium enhancement (Brown & Semelka, 1999). In a study of 18 patients with acute optic neuritis (2 with bilateral simultaneous disease) STIR imaging (TR 2000ms, TE 40ms, TI 150ms, 5mm contiguous slices, Picker 0.5T imager) was performed before and after injection of 0.02mmol/kg dimeglumine gadopentate (Youl *et al.*, 1991). Ten of the patients (one with bilateral simultaneous optic neuritis) had MRI twice, once a mean 6.4 days (range 2-13 days) after onset of symptoms and again a mean 27.8 days (range 20-32 days later). Clinical and electrophysiological examination was also performed at each occasion. Of the 31 examinations in total, gadolinium leakage was seen in 6/6 lesions where the time since onset of optic neuritis was less than seven days, in 7/8 lesions where time since onset was 7-13 days but in only 5/17 lesions where the age of the lesion was at least 14 days. Gadolinium leakage in the hyper-acute phase was associated with decreased visual acuity, pain on eye movement, an RAPD, swelling of the optic disc (p=0.001 for each clinical feature compared with the asymptomatic optic nerves) and decreased amplitude of the P100 component of VEP (p<0.001). There was a trend for patients with longer lesions to have worse visual acuity (acuity <6/9 in 4/5 patients with gadolinium leakage on $\geq$3 slices, compared with 4/8 studies with leakage on 1-2 slices, p=0.1). In those patients who had a follow-up MRI gadolinium leakage had ceased in 9/11 symptomatic optic nerves. This was associated with an improvement in all the above clinical features and increased P100 amplitude (p=0.02)

compared with the first examination. It was concluded that acute inflammation is associated with conduction block in the optic nerve and that resolution of inflammation plays an important role in the recovery process. As has been discussed these findings have been supported by work performed *in vitro*.

A recent report confirmed that gadolinium enhancement is a consistent feature of acute optic neuritis and that the lesion length had clinical significance at presentation (Kupersmith *et al.*, 2002). In this retrospective series 101/107 (94%) symptomatic optic nerves demonstrated enhancement following gadolinium on fat saturated T_1-weighted imaging. Optic nerves with $\geq$ 17mm enhancing segment on axial images had poorer baseline Snellen visual acuity (p=0.02), Humphrey 24-2 threshold perimetry (p=0.009) and colour vision on Ishihara plates (p=0.01). Canalicular involvement was associated with poorer colour vision (p=0.04). The location and length of the initial lesion however, was not predictive of the degree of visual recovery in the 93 patients (68 treated with corticosteroids) with clinical follow-up after six months.

Further studies are required to give a more accurate view of the temporal relationship between enhancement, visual impairment, and electrophysiology. The previous studies on optic neuritis used single- or double-dose gadolinium. Triple-dose (0.03ml/kg dimeglumine gadopentate) gadolinium increases the sensitivity for detecting enhancing lesions in MS by 66-75% compared with the use of single-dose gadolinium (Filippi *et al.*, 1996; Silver *et al.*, 1997). The sensitivity is further increased by introducing a delay between the injection and imaging and by using magnetisation transfer (MT) imaging (Silver *et al.*, 1997). It is not known yet whether the use of triple-dose Gd will add more information about prognosis in optic neuritis.

2.3.8 Optic nerve size

Optic nerve size can be judged on MRI both subjectively and objectively.

(i) Optic nerve swelling

Optic nerve swelling, suggesting the presence of acute inflammation and oedema, on STIR MRI was reported in three out of 37 cases (8%) of acute optic neuritis in the first

major imaging study performed that investigated the condition (Miller *et al.*, 1988). It had been thought to be a rare occurrence in optic neuritis and if swelling was present then a glioma or meningioma should be suspected (Cornblath & Quint, 1997). However, in a further study of acute optic neuritis using STIR imaging, swelling was reported in 12 out of 40 cases (40%) with, and in four out of 26 cases (15%), without canalicular involvement (Kapoor *et al.*, 1998). Also, using formal measurement of optic nerve size with callipers from the intraorbital optic nerve on hard copy STIR images (TR 2000ms, TE 40ms, TI 150ms, matrix 128x256, FOV 15cmx15cm, Picker 0.5T imager) from 10 patients Youl *et al.* (1996) reported that the mean area of symptomatic optic nerves with acute optic neuritis (mean disease duration 6 days) was 20.0 (standard deviation [SD] 2.7)mm^2 compared with 14.4 (SD 3.5)mm^2 for asymptomatic contralateral optic nerves (p=0.001). After a mean follow-up period of 28 days the mean area of the symptomatic optic nerves had decreased to 15.5 (SD 4.6)mm^2 (p=0.01) whereas the asymptomatic optic nerves had a mean area of 14.1 (SD 4.1)mm^2 (p=not significant [NS]). Both visual acuity and VEP amplitudes improved on follow-up whereas VEP latencies did not improve significantly. This suggested that resolution of acute inflammation was associated with resolution of optic nerve swelling.

(ii) Optic nerve atrophy

An expected end result of demyelination and axonal loss is atrophy of tissue. Measurements of CNS atrophy are used increasingly to monitor disease progression in both natural history studies and therapeutic trials (Miller *et al.*, 2002). Atrophy of tissue in MS could potentially result from both demyelination and axonal loss. However, axons contribute almost twice as much to the bulk of white matter as myelin (Miller *et al.*, 2002) and axonal loss would seem likely to be the more important determinant of atrophy. There have been many studies of brain and spinal cord atrophy in MS using MRI. These measures are either of the whole brain or a representative part, for example brain lateral ventricle volume or spinal cord area at C2/3. They tend to represent the global effects of disease rather than the effect of lesions on a single pathway. The latter could, in principle, be assessed in the optic nerve. Being able to quantify the degree of optic nerve atrophy following optic neuritis would be useful since, as already discussed, optic neuritis is a model for the effects of lesions in MS. This is technologically very demanding for a number of reasons. An appropriate fast pulse sequence with fat

saturation is required to produce high resolution images. The positioning of the patient and has to be reproducible for serial studies so that the scan-rescan variation is low and the measurement method has to be robust with low variation on repeat measurement.

Youl *et al.* (1996) also studied 22 patients with a mean disease duration of 60 days. Optic nerve area in both symptomatic and asymptomatic nerves was 16.8mm^2. After a mean of 405 days the patients were re-imaged. The mean area of symptomatic nerves decreased to 12.8 (SD 4.2)mm^2 (p<0.001) and the asymptomatic nerves to 16.3 (SD 3.3)mm^2 (p=NS). This was despite improvement in visual acuity, VEP amplitude (p=0.03) and VEP latency (p=NS) in the affected eyes. The STIR sequence Youl *et al.* used had the disadvantages of low resolution (pixel size 1.2x0.6mm), the presence of high signal from CSF obscuring the edge of the optic nerve and the inclusion of optic nerve sheath leading to an overestimation of optic nerve area.

FSE images have also been assessed for optic nerve atrophy by manual measurement of nerve diameter in papilloedema and autosomal dominant optic atrophy but as with STIR, high signal from CSF within the nerve sheath mitigates against accurate delineation of the nerve itself (Mashima *et al.*, 1996; Votruba *et al.*, 2000).

The combined CSF and fat suppression of SPIR-FLAIR imaging has allowed optic nerve atrophy to be detected qualitatively following optic neuritis. Inter-observer assessment of optic nerve size was 1.0 using a weighted Cohen κ test for SPIR-FLAIR compared with 0.85 for SPIR and 0.61 for STIR (sequences which were not CSF suppressed) (Jackson *et al.*, 1998).

Recently, Inglese *et al.* (2002) imaged 30 patients with RRMS and SPMS who had had a previous episode of optic neuritis. A T_1-weighted spin echo (TR 500ms, TE 14ms, matrix 224x512, FOV 15.6cmx25cm, 3mm slices with 0.3mm gap, 1.5T imager) sequence was used. The mean volume of the optic nerves was calculated from the mean areas from 11 slices using a local thresholding segmentation technique. The mean volume was 93.3 (SD 3.5)ml in 18 age-matched controls, 89.2 (SD 9.8)ml for clinically healthy nerves (n=18), 89.4 (SD 11.0)ml for diseased optic nerves with visual recovery to at least 20/25 (n=20) and 79.0 (SD 9.8)ml for diseased optic nerves with vision worse than 20/25 (n=22) (p=0.002, versus optic nerves with good recovery). Optic nerve

volume was correlated with both visual acuity (r_S=0.39, p=0.01) and VEP P100 latency (r_S=-0.31, p=0.05). The functional significance of optic nerve atrophy was therefore apparent although the correlations were modest. Formal measures of reproducibility were not included in this study.

A formal quantitative study is required to assess whether a CSF and lipid suppressed sequence is of use in the detection of optic nerve atrophy. For quantitative assessment it would be helpful if high signal from affected optic nerves is also suppressed - to enable more accurate blinding between affected and unaffected nerves and between patients and controls. It would also be of benefit for signal-intensity based automated contouring techniques to avoid potential bias in manual outlining. The SPIR-FLAIR sequence would not be suitable as it is T_2-weighted and optic nerve lesions give high signal. A fat-saturated fast FLAIR sequence that is less T_2-weighted may be of use here and would warrant investigation.

The relationship between optic nerve swelling and atrophy needs elucidating further, combining this with other imaging modalities such as fat saturated post-gadolinium T_1-weighted spin-echo imaging. The temporal and functional relationship between gadolinium enhancement, optic nerve swelling and optic nerve atrophy can then be elucidated.

2.3.9 Magnetisation transfer imaging

MT imaging provides a means by which tissues can be examined in more detail, going beyond the T_1 and T_2 characteristics. There follows a description of its physical basis (Wolff & Balaban, 1989; McGowan, 1999; Barker, 2000; Van Buchem & Tofts, 2000). In tissues water can be thought to exist in two states: "free" as in intra- and extracellular fluid and "bound" which consists of water involved in cellular membranes and myelin sheath. As has been discussed the relaxation characteristics of protons depends in part on the macromolecular environment (tissue) in which the protons lie. The bound water has restricted motion, short T_2 relaxation (~20μs compared to 80ms for free water), a resonant frequency close to that of free water and is present at a much lower concentration than free water in most tissues such that, when using conventional imaging techniques, signal from this pool is not included. The bandwidth for the bound

water is however much broader than for free water (≥ 10kHz compared with ~200Hz) (Figure 2.7)

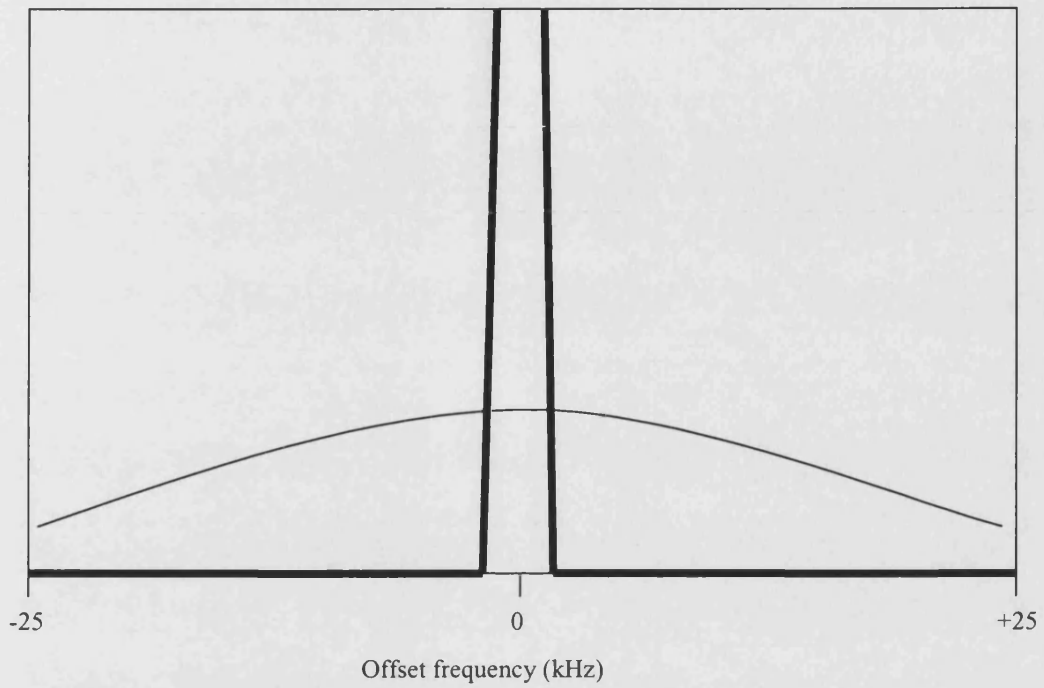

Figure 2.7: Simulated spectrum for bound (fine line) and free water (bold line). The areas under the curves are in the ratios of the water concentrations.

If an RF pulse is applied in the absence of a gradient with a frequency that includes the bound protons but not the free protons (ie an appropriate offset frequency) the bound protons can be partially saturated. There then follows an exchange of energy (magnetisation transfer) between the bound and free protons by chemical exchange or spin-spin interaction (cross-relaxation). If an attempt is then made to image the free protons, the signal from them will be reduced in proportion to the degree of exchange that has occurred with the bound protons. Use of MT therefore allows the hitherto invisible bound water to be examined and provides a means of increasing contrast. It also provides a means of producing quantitative images by calculating the degree of exchange between bound and free protons. If images are produced of the same slice both with and without an MT pre-pulse the MT ratio (MTR) can be calculated which is an indication of the amount of signal reduction that has occurred due to the MT pulse. It is calculated using the formula:

$MTR = [(M_0-M_S) / M_0] \times 100$ percent units

Where M_0 is the signal intensity in absence of the MT pre-pulse and M_S is the signal intensity in the presence of the MT pre-pulse. By custom the MTR is expressed as percent units (pu). The higher the MTR, the greater the reduction in signal and hence the greater the bound water pool is. It is not an absolute measure but is dependent on the amplitude and frequency offset of the MT pulse as well as the time delay between the MT pulse and the excitation pulse. It also varies between imagers and in the same imager due to coil non-uniformity, thus requiring accurate repositioning of patients in serial studies.

The MT sequence for MTR calculation requires low T_1-weighting (as the MT pulse shortens the T_1 time of tissues) and minimal motion between the M_0 and M_S images. GE imaging is usually used due to its low T_1-weighting (Barker, 2000). It does not include a 180° refocusing pulse, instead the signal is produced following a reversal of the gradient pulses (Brown & Semelka, 1999). Usually flip angles <90° are used with a short TR which decreases imaging time and power deposition to the patient.

Analysis of the images to give the MTR can be done in two ways. The conventional approach is to examine an ROI placed manually or using semi-automated techniques. This is useful when examining a particular tissue or a lesion. The positioning of the ROI is important to avoid partial volume pixels contaminated from adjacent tissues. The ROI also has to be accurately re-positioned both on the same image and in serial studies to ensure reproducibility and confidence that any changes detected are real and not artefactual due to variation in ROI placement. An alternative approach is to generate histograms containing information from all the pixels in the tissue to be examined. This can give an indication of the global burden of disease and can detect subtle changes in what appears to be normal tissue. Again reproducible segmentation and the avoidance of partial volume pixels are important.

MT imaging has been combined with histopathological examination to give an indication of the physical basis of the MT effect:

(i) Magnetisation transfer imaging in experimental allergic encephalomyelitis

MTR calculation has been performed on lesions in guinea-pigs due to EAE in combination with histological analysis (Dousset *et al.*, 1992). The MTR of two identified acute lesions from two animals decreased over the first 12 days following immunisation with homologous spinal cord in Freund's adjuvant by 6-7% ($p<0.001$), although in one animal there was an initial early rise in MTR. Symptoms appeared around day 10. Clinical decline mirrored the decline in MTR. Histological examination was performed on day 14. The lesions were oedematous with a mononuclear cell infiltrate but had no demyelination.

The experiments were repeated in a relapsing EAE model in macacas fascicularis monkeys (Brochet & Dousset, 1999). The MTR decreased initially but then progressively increased. The degree of demyelination was related to the decrease in MTR. Remyelination was associated with a restoration of MTR to normal, although resolution of oedema was also thought to play a rôle. After repeated attacks the MTR did not return to the normal. This was related to mild astrogliosis.

Lesions produced by direct injection of lysophosphatidylcholine into the centrum semiovale of macacas fascicularis monkeys can produce both myelin and axonal damage. The MTR in these lesions showed a larger decrease than in the relapsing EAE model (Brochet & Dousset, 1999).

(ii) Magnetisation transfer imaging in a Wallerian degeneration model

Lexa *et al.* (1994) surgically ablated the visual cortices from one hemisphere of 10 cats. MT imaging was then performed at varying intervals with histological analysis. In the first two weeks following the ablation the MTR in the optic radiations were higher on the ablated side compared to the contralateral hemisphere ($p<0.02$) followed by a fall in MTR over the next two weeks ($p<0.01$). The initial rise in MTR was associated with the early phase of Wallerian degeneration with axonal collapse, increased axoplasmic density and collapse of myelin tubes. Later on demyelination occurred with gliosis.

These studies indicate that early changes due to inflammation and Wallerian degeneration may be associated with an early rise in MTR, possibly due to exposure of myelin fragments to extracellular tissue increasing the exchange of magnetisation. Low MTR results from a decreased capacity for exchange due to oedema, demyelination and gliosis. Axonal loss combined with demyelination results in even greater falls in MTR. Remyelination can result in restoration of MTR.

(iii) Magnetisation transfer imaging combined with histopathological examination in multiple sclerosis

In a post mortem study van Waesberghe *et al.* (1999) demonstrated a strong correlation (r_S=0.71) between MTR and axonal density but a weaker correlation between MTR and myelin density (r_S=0.45) in active demyelinating lesions. In all regions MTR correlated strongly with axonal density (r_S=0.83, p<0.0001).

(iv) Magnetisation transfer imaging in optic neuritis

Optic nerve MT imaging requires high resolution and a fast imaging sequence to minimise motion artefacts between the M_0 and M_S images. The optic nerve is small and therefore imaging does not produce enough pixels for meaningful histogram analysis. An ROI-based approach is therefore required. All the studies to date of MTR in the optic nerves have relied on manual placement of small ROIs, typically only of 4-8 pixels. This risks the exclusion of important information if the optic nerves are swollen, as in acute optic neuritis and the inclusion of partial volume pixels containing CSF and orbital fat in the presence of optic atrophy. Also, none of the studies have included an indication of reproducibility of the results. For these reasons the results should be viewed with some caution.

In a study of 39 patients with acute optic neuritis and 50 controls (selected from patients having brain imaging for other indications) Boorstein *et al.* (1997) placed 8 pixel ROIs in the intraorbital portions of optic nerves on MT images (TR 106ms, TE 5ms, flip angle 12°, matrix 256x192, FOV 16cmx16cm, 3mm slices, 1.5T imager, acquired both with and without a 19ms saturation pulse, amplitude 3.7μT, offset frequency 2kHz). The MTR was 41.1 (SD 1.2)pu in control optic nerves, 30.6 (SD 2.4)pu in 22 optic

nerves in which either a high signal lesion was present on T_2-weighted images or contrast-enhancement was seen and 36.3 (SD 1.6)pu in 12 of the remaining 18 patients who had no high signal lesion but who demonstrated a reduction in MTR. MTR was therefore more sensitive than conventional imaging at detecting abnormalities in diseased optic nerves although no clinical or electrophysiological correlations were presented.

Thorpe *et al.* (1995) imaged six controls and 20 patients between three months and 16 years following optic neuritis (five of whom had MS, three with both eyes affected). One slice was acquired in the intraorbital portion of each optic nerve incorporating a lesion where possible (TR 180ms, TE 8ms, flip angle 40°, matrix 256x256, FOV 16cmx16cm, 3mm slice, 1.5T imager, acquired both with and without a 64ms saturation pulse, effective bandwidth 78Hz, amplitude 14.5μT, offset frequency 1kHz). The MTR was calculated as described above and recorded from a four pixel ROI placed in the centre of the nerve. The mean MTR was 49pu in controls, 48pu in clinically healthy nerves and 42pu in diseased nerves ($p<0.005$ versus healthy nerves and control nerves). The MTR was correlated with VEP whole field latency ($r_S=-0.554$, $p<0.01$) but not Snellen visual acuity. Lesion length on T_2-weighted FSE images was correlated with visual acuity ($p<0.02$). The negative correlation between MTR and VEP latency supports the idea that MTR reduction may be due to demyelination. The lack of correlation with clinical measures is consistent with the complex relationship between demyelination and conduction discussed in the previous chapter.

In addition to the optic nerve atrophy measurements in MS described above Inglese *et al.* (2002) also measured MTR in the optic nerves using a four pixel ROI from the whole length of the optic nerve from a two-dimensional (2D) GE sequence (TR 640ms, TE 12ms, flip angle 20°, matrix 256x256, FOV 25cmx25cm, 15 contiguous 5mm slices, 1.5T imager, acquired both with and without a saturation pulse, Gaussian envelope duration 7.68ms, offset frequency 1.5kHz, flip angle 500°). The mean MTR was 35.3 (SD 2.4)pu in 18 age-matched controls, 35.1 (SD 4.7)pu for clinically healthy nerves (n=18), 34.6 (SD 3.6)pu for diseased optic nerves with visual recovery to at least 20/25 (n=20) and 29.6 (SD 4.1)pu for diseased optic nerves with vision worse than 20/25 (n=22) ($p<0.001$, versus optic nerves with good recovery). When MTR was correlated with clinical and electrophysiological tests opposite results to Thorpe *et al.* (1995) were

obtained. MTR correlated with visual acuity (r_S=0.49, p=0.01) but not VEP P100 latency (r_S=-0.10). A possible explanation for the latter finding was that the cohort was biased towards those with a limited visual recovery, over 50% having a visual acuity worse than 20/25. Axonal loss in the optic nerve may have been more pronounced in this group

The above studies used 2D GE imaging. It would be desirable to use a three-dimensional (3D) sequence to minimise partial volume effects by having the highest resolution possible. Partial volume voxels at the junction between the nerve and surrounding CSF cause a particular problem for MTR measurement. The optic nerve has a much greater surface area/volume ratio than the brain and therefore greater proportion of partial volume voxels. The proportion increases with atrophy and there is therefore a danger in studies of optic nerve MTR chronically after optic neuritis to be measuring decreased MTR due to increased measurement of these voxels rather than due to changes in the nerve substance itself. The segmentation technique, as well as the acquisition sequence, should be selected with care.

The temporal evolution of MTR changes after an acute attack of optic neuritis and the relationship with imaging, clinical and electrophysiological parameters needs to be clarified. It would be desirable to confirm by imaging the electrophysiological observation of remyelination in the recovery process.

2.3.10 Diffusion-weighted imaging

Diffusion of water molecules *in vivo* is affected by the structure of the tissue. In white matter tracts, of which the optic nerve is an example, the structure is in the form of tightly packed axons. Diffusion occurs preferentially along the orientation of the axons. In the direction orthogonal to the axons, cellular membranes act as a greater barrier to the water molecule, hindering and restricting the process of water diffusion. Because of the complexity of the diffusion mechanism in tissue *in vivo* the measurements are dependent on the observation time, ence the term "apparent diffusion coefficient" (ADC) was introduced to indicate this dependency and its difference from the free diffusion coefficient of water. The directional dependence of the ADC *in vivo* is called anisotropy and is one of several parameters which can be derived from the diffusion

tensor (Basser *et al.*, 1994). If the white matter tracts are disrupted or the permeability of axonal membranes is increased then the ADC will increase and the fractional anisotropy (FA), a measure of the alignment of tissues, will decrease.

Diffusion-weighted imaging (DWI) refers to any MRI technique which has been made sensitive to the properties of molecular motion. Usually a spin-echo pulse sequence is applied both with and without extra magnetic field gradient pulses, for diffusion encoding. The applied gradients do not affect stationary molecules but causes an un-refocused phase shift and hence loss of signal from molecules that move during the measurement period relative to the signal acquired when no diffusion gradient is applied. The amount of signal loss that can be measured in each voxel is determined by the *average* diffusion coefficient in that voxel.

Studies in MS have revealed increased ADC values and decreased FA values in both lesions and normal appearing white matter (Ciccarelli *et al.*, 2001; Filippi & Inglese, 2001). DWI of the optic nerves in optic neuritis presents many challenges, as previously reported (Wheeler-Kingshott *et al.*, 2002) and for the reasons discussed above. The optic nerves are small and mobile, therefore rapid high-resolution single-shot techniques would be desirable to reduce motion artefacts within and between each image (Barker, 2000). CSF contamination of the optic nerves may lead to artificial elevation of the ADC and orbital fat may cause chemical shift artefacts. Furthermore, the bones of the orbital canal and air-fluid interfaces from the adjacent sphenoid and ethmoid sinuses are sources of susceptibility artefacts, potentially causing severe image distortions when employing single-shot DW techniques such as EPI sequences.

To sample the full diffusion tensor it is necessary to acquire a minimum of seven images: one without any diffusion weighting and six with diffusion weighting applied along six non-colinear directions (Basser & Pierpaoli, 1998). This makes it very sensitive to motion occurring between each acquisition. Ideally, one would wish to implement a registration algorithm capable of correcting the possible variable spatial position of the ON. An alternative is to acquire several images with the same diffusion weighting and average them after reconstruction to determine the central position of the optic nerve, with the drawback of longer acquisition times. Hence, most DWI studies of optic nerve have concentrated on measuring the ADC along fewer directions (rather

than the full diffusion tensor) as fewer acquisitions are required (Iwasawa *et al.*, 1997; Freeman *et al.*, 1998; Wheeler-Kingshott *et al.*, 2002).

Iwasawa *et al.* (1997) studied the optic nerves with a spin-echo sequence which had low diffusion weighting ("b-factor" of 262.05s/mm^2) and cardiac gating for a single slice through the orbital optic nerve. Three acquisitions were performed with the diffusion gradients in the x, y and z directions respectively. Due to motion artefacts the ADC could only be measured in the y and z directions, and not always reliably then. The ADC was measured from a 1mm diameter circular region-of-interest (ROI) placed in the centre of the nerve. In seven controls the mean ADC was 982 (SD 741) x 10^{-6}mm^2/s in the y direction and 1559 (SD 675) x 10^{-6}mm^2/s in the z direction. In four nerves with acute optic neuritis the mean ADC was 843 (SD 742) x 10^{-6}mm^2/s in the y direction and 941 (SD 431) x 10^{-6}mm^2/s in the z direction. In nine nerves with previous optic neuritis the mean ADC was 1560 (SD 690) x10^{-6}mm^2/s in the y direction and 4180 (SD 1130) x 10^{-6}mm^2/s in the z direction (p<0.001 versus controls and acute optic neuritis).

EPI is a single-shot multi echo imaging technique, which allows high resolution with high SNR per unit time, but at the expense of susceptibility and chemical shift artefacts. For optic nerve DWI a fat- and CSF-suppressed zonal oblique multi-slice EPI (ZOOM-EPI) sequence has been recently developed (Wheeler-Kingshott *et al.*, 2002). This sequence uses a limited field-of-view along the phase-encoding direction, shortening the echo train length, which reduces susceptibility artefacts and therefore image distortions. In a pilot study ZOOM-EPI DWI was carried out on three controls. After off-line post-processing with magnitude signal averaging (and correction for the effects of the Raleigh noise distribution) the mean ADC from the optic nerves as a combination of the x, y and z gradients could be calculated over the length of the optic nerves and was found to be 1058 (SD 101) x 10^{-6}mm^2/s.

Recently, Chabert *et al.* (2002) developed an axial fast spin-echo acquisition which could measure the ADC and FA in individual optic nerves. In four volunteers the mean diffusivity was 1670 (SD 450) x 10^{-6}mm^2/s with a mean FA of 0.59 (SD 0.08), reflecting strong anisotropy in the optic nerve. The fibre directions followed the expected nerve fibre directions on anisotropy maps. The sequence was free of

susceptibility artefacts however it was neither fat- nor CSF-suppressed and so the results should be interpreted with caution.

DWI offers the potential to offer pathologically specific imaging with measures that are thought to be sensitive to changes in nerve structure, particularly axonal disruption. DWI will not be considered further in this work although application of DWI in both patients acutely affected by, and recovering from, optic neuritis would be of interest. The functional significance of any changes measured would need to be elucidated with reference to clinical and electrophysiological tests.

2.3.11 Functional magnetic resonance imaging

The above studies have all focused on the imaging properties of the optic nerves and the structural changes that have occurred due to optic neuritis. An alternative approach is to study the effect of optic neuritis on brain function. fMRI allows the study of brain function as it utilises the differing T_2* decay properties of oxygenated and de-oxygenated haemoglobin (Simon & McDonald, 2000). Increased activity in a certain area of the brain will cause increased blood flow in that area. The increased oxy-haemoglobin/deoxy-haemoglobin ratio causes a transient increase in signal on T_2*-weighted images, the BOLD or blood oxygen level dependent effect. Changes over time for each voxel can be measured. In a study of patients with unilateral optic neuritis an average 33% decreased activation in the occipital cortex was seen upon stimulation of the affected eye with red lights flashing at 8Hz compared with controls and 61% decreased activation upon stimulation of the contralateral unaffected eye (Rombouts *et al.*, 1998).

In a subsequent study, Werring *et al.* (2000) recruited seven patients who had recovered vision to 6/5 following unilateral optic neuritis and had no brain lesions on imaging. In controls, stimulation of either eye just led to activation in the occipital cortex. In patients, stimulation of the previously affected eye resulted in activation in the insula-claustrum, thalamus, lateral temporal and posterior parietal cortices as well as the occipital cortex. Stimulation of the clinically unaffected eye led to activation of the occipital cortex and right insula-claustrum only. The extra-occipital activation appeared delayed compared with the occipital activation. The volume of extra-occipital

activation correlated with VEP latency (r_S=0.71, p=0.005). These extra-occipital areas are known to have extensive connections with the visual system. It was therefore concluded that part of the recovery process following optic neuritis may be due to functional reorganisation of the cerebral response to visual stimulation.

Serial changes in occipital cortex activation have also been measured in the recovery period following acute optic neuritis (Langkilde *et al.*, 2002). Eleven patients with untreated monosymptomatic optic neuritis were imaged with fMRI using 8Hz pattern reversal checkerboard stimulation serially from a mean of 10 days after symptom onset, and again at 34, 70 and 461 days. The number of activated voxels and the median BOLD signal increased, when stimulating the affected eye, with recovery and correlated with Snellen visual acuity (p=0.014 and p=0.001 respectively). On binocular stimulation the BOLD signal peaked at day 30, in parallel with the period of largest functional recovery. These changes suggested that dynamic adaptive changes may contribute to recovery.

The dynamic changes in the recovery process in the extra-occipital areas need to be elucidated. Whole brain coverage of the acquisition would be desirable for this. A key question is whether the observed occipital and extra-occipital responses are necessary for recovery. The responses in patients with good versus poor recoveries, and how the responses relate to structural and electrophysiological changes in the optic nerves, need further investigation.

2.4 Aims of this thesis

The aims of the series of studies outlined in this thesis are to elucidate further the pathophysiology of optic neuritis and so gain further insights into the mechanisms behind relapse, recovery, partial recovery and persistent disability in MS.

2.4.1 Optic neuritis as a model for multiple sclerosis relapses

The major event in RRMS is the acute relapse. The majority of patients with MS present with such an event. Most early relapses are followed by complete or near complete recovery, however partial recovery or significant disability can result from an individual relapse, and is often seen in patients with established relapsing remitting disease. Study of relapses *in vivo* is therefore desirable. MRI provides a non-invasive means of study of patients and is very sensitive at detecting MS lesions (Miller *et al.*, 1998). It would be desirable to be able to study of individual lesion responsible for a relapse in order to understand better the pathophysiology of the condition. This should make prediction of the prognosis for recovery from a relapse better and could provide a means of monitoring treatment effects in future therapeutic trials of novel agents in acute MS relapse. Unfortunately, in the brain and spinal cord, it has been difficult to reliably identify the lesion that is responsible for the symptoms of an individual relapse (Behan *et al.*, 2000) and most new brain lesions which are apparent on MRI are clinically silent (Miller *et al.*, 1998). New methods of MRI acquisition and analysis in the brain have also been better at studying the global burden of the disease and its effects on disability and progression than in studying individual lesions.

There are also difficulties when trying to study disability and impairment in MS. The most commonly used test is the EDSS (Kurtzke, 1983). This is a 10-point ordinal scale combining observer-derived scores for visual, brainstem, pyramidal, cerebellar, sensory, sphincter and cerebral function with walking ability. The EDSS is simple to perform, but at lower scores it is weighted towards impairment and at higher scores it is weighted towards disability, particularly walking ability (Thompson & Hobart, 1998). It is also rater-dependent. Inter-rater reliability is reasonable with an intraclass correlation coefficient (ICC) of 0.78 but intra-rater reliability is variable (ICC 0.62-0.94) (Hobart *et al.*, 2000). The EDSS has limited use in monitoring individual relapses, being a

composite scale. The multiple sclerosis functional composite (MSFC) combines scores for 25-foot timed walk, 9-hole peg test and paced auditory serial addition test. It is less rater-dependent than EDSS with inter- and intra-rater ICC of 0.95 and 0.97 respectively (Cohen *et al.*, 2000). The MSFC is now used alongside the EDSS in clinical studies of MS, but again is less useful for investigating the effects of a single lesion. Arm function can be assessed using the Medical Research Council 0-5 scale of muscle strength and the Ashworth or the modified Ashworth spasticity scale (Sloan *et al.*, 1992). These also have the disadvantage of being rater-dependent. The 9-hole peg test and box-and-block tests are more responsive to change than use of the composite scores alone and can be used to monitor arm function serially (Goodkin *et al.*, 1988). However, the manual dexterity required to perform the test reflects motor, sensory and cerebellar function in the arm and makes study of a single system harder if impairments exist in other modalities.

In comparison with single symptomatic lesions elsewhere in the CNS, optic neuritis provides a more attractive model to study the effects of relapses in MS. As has been discussed, optic neuritis is a frequent manifestation of MS and has been regarded as a *forme fruste* of the disease (Ebers, 1985). The natural history of acute optic neuritis mirrors that of an acute MS relapse elsewhere in the CNS and the response to corticosteroid therapy is the same (Brusaferri & Candelise, 2000). The optic nerves can also be affected by chronic damage, seen with the loss of the nerve fibre layer in the retina in MS patients (Frisen & Hoyt, 1974) and STIR MRI signal change in the optic nerves of SPMS patients in the absence of previous episodes of optic neuritis (Davies *et al.*, 1998).

Patients with optic neuritis often seek medical attention early in the course of their illness and therefore, with appropriate access to eye hospitals, good case ascertainment is possible. Visual function can also be measured accurately in a rater-independent fashion. The full range of acuities from 6/6 or better through to NPL has been reported in approximately equal proportions (Perkin & Rose, 1979; Optic Neuritis Study Group, 1991). Reliance cannot, however be made solely on visual acuity as abnormalities using other visual tests can be detected in patients with acute optic neuritis and "normal" visual acuity of 6/6 (Frederiksen *et al.*, 1991) and on recovery visual acuity alone may be less sensitive than other visual tests to detect abnormal vision

(Frederiksen *et al.*, 1997). However, the use of logMAR visual acuity does allow for parametric statistical analysis (Ferris III *et al.*, 1982). The figure given is the logarithm of the minimum angle of resolution. The chart allows for testing of vision at non-standard distances giving scores up to +1.68, approximately 6/300 Snellen equivalent (one letter read at 1m distance). The worst score is +1.70 (no letters read) and therefore logMAR acuity cannot differentiate between patients with counting finger acuity or worse.

Visual field testing gives extra information about vision outside the macula. It was initially thought that the predominant defect was a central or paracentral scotoma (Perkin & Rose, 1979) however it has become apparent that any type of field defect may be possible (Beck, 1998). The principal means of testing visual field are with either the Humphrey visual field analyser (Allergen Humphrey, San Leandro, CA, USA) or Goldmann perimeter. For studies of optic neuritis the 30-2 programme (testing the central 30° of vision) of the Humphrey visual field analyser is used more often as it is automated, and with use of the company-supplied software, deviation of the patient's results from expected age-matched normal results can be derived. This is given in decibels (a logarithmic scale) and again, like logMAR acuity, allows for parametric statistical analysis. Although the test is rater-independent, results from patients with recovered optic neuritis do show increased variability compared with controls. Wall *et al.* (1998) recorded a mean within-subject SD for mean deviation of 0.46dB for same-day measurements and 0.36dB for weekly measurements in 10 healthy volunteers compared with 1.35dB and 3.10dB in 17 patients with recovered optic neuritis respectively. A number of factors may have been responsible including temperature effects and fatigue. There is also some evidence to suggest that response variability in visual field testing worsens with decreased sensitivity due to loss of functioning neural channels (Henson *et al.*, 2000).

Colour vision can be examined using Ishihara pseudoisochromatic colour plates (Kanehara and Co. Ltd., Tokyo, Japan) or the FM 100 test (Farnsworth, 1943). The Ishihara plates provide a useful and rapid screening test for the presence of an optic neuropathy (Sloan, 1942), however parametric analysis is not possible. The FM 100 test takes longer but allows for parametric analysis. It is not, however, reliable in patients with a visual acuity of worse than 6/60 (Katz, 1995).

Contrast sensitivity can be measured using spatial frequency gratings with 98% of optic neuritis patients showing decreased sensitivity at 6 cycles per degree (CPD) ranging down to 80% at 18 CPD (Wakakura *et al.*, 1999b). Pelli-Robson charts allow for more rapid assessment (Pelli *et al.*, 1988) and 98.2% of patients at presentation in the ONTT demonstrated some abnormality although again, parametric analysis is not possible (Optic Neuritis Study Group, 1991).

As well as accurate and reliable tests of visual function across a spectrum of different parameters it is also possible, as has been discussed, to measure the latency and amplitude of the VEP which gives information about the integrity of the visual conducting pathways (Halliday *et al.*, 1972). Finally, MRI, with appropriate fat saturation techniques, enables the symptomatic lesion in optic neuritis to be visualised (Gass *et al.*, 1996).

Developments in imaging technology and application now means that, potentially more pathologically specific imaging sequences can be applied to the study of the optic nerves (Barker, 2000). This thesis will investigate the application of these new imaging techniques, along with clinical and VEP measures, to the study of optic neuritis in order to gain new insights into the effect of individual lesions on structure and function in the CNS in the short- and long-term.

It will show that optic neuritis is a useful model to study some of the main features on MS namely relapse, remission, partial recovery and persistent disability. The study concentrates on the use of MRI in optic neuritis and the relationship between imaging results and clinical and electrophysiological measurements. At present there are poor predictors of recovery in optic neuritis. The use of new MRI sequences to aid in the prediction will be assessed. To combine the different parameters and to follow them over time multiparametric analysis will be needed. The aim will be to describe the natural history and to see what factors are important in predicting prognosis for recovery.

This thesis will concentrate on structural imaging of the optic nerve in optic neuritis. The cortical response to optic neuritis is being investigated in a parallel study in the NMR Research Unit by Dr. A.T. Toosy.

2.4.2 Magnetic resonance imaging in optic neuritis

Optic nerve MRI, especially quantitative MRI using the parameters mentioned in earlier sections, presents considerable difficulties. The sequences need careful setting up. Subject motion, especially optic nerve motion is a particular problem. Subjects need to be selected who can tolerate the moderately long acquisition times that are necessary for high resolution imaging. They need to be instructed to keep as still as possible and to avoid deliberate eye movements. Fixation on one spot for acquisitions of up to 20 minutes is not possible. Most success has been achieved by asking patients to close their eyes and to avoid deliberate eye movements as much as possible. Subjects are not discouraged from sleeping as the onset of rapid eye movement (REM) sleep usually occurs later then 60-100 minutes after sleep onset (Lesch & Spire, 1990).

Optic nerve imaging has the potential for poorer reproducibility compared to brain imaging, as a result of movement artefacts causing poor scan-rescan reproducibility and because of difficulty in segmenting the optic nerves from images due to their small size leading to poor measurement-remeasurement reproducibility.

Quality assurance is important, particularly in serial imaging studies, to ensure that the output from the imager remains stable. This takes two principal forms. The first is by serial imaging of phantoms to ensure that the gradients are stable (Barker & Tofts, 1992). This is useful for MT imaging and DWI. For atrophy measurements serial imaging of healthy controls will give an indication of the stability of the measurements over time (Leary *et al.*, 1999).

In addition the small size of the optic nerves means that there will be a greater proportion of partial volume voxels compared with other structures as the surface area to volume ratio increases as an object gets smaller. It should be borne in mind that measured changes may be as a result of this phenomenon rather than pathological changes in the nerve itself, for example when measuring MTR.

In summary, a thorough evaluation of optic nerve imaging requires that the reproducibility, accuracy and stability of the imaging measures be carefully considered and understood. Such a methodological approach is needed to ensure a sound interpretation of the results in patients with optic neuritis.

Chapter 3 Studies of Optic Nerve Atrophy Following Optic Neuritis

3.1 Detection of optic nerve atrophy following a single episode of unilateral optic neuritis by magnetic resonance imaging using a fat saturated short echo fast fluid-attenuated inversion recovery sequence.

3.1.1 Introduction

In MS, atrophy of the brain and spinal cord correlates with clinical progression and may indicate axonal loss (Losseff *et al.*, 1996a; Losseff *et al.*, 1996b; Simon *et al.*, 1999). As has been discussed optic neuritis provides an excellent model for studies to elucidate the pathogenetic mechanisms of disability in demyelinating diseases and development of a reliable imaging technique for quantifying atrophy in the optic nerve would facilitate such studies. However, MRI of the optic nerve presents many problems due to its size and tortuosity, the presence of high signal from orbital fat and the CSF-filled sheath around the nerve, and the potential for motion artefact due to eye movement (Gass *et al.*, 1995). A new imaging sequence is evaluated here: fat saturated short echo fast FLAIR (sTE fFLAIR) which suppresses the high signal from fat and CSF and demonstrates both optic nerves with in-plane resolution of $0.5mm^2$ and 3mm slice thickness in $13^1/_2$ minutes. This has enabled quantification of optic nerve atrophy following a single episode of unilateral optic neuritis.

3.1.2 Patients and methods

17 patients were recruited following a single episode of unilateral optic neuritis at the Neuro-ophthalmology clinic at Moorfields Eye Hospital, London and Neurology and Ophthalmology clinics at Addenbrooke's Hospital, Cambridge. Optic neuritis was diagnosed using previously agreed clinical criteria (Compston *et al.*, 1978). No patient had a history of visual disturbance affecting the contralateral eye, although two patients had clinically probable MS (CPMS) and five CDMS by the Poser criteria (Poser *et al.*, 1983). The remainder were classified as having a CIS. The patients' median age was 40 years (range 23-51 years) with a median time since the onset of optic neuritis of 21 months (range 3-81 months) (Table 3.1).

Subject	Gender	Age at assessment (years)	Time since onset (months)	Clinical status
1	F	23	21	CIS
2	M	34	24	CIS
3	F	51	81	CPMS
4	F	41	67	CPMS
5	F	44	66	CIS
6	M	42	27	CIS
7	F	40	50	CIS
8	F	43	3	CIS
9	F	29	29	CIS
10	F	29	3	CIS
11	F	25	10	CDMS
12	F	50	5	CIS
13	F	47	9	CDMS
14	M	36	5	CIS
15	F	28	13	CPMS
16	M	25	26	CDMS
17	M	50	7	CDMS

Table 3.1: Subject, gender, age at assessment, time since onset of optic neuritis and clinical status.

Ethical approval was obtained for the study from the joint ethics committee of the Institute of Neurology and the National Hospital for Neurology and Neursurgery; informed consent in writing was obtained from each subject, according to the Declaration of Helsinki. A clinical assessment was carried out including Snellen visual acuity and 24-2 or 30-2 Humphrey perimetry (Allergan-Humphrey Inc., San Leandro, CA, USA).

Optic nerve MRI was performed on a Signa 1.5T imager (General Electric, Milwaukee, Wisc., USA) with coronal-oblique sTE fFLAIR (TR=2740ms, TE=16ms, TI=1072ms, NEX 6, ETL 6, matrix size 512x384, FOV 24x18cm, 3mm contiguous slices) and coronal-oblique fat suppressed dual echo FSE (TR=2300ms, TEef=58/145ms, NEX 2, ETL 8, matrix size 512x384, 24x18cm rectangular FOV, 3mm contiguous slices) sequences. Eleven patients had axial-oblique dual echo FSE brain imaging

(TR=2400ms, TEef 15/105ms, NEX 2, ETL 8, matrix size 256x256, 24x18cm rectangular FOV, 5mm contiguous slices). We also studied 30 control subjects, median age 27 years (range 21-48 years), using the sTE fFLAIR sequence only. Repeat imaging was performed on 18 of the controls at a later date to determine the acquisition-reacquisition reproducibility. Control subjects had to be free of significant ophthalmological or neurological disease and were recruited by the use of advertising posters. During optic nerve imaging all subjects were asked to close their eyes and avoid eye movements if possible.

The images were analysed on Sun workstations (Sun Microsystem, Mountain View, CA., USA) using the DispImage display tool (Plummer, 1992). On the sTE fFLAIR images, the mean cross-sectional area of the intra-orbital portion of each optic nerve from patients and controls was calculated by a blinded observer from five consecutive 3mm slices from the orbital apex forwards using a computer-assisted contouring technique as previously described (Grimaud *et al.*, 1996). This portion of the optic nerve was chosen because of the ease of identification of the orbital apex, the fact that the nerve lies approximately orthogonal to the imaging plane and to allow comparison of a representative length of the optic nerve between subjects, given that there is variation in the length of the intra-orbital portion of the optic nerve between individuals (Blinkov & Glezier, 1968; Williams *et al.*, 1989; Tamraz, 1994; Sadun, 1998; Slamovits, 1998). A simple contouring technique was chosen rather than setting a 50% threshold between the optic nerve signal and background similar to studies on the spinal cord (Losseff *et al.*, 1996b) because the sequence had some T_2-weighting. The threshold in diseased optic nerves might therefore tend to be higher than healthy optic nerves leading to an underestimate of optic nerve area in diseased optic nerves. Each measurement was carried out three times over the course of one week. The FSE images were assessed for the presence, distribution and length of any optic nerve lesions.

3.1.3 Statistical methods

Statistical analysis was performed using the 'SPSS 9.5 for Windows' statistical package (SPSS Inc., Chicago, Ill., USA). To assess measurement reproducibility the within- and between-subject SD and, hence coefficient of variation (CV) and reliability coefficients, were obtained from random effects analysis of variance (Bland & Altman, 1996a; Bland

& Altman, 1996b; Bland & Altman, 1996c). The acquisition-reacquisition reproducibility was calculated similarly from the measurements produced from the two series of images in the 18 control subjects who had repeat imaging. Paired and independent samples *t* tests were used for the group analyses as appropriate. Analysis of correlations was by Spearman's rank correlation.

3.1.4 Results

The mean cross-sectional area of the diseased optic nerve was 11.2 (SD 2.3)mm^2 and that of the contralateral healthy nerve 12.9 (SD 1.8)mm^2 (p=0.006 compared with the diseased nerve) (Table 3.2, Figure 3.1 and Figure 3.2). The optic nerve mean area in the control group was 12.8 (SD 1.9)mm^2 (Figure 3.2). This was significantly larger than that of the diseased nerve (p=0.014), but not significantly different from the contralateral healthy nerve area (p=0.93).

No.	Snellen visual acuity		Optic nerve mean area (mm^2)		FSE image lesion length (mm)		Humphrey mean deviation (dB)	
	Diseased nerve	Healthy nerve	Diseased nerve	Healthy nerve	Intra-orbital	Total	Diseased nerve	Healthy nerve
1	6/36	6/9	12.6	13.9	21	30	-5.80	-2.53 *
2	6/5	6/5	9.0	10.5	21	24	-4.23	-2.76 *
3	6/6	6/5	8.2	11.2	24	27	-2.65	-1.65 *
4	6/5	6/5	10.9	13.2	3	3	-1.76	-1.12 *
5	6/6	6/5	9.6	12.0	12	12	-3.24	-1.18 *
6	6/6	6/6	12.1	12.3	15	24	-4.82	-4.18 *
7	6/5	6/5	10.8	13.0	12	21	-3.96	-6.71 *
8	6/9	6/5	10.0	10.3	15	15	------	------
9	6/6	6/6	7.3	12.7	0	12	-4.44	-6.37 *
10	6/12	6/5	12.8	14.0	0	18	-2.81	-0.19 †
11	6/18	6/9	9.1	15.1	12	21	-8.71	-4.15†
12	6/5	6/5	15.7	16.7	9	18	+0.4	-0.04 †
13	6/9	6/5	14.7	13.2	12	27	-2.96	-1.47 †
14	6/9	6/5	12.1	13.0	9	9	-1.62	-3.32 †
15	6/9	6/5	12.3	9.7	15	15	-2.81	-2.08 †
16	6/18	6/6	10.5	12.4	18	27	-5.31	-0.54 †
17	6/9	6/6	13.5	15.3	9	9	------	------

Table 3.2: Subject, Snellen visual acuity, optic nerve mean area, FSE image lesion length in the affected optic nerve and Humphrey mean deviation. * = 30-2, † = 24-2.

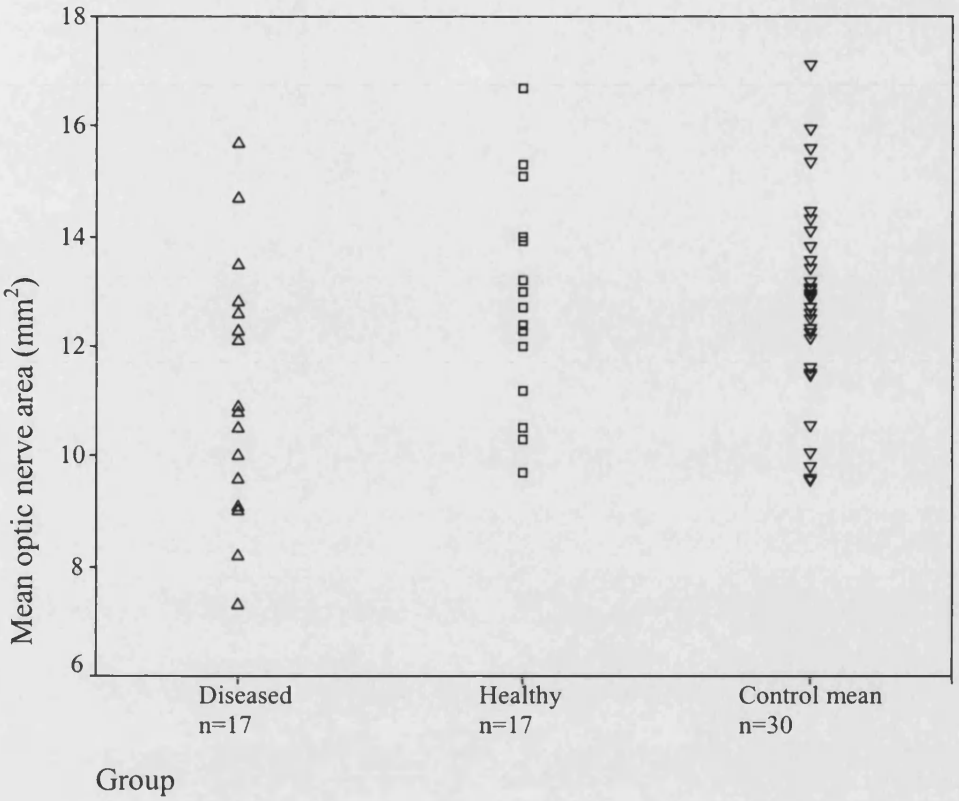

Figure 3.1: Scatter graph illustrating mean optic nerve area in affected optic nerves (n=17 eyes), the contralateral optic nerves in the patients (n=17 eyes), and control optic nerves (n=30, mean of each eye).

Figure 3.2: Coronal sTE fFLAIR image demonstrating right optic nerve atrophy (arrowed) in a 34 year old man (subject 2) two years after right optic neuritis.

There was a significant negative correlation between time since onset of the optic neuritis and the size of the affected optic nerve, expressed as the ratio of the mean area of the affected optic nerve over the mean area of the unaffected nerve (r_S= -0.59, p=0.012) (Figure 3.3).

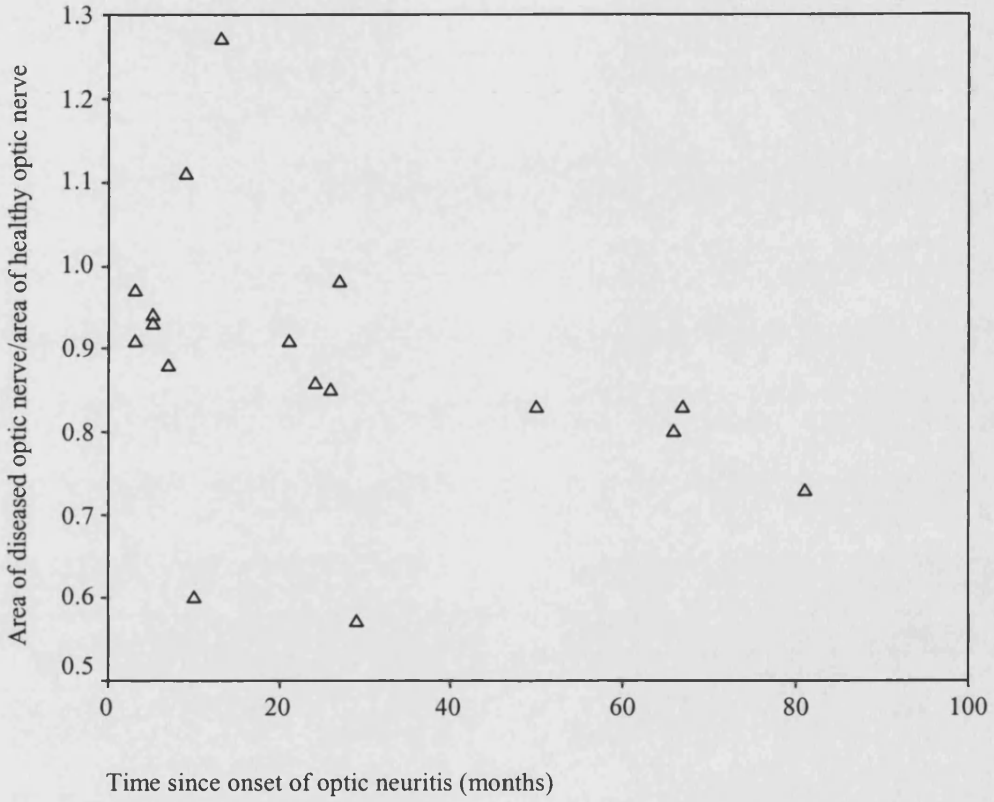

Figure 3.3: The relationship between time since onset of the optic neuritis and the size of the diseased optic nerve, expressed as the ratio of the mean area of the diseased optic nerve over the mean area of the healthy contralateral optic nerve (r_S= -0.59, p=0.012).

The measurement reproducibility results are given in Table 3.3. All patients had a high signal lesion in the affected optic nerve on T_2-weighted FSE images. There was no correlation between the total lesion length or intra-orbital lesion length and the area of the diseased optic nerve (Table 3.2). Five of the subjects had lesions in the contralateral optic nerve. In two of these cases, subjects 13 and 15, the contralateral nerve was smaller than the clinically diseased optic nerve (Table 3.2), but overall the ratio of nerve size (clinically affected versus contralateral nerve) was not significantly different between the groups with or without a contralateral optic nerve lesion (data not shown).

(a)

variable	mean area (mm^2)	within-subject SD	95% reference range[a]	CV (%)	reliability coefficient[b]
diseased nerves	11.2	0.75	± 1.47	6.7	0.90
healthy nerves	12.9	0.76	± 1.49	5.9	0.85
control left nerves	12.9	0.82	± 1.61	6.4	0.83
control right nerves	12.8	0.65	± 1.27	5.1	0.90

(b)

variable	mean area (mm^2)	within-subject SD	95% reference range[a]	CV (%)	reliability coefficient[b]
control left nerves	12.5	0.89	± 1.74	7.1	0.75
control right nerves	12.5	1.09	± 2.13	8.7	0.71

Table 3.3: Measurement reproducibility for the different subgroups.
(a) Measure-remeasure.
(b) Acquisition-reacquisition.

[a]1.96 x within-subject SD. 95% of measurements are expected to lie within this departure from the true value.

[b]The proportion of total variance due to between-subject variation. Under assumptions which are plausible here, one minus this value is the proportion of variation due to measurement error.

There was no significant difference in optic nerve area between patients with clinically isolated optic neuritis and those with CPMS or CDMS, between those with normal and abnormal brain imaging (data not shown), or between patients with poor or good recovery of visual acuity (Miller *et al.*, 1988). However, only four patients had a visual acuity of worse than 6/9 (Table 3.2).

Visual field data was available for 15 patients (Table 3.2). There was no significant difference in the mean deviations between the two eyes and there was no correlation between Humphrey mean deviation and mean area of the diseased optic nerve. Five of the patients had significant Humphrey mean deviations in the contralateral (clinically

unaffected) eyes, defined as -3.0dB (Beck *et al.*, 1993b), two of whom had lesions in the corresponding nerve, subjects 6 and 11.

3.1.5 Discussion

The sTE fFLAIR sequence provides good suppression of fat and excellent suppression of CSF, high spatial resolution and a relatively short acquisition time. This has enabled measurement of optic nerve area with sufficient reproducibility to show optic nerve atrophy following a single episode of unilateral optic neuritis.

Measurement of optic nerve area following optic neuritis has been attempted before, using manual methods from STIR images (Youl *et al.*, 1996). This sequence has the disadvantages of producing high signal from CSF obscuring the edge of the optic nerve and the inclusion of optic nerve sheath. The figure for optic nerve area was about 20% higher than with the sTE fFLAIR method (mean areas ranging from 14.1mm^2 to 16.8mm^2). FSE images have been previously assessed for optic nerve atrophy by manual measurement of nerve diameter in papilloedema and autosomal dominant optic atrophy but as with STIR, high signal from CSF within the nerve sheath mitigates against accurate delineation of the nerve itself (Mashima *et al.*, 1996; Votruba *et al.*, 2000). Formal measures of reproducibility were not included in these studies. A SPIR-FLAIR sequence has recently been described which demonstrated optic nerve atrophy following optic neuritis although again this was a qualitative study (Jackson *et al.*, 1998).

The presence of high signal lesions and visual field abnormalities in the clinically asymptomatic contralateral optic nerves has been previously described (Miller *et al.*, 1988; Beck *et al.*, 1993b) and is likely to reflect clinically silent foci of demyelination. Previous studies have also reported the presence of prolonged VEP latencies from the contralateral healthy eye (Miller *et al.*, 1988; Brusa *et al.*, 1999).

In post mortem studies the area of the optic nerve in normal adults has varied from 6.75 to 12.79mm^2 depending on the technique and which part of the nerve was studied (Donaldson & Bolton, 1891; Sylvester & Ari, 1961; Dolman *et al.*, 1980; Rimmer *et al.*, 1993). The discrepancy with the *in vivo* figures presented here, which are larger, could

be related to post mortem change and shrinkage in the fixation process. It could also reflect the fact that the post mortem areas were measured in a true coronal plane, whereas due to the angle and tortuosity of the nerve, the *in vivo* images may have been oblique to the nerve on some of the slices. Movement artefact may increase the apparent nerve area on imaging. Also, the semi-automated contouring method requires checking to make sure that other orbital structures, eg extra-ocular muscles, are not included in the outline when the nerve lies close to them. The manual correction may produce an over-estimation of the area by the inclusion of partial volume pixels.

The observation that the degree of atrophy is related to the disease duration is interesting. It suggests that atrophy is continuing, possibly as a result of low-grade axonal degeneration due to reduced survival capabilities of axons that exist in a persistently demyelinated state (Scolding & Franklin, 1998; McGavern *et al.*, 2000), or because of Wallerian degeneration distal to axonal damage in the primary lesion. The presence of axonal transection was striking in a recent pathological study of acute inflammatory multiple sclerosis plaques (Trapp *et al.*, 1998). Atrophy of the brain due to Wallerian degeneration does not appear radiologically until some months following other central nervous system lesions such as infarcts which cause axonal loss (Kuhn *et al.*, 1989), and this may explain the apparent progressive atrophy demonstrated here. The continuing atrophy is less likely to result from the recurrent sub-clinical optic nerve demyelination that is known to occur in multiple sclerosis (Feinsod & Hoyt, 1975) as this would be expected to affect both eyes and hence the contralateral optic nerve would be expected to diminish in size as well. In this study there was no overall significant difference in area between the contralateral optic nerves in patients and control optic nerves even though the patients were significantly older than the controls.

It has been shown here that a good recovery of visual acuity and Humphrey mean deviation is possible despite a significant degree of optic atrophy (mean 13% loss of optic nerve cross-sectional area). This suggests that there is redundancy in the anterior visual pathway or that significant cortical re-modelling of visual function has taken place. fMRI data suggest that an altered cortical response to visual stimulation can occur following an attack of optic neuritis (Rombouts *et al.*, 1998; Werring *et al.*, 2000).

Although this sequence has detected atrophy in the clinically diseased optic nerve following unilateral optic neuritis, the reproducibility of this method is not as high as for the studies of cerebral and spinal cord atrophy (Losseff *et al.*, 1996a; Losseff *et al.*, 1996b). The likely reasons for this are related to the smaller size of the optic nerves and greater liability for movement artefact.

3.2 Continuing optic nerve atrophy following optic neuritis: A serial magnetic resonance imaging study

3.2.1 Introduction

Atrophy of the brain and spinal cord occur in MS and are thought to be due predominantly to axonal loss (Losseff & Miller, 1998). In cross-sectional MRI series the degree of detected atrophy has been found to correlate well with measurements of disability (Losseff & Miller, 1998; Liu *et al.*, 1999). Short-term serial studies have demonstrated progressive atrophy, although poor correlations with changes in disability have been found (Stevenson *et al.*, 1998; Fox *et al.*, 2000). Longer follow-up improves the correlation with change in clinical status (Losseff & Miller, 1998; Rudick *et al.*, 1999). The previous chapter described a reproducible technique to measure orbital optic nerve mean area using a fat saturated sTE fFLAIR sequence which removes the high signal from both orbital fat and CSF in the sheath of the optic nerve. Optic nerve atrophy was demonstrated following optic neuritis and the degree of atrophy related to time since onset of the illness. The present report extends the observations of the previous chapter with a serial study to assess the degree of optic nerve atrophy that occurred over a one-year period in a cohort of patients following optic neuritis and to investigate the effect of atrophy on visual function. Using optic neuritis as a model, the study has implications for the effect of lesions in MS.

3.2.2 Patients and methods

Ten patients (six following one episode of optic neuritis, whom also featured in the previous study, two following two episodes in one eye and two following episodes in both eyes) were recruited from Neurology clinics at Addenbrooke's Hospital, Cambridge, UK. Six of the patients had CDMS, one had CPMS and three had clinically isolated optic neuritis (CIS) (Poser *et al.*, 1983). The patients' median age was 44 (range 25-55) years with a median time since the first episode of optic neuritis of 19.5 (range 3-252) months. Only one of the patients had corticosteroids in the acute phase of the optic neuritis. No patients received immunomodulatory therapy, either before or during the period of study. Ethical approval was obtained for the study from the joint ethics committee of the Institute of Neurology and the National Hospital for Neurology

and Neursurgery; informed consent in writing was obtained from each subject, according to the Declaration of Helsinki. Visual acuity using Snellen charts and pattern-reversal VEPs were recorded at baseline and after one year. Visual acuity was classed as poor (<6/9) or good (≥6/9) (Miller *et al.*, 1988). There were no further episodes of optic neuritis in any of the patients during the follow-up period.

MRI was performed on a Signa 1.5-T imager (General Electric, Milwaukee, Wisc., USA). The optic nerves were imaged with the sTE fFLAIR sequence (coronal-oblique, TR=2740ms, TE=16ms, TI=1072ms, NEX 6, ETL 6, matrix size 512x384, 24x18cm FOV, 3mm contiguous slices, acquisition time 13.5 minutes) and the brain was imaged with a dual echo FSE sequence (axial-oblique TR=2400ms, TEef 15/105ms, NEX 2, ETL 8, matrix size 256x256, 24x18cm rectangular FOV, 5mm contiguous slices). Imaging was performed at baseline and again at one year.

Between imaging sessions care was taken to accurately reposition the imaging field of view. In particular, the line from the anterior commissure to the posterior commissure on sagittal localiser images was used to ensure that the subjects' head angles were the same at each session.

The optic nerve images were analysed on Sun workstations (Sun Microsystem, Mountain View, CA., USA) using the DispImage display tool (Plummer, 1992). The mean cross-sectional area of the intra-orbital portion of each optic nerve was calculated by an observer blinded to patient identity from five consecutive 3mm slices anteriorly from the orbital apex using a computer-assisted contouring technique as previously described (Chapter 3.1). Each measurement was carried out on three separate occasions so that the reproducibility of the measurement could be calculated. The hard copy brain images were assessed for any lesions at baseline and any new brain lesions after one year.

3.2.3 Statistical methods

Statistical analysis was performed using the 'SPSS 9.5 for Windows' statistical package (SPSS Inc., Chicago, Ill., USA). To assess measurement reproducibility the within- and between-subject SDs and, hence CV and reliability coefficients, were obtained from

random effects analysis of variance (Bland & Altman, 1996a; Bland & Altman, 1996b; Bland & Altman, 1996c). Paired and independent samples *t* tests were used for the group analyses as appropriate. Analysis of correlations was by Spearman's rank correlation.

3.2.4 Results

The measurement reproducibility results are given in Table 3.4:

variable	mean area (mm^2)	within-subject SD	95% reference range[a]	CV (%)	reliability coefficient[b]
baseline diseased nerves	11.1	0.67	± 1.31	6.0	0.94
1-year diseased nerves	10.2	1.14	± 2.23	11.2	0.82
baseline healthy nerves	12.9	0.67	± 1.31	5.2	0.89
1-year healthy nerves	12.6	0.95	± 1.86	7.5	0.82

Table 3.4: Measurement reproducibility for the different subgroups.

[a]1.96 x within-subject SD. 95% of measurements are expected to lie within this departure from the true value.

[b]The proportion of total variance due to between-subject variation. Under assumptions which are plausible here, one minus this value is the proportion of variation due to measurement error.

At baseline the mean area of the diseased optic nerves was 11.1 (SD 2.7)mm^2 compared to 12.9 (SD 2.0)mm^2 for the healthy nerves ($p = 0.1$). Patients with CDMS or CPMS had smaller optic nerves than patients with CIS although the difference was not significant and the patients with MS also had a longer interval from onset of optic neuritis (data not shown). Seven diseased optic nerves had poor visual acuity and these were significantly smaller than the healthy optic nerves (p=0.02) (Figure 3.4).

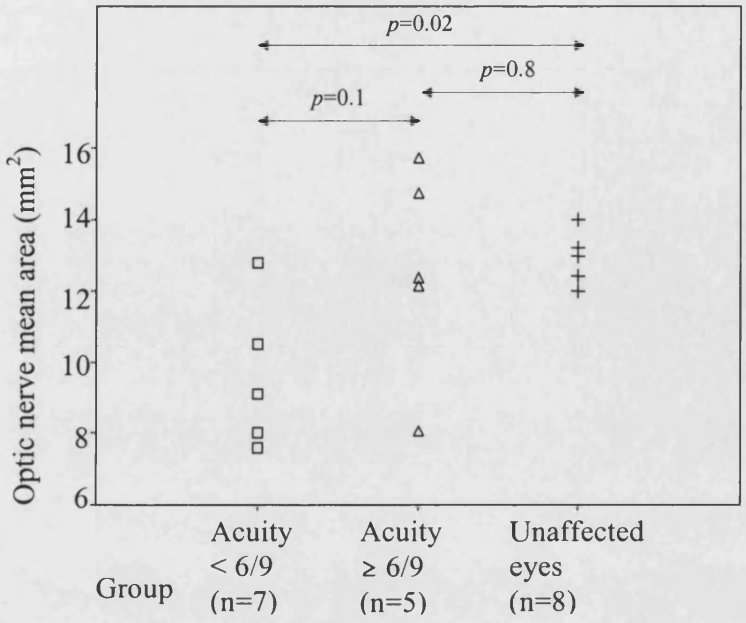

Figure 3.4: The relationship between optic nerve mean area at baseline and visual acuity for diseased eyes with poor recovery of visual acuity (<6/9) and good recovery of visual acuity (≥ 6/9), compared with healthy eyes.

Both the baseline VEP amplitude (r_S=0.65, p=0.02) (Figure 3.5) and VEP latency (r_S= -0.61, p=0.04) correlated significantly with the mean area of diseased optic nerves but not healthy optic nerves.

The mean area of diseased optic nerves decreased significantly over one year from 11.1 (SD 2.7)mm^2 to 10.2 (SD 2.4)mm^2 (p = 0.01) (Figures 3.6 and 3.7) whereas the healthy optic nerves did not change significantly (12.9 [SD 2.0]mm^2 to 12.6 [SD 2.0]mm^2, p = 0.6). After one year the difference in area between all diseased and healthy optic nerves became significant (p=0.04). There was a negative correlation between time since onset of the optic neuritis and change in mean area over time (r_S=-0.81, p=0.001).

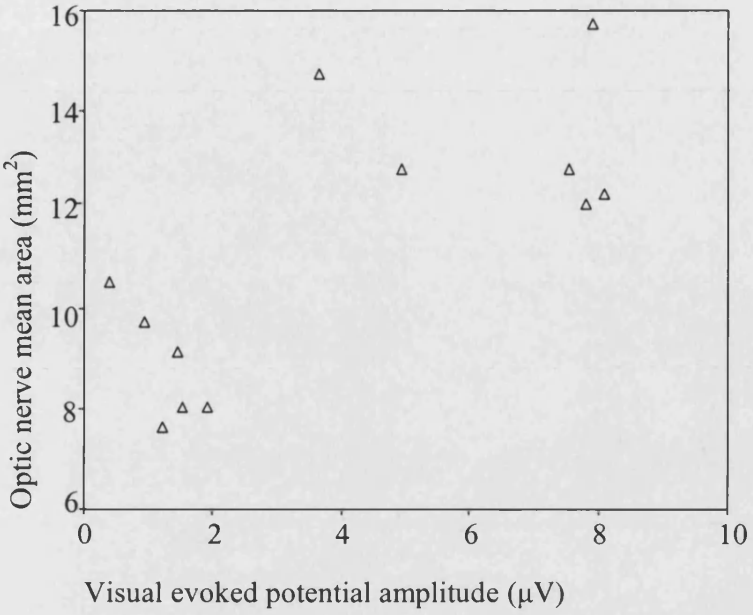

Figure 3.5: Graph demonstrating the relationship between diseased optic nerve mean area at baseline and visual evoked potential amplitude (r=0.65, p=0.02).

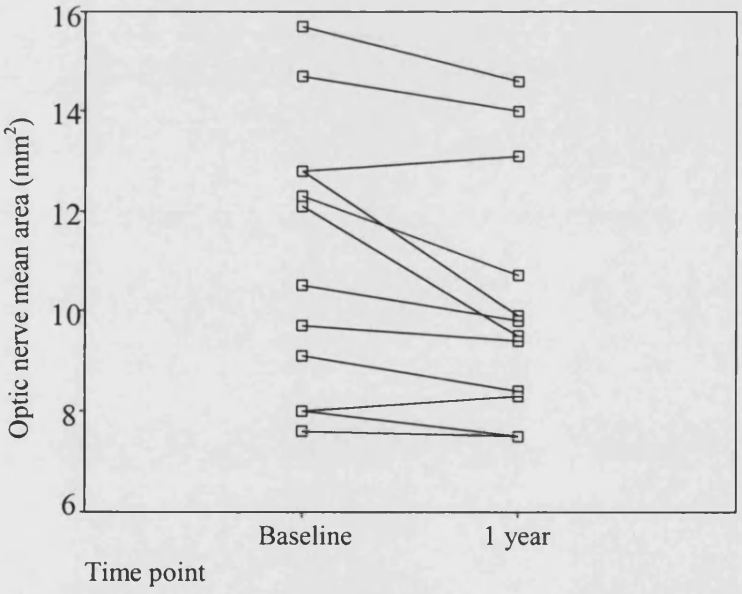

Figure 3.6: Change in optic nerve mean area over one year for optic nerves previously affected by optic neuritis. Baseline mean area 11.1mm^2, year one mean area 10.2mm^2 (p=0.01).

Figure 3.7: sTE fFLAIR images of the optic nerves of a 35 year old man. Left: five months after the onset of left optic neuritis (nerve arrowed). Right: one year later.

All patients had at least one lesion on brain imaging at baseline. Three patients had new brain lesions after one year. There was no difference in the progression of optic nerve atrophy between this group and the group with no new lesions. No patient had worsening visual acuity over this period despite the decreases in optic nerve mean area. There were no significant differences between the baseline and year-one VEP latencies and amplitudes in both symptomatic and asymptomatic optic nerves (data not shown).

3.2.5 Discussion

This study revealed that progressive atrophy occurs in optic nerves previously affected by optic neuritis. The correlation between the optic nerve mean area and VEP amplitude, and the suggestion that smaller optic nerves have worse visual acuities, provide indirect evidence that the observed atrophy is due to axonal loss although demyelination of axons with conduction block has also to be considered. The inverse correlation between time since onset of optic neuritis and extent of continuing atrophy indicates that the rate of atrophy is decreasing with time. In cases with a shorter time from onset, resolution of inflammation and oedema may contribute to the decrease in size of the optic nerve. However, the baseline measurement already showed a smaller nerve than in controls, suggesting that there was not much residual inflammation or oedema at this time. The prolonged and slowly evolving atrophy may reflect continuing axonal loss in a persistently demyelinated lesion or Wallerian degeneration secondary to axonal transection at the time of the optic neuritis (Perry & Anthony, 1999). It is unlikely to reflect further episodes of subclinical optic neuritis as these should equally

affect the contralateral optic nerves. These nerves showed no significant change in area after one year.

The lack of correlation between changes in optic nerve area and clinical data over the year may reflect the short period of follow-up and the relative insensitivity of Snellen charts for detecting change in visual acuity. Another possibility is that functional reorganisation in the visual system has occurred to preserve visual acuity (Werring *et al.*, 2000).

A mean 8% decrease in optic nerve area was recorded over the one-year follow-up period. This is greater than that seen in one-year serial studies on other areas of the central nervous system. Stevenson *et al.* (1998) showed a mean 3.2% decrease in spinal cord area in a mixed MS population and Simon *et al.* (1999) detected a 4.9% decrease in corpus callosum area in patients with RRMS. Studies using whole brain measures have showed smaller percentage decreases, 0.8% in brain volume (Fox *et al.*, 2000) and 0.7% in brain parenchymal fraction (Rudick *et al.*, 1999). These differences may be explained by the fact that the lesion in optic neuritis involves a greater proportion of the total optic nerve compared to lesions in the brain and spinal cord and hence may cause greater proportional atrophy.

The present study findings suggest that atrophy may evolve over several years following inflammatory demyelinating lesions in the central nervous system, albeit at a diminishing rate. This temporal dissociation between the initial lesion and the subsequent development of atrophy has important implications for interpreting the latter in natural history studies and treatment trials. Study of the effects of optic neuritis can therefore help in understanding the pathophysiology of MS. In a later chapter a prospective serial study will be described which will follow a cohort of patients from onset of optic neuritis in order to clarify the temporal evolution of atrophy and its relationship to other MRI, VEP and clinical measures.

3.3 Corticosteroids do not prevent optic nerve atrophy following optic neuritis

3.3.1 Introduction

Corticosteroids shorten the period of functional impairment following relapses in optic neuritis and MS, however they have not, thus far, been shown to affect the final level of function compared with placebo (Brusaferri & Candelise, 2000). There has been recent interest in the use of corticosteroids as neuro-protective agents by their effect of decreasing NO production by mononuclear cells (Compston & Coles, 2002). NO is toxic to axons *in vitro* (Smith *et al.*, 2001). Pulsed corticosteroid treatment has been reported to reduce the development of cerebral atrophy, a putative marker of neuronal loss (Miller *et al.*, 2002), over a five-year period in relapsing remitting MS (Zivadinov *et al.*, 2001). Optic nerve atrophy has been shown to develop following optic neuritis (Youl *et al.*, 1996). This study assesses whether a single course of IVMP during an attack of acute optic neuritis prevents the development of optic nerve atrophy following optic neuritis. MRI data from a recent randomised placebo-controlled trial of IVMP in acute optic neuritis were retrospectively evaluated (Kapoor *et al.*, 1998).

3.3.2 Patients and methods

The design, conduct and clinical results of the trial have been previously reported (Kapoor *et al.*, 1998). Briefly, 66 patients with a first episode of acute unilateral optic neuritis within 30 days of onset were enrolled into the study. The median duration of symptoms before randomisation was eight days (range 1-30). Six of the patients had CDMS, another 14 had CPMS and the rest had clinically isolated optic neuritis. They had their optic nerves imaged with a STIR sequence (TR 2500ms, TE 40ms, TI 175ms, matrix 256x128, FOV 16cmx16cm, 2 excitations, 5mm contiguous slices) and were then randomised to receive either 1g/day IVMP for three days or intravenous saline. Re-imaging was performed six months later. In addition, at six months, a detailed clinical assessment was performed including Snellen visual acuity, contrast sensitivity using the Pelli-Robson chart, 30-2 Humphrey visual field examination and colour vision using the FM 100 Hue test. Normal values were taken to be a visual acuity of 6/6 or better, contrast sensitivity of 1.65 or better, Humphrey mean deviation of -3dB or higher and the total error score of the FM 100 of less than 110 (Optic Neuritis Study Group,

1991; Steel & Waldock, 1998). Whole field and central field pattern-evoked VEPs were also recorded.

Only images that were acquired on a Signa 1.5T imager (General Electric, Milwaukee, WI) were available. Some early patients in the study were imaged on a Picker 0.5T imager and these images were not available for study. In total, images from 45 patients at baseline and 59 (30 given IVMP and 29 given placebo) patients after six months were examined. The images were transferred onto workstations (Sun Microsystems, Mountain View, CA). Mean optic nerve area was measured by an observer blinded to image identity, treatment group and acquisition order from two consecutive 5mm orbital slices from the orbital apex forwards using a semi-automated contouring technique as previously described (Chapter 3.1). Each measurement was carried out three times independently of each other. In a previously reported study of a different patient cohort, five consecutive 3mm orbital slices from an sTE fFLAIR sequence were measured (Chapter 3.1). It was not possible to measure a 15mm segment in all subjects from the STIR images as in some patients the most anterior slice occurred at the point that the nerve sheath dilated as it attached on the back of the globe leading to an artificially increased area; hence a 10mm segment was measured. This was less of a problem with the previous study because the sTE fFLAIR sequence suppresses the signal from CSF. The presence of high signal lesions in the measurement area was noted and lesion lengths at baseline and six-months were recorded from the data of the original study, measured by an experienced neuroradiologist (Kapoor *et al.*, 1998).

3.3.3 Statistical methods

The presence of nerve swelling at baseline and atrophy at six -months was assessed in terms of the ratio: diseased optic nerve area/healthy optic nerve area at the respective time points. Null hypotheses of ratio=1 were examined by paired t-tests on log nerve areas. The possible influence of a lesion in the measured portion of the nerve was examined by regression of log ratios on the presence of a lesion and its length. The association between atrophy and corticosteroid use was assessed by regression of the log ratio of six-month diseased optic nerve area/six-month healthy optic nerve area and six-month diseased area/baseline diseased optic nerve area on an indicator of corticosteroid use, adjusting for relevant baseline optic nerve area. The influence of the

presence of a baseline lesion was assessed by an interaction term. All paired tests or analyses involving both time points used only patients available at both time points. Associations between diseased optic nerve area at six months and VEP variables were assessed by linear regression on log diseased optic nerve area at six months; clinical variables were dichotomised about the threshold for the normal ranges and similarly assessed by logistic regression. To assess measurement reproducibility the within- and between-subject SD (and hence CV and reliability coefficients) were obtained from random effects analysis of variance (Bland & Altman, 1996a; Bland & Altman, 1996b; Bland & Altman, 1996c).

3.3.4 Results

Measurement reproducibility results are given in Table 3.5. At baseline optic nerve mean area was 18.4 (SD 3.8)mm^2 in diseased optic nerves and 17.8 (SD 3.6)mm^2 in healthy optic nerves (n=45). The estimated geometric mean ratio (diseased nerve area/healthy nerve area) was 1.035 (95% CI 0.96, 1.11; p=0.33). At baseline, high signal was present in the measurement area in 36/45 patients. The presence of a lesion did not affect the ratio, however the degree of swelling increased by 7.5% (95% CI 3.3%, 11.7%; p=0.001) for each slice that a high signal lesion was visible on.

After six months optic nerve mean area was 16.4 (SD 3.8)mm^2 in diseased optic nerves and 17.4 (SD 3.5)mm^2 in healthy optic nerves (Figure 3.8) (n=59). The estimated geometric mean ratio (diseased nerve area/healthy nerve area) was 0.93 (95% CI 0.87, 0.99; p=0.02). A lesion was present in 56/59 patients in the orbital portion measured at this time point. Neither the lesion length at baseline or six-months correlated with the degree of atrophy. There was no evidence of association between any of the clinical and VEP variables and six-month diseased nerve area.

variable	mean (mm^2)	within-subject SD	95% reference range[a]	CV (%)	reliability coefficient (95%CI)[b]
acute diseased nerve area	18.4	1.13	± 2.21	6.4	0.92 (0.88, 0.96)
acute healthy nerve area	17.8	1.21	± 2.37	6.8	0.89 (0.84, 0.94)
6-month diseased nerve area	16.4	0.76	± 1.49	4.6	0.96 (0.95, 0.98)
6-month healthy nerve area	17.4	1.11	± 2.18	6.4	0.91 (0.87, 0.95)

Table 3.5: Measurement reproducibility for the different subgroups.

[a]1.96 x within-subject SD. 95% of measurements are expected to lie within this departure from the true value.

[b]The proportion of total variance due to between-subject variation. Under assumptions which are plausible here, one minus this value is the proportion of variation due to measurement error.

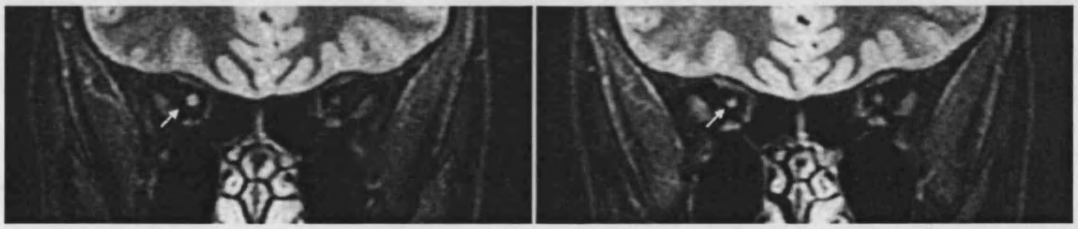

Figure 3.8: STIR MRI demonstrating optic nerve swelling at baseline (left) and optic nerve atrophy after six months (diseased nerve arrowed) in a 27 year old man with right optic neuritis.

The mean area of diseased optic nerves at six months in the IVMP group was 15.9 (SD 3.9)mm^2 (n=30) compared with 16.9 (SD 3.8)mm^2 in the placebo group (n=29). The ratio of six-month diseased/six-month healthy optic nerve area was 6.8% lower in the IVMP group than in the placebo group (95% CI, 16.1% lower, 3.6% higher, p=0.19). The ratio of six-month diseased optic nerve area/baseline diseased optic nerve area was 0.8% lower in the IVMP group than in the placebo group (95% CI 14.8% lower, 15.5%

higher, p=0.92). Neither the MS status nor the duration of symptoms before treatment was instigated affected these ratios.

3.3.5 Discussion

This technique was able to demonstrate optic nerve atrophy following optic neuritis with good reproducibility as witnessed by the high reliability coefficients. The area measurements are greater than those produced from sTE fFLAIR images as the measurements from the STIR images include the nerve sheath. Even though the measurements were of the optic nerve-sheath complex atrophy was still detected after six-months. At the time that the images were acquired during the trial the sTE fFLAIR sequence had not been developed and STIR was the preferred sequence for optic nerve lesion identification.

A study using sTE fFLAIR in a more chronic cohort of optic neuritis patients demonstrated that increasing optic nerve atrophy was associated with worse vision and decreased VEP amplitudes (Chapter 3.2). The lack of correlation between the clinical outcome measures and optic nerve mean area in the present study may be due to functional reorganization in the visual system in the early recovery process (Werring *et al.*, 2000), potentially achieved by utilising redundant optic nerve capacity (Frisen & Quigley, 1984). This plasticity may fail over time and this may be one explanation for the development of late clinical progression in MS.

There is no evidence from these data that a course of IVMP prevents the short-term development of optic nerve atrophy following acute optic neuritis. This is consistent with the lack of long-term functional benefit seen due to IVMP in both this and other studies.

Chapter 4 Recovery Following Acute Optic Neuritis

The following three sections detail the clinical, electrophysiological and quantitative MRI findings in a cohort of patients recruited with a first episode of acute unilateral optic neuritis to try and elucidate the mechanisms underlying initial visual impairment and subsequent recovery.

4.1 Visual recovery following acute optic neuritis: A clinical, electrophysiological and MRI study.

4.1.1 Introduction

As has been discussed, optic neuritis is one of the most common causes of acute visual loss in young adults living in temperate latitudes (Jin *et al.*, 1998). It has an incidence of 1-5 per 100,000/year (Rodriguez *et al.*, 1995; Jin *et al.*, 1998; MacDonald *et al.*, 2000). It may occur in isolation but there is a well known association with MS. Approximately 40-75% of patients affected by optic neuritis go on to develop MS (Francis *et al.*, 1987; Rodriguez *et al.*, 1995; Ghezzi *et al.*, 1999).

Although most patients make good recoveries from optic neuritis, about 10-15% of patients are left with significant visual impairment (Perkin & Rose, 1979; Beck, 1998). The degree of recovery does not seem to be related to age, gender, ethnicity, concurrent presence of multiple sclerosis, or abnormalities on brain MRI (Beck *et al.*, 1994). Generally, patients who are worst affected initially have a poorer prognosis, mainly related to the fact that recovery starts from a lower level compared with those who are mildly affected. Recovery however, is still possible. Of 66 patients presenting with a visual acuity of counting fingers or worse on entry to the ONTT, 61% recovered to 6/6 or better (Beck *et al.*, 1994). In another study, of 10 patients who presented with no light perception in the affected eye and a final diagnosis of demyelinating optic neuritis, six recovered to 6/9 or better (Slamovits *et al.*, 1991).

Corticosteroid therapy hastens recovery following acute optic neuritis and acute MS relapses. However, in all of the clinical trials to date no effect on final function has been demonstrated (Brusaferri & Candelise, 2000). IVIG was proposed to enhance

remyelination in order to promote recovery and to protect denuded axons from degeneration, however, in a randomised trial of 55 MS patients with persistent visual acuity loss after optic neuritis it did not significantly affect visual outcome (Noseworthy *et al.*, 2001).

Optic neuritis provides a useful model for study of MS relapses in general because it mirrors the natural history of relapse and recovery in MS. Also visual function can be measured accurately, electrophysiological tests provide insights into the effects on conduction in the visual pathways and MRI techniques with fat saturation enable the lesion in optic neuritis to be detected and studied (Gass *et al.*, 1996; Beck, 1998; Brusa *et al.*, 2001).

Gadolinium "enhancement" on MRI is a consistent feature in acute optic neuritis (Youl *et al.*, 1991; Kupersmith *et al.*, 2002). Its presence, an indicator of acute inflammation (Katz *et al.*, 1993), is associated with impairment of vision that improves on disappearance of the enhancement (Youl *et al.*, 1991). The length of the initial enhancing lesion however, was not shown to be related to the prognosis for recovery in one study that used a standard dose of gadolinium (0.1mmol/kg) (Kupersmith *et al.*, 2002).

This study reports the prospective follow-up of a cohort of patients who were recruited at presentation with a first attack of acute unilateral optic neuritis. Assessment was made using serial visual tests, electrophysiology, conventional and triple-dose gadolinium-enhanced MRI to examine which factors might be important in predicting prognosis for visual recovery. Triple-dose gadolinium (0.3mmol/kg) was chosen as it was known to increase the sensitivity for detecting enhancing brain lesions in MS by 66-75% compared with the use of single-dose (Filippi *et al.*, 1996; Silver *et al.*, 1997). This study assessed whether the potential for increased sensitivity for detecting the acute inflammatory lesion could lead to an improved ability for predicting prognosis based on the initial lesion length and the time that enhancement could be detected on serial imaging.

4.1.2 Patients and methods

Thirty-three patients with their first episode of acute unilateral optic neuritis within four weeks of onset of visual symptoms were recruited from the Neuro-Ophthalmology clinic of Moorfields Eye Hospital. The diagnosis of acute optic neuritis was based on previously agreed clinical criteria (Compston *et al.*, 1978). For the purposes of this study, patients under 18 years of age were excluded as being unable to consent to take part in the study and an upper age limit was put at 55 years of age as long as the rest of the clinical picture was consistent with acute optic neuritis. Patients were assessed for the diagnosis of MS according to the Poser criteria (Poser *et al.*, 1983). Patients with MS were eligible for the study as long as this was their first presentation with optic neuritis. Ethical approval was obtained for the study from the joint ethics committee of the Institute of Neurology and the National Hospital for Neurology and Neursurgery; informed consent in writing was obtained from each subject, in accordance with the Declaration of Helsinki

The demographics and clinical features of the patients are listed in Table 4.1. All 33 patients were assessed at baseline. Follow-up assessment was scheduled to occur two, four, eight, twelve, 26 and 52 weeks later. Twenty patients were assessed serially according to the above schedule (with some missing sessions) and twenty-two were assessed at one-year (Table 4.2).

Clinical assessment (at each visit)

Visual acuity

Best spectacle or pinhole-corrected visual acuity was measured using a retro-illuminated ETDRS chart and recorded as the 4m logMAR visual acuity (Ferris III *et al.*, 1982). When no letters could be correctly identified a score of 1.7 was assigned (Optic Neuritis Study Group, 1991). A visual acuity of 0.0 or better (equivalent to Snellen 6/6) was considered normal (Optic Neuritis Study Group, 1991; Steel & Waldock, 1998) and a poor recovery was assigned if the visual acuity at the last assessment was +0.2 or greater (equivalent to < Snellen 6/9) (Bradley & Whitty, 1967; (Miller *et al.*, 1988).

No.	Age	Gender	Side	Status	Delay -days*	Pain	Pain on eye movement	Phosphenes
1	30	♂	R	CPMS	12	Yes	No	No
2	29	♂	L	CIS	15	Yes	Yes	No
3	43	♀	L	CIS	14	Yes	Yes	Yes
4	38	♀	L	CIS	23	Yes	Yes	Yes
5	25	♀	L	CIS	7	Yes	Yes	No
6	26	♀	L	CIS	11	Yes	Yes	No
7	53	♀	L	CIS	18	Yes	Yes	No
8	25	♂	L	CIS	9	Yes	Yes	No
9	47	♀	R	CPMS	24	No	No	Yes
10	41	♂	L	CDMS	17	Yes	No	No
11	24	♀	R	CIS	14	Yes	Yes	No
12	33	♀	R	CIS	12	Yes	Yes	Yes
13	28	♀	R	CDMS	13	Yes	Yes	Yes
14	46	♂	L	CIS	10	Yes	Yes	No
15	34	♂	L	CIS	10	Yes	Yes	Yes
16	30	♀	R	CPMS	11	Yes	Yes	No
17	27	♀	R	CIS	15	Yes	Yes	No
18	40	♂	R	CIS	15	Yes	Yes	No
19	29	♀	R	CIS	8	Yes	Yes	Yes
20	19	♀	R	CDMS	21	Yes	Yes	No
21	22	♂	R	CIS	13	Yes	Yes	No
22	44	♂	R	CIS	18	No	No	No
23	27	♀	R	CIS	19	Yes	Yes	No
24	49	♀	L	CPMS	12	Yes	Yes	Yes
25	35	♀	R	CIS	9	No	No	Yes
26	23	♀	R	CIS	15	Yes	Yes	No
27	31	♂	R	CIS	10	Yes	Yes	No
28	23	♀	R	CIS	16	Yes	Yes	No
29	45	♀	L	CIS	14	Yes	Yes	No
30	22	♀	L	CPMS	11	Yes	Yes	No
31	39	♀	R	CIS	13	Yes	Yes	No
32	25	♀	L	CIS	13	Yes	Yes	Yes
33	27	♀	L	CIS	13	No	No	Yes

Table 4.1: Patient characteristics.

* Delay is the time since onset of visual symptoms to baseline session.

No.	Session (weeks)							Comments
	0	2	4	8	12	26	52	
1	✓	✓	✓					
2	✓	✓	✓	✓	✓	✓	✓	Healthy eye recurrences after 3 + 12 months
3	✓	✓	✓	✓	✓	✓	✓	Corticosteroid treatment
4	✓	✓	✓	✓	✓	✓	✓	No gadolinium-enhanced imaging
5	✓							No gadolinium-enhanced or brain imaging
6	✓	✓	✓		✓	✓	✓	
7	✓	✓	✓	✓	✓	✓	✓	
8	✓		✓		✓	✓	✓	
9	✓							No gadolinium
10	✓	✓	✓		✓	✓	✓	Congenital colour anomaly
11	✓	✓	✓	✓	✓	✓	✓	No gadolinium
12	✓	✓	✓	✓	✓	✓	✓	
13	✓							
14	✓	✓	✓	✓	✓	✓	✓	No gadolinium after baseline due to thrombophlebitis
15	✓	✓	✓	✓	✓	✓	✓	No gadolinium after baseline due to thrombophlebitis
16	✓		✓		✓	✓	✓	Healthy eye recurrence after 6 months
17	✓	✓	✓	✓	✓	✓	✓	
18	✓							
19	✓		✓	✓	✓	✓	✓	
20	✓							
21	✓	✓		✓	✓	✓	✓	Bilateral recurrence of optic neuritis after 3 months, treated with corticosteroids
22	✓		✓	✓	✓	✓	✓	
23	✓						✓	
24	✓		✓	✓	✓	✓	✓	
25	✓	✓	✓	✓	✓	✓	✓	
26	✓							
27	✓							
28	✓	✓	✓	✓	✓	✓	✓	Corticosteroid treatment
29	✓						✓	
30	✓							No gadolinium
31	✓						✓	
32	✓							
33	✓							

Table 4.2: Sessions that patients attended.

Visual field

The central 30° of the visual field was analysed using the 30-2 program on the Humphrey field analyser (Allergan-Humphrey Inc., San Leandro, CA, USA). Wide-angle lenses were used to correct refractive errors where necessary. The overall visual field mean deviation was compared with a reference field derived from control data provided by the manufacturer. A mean deviation of -35dB was assigned when vision was too poor to attempt the test (Kupersmith *et al.*, 2002). A mean deviation greater than or equal to -3.00dB was regarded as normal (Optic Neuritis Study Group, 1991; Wakakura *et al.*, 1999b) and a poor recovery was assigned if the mean deviation at the last assessment was less than or equal to -6.00dB (Keltner *et al.*, 1993).

The serial results from the above two parameters were chosen for detailed analysis because they give continuously variable measures that are amenable to statistical analysis.

Colour vision

Colour vision was assessed at each visit using the first 17 of the Ishihara Pseudoisochromatic Colour Plates 38 plates edition (Kanehara & Co. Ltd., Tokyo, Japan). Colour vision was scored as normal if 15 or more plates were correctly read (Fleishman *et al.*, 1987). In addition, at the one year visit, the FM 100 Hue test was performed in each eye (Farnsworth, 1943). It was not performed earlier for reasons of time and the poor performance of patients when visual acuity is poor (Katz, 1995). A square root of the error score of 10.5 or less was considered normal (Optic Neuritis Study Group, 1991).

Contrast sensitivity

Contrast sensitivity was assessed using standard Pelli-Robson charts at a distance of 1m (Pelli *et al.*, 1988). A score of 1.65 log units or higher was considered normal (Steel & Waldock, 1998).

Pupillary reaction

The presence of an RAPD was assessed using Levatin's swinging torch test (Levatin, 1959; Cox *et al.*, 1981).

Fundus examination

Fundus examination with an ophthalmoscope was performed and the presence of optic disc swelling or pallor commented upon.

Electrophysiological assessment of both diseased and healthy eyes
(at baseline, four, 12, 26 and 52 weeks)

VEP recording was done in a darkened room with the patient comfortably seated and the head supported. The patients wore appropriate corrective lenses when necessary. Five recording electrodes were attached to the scalp with paste in a symmetric lateral chain 5cm above the inion with an inter-electrode distance of 5cm. A sixth electrode was located 2.5cm above the inion. The common reference electrode was at Fz (10–20 System). Impedances were reduced to <5kΩ by prior skin preparation. The amplification band-pass was 0.16-1kHz and the sampling rate was 2kHz for 250ms after each stimulus. VEPs were recorded to reversal of achromatic checks on a computer monitor screen with a refresh rate of 100 Hz, each check subtending 40' at the eye. The brightness of the light checks was 60cd/m^2 and of the dark checks 4cd/m^2. Whole field VEPs were recorded at a viewing distance of 88cm so that the screen subtended 28° horizontal x 20° vertical. Central field recordings with a circular screen whose radius subtended 4° at the eye were also taken. The interval between reversals was 909ms. Two averages of 100 responses were made for whole field and three for central field VEPs, and these were averaged together after assessment of their consistency. The amplitude, measured from the preceding peak of opposite polarity, and latency of the P100 peaks were recorded. The results were compared with age-matched laboratory controls.

Conventional imaging (at baseline and one-year)

The optic nerves were imaged with a coronal-oblique fat suppressed dual echo FSE (TR=2300ms, TEef=58/145ms, 2 excitations, echo-train length 16, matrix size 512x384, 24x18cm rectangular FOV, 3mm contiguous slices) sequence (n=33 at baseline, n=22 at one-year). Brain imaging was also performed with an axial-oblique dual echo FSE (TR=2000ms, TEef=19/95ms, 2 excitations, echo-train length 8, matrix size 256x256, 24x18cm rectangular field of view, 5mm contiguous slices) sequence (n=32 at baseline, n=22 at one-year).

Between imaging sessions care was taken to accurately reposition the imaging field of view. In particular, the line from the anterior commissure to the posterior commissure on sagittal localiser images was used to ensure that the subjects' head angles were the same at each session.

An experienced radiologist (Dr K.A. Miszkiel), who was blinded to the lesion side and severity of visual loss, identified lesions on the proton density weighted FSE images at baseline and one year (in separate sessions), and determined their length as the number of consecutive slices involved multiplied by 3mm. The baseline brain FSE images were classified as abnormal if any lesions typical for demyelination were identified. Dissemination in space of the brain lesions was commented on according to the Barkhof criteria (although gadolinium-enhanced brain images were not acquired) (Barkhof *et al.*, 1997). The one-year images were assessed for the presence of any new lesions. Both sets of brain images were also evaluated for the presence of any optic radiation lesions. The brain images were then analysed on Sun workstations (Sun Microsystem, Mountain View, CA., USA) using the DispImage display tool (Plummer, 1992). The total brain and optic radiation lesion areas were calculated using a semi-automated contouring technique for the marked lesions as previously described (Grimaud *et al.*, 1996).

Triple-dose gadolinium-enhanced imaging (at baseline and until enhancement ceased)

Before and after administration of 0.3mmol/kg intravenous dimeglumine gadopentate (triple-dose gadolinium) the patients' optic nerves were imaged with a coronal-oblique fat-saturated T_1-weighted spin echo (TR 600ms, TE 20ms, 1 excitation, 256x192

matrix, 24x18cm FOV, 16 contiguous 3mm slices) sequence in 28 patients at baseline. The radiologist, blinded as above, identified and determined the length of any enhancing optic nerve lesions on the images. Serial imaging was performed on 15 of the patients after 2, 4, 8 and 12 weeks and gadolinium administered until enhancement was deemed to have ceased. The duration of enhancement was noted.

4.1.3 Statistical methods

VEP and imaging data were considered as continuous variables; colour vision on Ishihara charts and contrast sensitivity scores were considered as binary variables dichotomised about the normal values. Visual field mean deviation and logMAR visual acuity were considered as both continuous and binary variables dichotomised about the poor recovery thresholds.

Associations at fixed times

Linear regression was used to investigate associations between pairs of quantitative variables at fixed times, with additional predictor terms to assess interactions and confounding. Where Normality of residuals could not be assumed, non-parametric bias-corrected bootstrap CI were obtained using 1000 replicates (Carpenter & Bithell, 2000). T-tests or (where Normality could not be assumed) Wilcoxon Rank Sum tests were used to compare quantitative variables across two groups, and Pearson chi-square tests for associations between pairs of binary variables. Correlations were assessed using Pearson correlation coefficients.

Associations over multiple time points per subject

To investigate associations between pairs of quantitative variables across multiple time points, variance components regression models were used, estimating both within and between subject variation (Baltagi, 1995). Bootstrap inference was used when residuals showed some deviation from Normality.

As visual recovery appeared to approach an eventual recovery value, accordingly this was fitted using an exponential model which was able to fit this type of curve flexibly,

and which captured useful features of the trajectory by means of three estimated parameters, α, β, γ (Snedecor & Cochran, 1989):

$y_{ij} = \alpha_j + \beta_j \exp(-\gamma_j t_{ij}) + \varepsilon_{ij}$ $\quad\quad$ $\varepsilon_{ij} \sim N(0, \sigma^2)$

y_{ij} is the acuity score for the ith assessment of the jth subject, and t_{ij} is the time from onset at the ith assessment of subject j; ε_{ij} is the error term, assumed Normally distributed with mean 0, variance σ^2.

α_j is the asymptote, or 'eventual' recovery level, for subject j;

β_j is the extent of improvement in acuity from baseline to asymptote;

γ_j controls the trajectory shape for subject j;

Further: $-\beta_j\gamma_j$ is the estimated gradient at baseline, the 'initial recovery gradient', $(1/\gamma_j)\ln(\beta_j/[r - \alpha_j])$ is the estimated time to reach acuity score r, and $(1/\gamma_j)\ln(1/[1 - d])$ is the estimated time to achieve fraction d of the total extent of recovery β_j, for subject j. Since this type of non-linear model is difficult to fit in a multilevel context, the model was fitted for each subject separately giving subject-specific estimates, in particular, subject-specific eventual recovery levels (the predicted asymptote from the model, rather than the level at last assessment), initial recovery gradients, and times to achieve fractions of total recovery; these were then summarised or used in conventional regression models to investigate determinants of the trajectory. Bootstrap inference was used due to the non-Normal distribution of subject-specific estimates.

4.1.4 Results

Baseline Status

The patients' clinical characteristics and baseline visual and imaging results are given in Tables 4.3-4.5.

Baseline characteristics	Frequency
Time since onset	Median = 13 days, Range = 7-24
Age	Median = 30 years, Range = 19-53
Gender	Male = 10 (30.3%), Female = 23 (69.7%)
Side	Left = 15 (45.5%), Right = 18 (54.5%)
Clinical status	CDMS = 3 (9.1%), CPMS = 5 (15.1%), CIS = 25 (75.8%)
Pain	Present = 29 (87.9%), Absent = 4 (12.1%)
Pain on eye movement	Present = 27 (81.8%), Absent = 6 (18.2%)
Pain before visual loss	Present = 11 (33.3%), Absent = 22 (66.7%)
Phosphenes	Present = 11 (33.3%), Absent = 22 (66.7%)
RAPD	Present = 32 (97%), Absent = 1 (3%)
Swollen disc	Present = 19 (57.6%), Absent = 14 (42.4%)

Table 4.3: Baseline clinical status.

Test	Median	Range	No. (%) abnormal
logMAR acuity (and Snellen equivalent)	+1.02 (6/60)	+1.70 to -0.06 (NPL to 6/5)	30 (90.9%)
30-2 Humphrey mean deviation (dB)	-20.00	-35.00 to -2.47	32 (97%)
Ishihara plates correct out of 17 (n=32)*	1	0 to 16	30 (93.8%)
Pelli-Robson contrast sensitivity	0.75	0 to 1.65	32 (97%)
VEP whole field amplitude (μV)	2.1	0 to 18.1	n/a
VEP whole field latency (ms)	129.3	99.6 to 158.0	29 (87.9%) (inc. 9 flat responses)
VEP central field amplitude (μV) (n=32)†	1.3	0 to 8.6	n/a
VEP central field latency (ms) (n=32)†	134.1	99.6 to 165.7	31 (96.9%) (inc. 13 flat responses)

Table 4.4: Baseline clinical and electrophysiological results for diseased eyes.

* Colour vision not tested in one subject due to a congenital colour anomaly.

† One central field VEP not measured.

Imaging finding	Frequency
Lesion length on FSE	Median = 24mm, Range = 9-39mm
Canalicular involvement on FSE	Present = 31 (93.9%), Absent = 2 (6.1%)
Lesion length on Gd-enhanced T_1 CSE (n=28)	Median = 30mm, Range = 0-39mm
Canalicular involvement on Gd-enhanced T_1 CSE (n=28)	Present = 27 (96.4%), Absent = 1 (3.6%)
Duration of enhancement (n=16)*	Median = 62 days, Range = 0-113 days
Abnormal baseline brain imaging on FSE (n=32)	Present = 23 (71.9%), Absent = 9 (28.1%) Dissemination in space = 6 (18.8%)‡
Baseline brain lesion areas (n=32)	Median = 66.4mm^2, Range = 0-1829.1mm^2
Optic radiation lesions on FSE (n=32)	Present = 9 (28.1%), Absent = 23 (71.9%)
Optic radiation lesion areas (n=32)	Median = 0, Range = 0-349.8mm^2

Table 4.5: Imaging results at baseline.

* Including one patient with no enhancement at baseline.

‡ 5/6 patients with dissemination in space had CPMS or CDMS whereas 3 patients with CPMS did not have dissemination in space.

The symptomatic lesion on optic nerve FSE images was identified in all 33 cases with a median length of 24mm (range 9-39mm). Canalicular involvement was seen in all but two patients. Two patients showed chiasmal high signal at baseline and one patient had high signal in the contralateral healthy nerve but had no previous history of optic neuritis in this eye. In this case the vision measures in this eye were entirely normal, however the VEP central field latency was borderline abnormal at 111.8ms.

The symptomatic optic nerve lesion was identified on the enhanced images in 27/28 cases at baseline (Figure 4.1). The median lesion length at baseline was 30mm (range 0-39mm) with no chiasmal enhancement seen. Canalicular involvement was present in all but one case. Both pain on eye movement and optic disc swelling were related to the presence of enhancement of the anterior orbital optic nerve ($p=0.04$ and $p=0.01$ respectively). Seventeen patients had enhancement in the slice immediately posterior to the globe, 16 of whom had pain on eye movement and 13 of whom had optic disc

swelling (11 patients did not have anterior orbital enhancement, seven of whom had pain on eye movement and three of whom had optic disc swelling).

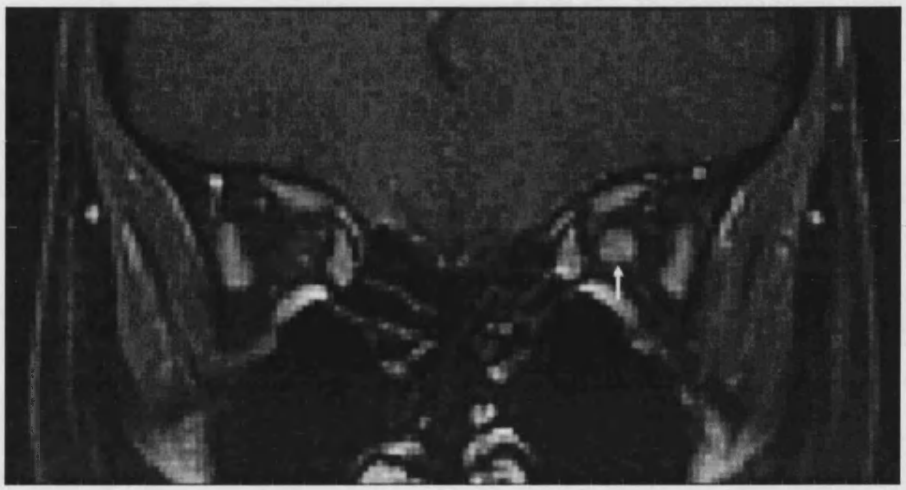

Figure 4.1: Triple-dose gadolinium-enhanced fat-saturated T_1-weighted image of a 42 year old woman 14 days from onset of acute left-sided optic neuritis (diseased optic nerve arrowed).

The lesion length on the baseline FSE images did not correlate significantly with logMAR visual acuity, visual field mean deviation or any of the VEP parameters. There was an association at baseline between lesion length on the triple-dose gadolinium-enhanced images and logMAR visual acuity ($r=0.38$, $p=0.044$), visual field mean deviation ($r=-0.57$, $p=0.002$) and VEP central field amplitude ($r=-0.41$, $p=0.035$).

Three patients received corticosteroids. The decision to treat with corticosteroids was made independently of the patients' involvement in the study. One patient was treated due to a slow recovery, one patient due to persistent pain and a slow recovery and the last patient was treated after bilateral recurrence of optic neuritis four months after the first episode.

<u>One-year status</u>

The one-year clinical and electrophysiological results are given in Table 4.6. Three patients had recurrences of optic neuritis in the year (1 patient with 2 episodes in contralateral eye, 1 patient with 1 episode in contralateral eye and 1 patient with

bilateral recurrence) and three other patients had relapses of MS. Twelve patients had a persistent RAPD and 21 had developed a pale optic disc.

Test	Median	Range	No. (%) abnormal
logMAR acuity (and Snellen equivalent)	-0.08 (6/5)	+0.62 to -0.2 (6/25 to 6/4)	7 (33.3%) 4 (19.0%) poor recovery
30-2 Humphrey mean deviation (dB)	-4.04	-13.78 to -1.00	13 (61.9%) 7 (33.3%) poor recovery
Ishihara plates correct out of 17 (n=20)*	15.5	1 to 17	10 (50.0%)
Pelli-Robson contrast sensitivity	1.50	0.9 to 1.65	11 (52.4%)
FM 100 hue square root of error score (n=20)*	8.94	34.12 to 4.90	9 (45%)
VEP whole field amplitude (μV)	8.0	1.5 to 35.9	n/a
VEP whole field latency (ms)	117.1	96.7 to 160.0	17 (81.0%)
VEP central field amplitude (μV)	5.5	1.0 to 16.8	n/a
VEP central field latency (ms)	115.2	95.3 to 171.1	19 (90.5%)

Table 4.6: Clinical and electrophysiological outcome at one year for diseased eyes (n=21 - one excluded due to bilateral recurrence of optic neuritis).

* Colour vision not tested in one subject due to a congenital colour anomaly

There was no association between baseline logMAR visual acuity, visual field mean deviation, FSE lesion length, brain or optic radiation lesion load and one year logMAR visual acuity or visual field mean deviation.

There was an association between baseline gadolinium-enhanced lesion length and visual outcome. The final recovery level in visual acuity was estimated to be worse by 0.02 (95% CI: 0.003, 0.04; p=0.03) logMAR units for every additional 3mm increase in baseline gadolinium-enhanced lesion length. However, there was a suggestion of non-linearity. The difference appeared to be mainly between patients with relatively short baseline lesions (lowest quartile, mean lesion length 14.0mm), and others. The final recovery level was 0.18 (99% CI: 0.02, 0.44; p<0.01) logMAR units lower between this lowest quartile and the other patients (Figure 4.2). This difference was not effectively

altered when adjusting for baseline logMAR score ($p<0.01$) indicating that the association between lesion length and outcome was independent of the baseline visual impairment.

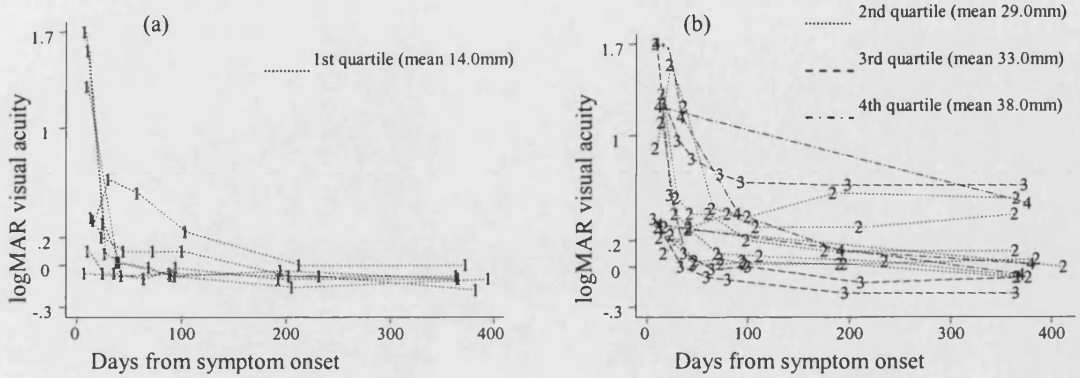

Figure 4.2: logMAR recovery over time by quartiles of baseline triple-dose gadolinium-enhanced lesion length.
(a) Patients in the first quartile.
(b) Patients in quartiles 2-4.

The final recovery level in visual field mean deviation was estimated as lower by 0.27dB (95% CI: 0.03, 0.60; p=0.03) for every additional 3mm increase in initial gadolinium-enhanced lesion length. However, there was evidence again that this relationship was not linear. The difference again appeared to be mainly between patients in the lowest quartile of lesion length and the others. The final recovery level was 2.55dB higher (99% CI: 0.22, 5.49; $p<0.01$) between this lowest quartile and the other patients (Figure 4.3). The other quartiles were not significantly different from each other. This difference was only slightly attenuated when adjusting for baseline visual field mean deviation to 2.26dB (97% CI: 0.03, 5.69; p=0.03).

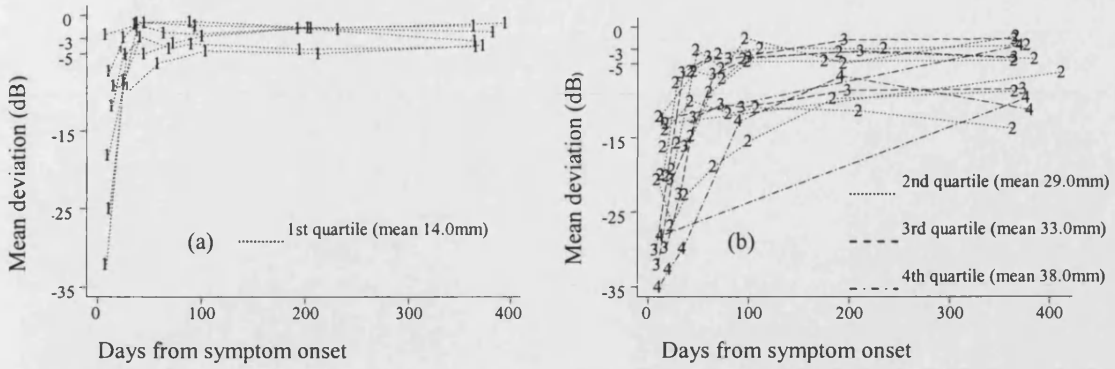

Figure 4.3: 30-2 Humphrey visual field mean deviation recovery over time by quartiles of baseline triple-dose gadolinium-enhanced lesion length.
(a) Patients in the first quartile.
(b) Patients in quartiles 2-4.

Six patients reported that their vision had returned to normal. Both logMAR visual acuity score and visual field mean deviation were poor predictors of "normal" vision at outcome. The presence of normal levels of contrast sensitivity (p=0.034, Wilcoxon rank sum), Ishihara colour vision (p=0.013, Wilcoxon rank sum) and having no RAPD (p=0.002, Pearson chi-squared) were however associated with self-reported normality. Patients reporting normal vision also had lower Farnsworth-Munsell square root of total error scores than those reporting abnormal vision (7.61 versus 15.64, 95% CI for difference in means of 8.03: 13.68, 3.06; p<0.001).

The median duration of gadolinium enhancement was 63 days (range 0-113 days). The duration of enhancement was associated with the initial gadolinium-enhanced lesion length, with five additional days of enhancement for each 3mm increase in baseline lesion length (r=0.56, p=0.024). The duration of enhancement was not however associated with visual outcome. The groups who had only baseline gadolinium-enhanced imaging and those who had serial enhanced imaging were well-matched in terms of initial visual impairment and initial lesion lengths.

The one-year imaging results are presented in Table 4.7.

One year imaging	Frequency
Lesion length on FSE (n=21)*	Median = 30mm, Range = 9-45mm
Canalicular involvement on FSE (n=21)*	Present = 20 (95.2%), Absent = 1 (4.8%)
New brain lesions on FSE‡	Present = 11 (50.0%), Absent =11 (50.0%)
Brain lesion areas	Median = 54.5mm^2, Range 0-767.3mm^2
New optic radiation lesions on FSE	Present = 4 (18.2%), Absent = 18 (81.8%)
Optic radiation lesion areas	Median = 0, Range = 0-318.2mm^2

Table 4.7: One year imaging results (n=22).

* One excluded due to bilateral recurrence of optic neuritis.

‡ No gadolinium enhanced brain imaging performed so dissemination in time could not be explored.

At one-year the median FSE lesion length was 30mm (range 9-45mm) and significantly longer than at baseline (mean change = 6.29mm, p=0.002). No new patients had chiasmal high signal at one year. No new high signal lesions were seen in the contralateral healthy optic nerves apart from those cases where new clinical events occurred. There was no association between one-year FSE lesion length, brain or optic radiation lesion load and one-year logMAR visual acuity or visual field mean deviation.

Visual recovery curves

logMAR acuity

From the whole cohort, 18 patients recovered to a logMAR acuity of less than +0.2, four did not (not including the patient with bilateral recurrence). This included a patient who recovered to logMAR +0.02 after 41 days and then was lost to follow-up. The median time to achieve 50% of the extent of eventual recovery was 11.1 days (95% CI: 8.3, 54.2) in patients with good recoveries and 17.1 days (96% CI: 9.7, 39.1) in patients with poor recovery. The 75th centile time to achieve 50% of eventual extent of recovery in patients with good recovery was 46.6 days (95% CI: 11.1, 131.2). The

estimated mean gradient at the start of recovery was -0.393 logMAR units per day in the patients with good recoveries and -0.002 logMAR units per day in poor-recovery patients (difference in mean gradients: 0.392, 95% CI: 0.03, 1.094; p=0.01). An illustration of the logMAR recovery curves for patients with good and poor eventual recoveries is given in Figure 4.4.

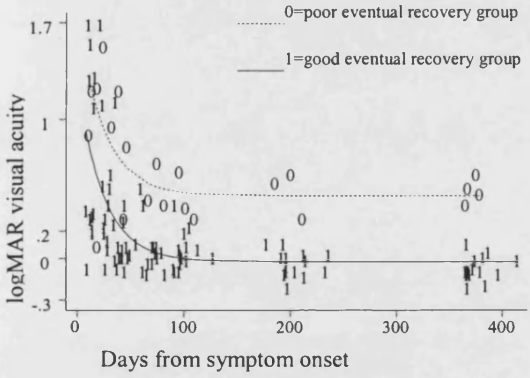

Figure 4.4: logMAR visual acuity recovery over time according to eventual recovery status

30-2 Humphrey visual field mean deviation

From the whole cohort, 15 patients recovered to a mean deviation of greater than -6.0dB, seven did not (not including the patient with bilateral recurrence). This cohort includes a patient who recovered to -2.93dB after 41 days and then was lost to follow-up. Two patients had their recovery status classified discordantly by the logMAR and visual field scores. The median time to achieve 50% of the extent of eventual recovery was 16.25 days (95% CI: 8.4, 35.2) in patients with good recoveries and 37.7 days (96% CI: 15.4, 96.7) in patients with poor recovery. The 75th centile time to achieve 50% of eventual extent of recovery in patients with good recovery was 25.3 days (95% CI 17.1, 38.1). The estimated mean gradient at the start of recovery was 4.60dB units per day in the patients with good recoveries and 0.99dB per day in poor-recovery patients (difference in mean gradients: 3.61, 95% CI 0.01, 9.08; p=0.02). An illustration of the visual field mean deviation recovery curves for patients with good and poor eventual recoveries is given in Figure 4.5.

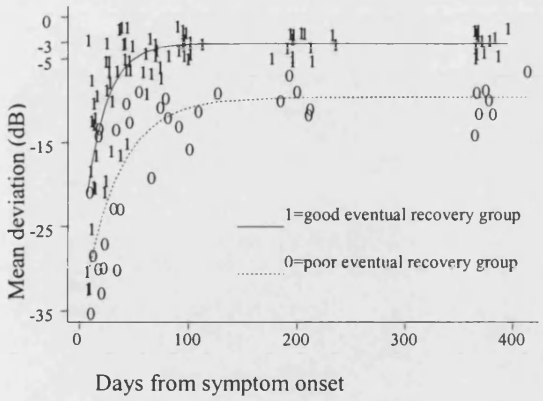

Figure 4.5: 30-2 Humphrey visual field mean deviation recovery over time according to eventual recovery status.

The quartile with shortest gadolinium-enhanced lesion length at baseline also had a borderline significant steeper gradient of Humphrey recovery than patients with longer lesions. The estimated mean gradient of recovery in shortest quartile was 7.94dB per day steeper than the estimated gradient in the remaining patients (95% CI 0, 22.63; P=0.05). The effect of initial lesion length on logMAR recovery was in the appropriate direction but not significant.

VEP data

There was no association between any of the baseline VEP variables and visual outcome. Patients with a good recovery of visual field mean deviation did though, have increased whole and central field amplitudes throughout the recovery process compared with patients with poor recovery. The mean differences between good- and poor-recovery patients were 5.02μV (95% CI 0.33, 9.71; p=0.036) for whole field amplitude and 2.29μV (95% CI 0.29, 4.56; p=0.047) for central field amplitude (Figure 4.6). There was however, no association between VEP latency and visual field recovery and between any VEP variable and logMAR recovery status.

The quartile with shortest gadolinium-enhanced lesion length at baseline had borderline significant higher time-averaged central field amplitude VEPs by a mean 2.26μV, 95% CI 0.03, 4.50; P=0.048) than longer lesion patients.

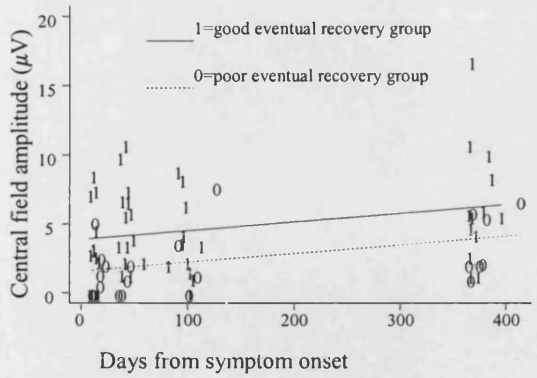

Figure 4.6: VEP central field amplitude over time according to eventual recovery status

Vision scores, averaged over time, tended to be better in patients with higher time-averaged whole and central field VEP amplitudes (see Table 4.8); moreover, within patients, at different times, better vision scores were associated with higher VEP amplitudes and lower central field latencies (Table 4.8).

VEP variable	logMAR visual acuity within subjects (change per unit)	logMAR visual acuity between subjects (change per unit)	Visual field mean deviation within subjects (dB) (change per unit)	Visual field mean deviation between subjects (dB) (change per unit)
Whole field amplitude (unit =1μV rise)	-0.07 (-0.1, -0.04) p<0.001	-0.03 (-0.05, -0.01) p=0.011	+1.23 (0.69, 1.76) p<0.001	+0.50 (0.11, 0.89) p=0.015
Whole field latency (unit =1ms rise)	No association	No association	No association	No association
Central field amplitude (unit =1μV rise)	-0.09 (-0.14, -0.05) p<0.001	-0.07 (-0.11, -0.02) p=0.005	+1.73 (0.85, 2.62) p<0.001	+1.21 (0.42, 2.01) p=0.005
Central field latency (unit =1ms rise)	+0.02 (0.01, 0.03) p<0.001	No association	-0.14 (-0.23, -0.37) p<0.007	No association

Table 4.8: The within and between subject relationships (95% bootstrap CI) between VEP parameters and both logMAR acuity and visual field mean deviation taking all available time points into account.

4.1.5 Discussion

Gadolinium enhancement of the optic nerves has been shown to correlate with the degree of expansion of the extracellular space and amount of inflammatory infiltrate in animal studies of experimental allergic encephalomyelitis with optic nerve involvement (Guy *et al.*, 1992). The initial enhanced lesion length in optic neuritis appeared to be important in our study in determining the amount of initial visual impairment confirming previous observations (Kupersmith *et al.*, 2002). This is consistent with acute inflammation causing conduction block in the optic nerve (Youl *et al.*, 1991). One previous study, which was a retrospective review of 93 patients out of a cohort of 107 who were followed to six-months after onset of optic neuritis did not find an association between acute enhancing lesion length or location and outcome (Kupersmith *et al.*, 2002). The use of triple-dose gadolinium in the present study was associated with an apparent high sensitivity for detecting the acute lesion in optic neuritis, although a comparative study with single-dose gadolinium was not performed. There was also an association, independent of baseline visual impairment, between the acute enhancing lesion length and outcome, although this was mostly due to patients with short inflammatory lesions having a good prognosis for recovery. This result suggests that the initial extent of inflammation has some importance in determining prognosis. It was not however possible to do quantitative measurements on the degree of enhancement apart from measuring lesion length. Canalicular involvement was thought previously to result in a poor prognosis (Miller *et al.*, 1988), but it was almost universal in this study, probably due to the increased sensitivity of the technique, and so no conclusions can be drawn.

Optic neuritis can usually be diagnosed on clinical grounds, however when there is clinical uncertainty imaging can also help in confirming the diagnosis and in ruling out other diagnoses such as a compressive lesion (Chapter 1). Routine use of triple-dose gadolinium for diagnostic imaging would have large cost implications and is not warranted in suspected optic neuritis. However, in future treatment trials of novel therapies in the acute phase to improve visual outcome in acute optic neuritis, use of triple-dose gadolinium may help in selecting patients who are more likely to have a poor prognosis.

Both optic disc swelling and pain on eye movement were related to the presence of enhancement of the optic nerve in the slice immediately posterior to the globe. The presence of optic disc swelling is consistent with local blood-nerve barrier breakdown with associated inflammation and oedema, although hold up of axonal transport and venous congestion may also contribute. The anterior optic nerve is the most mobile portion of the nerve and inflammation here may therefore be more likely to cause pain on eye movement. The observation of the presence of pain with orbital optic nerve enhancement was also made by Fazzone *et al.* (2003). 94.3% of patients with orbital enhancement experienced pain compared with only 32% of patients with enhancement confined to other portions of the optic nerve.

The duration of enhancement was longer than seen in previous studies. In nine out of 11 patients given single-dose gadolinium optic nerve "enhancement" using STIR MRI had ceased by a mean of 34.2 days since onset (Youl *et al.*, 1991). MS lesions have been shown to enhance for a mean 2.4±1.6 weeks in one study using triple-dose gadolinium (Tortorella *et al.*, 1999) and 3.7±1.9 weeks in another using single-dose gadolinium (Silver *et al.*, 1999). The longer duration that was observed here (median 63 days) may be due to the use of triple-dose rather than single dose gadolinium or this study being on symptomatic lesions which may have been more pathologically severe than the asymptomatic lesions studied in the brain serial triple-dose gadolinium imaging studies. The duration of enhancement did not influence outcome in this study, although there was a relationship between initial lesion length and duration of enhancement.

The use of arbitrary standards to determine if visual acuity and visual field scores had returned to normal vision did not always reflect the patients' views on whether their vision had returned to normal. The presence of normal contrast sensitivity and colour vision scores was associated with having subjectively normal vision at outcome; however these parameters are less amenable to statistical analysis compared with logMAR acuity and visual field mean deviation as they are not continuously variable.

The lesion on FSE images appeared to lengthen over the year. Possible explanations are Wallerian degeneration becoming apparent radiologically (Simon *et al.*, 2000), or extension of the primary demyelinating lesion. However, the absolute increase in lesion size was small (a mean of two slices on coronal imaging).

The baseline level of visual impairment appeared to be a poor predictor of visual outcome, but the visual field recovery curves showed a greater differentiation in shape between patients with good and poor recoveries, in particular regarding the initial gradient of recovery. 75% of patients, who recovered to a mean deviation of greater than -6.0dB, achieved half their recovery by 25 days. However, the confidence interval suggests this figure could have been as late as 40 days. It would be more desirable to give the 95% centile figure but this was not possible in this relatively small cohort.

The crucial period in recovery does appear to be within the first two months after onset. In one series, the mean period of recovery to Snellen 6/6 acuity, amongst those who reached this level, was 8.1 weeks and this was not affected by the severity of visual impairment at presentation (Perkin & Rose, 1979). Bradley and Whitty (1967), observed that vision had improved to normal (defined as Snellen acuity of 6/9 or better) in half after one month, and in three-quarters by six months. The recovery was slower in those with poor vision at onset (6/60 or worse). In the ONTT recovery of visual acuity was nearly complete by five weeks after onset of symptoms (Beck, 1998). Further, albeit slower, recovery has been seen up to one year following onset of the disease (Brusa *et al.*, 2001). It may be that a poor prognosis is fixed early on and is related to the intensity of the initial inflammatory process causing more extensive acute demyelination and axonal damage (Ferguson *et al.*, 1997; Trapp *et al.*, 1998). The slower recovery curves in these patients may then reflect attempts at repair with expression of new sodium channels on persistently demyelinated axons (Smith & McDonald, 1999) and cortical adaptation in the presence of axonal loss or persistent conduction block through demyelination (Werring *et al.*, 2000), rather than just resolution of inflammation and its effects on relatively normal axons which is associated with rapid recovery of vision (Youl *et al.*, 1991). It is interesting that corticosteroids speed up recovery without influencing outcome, probably reflecting their effect on suppressing inflammation. The association between lower VEP amplitudes and poorer vision during recovery suggests that the loss of functioning neural channels presents a bar to recovery. This would imply that axonal loss is important, although persistent conduction block in demyelinated fibres could give a similar picture. To counter such processes, neuroprotective or remyelination treatments may be required to improve visual outcome. Targeting of treatment to those with a poor prognosis will be

required. Also, if treatment is introduced too late then it may not influence outcome. Whilst these findings should be confirmed in a larger cohort they do suggest that the one- to two-month time window may be appropriate to identify those patients with a poorer prognosis. These patients may then be candidates for novel therapies. Some of these therapies may be invasive, such as cell-based remyelination requiring surgical introduction of the cells, emphasising the need for appropriate patient selection.

In conclusion, this study suggests that factors that are associated with a better prognosis are having a short acute lesion on triple-dose gadolinium-enhanced imaging, higher VEP amplitudes and a steeper gradient of the initial improvement in vision. These observations may have implications for the timing and strategy for implementing new treatments to improve visual outcome in optic neuritis, and potentially also for treatment of MS relapses in general, although it is less easy to define the symptomatic lesion in other parts of the CNS (Behan *et al.*, 2000). Also, lesions elsewhere may not be as easily accessible as the optic nerves are if cell-based remyelination therapies were to become available.

4.2 Serial magnetisation transfer imaging in acute optic neuritis

4.2.1 Introduction

As has been discussed in Chapter 2.3.9 MT imaging provides a means by which tissues can be examined in more detail (Wolff & Balaban, 1989), going beyond the more conventional MRI T_1 and T_2 characteristics (McGowan, 1999; Barker, 2000; Van Buchem & Tofts, 2000). Use of MT allows the otherwise invisible "bound" water associated with myelin sheaths to be examined. It also provides a means of producing quantitative images by calculating parameters related to the degree of exchange between bound and free protons; in particular the MTR.

Taken together the studies detailed in Chapter 2.3.9 suggest that:
(i) Early changes due to Wallerian degeneration may be associated with an early rise in MTR, possibly due to exposure of myelin fragments to extracellular tissue increasing the exchange of magnetisation.
(ii) Low MTR results from a decreased capacity for exchange due to oedema, demyelination and gliosis.
(iii) Axonal degeneration combined with demyelination results in even greater falls in MTR.
(iv) Remyelination may result in restoration of MTR.

The temporal evolution of MTR changes after an acute attack of optic neuritis and the relationship with imaging, clinical and electrophysiological parameters has not been previously studied. This report presents the results of a prospective serial study of optic nerve MTR using a high resolution 3D GE sequence in the above cohort of patients with acute unilateral optic neuritis. The key aims of the present study are:

(i) To quantify the MTR changes over time due to a symptomatic acute inflammatory demyelinating lesion.
(ii) To determine if the MTR changes over time mirror the electrophysiological and histopathological observations which suggest demyelination followed by remyelination in acute MS lesions. It would be desirable to confirm by imaging the electrophysiological observation of remyelination in the recovery process (Brusa *et al.*,

2001); such an outcome would support using MTR as a tool to investigate remyelination in the optic nerve and elsewhere in the CNS.
(iii) To explore whether the MTR measures either acutely, or during recovery, are associated with the degree of visual recovery.

4.2.2 Patients and methods

Twenty-nine patients with their first episode of acute unilateral optic neuritis (10 males, 19 females, median age 30 years, range 19-53 years), as part of the cohort described above, were recruited from the Neuro-Ophthalmology clinic, Moorfield's Hospital, London. The median delay from onset of visual symptoms to the first examination was 13 days (range 7-24 days). Three of the patients had CDMS, five had CPMS and 21 had clinically isolated optic neuritis (Poser *et al.*, 1983). All the patients were examined acutely and most after 2, 4, 8, 12, 26 and 52 weeks (n=21, with some missing time points for some of the patients).

MRI was performed on a Signa 1.5-T imager (General Electric, Milwaukee, Wisc., USA). The patients had their optic nerves imaged with a coronal 3D GE sequence (TR 23.1ms, TE 5.6ms, NEX 2, flip angle 12°, 256x192 matrix, 19x14.25cm FOV, in-plane resolution 0.75x0.75mm, 60x1.5mm contiguous slices, acquisition time 18mins) both with and without a pre-pulse to saturate the broad resonance of immobile macromolecular protons (offset frequency 2kHz, equivalent on-resonance flip angle 500°) and a fat-saturated dual echo FSE sequence (coronal-oblique, TR 2300ms, $TE_{effective}$ 58/145ms, ETL 8, NEX 2, 512x384 matrix, 24x18cm FOV, in-plane resolution 0.5x0.5mm, 16x3mm interleaved contiguous slices, 11min acquisition time).

In addition, 24 of the patients had their optic nerves imaged at baseline before and after intravenous administration of 0.3mmol/kg dimeglumine gadopentate (triple-dose gadolinium) with a coronal-oblique fat-saturated T_1-weighted spin echo sequence (TR 600ms, TE 20ms, 1 excitation, 256x192 matrix, 24x18cm FOV, 16 contiguous 3mm slices, 3min acquisition time). An experienced radiologist (Dr K.A. Miszkiel), blinded to the lesion side and severity of visual loss, identified and measured the length of any enhancing optic nerve lesions on the post-gadolinium images. Serial imaging following triple-dose gadolinium was performed on 15 of the patients after 2, 4, 8 and 12 weeks

until enhancement was deemed to have ceased. The duration of enhancement was noted.

Twenty-seven control subjects (11 male, 16 female, median age 32 years, range 21-58 years) were also imaged. Eight of the controls were imaged once, four were imaged twice and 15 were imaged on three separate occasions spread out over the course of one year. Control subjects had to be free of significant ophthalmological or neurological disease and were recruited by the use of advertising posters.

A quadrature birdcage head coil was used as both transmitter and receiver coil. Subjects were asked to close their eyes and avoid any deliberate eye movements during image acquisition. Between imaging sessions care was taken to accurately reposition the imaging field of view. In particular, the line from the anterior commissure to the posterior commissure on sagittal localiser images was used to ensure that the subjects' head angles were the same at each session.

At each visit the patients were examined. Best visual acuity with appropriate spectacle or pinhole correction was measured using a retro-illuminated ETDRS chart and recorded as the 4m logMAR visual acuity (Ferris III *et al.*, 1982). When no letters could be correctly identified a score of 1.7 was assigned (Optic Neuritis Study Group, 1991). The central 30° of the visual field was analysed using the 30-2 program on the Humphrey field analyser (Allergan-Humphrey Inc., San Leandro, CA, USA). Wide-angle lenses were used to correct refractive errors where necessary. The overall visual field mean deviation was compared with a reference field derived from control data provided by the manufacturer. A mean deviation of -35dB was assigned when vision was too poor to attempt the test (Kupersmith *et al.*, 2002). The above two parameters were chosen because they give continuously variable measures that are amenable to statistical analysis.

In addition, at baseline, 4, 12 and 52 weeks whole-field and central-field pattern-reversal VEPs were measured on each patient (Chapter 4.1) (Brusa *et al.*, 2001). Ethical approval was obtained for the study from the joint ethics committee of the Institute of Neurology and the National Hospital for Neurology and Neursurgery; informed consent

in writing was obtained from each subject, in accordance with the Declaration of Helsinki.

From the images, MTR was calculated on a voxel-by-voxel basis from the expression: 100x(Mo-Ms) / Mo pu where Ms and Mo represent signal intensities with and without the saturation pulse respectively. The calculated MTR maps (Figure 1) were displayed on workstations (Sun Microsystem, Mountain View, CA, USA) using the DispImage display tool (Plummer, 1992).

4.2.3 Segmentation methodology

For segmentation of the optic nerves on the images to give the mean MTR previous studies relied on manual placement of an ROI of 4-8 pixels within the nerve (Thorpe *et al.*, 1995; Boorstein *et al.*, 1997; Inglese *et al.*, 2002). As has been discussed this has the potential for poor reproducibility, loss of information if there is swelling of the optic nerves and partial volume effects from surrounding CSF and orbital fat if there is optic nerve atrophy. These changes are known to occur in the natural history of optic neuritis (Figure 4.7) (Youl *et al.*, 1996).

An evaluation of different segmentation techniques was performed to decide on the most optimum method to carry forward to the major study. Ten control datasets with repeat imaging and five patient datasets both acutely and after one year were selected for preliminary analysis. No automatic segmentation method exists for the optic nerve due to its small size and the close approximation to the brain in its intracranial portion and the extra-ocular muscles near the orbital apex (Figure 4.8).

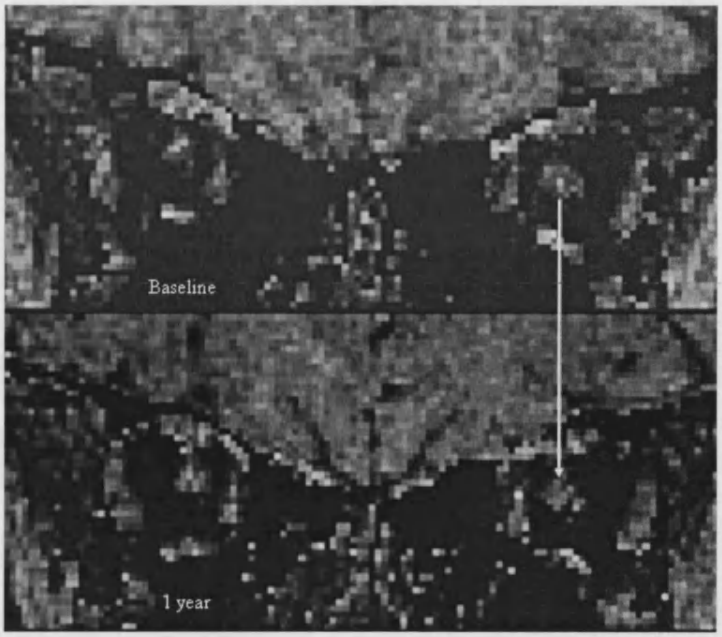

Figure 4.7: Baseline-52 week MTR maps of the orbital optic nerve in a patient with acute left-sided optic neuritis demonstrating change in optic nerve size over time (arrowed).

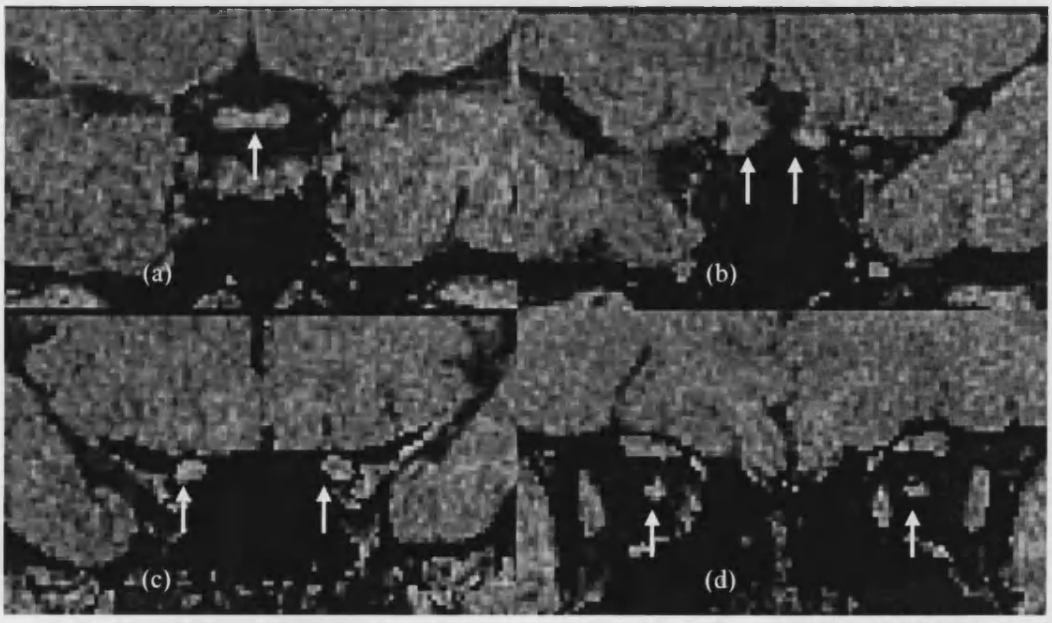

Figure 4.8: Optic nerve MTR maps from a control with optic nerves arrowed.
a) chiasm. b) intracranial.
c) intracanalicular. d) orbital.

A preliminary study was performed using the object strength method (Tofts *et al.*, 1997). The total excess intensity of the optic nerve in the orbit however was lower than in the canalicular and cranial portions because the background orbital fat had greater signal intensity than the air and bone surrounding the more posterior parts of the nerve (Figure 4.9). This methodology was not therefore explored further.

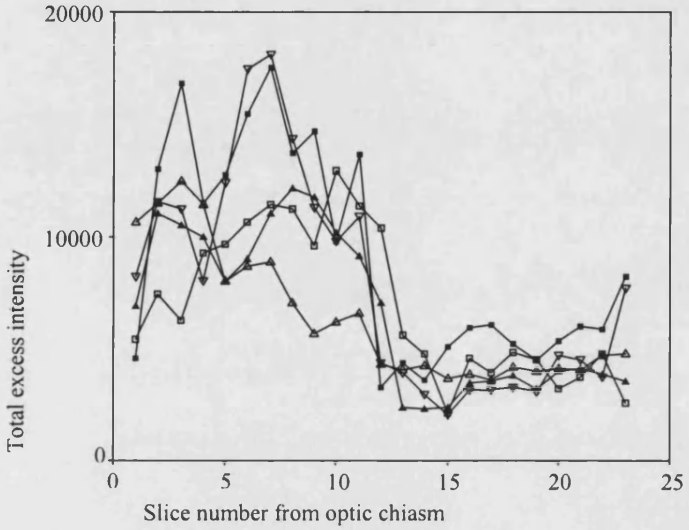

Figure 4.9: Total excess intensity from MTR maps versus position along the optic nerve for five randomly selected optic nerves. Note the sharp decrease in excess intensity which occurs upon entering the orbit.

Threshold-based contouring was tried, comparing a fixed threshold of 10pu, which was the threshold set for a previous MT study in the spinal cord to exclude partial volume pixels (Rovaris *et al.*, 2000), with a more conservative 30pu. These two thresholds were compared for both reproducibility and the ability to detect changes occurring in both the acute and chronic phase of optic neuritis. The analysis was performed by a blinded observer on the MTR maps, as the intraorbital optic nerve could not be identified on the M_o images due to high signal and chemical shift artefact from orbital fat (Figure 4.10). The signal from fat was suppressed on the MTR maps due to its low MTR. Some manual correction was needed particularly for the intracranial optic nerve, as the brain was often included in the initial ROI generated.

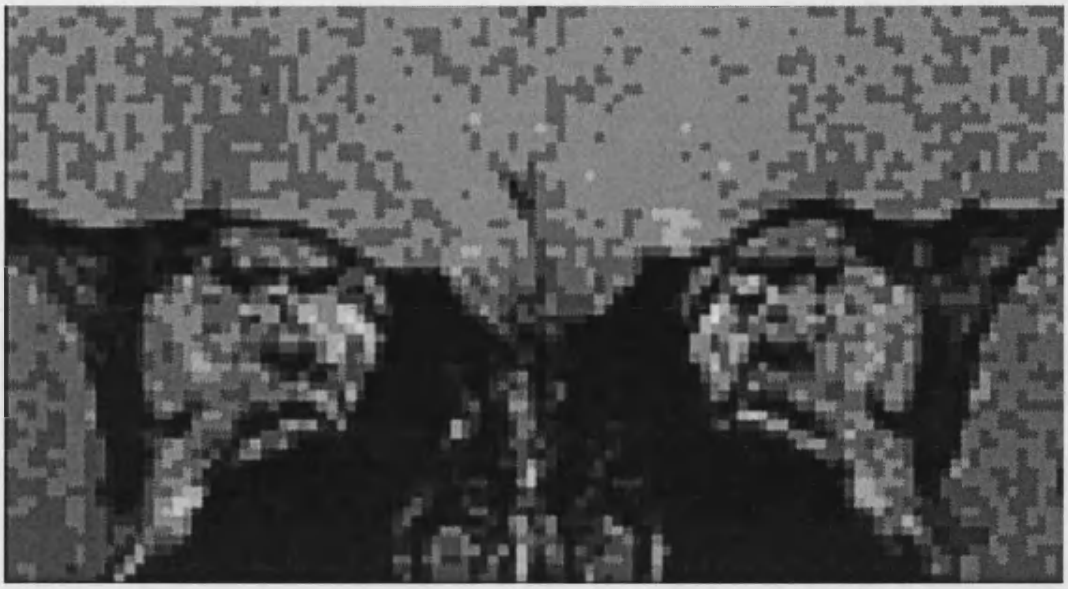

Figure 4.10: Orbital Mo image demonstrating high signal from orbital fat obscuring the optic nerves.

The measurement reproducibility of the two segmentation thresholds in given in Table 4.9 from random effects analysis of variance (Bland & Altman, 1996a; Bland & Altman, 1996b; Bland & Altman, 1996c) and the results in patients and controls is in Tables 4.10.

(a)

Threshold and side	Mean (pu)	Within-subject SD	95% reference range[a]	CV (%)[b]	Reliability coefficient[c]
10pu left	44.1	0.65	± 1.27	1.5	0.93
10pu right	42.7	0.65	± 1.27	1.5	0.82
30pu left	48.8	0.22	± 0.43	0.5	0.98
30pu right	47.9	0.50	± 0.98	1.0	0.99

(b)

Threshold and side	Mean (pu)	Within-subject SD	95% reference range[a]	CV (%)	Reliability coefficient[b]
10pu left	42.7	1.28	± 2.51	3.0	0.58
10pu right	42.7	1.14	± 2.23	2.7	0.62
30pu left	47.8	1.27	± 2.49	2.7	0.44
30pu right	47.8	1.03	± 2.02	2.2	0.67

Table 4.9: Measurement reproducibility for the different subgroups.
a) Measure-remeasure for 10 randomly selected datasets.
b) Acquisition-reacquisition for 10 controls.

[a]1.96 x within-subject SD. 95% of measurements are expected to lie within this departure from the true value.

[b]The proportion of total variance due to between-subject variation. Under assumptions which are plausible here, one minus this value is the proportion of variation due to measurement error.

Threshold	MTR (pu)		
	Control mean	Acute optic neuritis	Optic neuritis after 1 year
10 pu	42.7	43.6 p=0.4 v. control	40.1 p=0.01 v. control p=0.08 v. acute
30 pu	47.4	48.5 p=0.4 v. control	45.9 p=0.04 v. control p=0.1 v. acute

Table 4.10: Optic nerve MTR in patients and controls, comparisons using paired and independent samples *t* tests as appropriate.

This sequence produces high quality MT images and the fixed threshold contouring enables the measurement of MTR with both high reproducibility and sensitivity to detecting disease effects. The high reproducibility is a result of the segmentation using

fixed thresholds which are less dependent on the initialisation point and also because they are based on mean results over a number of slices. The 10pu threshold required more manual correction and potentially included more partial volume pixels, particularly in the orbit, as the background is not as uniform as in the spinal cord. The results suggest that changes in MTR due to optic neuritis can be measured, at least in the chronic phase, although this will need confirming in a larger cohort of patients. The 30pu threshold segmentation technique was more reproducible and is potentially more immune to partial volume effects and therefore the results will be more robust. Its use in the whole cohort of patients will now be considered.

4.2.4 Optic nerve segmentation

An observer, experienced in interpreting optic nerve images but blinded to subject identity and acquisition order, segmented the optic chiasmata and the optic nerves, from all the slices on which the nerves were visible, using threshold-based contouring with the threshold fixed at 30pu. The measurements made on the baseline imaging of the controls, plus 20 of the patients' scans (selected at random), were repeated so that the measurement reproducibility could be assessed.

Lesions were identified on the acute FSE images (intrinsically registered to the MT images as they were acquired together) by the radiologist (Dr. K. Miszkiel) and from their coordinates the part of the nerve occupied by a lesion could be identified on the MTR maps. The mean lesion and post-lesion MTR (ie the MTR in the section of the nerve between the lesion and the optic chiasm) could then be calculated. Formal co-registration was not possible due to the small size of the optic nerves and the fact that the nerves can move (semi-) independently of the surrounding tissue. Instead, at each subsequent time-point the same parts of the nerve were identified by using the optic chiasm as the reference point and counting the same number of slices from the anterior part of the chiasm.

In controls the optic nerve mean MTR varied with slice position from the optic chiasm reaching a peak in approximately the location of the optic canal (Figure 4.11).

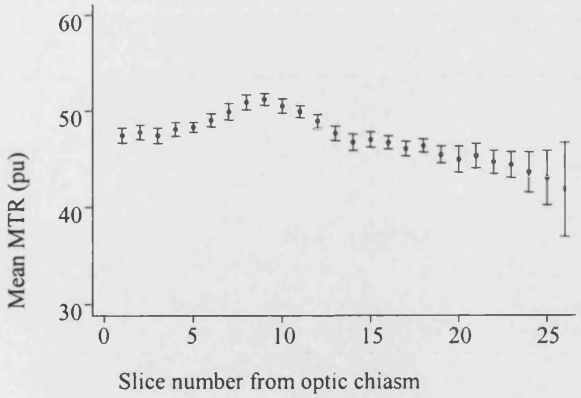

Figure 4.11: Mean MTR according to slice position from the optic chiasm anteriorly in controls. Error bars show ($\sqrt{2}/2$) x 95% confidence intervals. For first 16 slices n=27, for subsequent slices n = 26, 25, 23, 22, 20, 15, 11, 6, 4 and 2, respectively, reflecting the variation in length of the optic nerve in different individuals.

For analysis of lesion and post-lesion MTR, the ratio of the symptomatic optic nerve lesion mean MTR or post-lesion mean MTR to the corresponding part of the healthy contralateral optic nerve mean MTR was therefore used because the lesion length and position along the optic nerve varied between patients. This also had the effect of smoothing out any effects due to varying movement artefact between sessions, as any movement artefact due to head motion and conjugal eye movements tends to affect both eyes equally.

4.2.5 Statistical methods

To assess measurement reproducibility the within- and between-subject standard deviations (and hence CV and intraclass correlation coefficient) were obtained from random effects one way analysis of variance (Bland & Altman, 1996a; Bland & Altman, 1996b; Bland & Altman, 1996c). Variations in MTR variables over time were examined using random intercept (Goldstein, 1995) regression models with fixed linear and quadratic terms in time (there was no evidence that random slopes in time improved the fit). Baseline (time 0, the day of onset of visual symptoms) and 365 day values were estimated from these models, and patient versus control difference in gradient assessed, including a subject status by time interaction term. Time to nadir (minimum of the

quadratic curve) and value at nadir were functions of the linear and quadratic parameters, for which CI were obtained using a non-parametric bias-corrected bootstrap with 1000 replicates (Carpenter & Bithell, 2000). Bootstrap CI were also obtained where Normality of regression residuals could not confidently be assumed. Simple regression was used to examine relationships between 'time-averaged' variables (with one value per subject averaged over available time points); a subject status indicator was used to compare patients and controls (this is equivalent to a t-test). Eventual visual recovery levels were estimated for each patient as asymptotes of exponential models in time (Snedecor & Cochran, 1989). All analyses were carried out in Stata 7.0 (Stata Corporation, College Station, Texas, USA) except for random slopes models which were examined in MLwiN 1.10 (Centre for Multilevel Modelling, Institute of Education, London, UK).

One patient had bilateral recurrence of optic neuritis after 12 weeks and 2 patients had recurrences in their previously healthy contralateral optic nerves, one patient at both 12 and 52 weeks and one patient at 26 weeks. The data collected on these subjects after these events were excluded from the analysis.

4.2.6 Results

Measurement reproducibility figures (CV ranges 0.3-0.5%) are given in Table 4.11. The estimated mean MTR in control optic nerves at baseline was 47.8pu (95% CI 47.4, 48.2). This value showed no evidence of a systematic change according to the date of acquisition, nor was there evidence that mean MTR in controls changed significantly over one year: the estimated rate of change over the year was -0.00065pu/day (95% CI -0.0024, 0.0011), p=0.462. The time-averaged mean MTR in controls was 47.7pu (95% CI 47.5, 48.0) (Figure 4.12).

MTR variable	Mean (pu)	Within-subject SD	95% reference range[a]	CV (%)	Reliability coefficient (95%CI)[b]
Controls:					
Mean	47.8	0.17	± 0.34	0.4%	0.98 (0.96, 0.99)
Optic chiasm	48.4	0.21	± 0.41	0.4%	0.99 (0.98, 1.00)
Patients:					
Diseased optic nerve	45.9	0.21	± 0.41	0.5%	0.99 (0.98, 1.00)
Healthy optic nerve	47.7	0.17	± 0.33	0.3%	0.99 (0.99, 1.00)
Optic chiasm	46.7	0.18	± 0.36	0.4%	0.99 (0.98, 1.00)

Table 4.11: Measurement reproducibility for the different subgroups.

[a]1.96 x within-subject SD. 95% of measurements are expected to lie within this range of the true value, if the variable is approximately Normally distributed.

[b]The proportion of total variance due to between-subject variation (with 95% confidence intervals). Under assumptions which are plausible here, one minus this value is the proportion of variation due to measurement error.

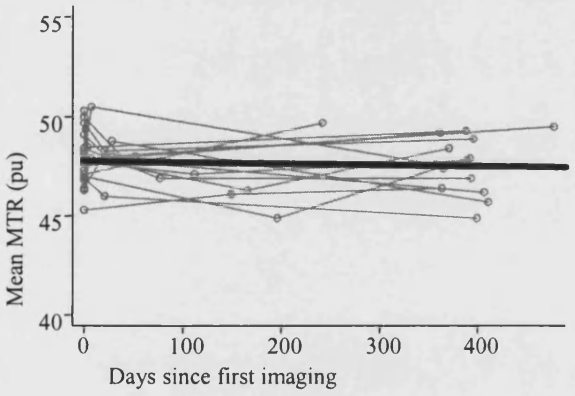

Figure 4.12: Mean MTR in controls over time with fitted line shown in bold.

The estimated mean MTR from healthy contralateral optic nerves from patients at baseline was 47.9pu (95% CI 47.5, 48.3). The gradient of change over one year was +0.00092pu/day (95% CI -0.0012, 0.0030), p=0.383, again suggesting that there was no significant change in MTR in the healthy contralateral eyes over one year. There was no evidence of any difference in time-averaged mean MTR between the healthy

contralateral nerves and controls (patient - control difference in means = 0.2813, 95% CI -0.2843, 0.8470, p=0.323).

The characteristics of mean MTR in diseased optic nerves and lesion MTR ratio are illustrated in Figures 4.13 and 4.14 and given in Table 4.12. The significant positive quadratic coefficients indicate a U-shape: an initial decline in MTR reaching a nadir at about 240 days followed by a slight increase. The estimated 365 day values remained significantly less than both baseline and control values although the increases compared with the nadir values were not significant (as shown by the appropriate 95% confidence limits).

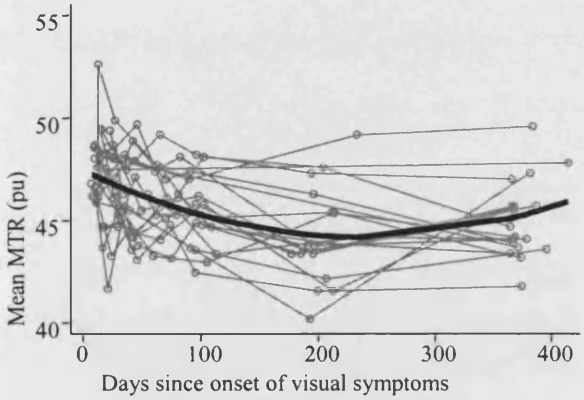

Figure 4.13: Mean MTR over time for whole of diseased optic nerves with fitted curve in bold.

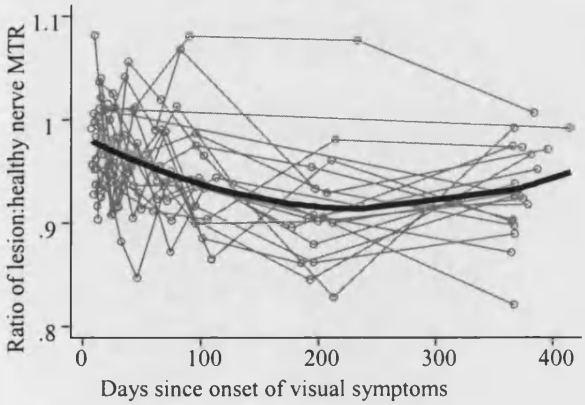

Figure 4.14: Ratio of MTR of the lesion: corresponding portion of healthy contralateral optic nerve over time with fitted curve in bold.

	Estimated time "0" value (95% CI)	Linear coefficient[a] (95% CI) P value	Quadratic coefficient (95% CI) P value	Time to nadir[b] (95% CI)[c]	Nadir value (95% CI)[c]	Estimated 365 day value (95% CI)
Diseased optic nerve MTR, pu	47.4 (46.8, 48.1)	-0.027 (-0.035, -0.019) P<0.001	$5.7x10^{-5}$ ($3.6 x10^{-5}$, $7.8 x10^{-5}$) P<0.001	239 (216, 277)	44.2 (43.7, 44.8)	45.1 (44.4, 45.8)
Ratio of diseased: healthy optic nerve MTR	0.99 (0.97, 1.00)	-0.00051 (-0.00072, -0.00030) P<0.001	$1x10^{-6}$ ($5x10^{-7}$, $1.6x10^{-6}$) P<0.001	246 (214, 313)	0.92 (0.91, 0.94)	0.94 (0.92, 0.95)
Ratio of lesion: healthy optic nerve MTR	0.98 (0.97, 1.00)	-0.00058 (-00083, -0.00033) P<0.001	$1.2x10^{-6}$ ($5.6x10^{-7}$, $1.8x10^{-6}$) P<0.001	241 (215, 289)	0.91 (0.90, 0.93)	0.93 (0.91, 0.95)

Table 4.12: Whole optic nerve and lesion MTR results in patients.

[a]Linear coefficient can be interpreted as the rate of daily decline at time "0".

[b]Days from time "0" (day of onset of visual symptoms).

[c]Bootstrap derived confidence intervals.

At the first assessment there was no significant difference in MTR between diseased optic nerves and control optic nerves (mean MTR in patients 47.3pu, mean MTR in controls 47.7, difference -0.4, 95% CI -1.2, 0.4, p=0.354). There was however a significant difference in the time-averaged mean MTR from diseased optic nerves and control optic nerves (46.2pu versus 47.7pu, difference in means -1.5, 95% CI -0.8, -2.1, p=0.0001).

The mean MTR ratios from post-lesion segment of diseased optic nerves and the mean MTR results from the optic chiasmata are given in Table 4.13. A linear model gave the best fit for these two variables and indicated a decline in both over time. In controls there was no evidence of change of chiasmal MTR over time (gradient -0.0013pu/day, 95% CI -0.0038, 0.0012, p=0.304). However, there was no statistical evidence of a difference in gradient between patients and controls, probably through insufficient power. At first assessment the chiasmal MTR was significantly less in patients than controls (47.1pu versus 48.3pu, p=0.023). There was also a significant difference between patients and controls for the time-averaged mean chiasmal MTR (46.8pu versus 48.0pu, p=0.004); and the 365 day estimated value for patients (46.0pu, 95% CI 45.3, 46.8) was lower than the control time-averaged mean (48.0pu, 95% CI 47.3, 48.7).

	Estimated time "0" value (95% CI)	Linear coefficient[a] (95% CI)	Estimated 365 day value (95% CI)
Ratio of post-lesion: healthy optic nerve MTR	0.98 (0.97, 0.99)[b]	$-9x10^{-5}$ ($-1.5x10^{-4}$, $-3x10^{-5}$)[b] p=0.01[b]	0.95 (0.93, 0.96)[b]
Chiasmal MTR, pu	47.2 (46.7, 47.7)	-0.0033 (-0.0058, -0.0007) p=0.013	46.0 (45.3, 46.8)

Table 4.13: Post-lesion and chiasmal MTR results from patients.

[a]This is interpreted as the estimated rate of change per day in the MTR variable.

[b]Bootstrap derived confidence intervals and P-value.

The relationship between the MTR variables and the clinical variables was complex. There was no linear relationship between any of the diseased optic nerve MTR variables and logMAR acuity or visual field mean deviation at baseline or one year. Although there appeared to be an association within patients between the MTR variables and vision (with the MTR variables appearing to fall as vision improved), this seemed to be an artefact of time: once time was entered into the model, the within-person MTR versus vision relationship lost statistical significance. However, eventual visual recovery level was improved in patients with higher time-averaged ratios of diseased:healthy optic nerve MTR; this was true for the whole optic nerve, for the lesion segment and for the post-lesion segment (Table 4.14).

There was no evidence of association between the acute lesion length (measured on either FSE or triple-dose gadolinium enhanced images) and any of the MTR variables. The median duration of gadolinium enhancement was 63 days (range 0-113 days). Again, the duration of enhancement was not associated with any of the MTR variables.

Ratio	Linear coefficients[a] (95% CI)[b] P-value	
	Visual field mean deviation recovery, dB	logMAR visual acuity recovery
Diseased optic nerve: healthy optic nerve MTR	0.95 (0.49, 1.57) p<0.001	-0.05 (-0.01, -0.08) p=0.007
Lesion: healthy optic nerve MTR	0.46 (0.08, 099) p=0.04	-0.03 (-0.002, -0.08) p=0.02
Post-lesion: healthy optic nerve MTR	0.79 (0.46, 1.12 p<0.001	-0.03 (-0.003, -0.07) p=0.03

Table 4.14: The relationship between time-averaged MTR ratios and visual recovery level.

[a]Interpreted as estimated change in eventual visual recovery level for each 0.01 rise in time-averaged MTR ratio.

[b]Bootstrap derived confidence intervals.

There were no significant direct linear relationships by cross-sectional analyses between the MTR variables and electrophysiological measurements. There was evidence that patients with higher time-averaged MTR values had shorter time-averaged VEP latencies. Whole field latency was lower by 5.3ms (95% CI 0.2, 10.3, p=0.043) and central field latency was lower by 6.1ms (95% CI 1.5, 10.7, p=0.012) (Figure 4.15) per 1pu rise in time-averaged diseased optic nerve MTR. There were no associations between time-averaged amplitude results and any time-averaged MTR variables.

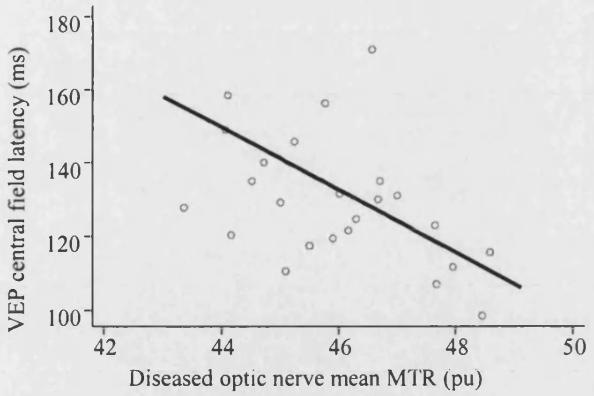

Figure 4.15: Time-averaged VEP central field latencies versus time-averaged diseased optic nerve MTR values.

4.2.7 Discussion

The use of a fixed threshold of 30pu enabled the optic nerves to be segmented with high reproducibility, although it should be noted that as the results reflect the mean MTR over the whole optic nerve, variations will tend to be, to an extent, smoothed out. The high threshold was chosen to exclude partial volume voxels which in patients might be expected to have a differential effect later in the study where optic nerve atrophy might be developing. This may also have limited the proportionate decrease in MTR values seen compared with previous studies in both MS and optic neuritis, by minimising the risk of a spurious reduction in MTR due to partial volume effects with inclusion of CSF in the optic nerve sheath. However, absolute MTR values between studies should not be directly compared as they vary according to the imager and sequence used.

The mean MTR in the healthy optic nerve varied with slice position, being highest in the optic canal, probably due to the more densely packed structure of the optic nerve within the confines of the bony canal (Figure 4.11). The decline in the orbital portion may be due to a looser structure as well as movement artefact in this portion of the optic nerve. There was also variation in length of the optic nerve between individuals leading to larger confidence intervals at the most anterior slices.

A quadratic model was used for both diseased optic nerve MTR and lesion MTR ratio because inspection of the raw data suggests that, on average, both declined to nadirs at around 240 days followed by small increases (Table 4.12, Figures 4.13 and 4.14). The one-year values however, were not significantly higher than the nadir values.

At the onset of optic neuritis, when visual impairment was at its worst, MTR values were unchanged. This finding is in contrast with acute brain lesions in MS where there is a rapid initial decrease in MTR. The normal MTR value in acute optic neuritis may result from a balance of two factors. Firstly, in the first two weeks after axonal transection, "acute" Wallerian degeneration may transiently increase MTR, probably due to increasing exposure of myelin fragments (Lexa *et al.*, 1994). Secondly, breakdown of the blood-optic nerve barrier, depicted using gadolinium enhancement, results in an inflammatory cellular infiltrate and an element of vasogenic oedema; the increase in interstitial fluid will decrease MTR. The optic nerve has a more compact structure with subdivision into fascicles of axons by fibrous septa and a surrounding optic sheath (Williams *et al.*, 1989). Vasogenic oedema may therefore be limited in the optic nerve, lessening the initial effects of oedema on MTR changes in the nerve. In comparison, acute MS lesions in the brain may show much larger initial reductions in MTR values (Dousset *et al.*, 1998; Silver *et al.*, 1998) because there is a much greater amount of interstitial fluid due to vasogenic oedema.

During the most rapid phase of visual recovery mean MTR was gradually declining. This decline did not reach a nadir until about 8 months. This discordance suggests that:
(i) There are factors leading to early visual recovery that are not reflected using MTR.
(ii) A continuing breakdown in tissue structure is occurring for several months following visual recovery.
The initial rapid recovery of vision may have been due to:
(i) Disappearance of inflammatory mediators of conduction block (e.g. nitric oxide) (Youl *et al.*, 1991).
(ii) Insertion of sodium channels along the inter-nodal membrane to restore axonal conduction (Moll *et al.*, 1991; Felts *et al.*, 1998).
(iii) Early remodelling of visual function and utilising redundant capacity at the level of central synaptic networks (Frisen & Quigley, 1984; Werring *et al.*, 2000).
None of these processes may have had a material effect on MTR.

The optic nerve mean MTR also continued to decline beyond when gadolinium enhancement, indicating inflammation, was last detected. The continued decline in MTR might be due to:

(i) Ongoing demyelination, as reflected by the relationship between time-averaged MTR and mean VEP central field latency.

(ii) Gradual clearance of myelin breakdown products (that continue to act as structural elements whilst present) resulting either from initial inflammatory myelin breakdown *per se* (Adams *et al.*, 1989) or as part of the prolonged degenerative phase of Wallerian degeneration (Lexa *et al.*, 1994).

The decline in MTR occurred for much longer in this study than studies of MS brain lesions (Dousset *et al.*, 1998; Silver *et al.*, 1998) possibly due to the different ultrastructure of the optic nerve compared with white matter tracts in the brain slowing clearance of myelin debris. In this context, it is noteworthy that in a rat optic nerve model of Wallerian degeneration myelin debris could be detected 22 months post-enucleation (Ludwin, 1990).

The decline in MTR appeared to reach a nadir after about 8 months, which may reflect arrest of demyelination and clearance of myelin debris. Remyelination in the lesion may have contributed to the subsequent trend for MTR to increase, a view supported by the significant relationship observed between time-averaged MTR and mean VEP central field latency. However, further follow up is needed to determine whether or not the increase in MTR is significant and sustained.

Over the whole period, lower time-averaged MTR ratios were associated with poorer visual outcome, which suggests that, although the relationship between MTR and vision is complex, the longer the time during which the diseased nerve MTR was lower than that of its fellow nerve (implying tissue disruption most likely due to demyelination and axonal loss) the worse the prognosis.

The continued linear decline in post-lesional and chiasmal MTR is probably solely due to Wallerian degeneration in the axons transected in the acute inflammatory lesion. The initial post-lesional MTR was not abnormally high, unlike what was seen in the case in the experimental transection study by Lexa *et al.* (1994), possibly due to inflammation in these regions not apparent on conventional imaging depressing MTR slightly. Also,

Wallerian degeneration is likely to be much less extensive in the optic nerve following optic neuritis, than in the above lesion study, probably affecting only about 10% of fibres compared with the 100% nerve section model.

If, in future trials of remyelination therapies, the optic nerves are chosen, then optic nerve MT imaging in combination with conventional imaging, VEP and clinical measures may be useful in assessing the response to treatment. The potential advantage of using optic nerve MT imaging to assess optic nerve structure over VEP measurement is the ability to visualise the optic nerves and to assess different parts of the optic nerve, including both the lesion and post-lesion segments. Electrophysiological measures can only give an indication of conduction in the whole optic pathway which may be influenced by changes in the optic tract, lateral geniculate body and optic radiation. MTR measures may also have a role in detecting remyelination of MS lesions elsewhere in the CNS.

4.3 A serial MRI study following optic nerve mean area in acute optic neuritis

4.3.1 Introduction

A reproducible technique to measure orbital optic nerve mean cross-sectional area was described in Chapter 3.1 and 3.2 using a fat-saturated sTE fFLAIR sequence which removes the high signal from both orbital fat and CSF in the sheath of the optic nerve. Optic nerve atrophy was demonstrated following optic neuritis and the degree of atrophy related to time since onset of the illness. Serial follow-up in a subgroup of patients demonstrated ongoing atrophy some years following the acute event in many of the patients. Poor baseline visual acuity (p=0.02), decreased VEP amplitudes (r_S=0.65, p=0.02) and increased latencies (r_S=-0.61, p=0.04) were associated with the degree of atrophy.

Although atrophy measures are widely used to monitor the course of MS, the mechanisms of progressive atrophy and axonal loss are not well understood. One potential mechanism for the development of ongoing atrophy is Wallerian degeneration due to axonal damage in focal MS lesions. This may result from inflammatory and post-inflammatory mechanisms. Axonal transection and loss has been shown to occur in acute inflammatory MS lesions (Ferguson *et al.*, 1997; Trapp *et al.*, 1998). However, axons are potentially vulnerable for a long time, perhaps months or years, in the post inflammatory lesion, if there is persistent demyelination and/or exposure to excitatory neurotoxic molecules including nitric oxide and glutamate (Smith & McDonald, 1999). In the brain and spinal cord, measures of atrophy, in general, correlate only modestly with lesion load measures but it is difficult to explore the relationship between atrophy and lesions in these regions of because it is not possible to study the effects of individual lesions within their relevant fibre tract (Miller *et al.*, 2002). As has been discussed, optic neuritis offers a unique opportunity to investigate individual inflammatory lesions and the consequences that they have for tissue volume loss.

This study focuses on the above cohort of patients recruited prospectively with their first episode of acute optic neuritis. The key aims of this study are:

(i) To quantify the extent of tissue volume changes due to an individual acute inflammatory demyelinating lesion within its fibre tract, previously observed to be swollen acutely and atrophied chronically.
(ii) To determine the time course of atrophy developing as a result of individual lesions.
(iii) To explore if any of the acute imaging, clinical or electrophysiological measures may help in predicting the likelihood of optic nerve atrophy developing: identifying such factors may help in selecting patients where therapies to prevent atrophy are most needed.
(iv) To determine whether the extent of early swelling or later atrophy are related to clinical, imaging or electrophysiological measures.
(v) To determine if there is any relationship between MTR, a putative marker for myelination and axonal integrity (Chapters 2.3.9 and 4.2) in the optic nerve and the development of optic nerve atrophy, in particular if higher MTR values, implying less demyelination, are associated with less atrophy development.

4.3.2 Patients and methods

Twenty-nine patients with their first episode of acute unilateral optic neuritis (10 males, 19 females, median age 30 years, range 19-53 years), as part of the cohort described above, were recruited from the Neuro-Ophthalmology clinic, Moorfields Hospital, London. The median delay from onset of visual symptoms to the first examination was 13 days (range 7-24 days). Three of the patients had CDMS, five had CPMS and 21 had clinically isolated optic neuritis (Poser *et al.*, 1983). All of the patients were examined acutely and then 21 were followed-up after 2, 4, 8, 12, 26 and 52 weeks (with some missing time points for some of the patients). Ethical approval was obtained for the study from the joint ethics committee of the Institute of Neurology and the National Hospital for Neurology and Neurosurgery; informed consent in writing was obtained from each subject, in accordance with the Declaration of Helsinki.

MRI was performed on a Signa 1.5-T imager (General Electric, Milwaukee, Wisc., USA). The patients' optic nerves were imaged with the sTE fFLAIR (coronal-oblique, TR=2740ms, TE=16ms, TI=1072ms, NEX 6, ETL 6, matrix size 512x384, 24x18cm field of view, in-plane resolution 0.47x0.47mm, 3mm interleaved contiguous slices, acquisition time 13.5 minutes) sequence, a fat-saturated FSE (coronal-oblique, TR

2300ms, TEef 58/145ms, ETL 8, NEX 2, 512x384 matrix, 24x18cm field of view, in-plane resolution 0.47x0.47mm, 3mm interleaved contiguous slices, 11min acquisition time) sequence and a three-dimensional GE (coronal, TR 23.1ms, TE 5.6ms, NEX 2, flip angle 12°, 256x192 matrix, 19x14.25cm field of view, in-plane resolution 0.74x0.74mm, 60x1.5mm contiguous slices, acquisition time 18mins) sequence both with and without a pre-pulse to saturate the broad resonance of immobile macromolecular protons (offset frequency 2kHz, equivalent on-resonance flip angle 500°). From these images, MTR was calculated on a voxel-by-voxel basis from the expression: 100x(Mo-Ms) / Mo pu where Ms and Mo represent signal intensities with and without the saturation pulse respectively.

In addition, 24 of the patients had their optic nerves imaged at baseline before and after intravenous administration of 0.3mmol/kg dimeglumine gadopentate (triple-dose gadolinium) with a coronal-oblique fat-saturated T_1-weighted spin echo (TR 600ms, TE 20ms, 1 excitation, 256x192 matrix, 24x18cm field of view, in-plane resolution 0.94x0.94mm, 16 interleaved contiguous 3mm slices) sequence. An experienced radiologist (Dr. K.A. Miszkiel), blinded to the lesion side and severity of visual loss, identified and measured the length of lesions on FSE images and any enhancing optic nerve lesions on the post-gadolinium T_1-weighted images. Serial imaging following triple-dose gadolinium was performed on 15 of the patients after 2, 4, 8 and 12 weeks until enhancement was deemed to have ceased. The duration of enhancement was noted.

Thirty-two control subjects (14 male, 18 female, median age 31 years, range 21-58 years) were also imaged. Ten of the controls were imaged once, six were imaged twice and 16 were imaged on three separate occasions spread out over the course of one year. Control subjects had to be free of significant ophthalmological or neurological disease and were recruited by the use of advertising posters.

A quadrature birdcage head coil was used as both transmitter and receiver coil. Subjects were asked to close their eyes and avoid any deliberate eye movements during image acquisition. Between imaging sessions care was taken to accurately reposition the imaging field of view. In particular, the line from the anterior commissure to the

posterior commissure on sagittal localiser images was used to ensure that the subjects' head angles were the same at each session.

At each visit the patients were examined. Best visual acuity with appropriate spectacle or pinhole correction was measured using a retro-illuminated ETDRS chart and recorded as the 4m logMAR acuity (Ferris III *et al.*, 1982). When no letters could be correctly identified a score of 1.7 was assigned (Optic Neuritis Study Group, 1991). The central 30° of the visual field was analysed using the 30-2 program on the Humphrey field analyser (Allergan-Humphrey Inc., San Leandro, CA, USA). Wide-angle lenses were used to correct refractive errors where necessary. The overall field mean deviation was compared with a reference field derived from control data provided by the manufacturer. A mean deviation of -35dB was assigned when vision was too poor to attempt the test (Kupersmith *et al.*, 2002). The above two parameters were chosen because they give continuously variable measures that are amenable to statistical analysis. In addition, at baseline, 4, 12 and 52 weeks whole-field and central-field pattern-reversal VEPs were measured on each patient (Chapter 4.1) (Brusa *et al.*, 2001).

The images were displayed on Unix workstations (Sun Microsystem, Mountain View, CA, USA) using the DispImage display tool (Plummer, 1992). The mean cross-sectional area of the intra-orbital portion of each optic nerve was calculated by an experienced observer blinded to image identity and acquisition order from five consecutive 3mm slices anteriorly from the orbital apex from the sTE fFLAIR images using a computer-assisted contouring technique as described in Chapter 3.1. The measurements were repeated from all of the controls' baseline imaging and 20 of the patients' images selected at random so that the measurement reproducibility could be calculated. The same observer segmented the whole optic nerves from the MTR maps using threshold-based contouring with the threshold fixed at 30pu, as performed in Chapter 4.2.

One patient had bilateral recurrence of optic neuritis after 12 weeks and 2 patients had recurrences in their previously healthy contralateral optic nerves, one patient at both 12 and 52 weeks and one patient at 26 weeks. The respective data from these time points and after have been discarded.

4.3.3 Statistical methods

To assess measurement reproducibility the within- and between-subject standard deviations (and hence CV and intraclass correlation coefficient) were obtained from random effects one way analysis of variance (Bland & Altman, 1996a; Bland & Altman, 1996b; Bland & Altman, 1996c).

Paired t-tests were used to assess differences between diseased and healthy contralateral optic nerve mean areas at fixed time points. Two sample t-tests were used for the comparison between diseased and control optic nerve mean areas both at fixed time points and for 'time-averaged' values (mean for each patient over available time points). Variation in healthy nerve area over time was examined using random intercept and fixed slope regression models (Goldstein, 1995) with linear term in time (there was no evidence that random slopes improved fit). Patient indicator x time interaction terms were used to assess patient versus control differences in gradients over time.

Patient-specific baseline and one year rates of decline and eventual levels of diseased optic nerve area were estimated by fitting exponential models in time (Snedecor & Cochran, 1989) for each patient, since multilevel non-linear models are difficult to fit. CIs and p-values for these estimates were obtained using a non-parametric bias-corrected bootstrap with 1000 replicates (Carpenter & Bithell, 2000). Figures 4.18 and 4.19 were generated using exponential models fitted to all patient data.

Linear regression was used to investigate associations at fixed time points between atrophy and other quantitative variables (VEP, visual acuity), and between time-averaged variables. Where Normality of residuals could not be assumed bootstrap confidence intervals and corresponding p-values were obtained; where outliers were present Spearman rank coefficients are reported.

All analyses were carried out in Stata 7.0 (Stata Corporation, College Station, Texas, USA) except for random slopes models which were examined in MLwiN 1.10 (Centre for Multilevel Modelling, Institute of Education, London, UK).

4.3.4 Results

Measurement reproducibility figures are given in Table 4.15. There was no evidence of a systematic change in mean area from controls according to the date of acquisition.

Variable	Mean (pu)	Within-subject SD	95% reference range[a]	CV (%)	Reliability coefficient (95% CI)[b]
Controls: Mean	13.5	0.55	± 1.07	4.0%	0.90 (0.84, 0.97)
Patients: Diseased optic nerves	13.6	0.65	± 1.26	4.8%	0.96 (0.93, 0.99)
Healthy optic nerves	12.7	0.67	± 1.31	5.3%	0.84 (0.70, 0.97)

Table 4.15: Measurement reproducibility for the different subgroups.
[a]1.96 x within-subject SD. 95% of measurements are expected to lie within this range of the true value, if the variable is approximately Normally distributed.
[b]= The proportion of total variance due to between-subject variation. Under assumptions which are plausible here, one minus this value is the proportion of variation due to measurement error.

Control mean areas

At baseline the mean area of control optic nerves was 13.6 (SD 1.8)mm^2. There were no significant differences between right or left optic nerves or in optic nerve mean area between males and females. The control mean area at 52 weeks was 13.1 (SD 1.8)mm^2 to give a time-averaged mean of 13.5 (SD 1.6)mm^2 and gradient of change of -0.001mm^2/day (95% CI -0.003, 0.001; p=0.36).

Patients: Baseline mean areas

At baseline the mean area of diseased optic nerves was 16.1 (SD 3.1)mm^2, 20.1% higher than the 13.4 (SD 2.0)mm^2 for healthy contralateral optic nerves (mean

difference=2.7mm^2, 95% CI 1.8, 3.7; p<0.0001 for hypothesis of zero difference) and 18.4% higher than the 13.6mm^2 for controls (mean difference=2.5mm^2 95% CI 1.2, 3.8; p=0.0003).

Patients: 52 week mean areas

At 52 weeks the mean area of diseased optic nerves was 11.3 (SD 2.2)mm^2, 11.7% lower than the 12.8 (SD 1.5)mm^2 for healthy contralateral optic nerves (mean difference=-1.5, 95% CI -0.1, -2.8; p=0.032) and 13.7% lower than the 13.1mm^2 for controls (mean difference=-1.8, 95% CI -0.5, -3.2; p=0.008) (Figure 4.16).

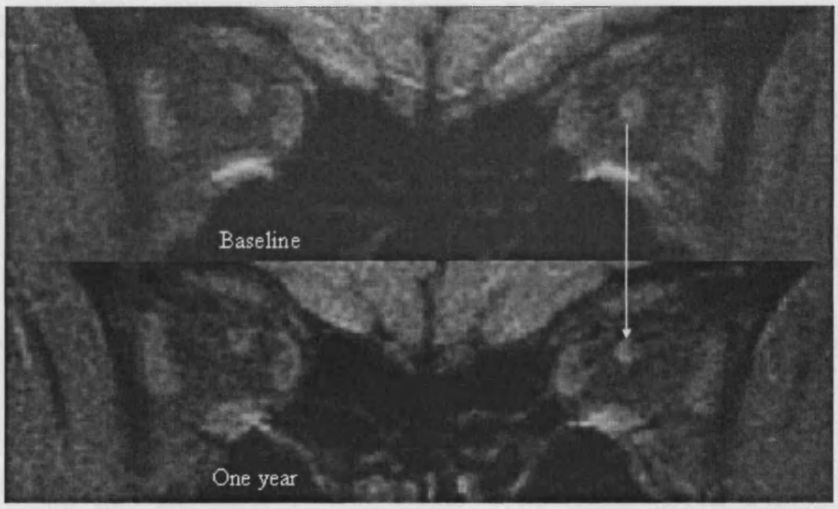

Figure 4.16: Baseline and one-year images from a 42 year-old woman with left-sided optic neuritis. The first imaging was performed 14 days after onset of visual symptoms.

Patient healthy contralateral optic nerve mean area trajectories

There was no evidence of change in area of healthy contralateral optic nerves over time (gradient=-0.00072mm^2/day, 95% CI -0.0029, 0.0015; p= 0.52) (Figure 4.17). There was also no evidence of any difference in time-averaged values between the patients' healthy contralateral optic nerves (mean 13.15 [SD 1.0]mm^2) and control optic nerves (13.5mm^2), difference 0.35mm^2 (95% CI 0.3, 1.0; p=0.32).

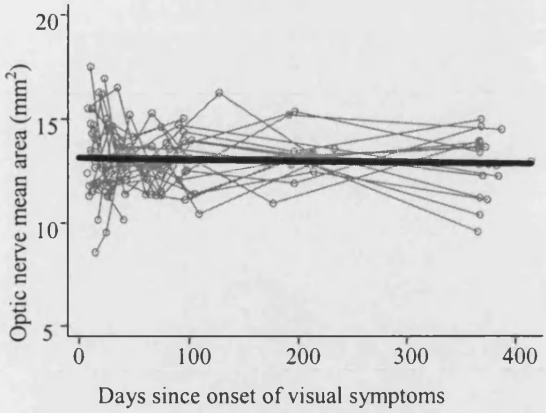

Figure 4.17: Contralateral healthy optic nerve mean area over time with linear model prediction shown in bold.

Patient diseased optic nerve mean area trajectories

The diseased optic nerve mean area declined over time, from initial swelling, to later atrophy. The best fitting model to describe the changes was an exponential (Figure 4.18 for mean area and Figure 4.19 for ratio of diseased: healthy optic nerve mean area). The median gradient of decline in mean area at baseline (reported as median due to three outliers) was -0.26mm^2/day (95% CI -0.35, -0.050). Significant ongoing decrease in area was still apparent after one-year. The mean gradient at 365 days was -0.0018mm^2/day (95% CI -0.0038, -0.00051; $p<0.01$ for difference from hypothesis of zero gradient). There was no evidence of association between baseline diseased optic nerve area and outcome optic nerve area or with rate of decline of optic nerve area at either baseline or one-year.

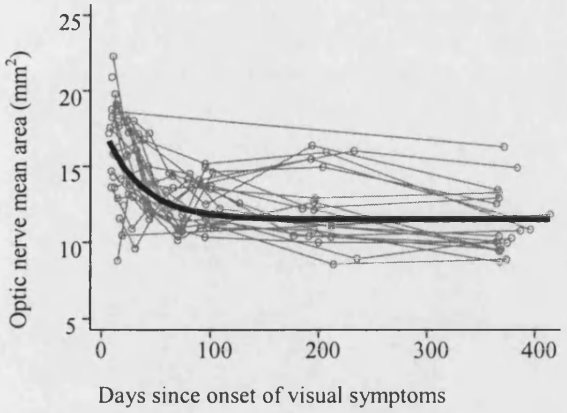

Figure 4.18: Diseased optic nerve mean area over time with predicted trajectory of mean area by applying exponential model to all data points ignoring subject (bold line).

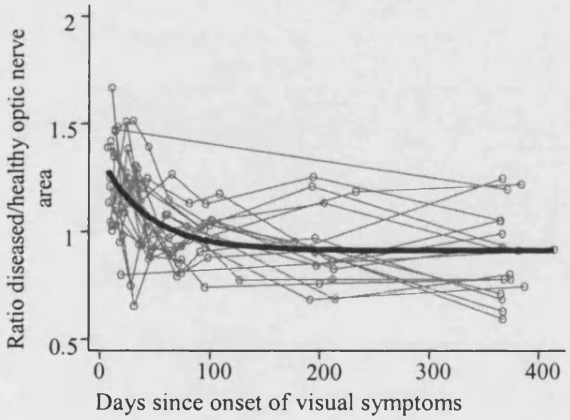

Figure 4.19: Ratio of diseased optic nerve: healthy optic nerve mean area over time with predicted trajectory of mean ratio by applying exponential model to all data points ignoring subject (bold line).

Associations with vision

Higher baseline diseased optic nerve mean area was correlated with worse baseline logMAR visual acuity (r_S=0.46, p=0.012) and with lower baseline visual field mean deviation (r_S=-0.55, p=0.002). However, at 52 weeks there was no direct evidence of

association between vision scores and diseased optic nerve mean area. There was also no evidence of association between vision scores at one-year and either baseline or one-year gradients of decrease in diseased optic nerve mean area.

Associations with VEP parameters

There was no evidence of association between baseline, rates of decline or one-year diseased optic nerve mean areas and any of the baseline, one-year or time-averaged VEP variables.

Associations with lesion lengths

The median baseline gadolinium-enhanced lesion length was 30mm (range 0-39mm) and the median duration of enhancement was 63.5 days (range 0-113 days). The baseline diseased optic nerve mean area was $0.2mm^2$ (95% CI 0.08, 0.3; p=0.001) higher for every additional 1mm of gadolinium-enhanced lesion length. However there was no association between baseline lesion length and initial or one-year rate of decline of optic nerve mean area, or one-year optic nerve mean area.

There was borderline evidence that the initial rate of decline in diseased optic nerve mean area was related to the length of time that enhancement was detected for, but not the one-year rate of decline: the baseline gradient of decline was less steep by $3.5mm^2$/day for each day that enhancement was detected for (95% CI 0.00099, 8.40; p=0.05).

The median baseline lesion length on FSE images was 21mm (range 9-39mm). There was no evidence of association between baseline lesion lengths on FSE images and baseline diseased optic nerve mean area or initial rates of decline of diseased optic nerve mean area. There was borderline evidence that the one-year rate of decline in diseased optic nerve mean area was less steep in the shortest quartile of baseline lesion length than in patients with longer lesions by $0.0019mm^2$/day (95% bootstrap CI $8.6x10^{-5}$, 0.0044; p=0.045).

Associations with MTR values

The MTR results have been previously reported (Chapter 4.2). There was some evidence that higher one-year diseased optic nerve mean area values were associated with higher baseline mean optic nerve MTR values. The one-year mean area was higher by 0.47mm^2 (95% bootstrap CI 0.022, 0.92; p=0.045) per 1pu rise in baseline mean MTR. There was a stronger association between one-year optic nerve mean area and time-averaged optic nerve MTR. The one-year mean area was higher by 0.76mm^2 (95% bootstrap CI 0.29, 1.13; p=0.009) per 1pu rise in time-averaged optic nerve MTR (Figure 4.20). However, there was no evidence of a direct association between one-year optic nerve mean area and one-year optic nerve mean MTR values.

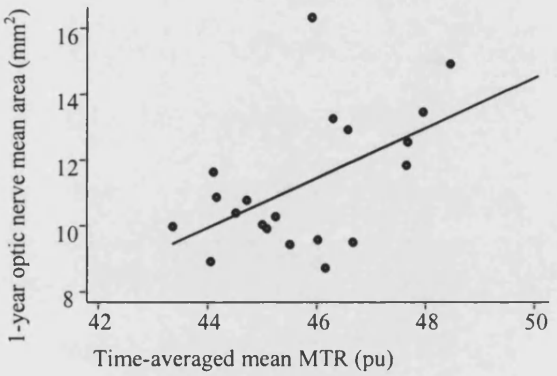

Figure 4.20: The relationship between one-year optic nerve mean area and time-averaged mean MTR.

4.3.5 Discussion

By prospectively studying a cohort of patients with acute optic neuritis using multiple MRI sequences, detailed clinical tests and VEPs, and in particular using the sTE fFLAIR sequence and a computer-assisted contouring technique to segment the optic nerves, it has been possible to extend the previous observations that optic nerve atrophy occurs following optic neuritis, and may continue to develop over several years. The measurement CV figures for optic nerve area were of the order of 5%, however the reliability coefficiency figures of approximately 0.9 suggest that the technique is reproducible, with 90% of the variability due to inter-subject variability and only 10%

due to measurement error (see Table 4.15). The reproducibility is not as good as for atrophy studies in the brain or spinal cord, reflecting the small size of the optic nerves and the greater potential for movement artefact. Higher resolution sequences or higher field imagers may help in future studies, although the former would be at the expense of increasing the acquisition time (Barker, 2000). At present, the sTE fFLAIR sequence presents the best compromise between high resolution and an acceptable acquisition time.

This study confirms, quantitatively, that optic nerve swelling occurs in acute optic neuritis, followed by the development of optic nerve atrophy over time. The results suggest an average increase in optic nerve mean area at baseline of approximately 20%. Optic nerve swelling on MRI had been previously thought to be a rare occurrence in acute optic neuritis and if swelling was present then it was recommended that a glioma or meningioma should be suspected (Cornblath & Quint, 1997). The present study is in agreement with other studies (Youl *et al.*, 1996; Kapoor *et al.*, 1998) which suggest that optic nerve swelling is actually common in acute optic neuritis. This swelling is probably due to acute inflammation with inflammatory cell infiltrates and vasogenic oedema. The observations that the amount of swelling was related to the lesion length on the gadolinium-enhanced images and the less steep decline in optic nerve mean area with increasing duration of enhancement support this conclusion, since the gadolinium enhancement has been shown to correlate with pathological features of inflammation in MS (Katz *et al.*, 1993; Bruck *et al.*, 1997). This study also supports the previous observation that acute inflammation causes impairment of vision (Youl *et al.*, 1991), with an association between the extent of acute optic nerve swelling and the degree of visual impairment in the acute phase.

The degree of initial swelling or acute enhancing lesion length was not associated with the degree of atrophy at one year, although there was a suggestion that the patients who had short acute FSE lesions had a decreased rate of continuing development of atrophy after one year. There was also an association between time-averaged optic nerve MTR and one-year optic nerve mean area. The presence of higher average MTR values implies less acute oedema and demyelination, although the degree of axonal integrity also contributes. The two mechanisms of Wallerian degeneration of axons previously discussed in Chapter 4.2, namely: transection in the acute inflammatory lesion and later

axonal death in persistently demyelinated axons; probably both contribute to the development of optic nerve atrophy which occurred over the year of follow up. More prolonged follow-up may help to determine if remyelination, inferred from increasing mean MTR values and shortening of VEP latencies, confers protection against continuing axonal degeneration, as measured by ongoing atrophy development. If this is the case then therapies to induce remyelination might be appropriate for neuroprotection.

The lack of association between the optic nerve mean area and visual impairment after one year could reflect the fact that few patients had substantial visual impairment and that the overall extent of tissue loss was small (mean decrease in area 12%). It is probable that the remaining axonal fibres are sufficient to enable restoration of vision once the phase of conduction block during acute inflammation has passed. Recovery of vision may also, in part, be due to central adaptation. This has been suggested by a functional MRI study of patients who recovered back to normal vision following optic neuritis and in whom there was activation involving extra-striate cortical regions (Werring *et al.*, 2000). Some of this reorganisation may be achieved by utilising redundant optic nerve capacity (Frisen & Quigley, 1984).

The data suggest that the decline in mean area from initial swelling to later atrophy followed an exponential curve. More prolonged follow-up will be undertaken to determine whether optic nerve atrophy continues to occur over several years, as suggested by the previous small study (Chapter 3.2). This previous study and another that has been published (Inglese *et al.*, 2002) suggest that in patients seen some years following optic neuritis there is an association between the degree of atrophy and visual impairment. Although it is hard to directly compare studies, the degree of tissue loss was not much greater than reported in the present study at one year. It may be that further episodes of optic neuritis (that could have been asymptomatic) had occurred leading to more demyelination and conduction block, or that failure of remyelination of the initial lesion with persistent demyelination may have predisposed, over time, to secondary axonal degeneration (Scolding & Franklin, 1998; McGavern *et al.*, 2000). In this case a small decrease in the number of critical macular axons may affect the ability of the visual system to compensate. The failure to compensate as axonal degeneration slowly but relentlessly occurs is one potential explanation for the development of

secondary progression in MS. Although progressive significant visual impairment is unusual in MS, evidence for progressive atrophy of the optic nerve over a long period of time would support the concept that progressive axonal loss may follow acute inflammatory demyelination.

In the brain and spinal cord measures of atrophy in MS reflect the global effects of the disease, which includes both old and new lesions and normal-appearing tissues. The observation here of swelling in the acute inflammatory lesion and atrophy in the more chronic post inflammatory lesion suggest that the concurrent presence of lesions of differing ages, as is often seen in the brain of patients with relapsing forms of MS, may introduce noise when using the measure of progressive brain atrophy as surrogate markers of axonal loss. The present observations support the study of optic neuritis as a model for the development of atrophy following inflammatory demyelinating lesions. A further implication of the present study is that disease modifying therapies for preventing acute inflammation have the potential to decrease the extent of tissue damage and axonal loss in MS. It also suggests that acute treatments during the inflammatory episode which prevent or reduce subsequent tissue loss should be sought. It was reported above (Chapter 3.3) that high dose IVMP failed to prevent optic nerve atrophy following an attack of optic neuritis consistent with the lack of long-term functional benefit from the therapy. Novel therapies for acute MS relapses are therefore required. In future treatment trials of such agents, inclusion of patients with optic neuritis and the use of combined clinical, electrophysiological and quantitative MRI measures including optic nerve size would be useful in assessing the response to treatment.

Chapter 5 Conclusions

The studies in this work have shown that optic neuritis is indeed a good model for the study of the effects of inflammatory demyelinating lesions. The lesion affects a defined pathway, with obvious clinical symptomatology that usually causes patients to present early. The effects on vision can be quantified reproducibly and VEP studies give an indication about how conduction in the optic pathways has been affected. This work has built on previous MRI studies on optic neuritis.

The acute lesion in optic neuritis is almost invariably associated with gadolinium enhancement, especially if triple-dose gadolinium is given. The finding of associations between the lesion length on triple-dose gadolinium-enhanced images and logMAR visual acuity ($r=0.38$, $p=0.044$), visual field mean deviation ($r=-0.57$, $p=0.002$) and VEP central field amplitude ($r=-0.41$, $p=0.035$) are in support of the view that the acute inflammatory lesion causes conduction block in the optic nerve (Youl *et al.*, 1991). There was also an association, not seen in a previous study using single-dose gadolinium (Kupersmith *et al.*, 2002), between the acute enhancing lesion length and outcome, although this was mostly due to patients with short inflammatory lesions having a good prognosis for recovery. The measurement of lesion length is a fairly crude way of determining the degree of acute inflammatory change as it does not reflect the signal intensity ("brightness") changes in the optic nerve due to gadolinium leakage. One possible solution is to look at the relative change before and after gadolinium in the T_1 properties of a tissue. This has been used in studies in the brain (Silver *et al.*, 2001), but requires registration of the pre- and post-gadolinium enhanced images. Due to the small size of the optic nerves this was not possible using current methodology. It may be feasible in future with if resolution can be improved, perhaps by using higher field imagers or new phased array receiver coils.

The baseline level of visual impairment in the study in Chapter 4.1 appeared to be a poor predictor of visual outcome, but the visual field recovery curves showed a greater differentiation in shape between patients with good and poor recoveries, in particular regarding the initial gradient of recovery. In combination with the observation that initial enhanced lesion length was associated with the final recovery level it may suggest that a poor prognosis is fixed early on. There has been a suggestion that the

reason that corticosteroids do not influence outcome, or the development of optic nerve atrophy as observed in Chapter 3.3, is that they are given too late to prevent acute axonal damage (Compston & Coles, 2002). Trials of corticosteroids in the hyperacute phase of optic neuritis would be required to test this hypothesis. Optic nerve imaging may be useful in helping select those patients who might be predicted to have a poor prognosis. It was previously thought that canalicular involvement led to a worse outcome (Miller *et al.*, 1988), although this has not been borne out in subsequent studies (Kapoor *et al.*, 1998; Kupersmith *et al.*, 2002) and it was almost universal in the study in Chapter 4.1, probably due to the increased sensitivity of the technique. The results in Chapter 4.1 suggest that patients with short lesion on triple-dose gadolinium enhanced imaging have a better prognosis, independent of the level of baseline visual impairment. Triple-dose gadolinium enhanced imaging may therefore be useful in selecting patients for future optic neuritis treatment trials, although the cost implications will bar its use in routine clinical practice.

Optic neuritis can usually be diagnosed on clinical grounds (Chapter 1). The principal use of MRI in these patients is to assess the brain for asymptomatic demyelinating lesions. This can then give an indication for the likely risk of subsequent MS (Optic Neuritis Study Group, 1997a; Optic Neuritis Study Group, 2003) and may drive the decision to initiate DMDs, although they are not currently licensed for this indication in the United Kingdom. In clinical practice, optic nerve MRI is most useful in ruling out other pathologies, especially if the clinical presentation is atypical (Chapter 1).

The results from the optic nerve MTR study (Chapter 4.2) were interesting in that initially the MTR in the diseased optic nerves were unchanged, in contrast to the situation in brain MS lesions. This may have been partly due to the ultrastructure of the optic nerve with its subdivision into fascicles (Williams *et al.*, 1989) limiting vasogenic oedema, although it has been demonstrated the swelling of the optic nerve does occur during acute optic neuritis (Chapter 4.3). The inflammatory infiltrate may also be more cellular which would tend to increase the number of sites for exchange of magnetisation (thus maintaining or increasing MTR). The subsequent prolonged decline followed by stabilisation and a small (but not significant) upturn may reflect slow clearance of myelin debris followed by remyelination. Studies with prolonged follow-up of patients with optic neuritis suggest that significant shortening of VEP latencies, implying

remyelination, occurs for 2-3 years (Brusa *et al.*, 1999; Brusa *et al.*, 2001). It is interesting to note that in these studies and in the study in Chapter 4.1, vision scores were not associated with VEP latencies but were associated with VEP amplitudes. This supports the view that vision requires functional axonal channels. These are affected initially by acute inflammation causing conduction block, and subsequently by the degree of axonal damage. Demyelination may not prevent visual recovery as has been discussed in Chapter 1.

Optic nerve atrophy measures may be most influenced by the degree of axonal damage. The studies in Chapters 3 and 4.3 suggest that atrophy is a consistent feature following optic neuritis. The measurement reproducibility figures were not as good as for studies of brain and spinal cord atrophy, due to the difficulties of imaging the optic nerves as outlines. However, the reliability coefficients of ~0.9 imply that most of the variation was due to inter-subject variability rather than measurement variability, thus the measure provides a meaningful biological outcome. Improvements in the imaging sequence for measuring optic nerve size should be possible in future. The ideal imaging sequence for this purpose should combine short acquisition time with high spatial resolution, high SNR and CSF and fat suppression. 3D double inversion recovery or 3D fast FLAIR sequences may give some improvements over the current 2D sequence. If so, it may be possible to re-format the images in other planes and so obtain images orthogonal to the nerve. An automated method to segment the nerves could also be considered. A method using a B-Spline active surface technique has been proposed (Coulon *et al.*, 2000). This has been tried in the spinal cord and gives good reproducibility results (Hickman *et al.*, 2003). The technique appeared however to be less sensitive at detecting small changes than existing semi-automated threshold contouring, both in the spinal cord (Hickman *et al.*, 2003) and when tested in the optic nerve on the sTE fFLAIR images (S.J. Hickman, unpublished observations). Further developments to active surface techniques are awaited.

There was no association between optic nerve mean area and vision scores in the patients studied with a short interval after the attack of optic neuritis (median 21 months in Chapter 3.1, six months in Chapter 3.3 and up to 12 months in Chapter 4.3) suggesting that initially the visual system can compensate for the damage to the afferent system, through redundancy in the system and/or more active reorganisation of cortical

response. In the cohort studied with a longer interval which had patients up to 252 months after their first attack of optic neuritis there was an association between optic nerve mean area and vision scores, in that the optic nerves with poor visual recovery (<6/9) were significantly smaller than healthy optic nerves (p=0.02). The ability to compensate may have been affected by either further attacks of optic neuritis that may have been subclinical or by ongoing loss of critical macular axonal fibres. The visual system may be able to compensate in the short-term but may fail over a longer period. It is also possible that the full extent of atrophy that results from an acute inflammatory/demyelinating lesion does not emerge for a long time (i.e. more than one year) because of protracted and slow clearance of debris associated with Wallerian degeneration.

The cohort of patients from the studies in Chapter 4 is being followed-up after both two and three years. This will help to show if the observation of prolonged shortening of VEP latencies, implying remyelination, in previous studies can be repeated. It will also be interesting to see if the small upturn in MTR in the optic nerves between 240 days and one-year after onset of optic neuritis in the study of Chapter 4.2 is sustained, or even progressive. If the association remains between VEP latency and optic nerve MTR then it supports the use of MTR as a tool to measure remyelination *in vivo*, especially as therapies to promote remyelination have been proposed (Compston & Coles, 2002). The association between time-averaged optic nerve MTR and one-year optic nerve mean area is interesting (Chapter 4.3). It implies that more pronounced damage of optic nerve integrity, probably as a combination of vasogenic oedema, demyelination and axonal transaction, leads to more long-term tissue damage. Prolonged follow-up may help to determine if remyelination, inferred from increasing mean MTR values and shortening of VEP latencies, may confer protection against continuing axonal degeneration, as measured by ongoing atrophy development. The amount of ongoing axonal degeneration is likely to be small as the long-term visual outcome following optic neuritis is very good (Optic Neuritis Study Group, 2004). Poor visual outcome (and increasing optic nerve atrophy as seen in Chapter 3.2) usually occurs due to recurrent attacks of optic neuritis.

The use of arbitrary standards to determine if vision had returned to normal did not always reflect the patients' views on whether their vision had returned to normal in

Chapter 4.1. Pelli-Robson contrast sensitivity and Ishihara colour vision scores appeared to be more discriminatory however these parameters are less amenable to statistical analysis compared with logMAR acuity and visual field mean deviation as they are not continuously variable. FM 100 Hue colour vision scores seemed to be able to discriminate between good subjective recovery and not as well as providing a continuously variable score for statistical analysis. The test however takes a long time to perform (~15 minutes per eye) and is unreliable when vision is worse than 6/60 (Katz, 1995), as is common in the acute stages of optic neuritis. Future methods of testing could include rarebit perimetry which appears to be more sensitive for detecting optic nerve damage by being able to probe for damage within receptive fields (Frisen, 2002; Frisen, 2003). It also has the advantage of being very fast to perform (one minute for each pass, although multiple passes are usually performed). Psychophysical testing may be useful in differentiating between magnocellular and parvocellular damage. In optic neuritis and MS the parvocellular pathway is thought to be affected more (Wall, 1990; Caruana *et al.*, 2000; Evangelou *et al.*, 2001). Again, psychophysical testing is time consuming (60-75 minutes) and may not be able to distinguish between preferential damage to either system where there is profound visual loss. Chromatic (particularly red) perimetry could be considered (Frisen, 2002).

At present results of quantitative imaging studies can only be correlated with tests of visual function or of electrical conduction to validate them. Radiological-pathological studies are useful and have been performed successfully in the brain and spinal cord (van Waesberghe *et al.*, 1999; De Groot *et al.*, 2001; Mottershead *et al.*, 2003). Autopsy MRI of the optic nerves has not previously been performed. Any tissue would have to be carefully handled and due to the small size of the optic nerves and *post mortem* or fixation artefacts may have a profound influence on the results. There would not however be difficulties with orbital fat or CSF, nor movement artefact. Acquisition times *post mortem* can be much longer than could be tolerated *in vivo* and so higher spatial resolution would be possible. Another way of trying to assess the degree of axonal damage in the optic nerves, which is possible *in vivo*, is to image the RNFL. Atrophy of fibres of the RNFL has been described in MS (Frisen & Hoyt, 1974). Recently attempts have been made to try and quantify this loss. Two techniques that have been employed are scanning laser polarimetry (SLP) (Steel & Waldock, 1998) and ocular coherence tomography (OCT) (Parisi *et al.*, 1999; Drexler *et al.*, 2001). These

can both give an indication of the thickness of the nerve fibre layer and have both been applied in patients following optic neuritis. Steel and Waldock (1998) found evidence of RNFL loss in 29/33 eyes previously affected by optic neuritis, although there was no correlation between SLP scores and other clinical tests. Parisi *et al.* (1999) measured RNFL thickness with OCT in 14 patients with MS who had had previous optic neuritis. Mean overall RNFL thickness was 111.11±11.87μm in 14 control eyes, 82.73±10.73μm in clinically healthy eyes from MS patients and 59.79±10.80μm in eyes previously affected by optic neuritis ($p<0.01$ compared with both controls and clinically healthy eyes). RNFL thickness correlated with PERG P50 latency and P50 to N95 amplitude but not VEP scores. It would be interesting to combine studies using both a measure of axonal integrity, such as the two methods mentioned above, and quantitative optic nerve imaging to try and quantify the amount of damage that occurs in the axonal pathways both within the retina and in the optic nerve. Should such studies reveal a correlation between RNFL thickness and an MR measure, it would further support using that MR measure (e.g. atrophy) as a surrogate markers of axonal loss.

Optic nerve MRI in optic neuritis/MS has developed from initial studies with STIR that could give an indication of lesion length and anatomical distribution of any lesion, through more sensitive means of detecting abnormalities in the visual pathway using sequences such as fat-saturated FSE and gadolinium enhancement, to the situation now where techniques such as atrophy and MT imaging that have been initially employed in the brain and spinal cord have been applied to the optic nerve. These techniques have gone some way to overcome the difficulties that imaging the optic nerve causes. In quantitative studies, reproducibility figures have not been as high as in studies of the brain and spinal cord. The techniques have though been sensitive to disease effects and in many studies produced results that correlate with measures of visual function and conduction in the optic pathways. Further refinements may be possible using higher field strengths or more sensitive coils. Another class of imaging technique that is being developed for optic nerve imaging is DWI as outlined in Chapter 2. DWI offers the potential to offer pathologically specific imaging with measures that are thought to be sensitive to changes in nerve structure, particularly axonal disruption. Further studies in optic neuritis using DWI are awaited.

In conclusion, quantitative MRI of the optic nerves in optic neuritis can help to give insights into the evolution of the condition. Optic neuritis is a model for MS relapses in general. In future treatment trials of novel therapies that aim to improve outcome following MS relapses optic neuritis would be a useful testing ground. In such trials optic nerve MRI with some of the techniques outlined in this work could be used to screen patients and in assessing response to treatment. With further developments in MR technology, it is possible to foresee that future studies of the optic nerve, using advanced MRI, VEP and clinical evaluation, will not only define reliable imaging markers for specific pathological features in optic neuritis and MS, but will also elucidate the pathophysiological mechanisms for functional recovery and its failure.

Chapter 6 Reference List

Acheson J. Optic nerve and chiasmal disease. *J Neurol* 2000;**247**:587-596.

Adachi-Usami E. Optic neuritis: from diagnosis to optic nerve transplantation. *Jpn J Ophthalmol* 2001;**45**:320-321.

Adams CW, Poston RN, Buk SJ. Pathology, histochemistry and immunocytochemistry of lesions in acute multiple sclerosis. *J Neurol Sci* 1989;**92**: 291-306.

Anderson DR, Hoyt WF. Ultrastructure of intraorbital portion of human and monkey optic nerve. *Arch Ophthalmol* 1969;**82**:506-530.

Balazsi AG, Rootman J, Drance SM, Schulzer M, Douglas GR. The effect of age on the nerve fiber population of the human optic nerve. *Am J Ophthalmol* 1984;**97**:760-766.

Baltagi H. *Econometric Analysis of Panel Data.* New York: John Wiley & Sons; 1995.

Barker GJ. Technical issues for the study of the optic nerve with MRI. *J Neurol Sci* 2000;**172(Suppl.1)**:S13-S16.

Barker GJ, Tofts PS. Semiautomated quality assurance for quantitative magnetic resonance imaging. *Magn Reson Imaging* 1992;**10**:585-595.

Barkhof F, Filippi M, Miller DH, Scheltens P, Campi A, Polman CH, Comi G, Ader HJ, Losseff N, Valk J. Comparison of MRI criteria at first presentation to predict conversion to clinically definite multiple sclerosis. *Brain* 1997;**120**:2059-2069.

Barnes D. Treatment of acute relapses. In: Hawkins CP, Wolinsky JS, eds. *Principles of treatments in multiple sclerosis.* Oxford: Butterworth-Heinemann; 2000, pp. 14-22.

Basser PJ, Mattiello J, LeBihan D. MR diffusion tensor spectroscopy and imaging. *Biophys J* 1994;**66**:259-267.

Basser PJ, Pierpaoli C. A simplified method to measure the diffusion tensor from seven MR images. *Magn Reson Med* 1998;**39**:928-934.

Beck RW. The Optic Neuritis Treatment Trial: Three-year follow-up results. *Arch Ophthalmol* 1995;**113**:136-137.

Beck RW. Optic Neuritis. In: Miller NR, Newman NJ, eds. *Walsh and Hoyt's Clinical Neuro-Ophthalmology, 5th ed.* Baltimore: Williams and Wilkins. 1998, pp. 599-647.

Beck RW, Cleary PA. Optic Neuritis Treatment Trial. One-year follow-up results. *Arch Ophthalmol* 1993a;**111**:773-775.

Beck RW, Cleary PA. Recovery from severe visual loss in optic neuritis. *Arch Ophthalmol* 1993b;**111**:300.

Beck RW, Cleary PA, Anderson MM Jr, Keltner JL, Shults WT, Kaufman DI, Buckley EG, Corbett JJ, Kupersmith MJ, Miller NR, Optic Neuritis Study Group. A randomized, controlled trial of corticosteroids in the treatment of acute optic neuritis. *N Engl J Med* 1992;**326**:581-588.

Beck RW, Cleary PA, Backlund JC. The course of visual recovery after optic neuritis. Experience of the Optic Neuritis Treatment Trial. *Ophthalmology* 1994;**101**: 1771-1778.

Beck RW, Cleary PA, Trobe JD, Kaufman DI, Kupersmith MJ, Paty DW, Brown CH, Optic Neuritis Study Group. The effect of corticosteroids for acute optic neuritis on the subsequent development of multiple sclerosis. *N Engl J Med* 1993a;**329**:1764-1769.

Beck RW, Kupersmith MJ, Cleary PA, KatzB. Fellow eye abnormalities in acute unilateral optic neuritis. Experience of the Optic Neuritis Treatment Trial. *Ophthalmology* 1993b;**100**:691-697.

Behan CMH, Hickman SJ, Scolding NJ, Miller DH, Compston DAS. Identification of the clinically symptomatic lesion in multiple sclerosis - implications for remyelination therapy. *Rev Neurol (Paris)* 2000;**156(Suppl.3)**:S28.

Berger T, Rubner P, Schautzer F, Egg R, Ulmer H, Mayringer I, Dilitz E, Deisenhammer F, Reindl M. Antimyelin antibodies as predictor of clinically definite multiple sclerosis after a first demyelinating event. *N Engl J Med* 2003;**349**:139-145.

Biousse V, Trichet C, Bloch-Michel E, Roullet E. Multiple sclerosis associated with uveitis in two large clinic-based series. *Neurology* 1999;**52**:179-181.

Bland JM, Altman DG. Measurement error and correlation coefficients. *Br Med J* 1996a;**313**:41-42.

Bland JM, Altman DG. Measurement error proportional to the mean. *Br Med J* 1996b;**313**:106.

Bland JM, Altman DG. Measurement error. *Br Med J* 1996;**313**:744.

Blinkov SM, Glezier II. The cranial nerves. In: *The human brain in figures and tables.* New York: Plenum Press; 1968, pp. 94-122.

Boorstein JM, Moonis G, Boorstein SM, Patel YP, Culler AS. Optic neuritis: Imaging with magnetization transfer. *AJR Am J Roentgenol* 1997;**169**:1709-1712.

Bowden AN, Bowden PM, Friedmann AI, Perkin GD, Rose FC. A trial of corticotrophin gelatin injection in acute optic neuritis. *J Neurol Neurosurg Psychiatry* 1974;**37**:869-873.

Bradley WG, Whitty CW. Acute optic neuritis: Its clinical features and their relation to prognosis for recovery of vision. *J Neurol Neurosurg Psychiatry* 1967;**30**:531-538.

Brady KM, Brar AS, Lee AG, Coats DK, Paysse EA, Steinkuller PG. Optic neuritis in children: Clinical features and visual outcome. *J AAPOS* 1999;**3**:98-103.

Brex PA, Ciccarelli O, O'Riordan JI, Sailer M, Thompson AJ, Miller DH. A longitudinal study of abnormalities on MRI and disability from multiple sclerosis. *N Engl J Med* 2002;**346**:158-164.

Brex PA, O'Riordan JI, Miszkiel KA, Moseley IF, Thompson AJ, Plant GT, Miller DH. Multisequence MRI in clinically isolated syndromes and the early development of MS. *Neurology* 1999;**53**:1184-1190.

Brinkmeier H, Aulkemeyer P, Wollinsky KH, Rudel R. An endogenous pentapeptide acting as a sodium channel blocker in inflammatory autoimmune disorders of the central nervous system. *Nat Med* 2000;**6**:808-811.

British National Formulary. London: British Medical Association, Royal Pharmaceutical Society of Great Britain; 2003.

Brochet B, Dousset V. Pathological correlates of magnetization transfer imaging abnormalities in animal models and humans with multiple sclerosis. *Neurology* 1999;**53**:S12-S17.

Brown MA, Semelka RC. MR imaging abbreviations, definitions, and descriptions: A review. *Radiology* 1999;**213**: 647-662.

Bruck W, Bitsch A, Kolenda H, Bruck Y, Stiefel M, Lassmann H. Inflammatory central nervous system demyelination: Correlation of magnetic resonance imaging findings with lesion pathology. *Ann Neurol* 1997;**42**:783-793.

Brusa A, Jones SJ, Kapoor R, Miller DH, Plant GT. Long-term recovery and fellow eye deterioration after optic neuritis, determined by serial visual evoked potentials. *J Neurol* 1999;**246**:776-782.

Brusa A, Jones SJ, Plant GT. Long-term remyelination after optic neuritis: A 2-year visual evoked potential and psychophysical serial study. *Brain* 2001;**124**:468-479.

Brusaferri F, Candelise L. Steroids for multiple sclerosis and optic neuritis: a meta-analysis of randomized controlled clinical trials. *J Neurol* 2000;**247**:435-442.

Campos EC, Enoch JM, Fitzgerald CR, Benedetto MD. A simple psychophysical technique provides early diagnosis in optic neuritis. *Doc Ophthalmol* 1980;**49**:325-335.

Carmody RF, Mafee MF, Goodwin JA, Small K, Haery C. Orbital and optic pathway sarcoidosis: MR findings. *AJNR Am J Neuroradiol* 1994;**15**:775-783.

Carpenter J, Bithell J. Bootstrap confidence intervals: When, which, what? A practical guide for medical statisticians. *Stat Med* 2000;**19**:1141-1164.

Carroll WM, Jennings AR, Mastaglia FL. The origin of remyelinating oligodendrocytes in antiserum-mediated demyelinative optic neuropathy. *Brain* 1990;**113**:953-973.

Caruana PA, Davies MB, Weatherby SJM, Williams R, Haq N, Foster DH, Hawkins CP. Correlation of MRI lesions with visual psychophysical deficit in secondary progressive multiple sclerosis. *Brain* 2000;**123**:1471-1480.

Chabert S, Molko N, Cointepas Y, Le Roux P, Le Bihan D. "Functional" diffusion tensor imaging of the optic nerve using a non CPMG fast spin echo sequence. *Proc Intl Soc Magn Reson Med* 2002;**10**:1115.

Charcot JM. *Lectures on the Diseases of the Nervous System.* London: The New Sydenham Society; 1877, pp. 191-192.

Charles P, Reynolds R, Seilhean D, Rougon G, Aigrot MS, Niezgoda A, Zalc B, Lubetzki C. Re-expression of PSA-NCAM by demyelinated axons: An inhibitor of remyelination in multiple sclerosis? *Brain* 2002;**125**:1972-1979.

Chou PI, Sadun AA, Lee H. Vasculature and morphometry of the optic canal and intracanalicular optic nerve. *J Neuroophthalmol* 1995;**15**:186-190.

Ciccarelli O, Werring DJ, Wheeler-Kingshott CA, Barker GJ, Parker GJ, Thompson AJ, Miller DH. Investigation of MS normal-appearing brain using diffusion tensor MRI with clinical correlations. *Neurology* 2001;**56**:926-933.

Cohen JA, Fischer JS, Bolibrush DM, Jak AJ, Kniker JE, Mertz LA, Skaramagas TT, Cutter GR. Intrarater and interrater reliability of the MS functional composite outcome measure. *Neurology* 2000;**54**:802-806.

Cole SR, Beck RW, Moke PS, Kaufman DI, Tourtellotte WW, Optic Neuritis Study Group. The predictive value of CSF oligoclonal banding for MS 5 years after optic neuritis. *Neurology* 1998;**51**:885-887.

Coles AJ, Wing MG, Molyneux P, Paolillo A, Davie CM, Hale G, Miller D, Waldmann H, Compston A. Monoclonal antibody treatment exposes three mechanisms underlying the clinical course of multiple sclerosis. *Ann Neurol* 1999;**46**:296-304.

Comi G, Filippi M, Barkhof F, Durelli L, Edan G, Fernandez O, Hartung H, Seeldrayers P, Sorensen PS, Rovaris M, Martinelli V, Hommes OR. Effect of early interferon treatment on conversion to definite multiple sclerosis: a randomised study. *Lancet* 2001;**357**:1576-1582.

Committee on Safety of Medicines. Severe chickenpox associated with systemic corticosteroids. *Current problems in Pharmacovigilance.* London: Committee on Safety of Medicines 1994;**20**.

Compston A, Coles A. Multiple sclerosis. *Lancet* 2002;**359**:1221-1231.

Compston DA, Batchelor JR, Earl CJ, McDonald WI. Factors influencing the risk of multiple sclerosis developing in patients with optic neuritis. *Brain* 1978;**101**:495-511.

Cornblath WT, Quint DJ. MRI of optic nerve enlargement in optic neuritis. *Neurology* 1997;**48**:821-825.

Coulon O, Parker GJM, Schnabel JA, Arridge SR. A B-spline active surface method for segmentation of the optic nerve. *Proc Intl Soc Magn Reson Med* 2000;**8**:1760.

Cox TA, Thompson HS, Corbett JJ. Relative afferent pupillary defects in optic neuritis. *Am J Ophthalmol* 1981;**92**:685-690.

Dalton CM, Brex PA, Miszkiel KA, Hickman SJ, MacManus DG, Plant GT, Thompson AJ, Miller DH. Application of the new McDonald criteria to patients with clinically isolated syndromes suggestive of multiple sclerosis. *Ann Neurol* 2002;**52**:47-53.

Davies MB, Williams R, Haq N, Pelosi L, Hawkins CP. MRI of optic nerve and postchiasmal visual pathways and visual evoked potentials in secondary progressive multiple sclerosis. *Neuroradiology* 1998;**40**:765-770.

Davis FA, Bergen D, Schauf C, McDonald I, Deutsch W. Movement phosphenes in optic neuritis: a new clinical sign. *Neurology* 1976;**26**:1100-1104.

De Groot CJ, Bergers E, Kamphorst W, Ravid R, Polman CH, Barkhof F, van der Valk P. Post-mortem MRI-guided sampling of multiple sclerosis brain lesions: Increased yield of active demyelinating and (p)reactive lesions. *Brain* 2001;**124**: 1635-1645.

de Preux J, Mair WG. Ultrastructure of the optic nerve in Schilder's disease, Devic's disease and disseminated sclerosis. *Acta Neuropathol (Berl)* 1974;**30**:225-242.

Dolman CL, McCormick AQ, Drance SM. Aging of the optic nerve. *Arch Ophthalmol* 1980;**98**:2053-2058.

Donaldson HH, Bolton TL. The size of several cranial nerves in man as indicated by the areas of their cross-sections. *Am J Psychol* 1891;**4**:224-229.

Dousset V, Gayou A, Brochet B, Caille JM. Early structural changes in acute MS lesions assessed by serial magnetization transfer studies. *Neurology* 1998;**51**:1150-1155.

Dousset V, Grossman RI, Ramer KN, Schnall MD, Young LH, Gonzalez-Scarano F, Lavi E, Cohen JA. Experimental allergic encephalomyelitis and multiple sclerosis: lesion characterization with magnetization transfer imaging. *Radiology* 1992;**182**:483-491.

Drexler W, Morgner U, Ghanta RK, Kartner FX, Schuman JS, Fujimoto JG. Ultrahigh-resolution ophthalmic optical coherence tomography. *Nat Med* 2001;**7**:502-507.

Dunker S, Wiegand W. Prognostic value of magnetic resonance imaging in monosymptomatic optic neuritis. *Ophthalmology* 1996;**103**:1768-1773.

Dunya IM, Frangieh GT, Heilman CB, Miranda MR, Rand LI, Hedges TR. Anterior clinoid mucocele masquerading as retrobulbar neuritis. *Ophthal Plast Reconstr Surg* 1996;**12**:171-173.

Ebers GC. Optic neuritis and multiple sclerosis. *Arch Neurol* 1985;**42**:702-704.

Ebers GC. Preventing multiple sclerosis? *Lancet* 2001;**357**:1547.

Eggenberger ER. Inflammatory optic neuropathies. *Ophthalmol Clin North Am* 2001;**14**:73-82.

Enoch JM, Campos EC, Bedell HE. Visual resolution in a patient exhibiting a visual fatigue or saturation-like effect: Probable multiple sclerosis. *Arch Ophthalmol* 1979;**97**:76-78.

Evangelou N, Konz D, Esiri MM, Smith S, Palace J, Matthews PM. Size-selective neuronal changes in the anterior optic pathways suggest a differential susceptibility to injury in multiple sclerosis. *Brain* 2001;**124**:1813-1820.

Farnsworth D. The Farnsworth-Munsell 100-hue and dichotomous tests for color vision. *J Opt Soc Am* 1943;**33**:568-578.

Fazzone HE, Lefton DR, Kupersmith MJ. Optic neuritis: Correlation of pain and magnetic resonance imaging. *Ophthalmology* 2003;**110**:1646-1649.

Feinsod M, Hoyt WF. Subclinical optic neuropathy in multiple sclerosis. How early VER components reflect axon loss and conduction defects in optic pathways. *J Neurol Neurosurg Psychiatry* 1975;**38**:1109-1114.

Felts PA, Baker TA, Smith KJ. Conduction in segmentally demyelinated mammalian central axons. *J Neurosci* 1997;**17**:7267-7277.

Felts PA, Deerinck TJ, Ellisman MH, Levinson SR, Schwarz TL, Smith KJ. Sodium and potassium channel immunolocalization in demyelinated and remyelinated central axons. *Neuropathol Appl Neurobiol* 1998;**24**:154-155.

Ferguson B, Matyszak MK, Esiri MM, Perry VH. Axonal damage in acute multiple sclerosis lesions. *Brain* 1997;**120**:393-399.

Ferris FL III, Kassoff A, Bresnick GH, Bailey I. New visual acuity charts for clinical research. *Am J Ophthalmol* 1982;**94**:91-96.

ffrench-Constant C, Raff MC. Proliferating bipotential glial progenitor cells in adult rat optic nerve. *Nature* 1986;**319**:499-502.

Filippi M, Inglese M. Overview of diffusion-weighted magnetic resonance studies in multiple sclerosis. *J Neurol Sci* 2001;**186(Suppl.1)**:S37-S43.

Filippi M, Yousry T, Campi A, Kandziora C, Colombo B, Voltz R, Martinelli V, Spuler S, Bressi S, Scotti G, Comi G. Comparison of triple dose versus standard dose gadolinium-DTPA for detection of MRI enhancing lesions in patients with MS. *Neurology* 1996;**46**:379-384.

Fleishman JA, Beck RW, Linares OA, Klein JW. Deficits in visual function after resolution of optic neuritis. *Ophthalmology* 1987;**94**:1029-1035.

Fog T. The topography of plaques in multiple sclerosis. *Acta Neurol Scand* 1965;**41(Suppl.15)**:1-161.

Fox NC, Jenkins R, Leary SM, Stevenson VL, Losseff NA, Crum WR, Harvey RJ, Rossor MN, Miller DH, Thompson AJ. Progressive cerebral atrophy in MS: A serial study using registered, volumetric MRI. *Neurology* 2000;**54**:807-812.

Francis DA, Compston DA, Batchelor JR, McDonald WI. A reassessment of the risk of multiple sclerosis developing in patients with optic neuritis after extended follow-up. *J Neurol Neurosurg Psychiatry* 1987;**50**:758-765.

Franklin RJ. Why does remyelination fail in multiple sclerosis? *Nat Rev Neurosci* 2002;**3**:705-714.

Frederiksen JL, Larsson HB, Ottovay E, Stigsby B, Olesen J. Acute optic neuritis with normal visual acuity. Comparison of symptoms and signs with psychophysiological, electrophysiological and magnetic resonance imaging data. *Acta Ophthalmol (Copenh)* 1991;**69**:357-366.

Frederiksen JL, Petrera J. Serial visual evoked potentials in 90 untreated patients with acute optic neuritis. *Surv Ophthalmol* 1999;**44(Suppl.1)**:S54-S62.

Frederiksen JL, Sorensen TL, Sellebjerg FT. Residual symptoms and signs after untreated acute optic neuritis. A one-year follow-up. *Acta Ophthalmol Scand* 1997;**75**:544-547.

Freeman AJ, Ballinger R, Werner M, Guy J. Diffusion weighted EPI of the human optic nerve at 3T. *Proc Intl Soc Magn Reson Med* 1998;**6**:1265.

Frisen L. New, sensitive window on abnormal spatial vision: Rarebit probing. *Vision Research* 2002;**42**:1931-1939.

Frisen L. Spatial vision in visually asymptomatic subjects at high risk for multiple sclerosis. *J Neurol Neurosurg Psychiatry* 2003;**74**:1145-1147.

Frisen L, Hoyt WF. Insidious atrophy of retinal nerve fibers in multiple sclerosis. Funduscopic identification in patients with and without visual complaints. *Arch Ophthalmol* 1974;**92**:91-97.

Frisen L, Quigley HA. Visual acuity in optic atrophy: a quantitative clinicopathological analysis. *Graefes Arch Clin Exp Ophthalmol* 1984;**222**:71-74.

Gartner S. Optic neuropathy in multiple sclerosis. *Arch Ophthalmol* 1953;**50**:718-726.

Gass A, Barker GJ, MacManus D, Sanders M, Riordan-Eva P, Tofts PS, Thorpe J, McDonald WI, Moseley IF, Miller DH. High resolution magnetic resonance imaging of the anterior visual pathway in patients with optic neuropathies using fast spin echo and phased array local coils. *J Neurol Neurosurg Psychiatry* 1995;**58**:562-569.

Gass A, Moseley IF. The contribution of magnetic resonance imaging in the differential diagnosis of optic nerve damage. *J Neurol Sci* 2000;**172(Suppl.1)**:S17-S22.

Gass A, Moseley IF, Barker GJ, Jones S, MacManus D, McDonald WI, Miller DH. Lesion discrimination in optic neuritis using high-resolution fat-suppressed fast spin-echo MRI. *Neuroradiology* 1996;**38**:317-321.

Gass JD. The acute zonal outer retinopathies. *Am J Ophthalmol* 2000;**130**:655-657.

Ghezzi A, Martinelli V, Torri V, Zaffaroni M, Rodegher M, Comi G, Zibetti A, Canal N. Long-term follow-up of isolated optic neuritis: the risk of developing multiple sclerosis, its outcome, and the prognostic role of paraclinical tests. *J Neurol* 1999;**246**:770-775.

Goldberg RA, Hannani K, Toga AW. Microanatomy of the orbital apex. Computed tomography and microcryoplaning of soft and hard tissue. *Ophthalmology* 1992;**99**:1447-1452.

Goldstein H. *Multilevel statistical models*. London: Arnold; 1995.

Goodkin DE, Hertsgaard D, Seminary J. Upper extremity function in multiple sclerosis: improving assessment sensitivity with box-and-block and nine-hole peg tests. *Arch Phys Med Rehabil* 1988;**69**:850-854.

Gould ES, Bird AC, Leaver PK, McDonald W I. Treatment of optic neuritis by retrobulbar injection of triamcinolone. *Br Med J* 1977;**i**:1495-1497.

Grimaud J, Lai M, Thorpe J, Adeleine P, Wang L, Barker GJ, Plummer DL, Tofts PS, McDonald WI, Miller DH. Quantification of MRI lesion load in multiple sclerosis: A comparison of three computer-assisted techniques. *Magn Reson Imaging* 1996;**14**: 495-505.

Grossman RI, Kappos L, Wolinsky JS. The contribution of magnetic resonance imaging in the differential diagnosis of the damage of the cerebral hemispheres. *J Neurol Sci* 2000;**172(Suppl.1)**:S57-S62.

Guy J. New therapies for optic neuropathies: Development in experimental models. *Curr Opin Ophthalmol* 2000;**11**:421-429.

Guy J, Fitzsimmons J, Ellis EA, Beck B, Mancuso A. Intraorbital optic nerve and experimental optic neuritis. Correlation of fat suppression magnetic resonance imaging and electron microscopy. *Ophthalmology* 1992;**99**:720-725.

Halliday AM, McDonald WI, Mushin J. Delayed visual evoked response in optic neuritis. *Lancet* 1972;**i**:982-985.

Halliday AM, McDonald WI, Mushin J. Delayed pattern-evoked responses in optic neuritis in relation to visual acuity. *Trans Ophthalmol Soc UK* 1973a;**93**:315-324.

Halliday AM, McDonald WI, Mushin J. Visual evoked response in diagnosis of multiple sclerosis. *Br Med J* 1973b;**4**:661-664.

Harding GFA, Wright CE. Visual evoked potentials in acute optic neuritis. In: Hess RF, Plant GT, eds. *Optic neuritis*. Cambridge: Cambridge University Press; 1986, pp. 230-254.

Hashemi RH, Bradley WG Jr. *MRI the basics*. Baltimore: Lippincott Williams and Wilkins; 1997.

Hauser SL, Oksenberg JR, Lincoln R, Garovoy J, Beck RW, Cole SR, Moke PS, Kip KE, Gal RL, Long DT. Interaction between HLA-DR2 and abnormal brain MRI in optic neuritis and early MS. *Am J Ophthalmol* 2000;**130**:690-691.

Hayreh SS, Massanari RM, Yamada T, Hayreh SM. Experimental allergic encephalomyelitis. I. Optic nerve and central nervous system manifestations. *Invest Ophthalmol Vis Sci* 1981;**21**:256-269.

Hendrick RE. The AAPM/RSNA physics tutorial for residents. Basic physics of MR imaging: An introduction. *Radiographics* 1994;**14**:829-846.

Hennig J, Nauerth A, Friedburg H. RARE imaging: A fast imaging method for clinical MR. *Magn Reson Med* 1986;**3**:823-833.

Henson DB, Chaudry S, Artes PH, Faragher EB, Ansons A. Response variability in the visual field: Comparison of optic neuritis, glaucoma, ocular hypertension, and normal eyes. *Invest Ophthalmol Vis Sci* 2000;**41**:417-421.

Hickman SJ, Coulon O, Parker GJM, Barker GJ, Stevenson VL, Chard DT, Arridge SR, Thompson AJ, Miller DH. Application of a B-spline active surface technique to the measurement of cervical cord volume in multiple sclerosis from 3D MR images. *J Magn Reson Imaging* 2003;**18**:368-371.

Hobart J, Freeman J, Thompson A. Kurtzke scales revisited: the application of psychometric methods to clinical intuition. *Brain* 2000;**123**:1027-1040.

Holder GE. Pattern electroretinography (PERG) and an integrated approach to visual pathway diagnosis. *Prog Retin Eye Res* 2001;**20**:531-561.

Horowitz AL. *MRI physics for radiologists: A visual approach, 3rd ed.* New York: Springer-Verlag Inc.; 1994.

Horsfield MA. Imaging the cerebral hemispheres: Technical issues. *J Neurol Sci* 2000;**172(Suppl.1)**:S54-S56.

Horton JC. Mistaken treatment of anterior ischaemic optic neuropathy with interferon β-1a. *Ann Neurol* 2002;**52**:129.

Hu P, Pollard J, Hunt N, Taylor J, Chan-Ling T. Microvascular and cellular responses in the optic nerve of rats with acute experimental allergic encephalomyelitis (EAE). *Brain Pathol* 1998;**8**:475-486.

Ikeda H, Tansey EM. Virus-induced demyelination in the optic nerve of the mouse. I: Morphological and axonal transport studies. In: Hess RF, Plant GT, eds. *Optic neuritis*. Cambridge: Cambridge University Press; 1986, pp. 255-270.

Inglese M, Ghezzi A, Bianchi S, Gerevini S, Sormani MP, Martinelli V, Comi G, Filippi M. Irreversible disability and tissue loss in multiple sclerosis: A conventional and magnetization transfer magnetic resonance imaging study of the optic nerves. *Arch Neurol* 2002;**59**:250-255.

Iwasawa T, Matoba H, Ogi A, Kurihara H, Saito K, Yoshida T, Matsubara S, Nozaki A. Diffusion-weighted imaging of the human optic nerve: A new approach to evaluate optic neuritis in multiple sclerosis. *Magn Reson Med* 1997;**38**:484-491.

Jackson A, Sheppard S, Laitt RD, Kassner A, Moriarty D. Optic neuritis: MR imaging with combined fat- and water-suppression techniques. *Radiology* 1998;**206**:57-63.

Jacobs LD, Beck RW, Simon JH, Kinkel RP, Brownscheidle CM, Murray TJ, Simonian NA, Slasor PJ, Sandrock AW, CHAMPS Study Group. Intramuscular interferon beta-1a therapy initiated during a first demyelinating event in multiple sclerosis. *N Engl J Med* 2000;**343**:898-904.

Jin YP, Pedro-Cuesta J, Soderstrom M, Link H. Incidence of optic neuritis in Stockholm, Sweden, 1990-1995: II. Time and space patterns. *Arch Neurol* 1999;**56**:975-980.

Jin YP, Pedro-Cuesta J, Soderstrom M, Stawiarz L, Link H. Incidence of optic neuritis in Stockholm, Sweden 1990-1995: I. Age, sex, birth and ethnic-group related patterns. *J Neurol Sci* 1998;**159**:107-114.

John GR, Shankar SL, Shafit-Zagardo B, Massimi A, Lee SC, Raine CS, Brosnan CF. Multiple sclerosis: Re-expression of a developmental pathway that restricts oligodendrocyte maturation. *Nat Med* 2002;**8**:1115-1121.

Johnson G, Miller DH, MacManus D, Tofts PS, Barnes D, du Boulay EP, McDonald WI. STIR sequences in NMR imaging of the optic nerve. *Neuroradiology* 1987;**29**:238-245.

Jonas JB, Müller-Bergh JA, Schlötzer-Schrehardt UM, Nauman GOH. Histomorphometry of the human optic nerve. *Invest Ophthalmol Vis Sci* 1990;**31**: 736-744.

Jones SJ. Visual evoked potentials after optic neuritis. Effect of time interval, age and disease dissemination. *J Neurol* 1993;**240**:489-494.

Kakisu Y, Adachi-Usami E, Fujimoto N. Pattern visually evoked cortical potential and magnetic resonance imaging in optic neuritis. *J Clin Neuroophthalmol* 1991;**11**: 205-212.

Kansu T, Kirkali P, Kansu E, Zileli T. Optic neuropathy in Behçet's disease. *J Clin Neuroophthalmol* 1989;**9**:277-280.

Kapoor R, Davies M, Blaker PA, Hall SM, Smith KJ. Blockers of sodium and calcium entry protect axons from nitric oxide-mediated degeneration. *Ann Neurol* 2003;**53**:174-180.

Kapoor R, Miller DH, Jones SJ, Plant GT, Brusa A, Gass A, Hawkins CP, Page R, Wood NW, Compston DA, Moseley IF, McDonald WI. Effects of intravenous methylprednisolone on outcome in MRI-based prognostic subgroups in acute optic neuritis. *Neurology* 1998;**50**:230-237.

Katz B. The dyschromatopsia of optic neuritis: A descriptive analysis of data from the Optic Neuritis Treatment Trial. *Trans Am Ophthalmol Soc* 1995;**93**:685-708.

Katz D, Taubenberger JK, Cannella B, McFarlin DE, Raine CS, McFarland HF. Correlation between magnetic resonance imaging findings and lesion development in chronic, active multiple sclerosis. *Ann Neurol* 1993;**34**:661-669.

Kaufman DI, Trobe JD, Eggenberger ER, Whitaker JN. Practice parameter: The role of corticosteroids in the management of acute monosymptomatic optic neuritis. Report of the Quality Standards Subcommittee of the American Academy of Neurology. *Neurology* 2000;**54**:2039-2044.

Keltner JL, Johnson CA, Spurr JO, Beck RW, Optic Neuritis Study Group. Baseline visual field profile of optic neuritis. The experience of the Optic Neuritis Treatment Trial. *Arch Ophthalmol* 1993;**111**:231-234.

Keltner JL, Johnson CA, Spurr JO, Beck RW. Visual field profile of optic neuritis. One-year follow-up in the Optic Neuritis Treatment Trial. *Arch Ophthalmol* 1994;**112**:946-953.

Kermode AG, Thompson AJ, Tofts P, MacManus DG, Kendall BE, Kingsley DP, Moseley IF, Rudge P, McDonald WI. Breakdown of the blood-brain barrier precedes symptoms and other MRI signs of new lesions in multiple sclerosis. Pathogenetic and clinical implications. *Brain* 1990;**113**:1477-1489.

Kidd D, Burton B, Plant GT, Graham EM. Chronic relapsing inflammatory optic neuropathy (CRION): A newly recognised steroid responsive syndrome seemingly distinct from sarcoidosis. *Brain* 2003;**126**:276-284.

Kornek B, Storch MK, Weissert R, Wallstroem E, Stefferl A, Olsson T, Linington C, Schmidbauer M, Lassmann H. Multiple sclerosis and chronic autoimmune encephalomyelitis: A comparative quantitative study of axonal injury in active, inactive, and remyelinated lesions. *Am J Pathol* 2000;**157**:267-276.

Kriss A, Francis DA, Cuendet F, Halliday AM, Taylor DS, Wilson J, Keast-Butler J, Batchelor JR, McDonald WI. Recovery after optic neuritis in childhood. *J Neurol Neurosurg Psychiatry* 1988;**51**:1253-1258.

Kuhn MJ, Mikulis DJ, Ayoub DM, Kosofsky BE, Davis KR, Taveras JM. Wallerian degeneration after cerebral infarction: Evaluation with sequential MR imaging. *Radiology* 1989;**172**:179-182.

Kunii N, Goto N, Matsumoto K, Kawamura N. Morphometric comparison of the human optic nerve fiber with various other human nerve fibers. *Neurol Med Chir (Tokyo)* 1999;**39**:922-926.

Kupersmith MJ, Alban T, Zeiffer B, Lefton D. Contrast-enhanced MRI in acute optic neuritis: relationship to visual performance. *Brain* 2002;**125**:812-822.

Kurtzke JF. Rating neurologic impairment in multiple sclerosis: An expanded disability status scale (EDSS). *Neurology* 1983;**33**:1444-1452.

Langkilde AR, Rostrup E, Olsen DB, Jensen J, Frederiksen JL, Lauritzen M, Larsson HBW. Increased visual cortical activation in the recovery period from optic neuritis - a serial fMRI study. *Proc Intl Soc Magn Reson Med* 2002;**10**:1534.

Leary SM, Parker GJ, Stevenson VL, Barker GJ, Miller DH, Thompson AJ. Reproducibility of magnetic resonance imaging measurements of spinal cord atrophy: The role of quality assurance. *Magn Reson Imaging* 1999;**17**:773-776.

Lee AG, Lin DJ, Kaufman M, Golnik KC, Vaphiades MS, Eggenberger E. Atypical features prompting neuroimaging in acute optic neuropathy in adults. *Can J Ophthalmol* 2000;**35**:325-330.

Lee DH, Simon JH, Szumowski J, Feasby TE, Karlik SJ, Fox AJ, Pelz DM. Optic neuritis and orbital lesions: Lipid-suppressed chemical shift MR imaging. *Radiology* 1991;**179**:543-546.

Lesch DR, Spire J-P. Clinical electroencephalography. In: Thorpy MJ, ed. *Handbook of sleep disorders*. New York: Marcel Dekker Inc.; 1990, pp. 13-31.

Levatin P. Pupillary escape in disease of the retina or optic nerve. *Arch Ophthalmol* 1959;**62**:768-779.

Lexa FJ, Grossman RI, Rosenquist AC. Dyke Award paper. MR of Wallerian degeneration in the feline visual system: Characterization by magnetization transfer rate with histopathologic correlation. *AJNR Am J Neuroradiol* 1994;**15**:201-212.

Lightman S, McDonald WI, Bird AC, Francis DA, Hoskins A, Batchelor JR, Halliday AM. Retinal venous sheathing in optic neuritis. Its significance for the pathogenesis of multiple sclerosis. *Brain* 1987;**110**: 405-414.

Liu C, Edwards S, Gong Q, Roberts N, Blumhardt LD. Three dimensional MRI estimates of brain and spinal cord atrophy in multiple sclerosis. *J Neurol Neurosurg Psychiatry* 1999;**66**:323-330.

Liu C, Youl B, Moseley I. Magnetic resonance imaging of the optic nerve in extremes of gaze. Implications for the positioning of the globe for retrobulbar anaesthesia. *Br J Ophthalmol* 1992;**76**:728-733.

Losseff NA, Miller DH. Measures of brain and spinal cord atrophy in multiple sclerosis. *J Neurol Neurosurg Psychiatry* 1998;**64(Suppl.1)**:S102-S105.

Losseff NA, Wang L, Lai HM, Yoo DS, Gawne-Cain ML, McDonald WI, Miller DH, Thompson AJ. Progressive cerebral atrophy in multiple sclerosis. A serial MRI study. *Brain* 1996a;**119**:2009-2019.

Losseff NA, Webb SL, O'Riordan JI, Page R, Wang L, Barker GJ, Tofts PS, McDonald WI, Miller DH, Thompson AJ. Spinal cord atrophy and disability in multiple sclerosis. A new reproducible and sensitive MRI method with potential to monitor disease progression. *Brain* 1996b;**119**:701-708.

Lucchinetti C, Bruck W, Parisi J, Scheithauer B, Rodriguez M, Lassmann H. Heterogeneity of multiple sclerosis lesions: Implications for the pathogenesis of demyelination. *Ann Neurol* 2000;**47**:707-717.

Ludwin SK. Phagocytosis in the rat optic nerve following Wallerian degeneration. *Acta Neuropathol (Berl)* 1990;**80**:266-273.

MacDonald BK, Cockerell OC, Sander JW, Shorvon SD. The incidence and lifetime prevalence of neurological disorders in a prospective community-based study in the UK. *Brain* 2000;**123**:665-676.

Malinowski SM, Pulido JS, Folk JC. Long-term visual outcome and complications associated with pars planitis. *Ophthalmology* 1993;**100**:818-824.

Mashima Y, Oshitari K, Imamura Y, Momoshima S, Shiga H, Oguchi Y. High-resolution magnetic resonance imaging of the intraorbital optic nerve and subarachnoid space in patients with papilledema and optic atrophy. *Arch Ophthalmol* 1996;**114**:1197-1203.

McCluskey PJ, Watson PG, Lightman S, Haybittle J, Restori M, Branley M. Posterior scleritis: Clinical features, systemic associations, and outcome in a large series of patients. *Ophthalmology* 1999;**106**:2380-2386.

McDonald I. Diagnostic methods and investigation in multiple sclerosis. In: Compston A, Ebers G, Lassman H, McDonald I, Matthews B, Wekerle H, eds. *McAlpine's multiple sclerosis*. London: Churchill Livingstone; 1998, pp. 251-279.

McDonald WI. Pathophysiology of conduction in central nerve fibres. In: Desmedt JE, ed. *Visual evoked potentials in man: New developments*. Oxford: Clarendon Press; 1977, pp. 427-437.

McDonald WI. In: Hess RF, Plant GT, eds. The pathogenesis of optic neuritis. *Optic neuritis*. Cambridge: Cambridge University Press; 1986, pp. 42-50.

McDonald WI, Compston A, Edan G, Goodkin D, Hartung H-P, Lublin FD, McFarland HF, Paty DW, Polman CH, Reingold SC, Sandberg-Wollheim M, Sibley W, Thompson A, van den Noort S, Weinshenker BY, Wolinsky JS. Recommended diagnostic criteria for multiple sclerosis: Guidelines from the International Panel on the diagnosis of multiple sclerosis. *Ann Neurol* 2001;**50**:121-127.

McDonald WI, Sears TA. The effects of experimental demyelination on conduction in the central nervous system. *Brain*;1970:**93**:583-598.

McGavern DB, Murray PD, Rivera-Quinones C, Schmelzer JD, Low PA, Rodriguez M. Axonal loss results in spinal cord atrophy, electrophysiological abnormalities and neurological deficits following demyelination in a chronic inflammatory model of multiple sclerosis. *Brain* 2000;**123**:519-531.

McGowan JC. The physical basis of magnetization transfer imaging. *Neurology* 1999;**53**:S3-S7.

McKee MD, Waddell JP, Kudo PA, Schemitsch EH, Richards RR. Osteonecrosis of the femoral head in men following short-course corticosteroid therapy: A report of 15 cases. *CMAJ* 2001;**164**:205-206.

Medana I, Martinic MA, Wekerle H, Neumann H. Transection of major histocompatibility complex class I-induced neurites by cytotoxic T lymphocytes. *Am J Pathol* 2001;**159**:809-815.

Miller DH, Barkhof F, Frank JA, Parker GJ, Thompson AJ. Measurement of atrophy in multiple sclerosis: Pathological basis, methodological aspects and clinical relevance. *Brain* 2002;**125**:1676-1695.

Miller DH, Grossman RI, Reingold SC, McFarland HF. The role of magnetic resonance techniques in understanding and managing multiple sclerosis. *Brain* 1998;**121**:3-24.

Miller DH, Newton MR, van der Poel JC, du Boulay EP, Halliday AM, Kendall BE, Johnson G, MacManus DG, Moseley IF, McDonald WI. Magnetic resonance imaging of the optic nerve in optic neuritis. *Neurology* 1988;**38**:175-179.

Miller DH, Thompson AJ, Morrissey SP, MacManus DG, Moore SG, Kendall BE, Moseley IF, McDonald WI. High dose steroids in acute relapses of multiple sclerosis: MRI evidence for a possible mechanism of therapeutic effect. *J Neurol Neurosurg Psychiatry* 1992;**55**:450-453.

Miller NR, Newman NJ, eds. *Walsh and Hoyt's Clinical Neuro-Ophthalmology, 5th ed.* Baltimore: Williams and Wilkins; 1998.

Miller NR, Savino PJ, Schneider T. Rapid growth of an intracranial aneurysm causing apparent retrobulbar optic neuritis. *J Neuroophthalmol* 1995;**15**:212-218.

Mogenson PH. Histopathology of anterior parts of the optic pathway in patients with multiple sclerose. *Acta Ophthalmol (Copenh)* 1990;**68**:218-220.

Moll C, Mourre C, Lazdunski M, Ulrich J. Increase of sodium channels in demyelinated lesions of multiple sclerosis. *Brain Res* 1991;**556**:311-316.

Morales DS, Siatkowski RM, Howard CW, Warman R. Optic neuritis in children. *J Pediatr Ophthalmol Strabismus* 2000;**37**:254-259.

Mottershead JP, Schmierer K, Clemence M, Thornton JS, Scaravilli F, Barker GJ, Tofts PS, Newcombe J, Cuzner ML, Ordidge RJ, McDonald WI, Miller DH. High field MRI correlates of myelin content and axonal density in multiple sclerosis - a post-mortem study of the spinal cord. *J Neurol* 2003;**250**:1293-1301.

Noseworthy JH, O'Brien PC, Petterson TM, Weis J, Stevens L, Peterson WK, Sneve D, Cross SA, Leavitt JA, Auger RG, Weinshenker BG, Dodick DW, Wingerchuk DM, Rodriguez M. A randomized trial of intravenous immunoglobulin in inflammatory demyelinating optic neuritis. *Neurology* 2001;**56**:1514-1522.

Optic Neuritis Study Group. The clinical profile of optic neuritis. Experience of the Optic Neuritis Treatment Trial. *Arch Ophthalmol* 1991;**109**:1673-1678.

Optic Neuritis Study Group. The 5-year risk of MS after optic neuritis. Experience of the Optic Neuritis Treatment Trial. *Neurology* 1997a;**49**:1404-1413.

Optic Neuritis Study Group. Visual function 5 years after optic neuritis: Experience of the Optic Neuritis Treatment Trial. *Arch Ophthalmol* 1997b;**115**:1545-1552.

Optic Neuritis Study Group. High- and low-risk profiles for the development of multiple sclerosis within 10 years after optic neuritis. Experience of the Optic Neuritis Treatment Trial. *Arch Ophthalmol* 2003;**121**:944-949.

Optic Neuritis Study Group. Visual function more than 10 years after optic neuritis: Experience of the Optic Neuritis Treatment Trial. *Am J Ophthalmol* 2004;**137**:77-83.

Parisi V, Manni G, Spadaro M, Colacino G, Restuccia R, Marchi S, Bucci MG, Pierelli F. Correlation between morphological and functional retinal impairment in multiple sclerosis patients. *Invest Ophthalmol Vis Sci* 1999;**40**:2520-2527.

Parkin PJ, Hierons R, McDonald WI. Bilateral optic neuritis. A long-term follow-up. *Brain* 1984;**107**:951-964.

Pelli DG, Robson JG, Wilkins AJ. The design of a new letter chart for measuring contrast sensitivity. *Clin Vision Sci* 1988;**2**:187-199.

Perkin GD, Rose FC. *Optic neuritis and its differential diagnosis*. Oxford: Oxford University Press; 1979.

Perry VH, Anthony DC. Axon damage and repair in multiple sclerosis. *Philos Trans R Soc Lond B Biol Sci* 1999;**354**:1641-1647.

Persson HE, Sachs C. Visual evoked potentials elicited by pattern reversal during provoked visual impairment in multiple sclerosis. *Brain* 1981;**104**:369-382.

Pitt D, Werner P, Raine CS. Glutamate excitotoxicity in a model of multiple sclerosis. *Nat Med* 2000;**6**:67-70.

Plummer DL. DispImage: A display and analysis tool for medical images. *Rivista di Neuroradiologia* 1992;**5**:489-495.

Poser CM, Brinar VV. Problems with diagnostic criteria for multiple sclerosis. *Lancet* 2001;**358**:1746-1747.

Poser CM, Paty DW, Scheinberg L, McDonald WI, Davis FA, Ebers GC, Johnson KP, Sibley WA, Silberberg DH, Tourtellotte WW. New diagnostic criteria for multiple sclerosis: guidelines for research protocols. *Ann Neurol* 1983;**13**:227-231.

Prineas JW, Barnard RO, Kwon EE, Sharer LR, Cho ES. Multiple sclerosis: Remyelination of nascent lesions. *Ann Neurol* 1993;**33**:137-151.

Prineas JW, Connell F. Remyelination in multiple sclerosis. *Ann Neurol* 1979;**5**:22-31.

Purvin V, Kawasaki A, Jacobson DM. Optic perineuritis: Clinical and radiographic features. *Arch Ophthalmol* 2001;**119**:1299-1306.

Raine CS, Cross AH. Axonal dystrophy as a consequence of long-term demyelination. *Lab Invest* 1989;**60**:714-725.

Raine CS, Traugott U, Nussenblatt RB, Stone SH. Optic neuritis and chronic relapsing experimental allergic encephalomyelitis: Relationship to clinical course and comparison with multiple sclerosis. *Lab Invest* 1980;**42**:327-335.

Ramsaransing G, Maurits N, Zwanikken C, De Keyser J. Early prediction of a benign course of multiple sclerosis on clinical grounds: A systematic review. *Mult Scler* 2001;**7**:345-347.

Rao NA. Demyelinating optic neuritis. *Comp Pathol Bull* 1979;**2**:3-4.

Rao NA, Tso MO, Zimmerman EL. Experimental allergic optic neuritis in guinea pigs: Preliminary report. *Invest Ophthalmol Vis Sci* 1977;**16**:338-342.

Rasminsky M. The effects of temperature on conduction in demyelinated single nerve fibers. *Arch Neurol* 1973;**28**:287-292.

Rawson MD, Liversedge LA. Treatment of retrobulbar neuritis with corticotrophin. *Lancet* 1969;**ii**:222.

Rawson MD, Liversedge LA, Goldfarb G. Treatment of acute retrobulbar neuritis with corticotrophin. *Lancet* 1966;**ii**:1044-1046.

Ray S, Gragoudas E. Neuroretinitis. *Int Ophthalmol Clin* 2001;**41**:83-102.

Redford EJ, Kapoor R, Smith KJ. Nitric oxide donors reversibly block axonal conduction: Demyelinated axons are especially susceptible. *Brain* 1997;**120**:2149-2157.

Repka MX, Quigley HA. The effect of age on normal human optic nerve fiber number and diameter. *Ophthalmology* 1989;**96**:26-32.

Reynolds J, Jones T, Madden J, Schofield S. Chickenpox and steroid cards. Amended card is used in Oxford. *Br Med J* 1996;**312**:1608-1609.

Rimmer S, Keating C, Chou T, Farb MD, Christenson PD, Foos RY, Bateman JB. Growth of the human optic disk and nerve during gestation, childhood, and early adulthood. *Am J Ophthalmol* 1993;**116**:748-753.

Rivera-Quinones C, McGavern D, Schmelzer JD, Hunter SF, Low PA, Rodriguez M. Absence of neurological deficits following extensive demyelination in a class I-deficient murine model of multiple sclerosis. *Nat Med* 1998;**4**:187-193.

Rizzo JF III, Lessell S. Risk of developing multiple sclerosis after uncomplicated optic neuritis: A long-term prospective study. *Neurology* 1988;**38**:185-190.

Rodriguez M, Siva A, Cross SA, O'Brien PC, Kurland LT. Optic neuritis: A population-based study in Olmsted County, Minnesota. *Neurology* 1995;**45**:244-250.

Rombouts SA, Lazeron RH, Scheltens P, Uitdehaag BM, Sprenger M, Valk J, Barkhof F. Visual activation patterns in patients with optic neuritis: An fMRI pilot study. *Neurology* 1998;**50**:1896-1899.

Rosenberg ML, O'Connor P, Carter J. Idiopathic unilateral disc edema. The big blind spot syndrome. *J Clin Neuroophthalmol* 1984;**4**:181-184.

Rovaris M, Bozzali M, Santuccio G, Iannucci G, Sormani MP, Colombo B, Comi G, Filippi M. Relative contributions of brain and cervical cord pathology to multiple sclerosis disability: A study with magnetisation transfer ratio histogram analysis. *J Neurol Neurosurg Psychiatry* 2000;**69**:723-727.

Rudick RA, Fisher E, Lee JC, Simon J, Jacobs L, Multiple Sclerosis Collaborative Research Group. Use of the brain parenchymal fraction to measure whole brain atrophy in relapsing-remitting MS. *Neurology* 1999;**53**:1698-1704.

Rush JA, Kennerdell JS, Martinez AJ. Primary idiopathic inflammation of the optic nerve. *Am J Ophthalmol* 1982;**93**:312-316.

Rushton D. Use of the Pulfrich pendulum for detecting abnormal delay in the visual pathway in multiple sclerosis. *Brain* 1975;**98**:283-296.

Sabel BA, Kasten E, Kreutz MR. Recovery of vision after partial visual system injury as a model of postlesion neuroplasticity. *Adv Neurol* 1997;**73**:251-276.

Sadun AA. Anatomy and physiology of the optic nerve. In: Miller NR, Newman NJ, eds. *Walsh and Hoyt's Clinical Neuro-Ophthalmology*. Baltimore:Williams and Wilkins; 1998, pp. 57-83.

Samtani V, Smith KJ. Remyelinated central axons are vulnerable to damage caused by electrical impulse activity. *Mult Scler* 1999;**5(Suppl.1)**:S4.

Sandberg-Wollheim M, Bynke H, Cronqvist S, Holtas S, Platz P, Ryder LP. A long-term prospective study of optic neuritis: Evaluation of risk factors. *Ann Neurol* 1990;**27**:386-393.

Saul RF, Hayat G, Selhorst JB. Visual evoked potentials during hyperthermia. *J Neuroophthalmol* 1995;**15**:70-78.

Schauf CL, Davis FA. Impulse conduction in multiple sclerosis: A theoretical basis for modification by temperature and pharmacological agents. *J Neurol Neurosurg Psychiatry* 1974;**37**:152-161.

Scolding N, Franklin R. Axon loss in multiple sclerosis. *Lancet* 1998;**352**:340-341.

Selhorst JB, Saul RF. Uhthoff and his symptom. *J Neuroophthalmol* 1995;**15**:63-69.

Sellebjerg F, Nielsen HS, Frederiksen JL, Olesen J. A randomized, controlled trial of oral high-dose methylprednisolone in acute optic neuritis. *Neurology* 1999;**52**:1479-1484.

Sharief MK. Cytokines in multiple sclerosis: Pro-inflammation or pro-remyelination? *Mult Scler* 1998;**4**:169-173.

Shields DC, Tyor WR, Deibler GE, Banik NL. Increased calpain expression in experimental demyelinating optic neuritis: An immunocytochemical study. *Brain Res* 1998;**784**:299-304.

Silver N, Lai M, Symms M, Barker G, McDonald I, Miller D. Serial gadolinium-enhanced and magnetization transfer imaging to investigate the relationship between the duration of blood-brain barrier disruption and extent of demyelination in new multiple sclerosis lesions. *J Neurol* 1999;**246**:728-730.

Silver NC, Good CD, Barker GJ, MacManus DG, Thompson AJ, Moseley IF, McDonald WI, Miller DH. Sensitivity of contrast enhanced MRI in multiple sclerosis. Effects of gadolinium dose, magnetization transfer contrast and delayed imaging. *Brain* 1997;**120**:1149-1161.

Silver NC, Lai M, Symms MR, Barker GJ, McDonald WI, & Miller DH. Serial magnetization transfer imaging to characterize the early evolution of new MS lesions. *Neurology* 1998;**51**:758-764.

Silver NC, Tofts PS, Symms MR, Barker GJ, Thompson AJ, Miller DH. Quantitative contrast-enhanced magnetic resonance imaging to evaluate blood-brain barrier integrity in multiple sclerosis: A preliminary study. *Mult Scler* 2001;7:75-82.

Simon JH, Jacobs LD, Campion MK, Rudick RA, Cookfair DL, Herndon RM, Richert JR, Salazar AM, Fischer JS, Goodkin DE, Simonian N, Lajaunie M, Miller DE, Wende K, Martens-Davidson A, Kinkel RP, Munschauer FE III, Brownscheidle CM, The

Multiple Sclerosis Collaborative Research Group (MSCRG). A longitudinal study of brain atrophy in relapsing multiple sclerosis. *Neurology* 1999;**53**:139-148.

Simon JH, Kinkel RP, Jacobs L, Bub L, Simonian N. A Wallerian degeneration pattern in patients at risk for MS. *Neurology* 2000;**54**:1155-1160.

Simon JH, McDonald WI. Assessment of optic nerve damage in multiple sclerosis using magnetic resonance imaging. *J Neurol Sci.* 2000;**172(Suppl.1)**:S23-S26.

Slagsvold JE. Pulfrich pendulum phenomenon in patients with a history of acute optic neuritis. *Acta Ophthalmol (Copenh)* 1978;**56**:817-826.

Slamovits TL. Anatomy and physiology of the optic chiasm. In: Miller NR, Newman NJ, eds. *Walsh and Hoyt's Clinical Neuro-Ophthalmology.* Baltimore:Williams and Wilkins; 1998, pp. 85-100.

Slamovits TL, Rosen CE, Cheng KP, Striph GG. Visual recovery in patients with optic neuritis and visual loss to no light perception. *Am J Ophthalmol* 1991;**111**:209-214.

Sloan LL. The use of pseudo-isochromatic charts in detecting central scotomas due to lesions in the conducting pathways. *Am J Ophthalmol* 1942;**25**:1352-1356.

Sloan RL, Sinclair E, Thompson J, Taylor S, Pentland B. Inter-rater reliability of the modified Ashworth Scale for spasticity in hemiplegic patients. *Int J Rehabil Res* 1992;**15**:158-161.

Smith KJ, Blakemore WF, McDonald WI. The restoration of conduction by central remyelination. *Brain* 1981;**104**:383-404.

Smith KJ, Kapoor R, Hall SM, Davies M. Electrically active axons degenerate when exposed to nitric oxide. *Ann Neurol* 2001;**49**:470-476.

Smith KJ, Lassmann H. The role of nitric oxide in multiple sclerosis. *Lancet Neurol* 2002;**1**:232-241.

Smith KJ, McDonald WI. The pathophysiology of multiple sclerosis: The mechanisms underlying the production of symptoms and the natural history of the disease. *Philos Trans R Soc Lond B Biol Sci* 1999;**354**:1649-1673.

Smith KJ, McDonald WI, & Blakemore WF. Restoration of secure conduction by central demyelination. *Trans Am Neurol Assoc* 1979;**104**:25-29.

Snedecor GW, Cochran WG. *Statistical Methods, 8th ed.* Ames, Iowa: Iowa State University Press; 1989, pp. 398-403.

Soila KP, Viamonte M Jr, Starewicz PM. Chemical shift misregistration effect in magnetic resonance imaging. *Radiology* 1984;**153**:819-820.

Steel DH, Waldock A. Measurement of the retinal nerve fibre layer with scanning laser polarimetry in patients with previous demyelinating optic neuritis. *J Neurol Neurosurg Psychiatry* 1998;**64**:505-509.

Stevenson VL, Leary SM, Losseff NA, Parker GJ, Barker GJ, Husmani Y, Miller DH, Thompson AJ. Spinal cord atrophy and disability in MS: A longitudinal study. *Neurology* 1998;**51**:234-238.

Sylvester PE, Ari K. The size and growth of the human optic nerve. *J Neurol Neurosurg Psychiatry* 1961;**24**:45-49.

Taber KH, Herrick RC, Weathers SW, Kumar AJ, Schomer DF, Hayman LA. Pitfalls and artifacts encountered in clinical MR imaging of the spine. *Radiographics* 1998;**18**:1499-1521.

Tamraz J. Neuroradiologic investigation of the visual system using magnetic resonance imaging. *J Clin Neurophysiol* 1994;**11**:500-518.

Tansey EM, Ikeda H. Virus-induced demyelination in the optic nerve of the mouse. II: Electrophysiological studies. In: Hess RF, Plant GT, eds. *Optic neuritis*. Cambridge: Cambridge University Press; 1986, pp. 271-282.

Thompson AJ, Hobart JC. Multiple sclerosis: Assessment of disability and disability scales. *J Neurol* 1998;**245**:189-196.

Thorpe JW, Barker GJ, Jones SJ, Moseley I, Losseff N, MacManus DG, Webb S, Mortimer C, Plummer DL, Tofts PS, McDonald WI, Miller DH. Magnetisation transfer ratios and transverse magnetisation decay curves in optic neuritis: Correlation with clinical findings and electrophysiology. *J Neurol Neurosurg Psychiatry* 1995;**59**:487-492.

Tofts PS, Silver NC, Barker GJ, Lai M, Gass A. Object strength - a reproducible lesion measure that is insensitive to partial volume errors. *Proc Int Soc Magn Reson Med* 1997;**5**:49.

Tortorella C, Codella M, Rocca MA, Gasperini C, Capra R, Bastianello S, Filippi M. Disease activity in multiple sclerosis studied by weekly triple-dose magnetic resonance imaging. *J Neurol* 1999;**246**:689-692.

Trapp BD, Peterson J, Ransohoff RM, Rudick R, Mork S, Bo L. Axonal transection in the lesions of multiple sclerosis. *N Engl J Med* 1998;**338**:278-285.

Trauzettel-Klosinski S, Axmann D, Diener HC. The Tubingen study on optic neuritis treatment: A prospective randomized and controlled trial. *Clin Vision Sci* 1993;**8**:385-394.

Trobe JD, Sieving PC, Guire KE, Fendrick AM. The impact of the Optic Neuritis Treatment Trial on the practices of ophthalmologists and neurologists. *Ophthalmology* 1999;**106**:2047-2053.

Tso MO, Shih CY, McLean IW. Is there a blood-brain barrier at the optic nerve head? *Arch Ophthalmol* 1975;**93**:815-825.

Ulrich J, Groebke-Lorenz W. The optic nerve in multiple sclerosis: A morphological study with retrospective clinico-pathological correlations. *Neuro-ophthalmology* 1983;**3**:149-159.

Van Buchem MA, Tofts PS. Magnetization transfer imaging. *Neuroimaging Clin N Am* 2000;**10**:771-788.

van Engelen BG, Hommes OR, Pinckers A, Cruysberg JR, Barkhof F, Rodriguez M. Improved vision after intravenous immunoglobulin in stable demyelinating optic neuritis. *Ann Neurol* 1992;**32**:834-835.

van Waesberghe JH, Kamphorst W, De Groot CJ, van Walderveen MA, Castelijns JA, Ravid R, Lycklama a Nijeholt GJ, van de Valk P, Polman CH, Thompson AJ, Barkhof F. Axonal loss in multiple sclerosis lesions: Magnetic resonance imaging insights into substrates of disability. *Ann Neurol* 1999;**46**:747-754.

Vine AK. Severe periphlebitis, peripheral retinal ischemia, and preretinal neovascularization in patients with multiple sclerosis. *Am J Ophthalmol* 1992;**113**: 28-32.

Votruba M, Leary S, Losseff N, Bhattacharya SS, Moore AT, Miller DH, Moseley IF. MRI of the intraorbital optic nerve in patients with autosomal dominant optic atrophy. *Neuroradiology* 2000;**42**:180-183.

Wakakura M, Mashimo K, Oono S, Matsui Y, Tabuchi A, Kani K, Shikishima K, Kawai K, Nakao Y, Tazawa Y, Kiyosawa M, Abe H, Ohba N, Yago K, Maeda S, Sugita M, Ishikawa S, Optic Neuritis Treatment Trial Multicenter Cooperative Research Group (ONMRG). Multicenter clinical trial for evaluating methylprednisolone pulse treatment of idiopathic optic neuritis in Japan. *Jpn J Ophthalmol* 1999a;**43**:133-138.

Wakakura M, Minei-Higa R, Oono S, Matsui Y, Tabuchi A, Kani K, Shikishima K, Kawai K, Nakao Y, Tazawa Y, Kiyosawa M, Abe H, Ohba N, Yago K, Maeda S, Sugita M, Ishikawa S, Optic Neuritis Treatment Trial Multicenter Cooperative Research Group (ONMRG). Baseline features of idiopathic optic neuritis as determined by a multicenter treatment trial in Japan. *Jpn J Ophthalmol* 1999b;**43**:127-132.

Wall M. Loss of P retinal ganglion cell function in resolved optic neuritis. *Neurology* 1990;**40**:649-653.

Wall M, Johnson CA, Kutzko KE, Nguyen R, Brito C, Keltner JL. Long- and short-term variability of automated perimetry results in patients with optic neuritis and healthy subjects. *Arch Ophthalmol* 1998;**116**:53-61.

Waller A. Experiments on the section of glossopharyngeal and hypoglossal nerves of the frog and observations of the alterations produced thereby in the structure of their primitive fibres. *Philos Trans R Soc Lond B Biol Sci* 1850;**140**:423-429.

Wenning GK, Wietholter H, Schnauder G, Muller PH, Kanduth S, Renn W. Recovery of the hypothalamic-pituitary-adrenal axis from suppression by short-term, high-dose intravenous prednisolone therapy in patients with MS. *Acta Neurol Scand* 1994;**89**:270-273.

Werring DJ, Bullmore ET, Toosy AT, Miller DH, Barker GJ, MacManus DG, Brammer MJ, Giampietro VP, Brusa A, Brex PA, Moseley IF, Plant GT, McDonald WI, Thompson AJ. Recovery from optic neuritis is associated with a change in the distribution of cerebral response to visual stimulation: A functional magnetic resonance imaging study. *J Neurol Neurosurg Psychiatry* 2000;**68**:441-449.

Wheeler-Kingshott CA, Parker GJ, Symms MR, Hickman SJ, Tofts PS, Miller DH, Barker GJ. ADC mapping of the human optic nerve: Increased resolution, coverage, and reliability with CSF-suppressed ZOOM-EPI. *Magn Reson Med* 2002;**47**;24-31.

Wilkins A, Majed H, Layfield R, Compston A, Chandran S. Oligodendrocytes promote neuronal survival and axonal length by distinct intracellular mechanisms: A novel role for oligodendrocyte-derived glial cell line-derived neurotrophic factor. *J Neurosci* 2003;**23**:4967-4974.

Williams PL, Warwick R, Dyson M, Bannister LH. *Gray's Anatomy, 37th ed.* Edinburgh: Churchill Livingstone; 1989.

Wisniewski HM, Oppenheimer D, McDonald WI. Relation between myelination and function in MS and EAE. *J Neuropathol Exp Neurol* 1976;**35**:327.

Wolff SD, Balaban RS. Magnetization transfer contrast (MTC) and tissue water proton relaxation in vivo. *Magn Reson Med* 1989;**10**:135-144.

Youl BD, Turano G, Miller DH, Towell AD, MacManus DG, Moore SG, Jones SJ, Barrett G, Kendall BE, Moseley IF, Tofts PS, Halliday AM, McDonald WI. The pathophysiology of acute optic neuritis. An association of gadolinium leakage with clinical and electrophysiological deficits. *Brain* 1991;**114**:2437-2450.

Youl BD, Turano G, Towell AD, Barrett G, MacManus DG, Moore SG, Miller DH, Jones SJ, du Boulay EP, Kendall BE, Moseley IF, McDonald WI. Optic neuritis: Swelling and atrophy. *Electroencephalogr Clin Neurophysiol Suppl* 1996;**46**:173-179.

Zacks DN, D'Amico DJ. Maculopathies that resemble optic neuropathies. *Int Ophthalmol Clin* 2001;**41**;61-71.

Zajicek JP, Scolding NJ, Foster O, Rovaris M, Evanson J, Moseley IF, Scadding JW, Thompson EJ, Chamoun V, Miller DH, McDonald WI, Mitchell D. Central nervous system sarcoidosis - diagnosis and management. *QJM* 1999;**92**:103-117.

Zhu B, Moore GR, Zwimpfer TJ, Kastrukoff LF, Dyer JK, Steeves JD, Paty DW, Cynader MS. Axonal cytoskeleton changes in experimental optic neuritis. *Brain Res* 1999;**824**:204-217.

Zivadinov R, Rudick RA, De Masi R, Nasuelli D, Ukmar M, Pozzi-Mucelli RS, Grop A, Cazzato G, Zorzon M. Effects of IV methylprednisolone on brain atrophy in relapsing- remitting MS. *Neurology* 2001;**57**:1239-1247.